Universidade de Aveiro Departamento de Química
2017

Helena Isabel Sousa Passos

Desenvolvimento e caracterização de novas plataformas de extração com sistemas aquosos bifásicos compostos por líquidos iónicos

Development and characterization of new extraction platforms using ionic-liquid-based aqueous biphasic systems

Universidade de Aveiro Departamento de Química
2017

Helena Isabel Sousa Passos

Desenvolvimento e caracterização de novas plataformas de extração com sistemas aquosos bifásicos compostos por líquidos iónicos

Development and characterization of new extraction platforms using ionic-liquid-based aqueous biphasic systems

Tese apresentada à Universidade de Aveiro para cumprimento dos requisitos necessários à obtenção do grau de Doutor em Engenharia Química, realizada sob a orientação científica do Professor Doutor João Manuel da Costa e Araújo Pereira Coutinho, Professor Catedrático do Departamento de Química, CICECO, da Universidade de Aveiro, e coorientação da Doutora Mara Guadalupe Freire Martins, Investigadora Coordenadora do Departamento de Química, CICECO, da Universidade de Aveiro.

Apoio financeiro do POCTI no âmbito do III Quadro Comunitário de Apoio.

O doutorando agradece o apoio financeiro da FCT e da FSE no âmbito do III Quadro Comunitário de Apoio (SFRH/BD/85248/2012). Parte da investigação que conduziu aos resultados aqui apresentados foi financiada pelo Conselho Europeu de Investigação ao abrigo do Sétimo Programa-Quadro da União Europeia (FP7/2007-2013)/ERC no. 337753.

Ao Bruno e aos meus pais, pela paciência, dedicação
e amor incondicional que me trouxe até aqui...

o júri

presidente

Prof. Dr. Eduardo Anselmo Ferreira da Silva
Professor Catedrático do Departamento de Geociências da Universidade de Aveiro

Prof. Dr. João Manuel da Costa e Araújo Pereira Coutinho
Professor Catedrático do Departamento de Química da Universidade de Aveiro

Prof. Dr. José António Teixeira
Professor Catedrático da Universidade do Minho

Prof.ª Dr.ª Ana Maria Soto Campos
Professora Catedrática da Universidade de Santiago de Compostela, Espanha

Drª Isabel Maria Delgado Jana Marrucho Ferreira
Professora Associada do Instituto Superior Técnico de Lisboa

Drª Sónia Patrícia Marques Ventura
Investigadora Auxiliar do Departamento de Química da Universidade de Aveiro

Dr. António Palma Madeira
Estagiário de Pós-doutoramento do Departamento de Química da Universidade de Aveiro

Drª Isabelle Billard
Directrice de Recherche, Centre National de la Recherche Scientifique, Universidade de Grenoble Alpes, França

agradecimentos

São muitas as pessoas que de alguma forma contribuíram para o desenvolvimento desta tese e a quem eu tenho que agradecer...

Em primeiro lugar, quero deixar um muito obrigada aos meus orientadores pelo acompanhamento excecional, total disponibilidade e permanente motivação. Em particular, agradeço ao Prof. João pelo desafio que me colocou, por me ter levado a quebrar barreiras e, acima de tudo, por me ter feito crescer. À Mara tenho que agradecer o apoio incondicional, a confiança que sempre depositou em mim, bem como a paixão contagiante que me transmitiu todos os dias. Obrigada aos dois, por me terem ajudado a traçar o caminho que me trouxe até aqui.

Agradeço ao PATh, aos que cá estão e aos que estiveram, sem exceção!, por terem estado presentes nos melhores momentos, mas também nos menos bons, por me terem deixado partilhar tantas aventuras e por me fazerem sentir que fiz parte desta família...

Inês e Ana Maria, cada uma à sua maneira, mas ambas foram uma peça indispensável neste percurso. Ana Maria, obrigada por teres estado sempre por perto, por me teres deixado partilhar contigo todos os momentos, os bons e os mais difíceis. Obrigada pela tua amizade, apoio e confiança. Inês, nunca percebi o porquê, mas precisamos de poucas palavras para nos entendermos. Talvez por isso eu sinta que, mesmo longe, mesmo passados meses sem nos vermos, tu estiveste e estarás sempre lá, a minha melhor amiga para o que der e vier...

À minha família e amigos, um muito obrigada pelo vosso carinho e apoio. Um especial obrigada aos meus padrinhos e à minha avó, obrigada por acreditarem em mim e por estarem sempre presentes.

Pai e Mãe, não há palavras suficientes para expressar o quanto eu gosto de vocês e o quanto vos agradeço por todas as oportunidades que me deram na vida. Obrigada por estarem sempre do meu lado e pelo vosso apoio incondicional.

Bruno, obrigada por teres aceite percorrer esta estrada comigo e me teres apoiado até ao fim...

palavras-chave

Sistemas aquosos bifásicos, líquidos iónicos, extração, caracterização, sistemas ternários e quaternários, misturas, polaridade

resumo

Devido às suas propriedades únicas, sendo a sua capacidade de *tailoring* uma das mais importantes, os líquidos iónicos são atualmente considerados potenciais substitutos dos solventes orgânicos voláteis comumente utilizados pela indústria, o que levou a uma investigação crescente da sua aplicação em diversas áreas. Contudo, para além da utilização de líquidos iónicos hidrofóbicos na formação de sistemas bifásicos com água e/ou em meios aquosos, na última década, introduziram-se os líquidos iónicos hidrofílicos como constituintes de sistemas aquosos bifásicos – sistemas do tipo líquido-líquido compostos por duas fases aquosas e mais benignos – conduzindo a uma melhor *performance* de extração e seletividade para um vasto número de compostos. Tendo em conta todas estas vantagens, esta tese tem como objetivo o estudo científico e tecnológico de sistemas aquosos bifásicos constituídos por líquidos iónicos, envolvendo o desenvolvimento de novos processos de separação mais eficientes.

Com o intuito de desenvolver plataformas de extração/separação mais eficientes, este trabalho inicia-se com o estudo de novos compostos e suas misturas na formação de sistemas aquosos bifásicos. A caracterização das propriedades das fases em equilíbrio e a descrição dos mecanismos que regem a formação destes sistemas, bem como a partição de diversos solutos entre as fases, são temas abordados no segundo capítulo. Por último, e como um exemplo de possível aplicação destes novos sistemas, estudou-se a sua utilização na extração e pré-concentração de compostos que apresentam riscos para a saúde humana e ambiente.

A elevada versatilidade dos sistemas aquosos bifásicos constituídos por líquidos iónicos, bem como a sua elevada *performance* na extração dos mais diversos compostos, foram aqui demonstrados, confirmando o potencial destes sistemas como processos de separação alternativos. No entanto, e como comprovado neste trabalho, ainda é necessário prosseguir com a investigação em sistemas aquosos bifásicos constituídos por líquidos iónicos, principalmente visando o seu *scale-up* e utilização final pela indústria.

keywords

Aqueous biphasic systems, ionic liquids, extraction, characterization, ternary and quaternary systems, mixtures, polarity

abstract

Due to their unique properties, being one of the most important their tailoring ability, ionic liquids (ILs) have been investigated in several fields and proposed as alternatives to hazardous volatile organic compounds commonly used by industries. In addition to the use of hydrophobic ILs in the formation of biphasic systems with water and/or in aqueous media, in the past decade, hydrophilic ILs were introduced as phase-forming components of aqueous biphasic systems (ABS) – more benign liquid-liquid systems composed of two aqueous-rich phases – able to provide improved extraction performance with increased selectivity for a large range of compounds. Based on these advantages, this thesis aims to gather a deeper scientific and technological knowledge on IL-based ABS, through the development and characterization of novel and more efficient separation processes.

Aiming at developing ABS with tailored and better extraction performance, this work starts with a comprehensive investigation on the use of new phase-forming components and their mixtures, and their impact on the formation of liquid-liquid systems. The characterization of the properties of the coexisting phases and the description of the mechanisms which rule the formation of IL-based ABS, as well as the partition behavior of several solutes between the phases, are addressed in the second chapter. Finally, the use of these novel IL-based systems in the extraction and pre-concentration of compounds of human and environmental concern is addressed as a main example of these systems applications.

The high versatility of IL-based ABS, as well as their high extraction performance and selectivity, were here demonstrated, confirming their potential within separation processes. Nevertheless, and as proved in this work, additional research on IL-based ABS is still required so that these systems can be finally scaled-up and used by industries.

CONTENTS

LIST OF TABLES

LIST OF FIGURES

NOMENCLATURE

List of symbols

$\mathrm{p}K_a$	acidic dissociation constant	$[IL]_{SS}$	IL molality at saturation solubility
γ_i	activity coefficient of component i	ΔS_{hyd}	molar entropy of hydration
$\varepsilon^{A_iB_i}/k_B$	association-energy parameter of component i	a	molar Helmholtz energy
$k^{A_iB_i}$	association-volume parameter of component i	x_i	mole fraction of component i
k_{ij}	binary interaction parameter for components i and j	M_w	molecular weight
k_B	Boltzmann constant	NP	number of experimental data
$\delta(C_i)$	chemical shift of carbon atom in position i	K_{ow}	octanol-water partition coefficient
$[i]$	concentration of component i	K_i	partition coefficient of component i
$[i]_j$	concentration of component i in the phase j	p	pressure
R^2	correlation coefficient	α	ratio between the weight of the salting-out specie rich phase and the total weight of the mixture **or** hydrogen bond acidity **or** degree of dissociation
ρ	density	F	ratio of variance
π^*	dipolarity/polarizability	σ_i	segment diameter of component i
u_i/k_B	dispersion-energy parameter of component i	m_i^{seg}	segment number of component i
G_{Max}^E	excess Gibbs function	S	selectivity
$EE_i\%$	extraction efficiency percentage of component i	σ or SD	standard deviation
U_0	flow rate	T	temperature
φ_i	fugacity coefficient of component i	t	time
ΔG_{hyd}	Gibbs energy of ion hydration	η	viscosity
β	hydrogen bond basicity	V	volume
E_{HB}	hydrogen-bonding interaction energies	w_i^j	weight of component i in the phase j
R	ideal gas constant		

List of abbreviations

AA	amino acid	LSER	linear solvation energy relationship
AAD	average absolute deviation	M	mixture
ABS	aqueous biphasic systems	MES	2-(*N*-morpholino)ethanesulfonic acid
AD	absolute deviation	MS	mass spectrometry
ARD	average relative deviation	MuPS	aqueous multiphase systems
Azo	azocasein	NMR	nuclear magnetic resonance
BPA	bisphenol A	NRTL	Non-Random Two-Liquid
CHES	*N*-cyclohexyl-2-aminoethanesulfonic acid	PB	pigment blue
COSMO-RS	COnductor-like Screening MOdel for Realistic Solvation	PC-SAFT	Perturbed-Chain Statistical Associating Fluid Theory
CPC	centrifugal partition chromatography	PEG	poly(ethylene glycol)
Cyt	cytochrome C	Phe	phenylalanine
DES	deep eutectic solvents	PIL	protic ionic liquid
DLLME	dispersive liquid–liquid micro extraction	PPG	poly(propylene glycol)
DNP-AA	dinitrophenyl-amino acids	PyO	pyridine-*N*-oxide
E2	17β-estradiol	SLE	solid-liquid extraction
EDCs	endocrine disrupting compounds	SPE	solid-phase extraction
EE2	17α-ethinylestradiol	SWCF-VR	Square-Well Chain Fluid with Variable Range
EoS	equation of state	TES	*N*-tris(hydroxymethyl)methyl-2-aminoethanesulfonic acid
FTIR	Fourier transform infrared spectroscopy	TL	tie-line
GBs	Good's buffers	TLL	tie-line length
GC	gas chromatography	Tricine	*N*-tris(hydroxymethyl) methylglycine
HBA	hydrogen bond acceptor	Trp	tryptophan
HBD	hydrogen bond donor	TSP	trimethylsilyl propanoic acid
HEPES	4-(2-hydroxyethyl)-1-piperazineethanesulfonic acid	Tyr	tyrosine
HPLC	high performance liquid chromatography	UCST	upper critical solution temperature
HSQC	heteronuclear single quantum coherence	UNIFAC	UNIversal Functional Activity Coefficients
IL	ionic liquid	USEPA	United States Environmental Protection Agency
KT	Kamlet-Taft	UV-Vis	ultraviolet-visible
LC	liquid chromatography	VLE	vapor-liquid equilibrium
LCST	lower critical solution temperature	VOC	volatile organic compound
LLE	liquid-liquid equilibrium		

Abbreviation of the ionic liquids cations

$[C_1C_1im]^+$	1,3-dimethylimidazolium	$[N_{11(13)(C7H7)}]^+$	cocoalkonium
$[C_1im]^+$	1-methylimidazolium	$[N_{11[2(N110)]0}]^+$	*N*,*N*-dimethyl-*N*-(*N´*,*N´*dimethylaminoethyl)ammonium
$[C_2C_1im]^+$	1-ethyl-3-methylimidazolium	$[N_{111(2OH)}]^+$	cholinium
$[C_2C_1pyr]^+$	1-ethyl-1-methylpyrrolidinium	$[N_{1120}]^+$	*N*,*N*-dimethyl-*N*-ethylammonium
$[C_3C_1im]^+$	1-propyl-3-methylimidazolium	$[N_{1220}]^+$	*N*,*N*-diethyl-*N*-methylammonium
$[C_3C_1py]^+$	1-propyl-3-methylpyridinium	$[N_{2000}]^+$	ethylammonium
$[C_4C_1im]^+$	1-butyl-3-methylimidazolium	$[N_{2220}]^+$	triethylammonium
$[C_4C_1pip]^+$	1-butyl-1-methylpiperidinium	$[N_{4444}]^+$	tetrabutylammonium
$[C_4C_1py]^+$	1-butyl-3-methylpyridinium	$[OHC_2C_1im]^+$	1-(2-hydroxyethyl)-3-methylimidazolium
$[C_4C_1pyr]^+$	1-butyl-1-methylpyrrolidinium	$[P_{4441}]^+$	tributylmethylphosphonium
$[C_6C_1im]^+$	1-hexyl-3-methylimidazolium	$[P_{4442}]^+$	tributylethylphosphonium
$[C_8C_1im]^+$	1-methyl-3-octylimidazolium	$[P_{4444}]^+$	tetrabutylphosphonium
$[N_{(10)(10)11}]^+$	didecyldimethylammonium	$[P_{666,14}]^+$	trihexyltetradecylphosphonium
$[N_{1(2OH)(TH)(TH)}]^+$	dihydrogenated tallowoylethyl hydroxyethylmonium		

Abbreviation of the ionic liquids anions

$[Ace]^-$	acetate	$[DHP]^-$	dihydrogenphosphate
$[BF_4]^-$	tetrafluoroborate	$[DMP]^-$	dimethylphosphate
$[But]^-$	butanoate	$[Gly]^-$	glycolate
$[C_2H_5SO_4]^-$	ethylsulfate	$[HSO_4]^-$	hydrogensulfate
$[C_7H_{15}CO_2]^-$	octanoate	$[Lac]^-$	lactate
$[C_7H_7CO_2]^-$	phenylacetate	$[N(CN)_2]^-$	dycianamide
$[C_8H_{17}SO_4]^-$	octylsulfate	$[NO_3]^-$	nitrate
$[CF_3CO_2]^-$	trifluoroacetate	$[NTf_2]^-$	bis-(trifluoromethylsulfonyl)amide
$[CF_3SO_3]^-$	trifluoromethanesulfonate	$[PF_6]^-$	hexafluorophosphate
$[CH_3CO_2]^-$	acetate	$[Pro]^-$	propanoate
$[CH_3SO_3]^-$	methanesulfonate	$[SCN]^-$	thiocyanate
$[CH_3SO_4]^-$	methylsulfate	$[TOS]^-$	tosilate
$[DBP]^-$	dibutylphosphate	Br^-	bromide
$[DEP]^-$	diethylphosphate	Cl^-	chloride
$[DHC]^-$	dihydrogencitrate		

List of common salts

$(NH_4)_2SO_4$	ammonium sulfate	$KNaC_4H_4O_6$	potassium sodium tartrate
$Al_2(SO_4)_3$	aluminum sulfate	LiBr	lithium bromide
$AlPO_4$	aluminum phosphate	Na_2CO_3	sodium carbonate
K_2CO_3	potassium carbonate	Na_2HPO_4	disodium phosphate
K_2HPO_4	dipotassium phosphate	Na_2SO_4	sodium sulfate
$K_3C_6H_5O_7$	potassium citrate	NaBr	sodium bromide
K_3PO_4	tripotassium phosphate	$NaCH_3CO_2$	sodium acetate
KCH_3CO_2	potassium acetate	NaCl	sodium chloride
KH_2PO_4	sodium acetate		

1. Ionic-liquid-based aqueous biphasic systems:

A brief introduction

1.1. Ionic liquids (ILs)

In the past decades, the word "green" acquired a new meaning in chemistry-related fields. The introduction of the twelve principles of green chemistry played a major role in the development of "green engineering",[1] and the importance of sustainable development and "green chemistry" changed the way chemical processes and products are designed. The maximization on the use of raw materials, and the minimization of losses and energy consumption, and of the environmental and health impacts of chemical processes and products, became a priority. To this end, more sustainable and environmentally friendly approaches have been developed.[1] Some of these attempts address the use of renewable sources, such as biomass, and solvents such as water, supercritical CO_2, ionic liquids (ILs), and natural deep eutectic mixtures.[2] In this context, this work is focused on the development of novel separation and purification platforms based on aqueous solutions of ILs.

ILs are salts with melting temperatures below 373 K – a result of their low-charge density and low symmetry ions.[3] These salts are usually composed of a large organic cation and an organic or inorganic anion, and are generally described as "designer solvents" since there is a large degree of cation/anion combinations, boosting them with the possibility of tuning their properties, such as their thermophysical properties, biodegradation ability or toxicological features, as well as their hydrophobicity and solution behavior.[4–7]

The synthesis of ILs was reported for the first time at the beginning of the 20th century, by Paul Walden.[8] Walden synthesized a salt, ethylammonium nitrate, $[N_{2000}][NO_3]$, with a melting point of 284 K, when searching for new explosives for the replacement of nitroglycerin.[8] Although some patents involving ILs were published after this finding, in particular during the World War II,[9–11] only in the past two decades, with the appearance of air- and water-stable ILs, as well as of task-specific compounds, the research on the synthesis of novel ILs and on their applications has increased.[12] The number of articles and patents concerning ILs, and published between 1990 and 2016, are depicted in **Figure 1.1**.

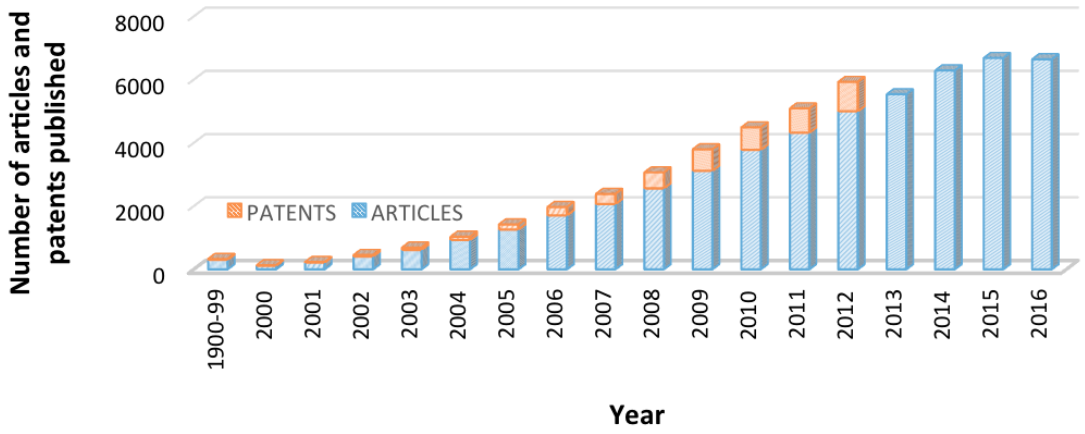

Figure 1.1. Number of articles and patents *per* year involving ILs. Values taken from *ISI Web of Knowledge* in January 11, 2017.

Nowadays, amongst the large range of ILs that can be synthesized, the most commonly studied cations are nitrogen-based, namely pyrrolidinium-, imidazolium-, piperidinium- pyridinium- and quaternary-ammonium, combined with anions such as chloride (Cl^-), bromide (Br^-), acetate ($[CH_3CO_2]^-$), hexafluorophosphate ($[PF_6]^-$), tetrafluoroborate ($[BF_4]^-$) and bis(trifluoromethylsulfonyl)imide ($[NTf_2]^-$). In **Figure 1.2** are depicted some of the most common ILs cations and anions chemical structures. However, the development of novel ILs is fast moving away from the more hydrophobic and fluorinated anions ($[PF_6]^-$, $[BF_4]^-$, etc.) towards less toxic and biodegradable alternatives, namely derivatives from carboxylic acids and amino-acid-based anions.[13,14] The search on ILs produced from renewable resources, more biodegradable and biocompatible, has also led to the synthesis of, for instance, cholinium- and amino-acid-based cations,[15] and more recently to derivatives of mandelic acid.[16,17] The synthesis of more biodegradable and low-toxicity ILs has considerably increased in the past few years, and several ILs are already classified as 'biodegradable' (at least 60 % of the compound is biodegraded within 28 days).[18]

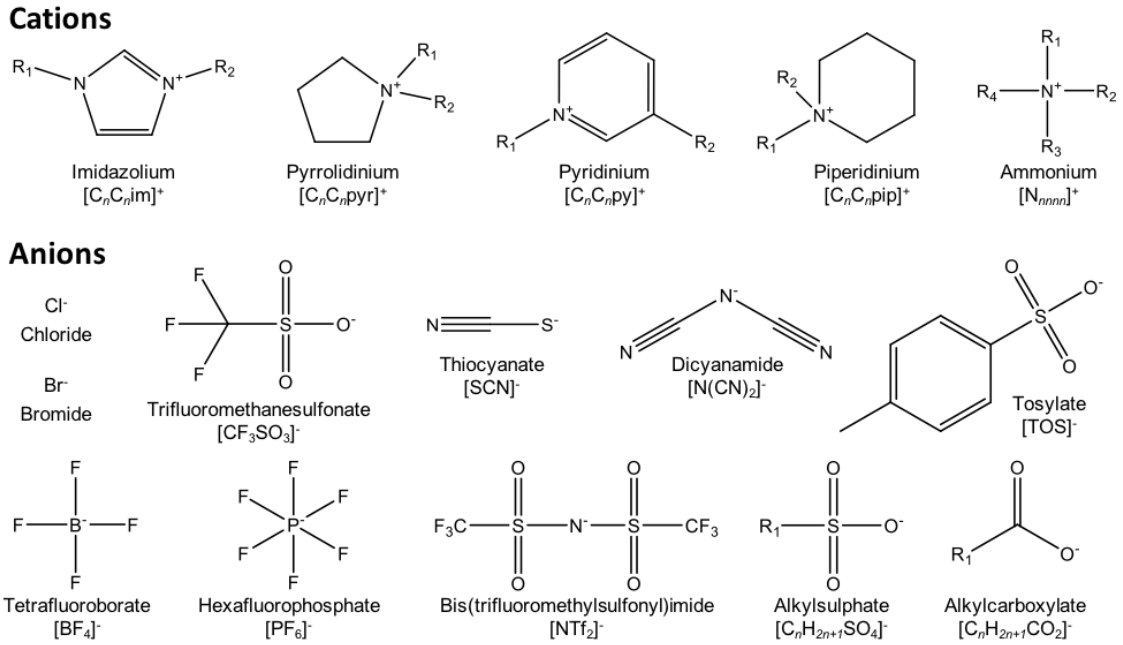

Figure 1.2. Chemical structures of ILs ions.

Due to their ionic character, most aprotic ILs exhibit unique properties, namely a negligible vapor pressure, low flammability, high thermal and chemical stabilities, broad liquid temperature range, high solvation ability for organic, inorganic and organometallic compounds, and improved selectivity.[19–21] All these features make of them potential alternatives to the volatile organic compounds (VOCs) commonly used in the most diverse applications, namely in biphasic catalysis, organic synthesis, polymerization, separation and extraction processes, and in the dissolution of biomaterials.[4,22–25] Moreover, ILs also demonstrated a good performance in biocatalysis, some of them providing a non-denaturing environment for biomolecules and maintaining the protein structure and enzymatic activity.[26]

Although more than 100 years have passed since the synthesis of the first IL,[8] there is still much to explore and to learn with these compounds. The research on their synthesis, characterization and applications is still under continuous development.

1.2. Aqueous biphasic systems (ABS)

In biotechnological processes, the separation and purification stages usually require numerous steps which further imply a high energetic and chemical consumption, and may represent up to 60 % of the final product cost, reaching 90 % in some cases.[27] There have been considerable efforts addressing the development of fast and cost-effective separation techniques, namely in liquid-liquid extractions. These separation processes take into account the relative

solubility and the partition behavior of the target compounds between two immiscible liquids, one of which is, for biocompounds, usually water, and the other an organic solvent. Liquid-liquid extraction processes are technologically simple, of low cost, highly effective for the separation of a large range of compounds or materials, and can be used at several scales, from microanalysis to production processes.[28,29] The liquid-liquid extraction of value-added biomolecules is typically carried out using VOCs – which are often poorly biocompatible media that may lead to the denaturation of enzymes and proteins and other labile biomolecules – due their immiscibility with aqueous media where biomolecules tend to be present.[27,30]

In the 50's, aqueous biphasic systems (ABS) appeared as a more benign liquid-liquid separation process. These systems consist of two immiscible aqueous-rich phases and can be created by the mixture of two polymers, a polymer with a salt or two salts.[31] Liquid-liquid extraction by ABS has been intensively explored and used to separate and purify several biological products,[31–33] and also to recover metal ions, drugs, small organic compounds and inorganic particles from complex mixtures, among others.[34,35] The macroscopic aspect of an ABS is shown in **Figure 1.3**.

Figure 1.3. Macroscopic aspect of an ABS.

The mechanisms which rule the formation of an ABS and the partition behavior of solutes between the phases are truly complex, comprising some attempts based on the hydration enthalpy and entropy net balance to better understand the liquid-liquid demixing phenomenon.[36] Moreover, specific interactions involved in the demixing of the phases are highly dependent on the type of ABS, *i.e.*, the chemical nature of their constituents[37], turning thus the understanding of the involved molecular-level mechanisms even more difficult to be appraised.

In a simple way, the demixing of two aqueous-rich phases, and consequent formation of an ABS, occurs due to the competition of different species for the formation of hydration complexes. ABS composed of two polymers (*e.g.* dextran and poly(ethylene glycol) (PEG)), and a polymer and a salt (*e.g.* PEG and phosphate-, sulfate- or citrate-based salts), have been studied and used for many years.[38,39] When two polymers of different nature are mixed in an aqueous solution, the formation of large aggregates occurs and consequently the polymers tend to separate into two different aqueous phases due to steric exclusion.[36] Similarly, when a high charge density salt is mixed with a polymer, the salt will 'capture' a large amount of water inducing the exclusion of the

polymer to a second aqueous phase, occurring a salting-out effect of the salt over the polymer in aqueous media.[36]

The ternary compositions of ABS can be represented in a triangular (**Figure 1.4 A**) or in an orthogonal phase diagram (**Figure 1.4 B**). In both it is possible to identify the solubility curve, also frequently designated by binodal curve, that separates the monophasic from the biphasic region, and which depends on certain conditions, namely on the pH, temperature and pressure.[40] The knowledge of the biphasic region, initial mixture and individual phases compositions is crucial to any extraction process design and operation, as well as to understand the mechanisms which rule the partition of a solute between the two aqueous phases. For example, in the biphasic region, an initial mixture of composition *E* results in two coexisting phases with the composition represented by two extreme points, *D* and *F*, in the binodal curve. The connection between these two points forms a well-defined line (*DEF*), named tie-line (TL). Different mixture points along the same TL will always result in the formation of two phases with the compositions *D* and *F*, but with different mass or volume ratios (V_R) – *cf.* **Figure 1.4 B**. The difference between the compositions of the two coexisting phases is numerically described by the tie-line length (TLL). Higher TLL values reflect higher differences between the bottom and top phases' compositions and are often used to correlate the partition of solutes between the two phases. The point *C* in the solubility curve is known as the critical point and represents the mixture in which the composition of the coexisting phases became equal and the biphasic system ceases to exist (TLL = 0). The orthogal representation, where water concentration is omitted (the origin of the orthogonal axis represents the pure water), is the most used type in the ABS-related literature, since it allows the use of any units of concentration, while in a triangular representation, the concentration units are restricted to mass and/or molar fraction.

Beyond polymer-polymer and polymer-salt, the most characterized and more conventional ternary systems, other types of ABS can be found in the literature.[41] In **Table 1.1** are summarized some of the different types of ABS previously reported and some examples of their phase-forming compounds, as well as the advantages and drawbacks associated to the application of each ABS type.

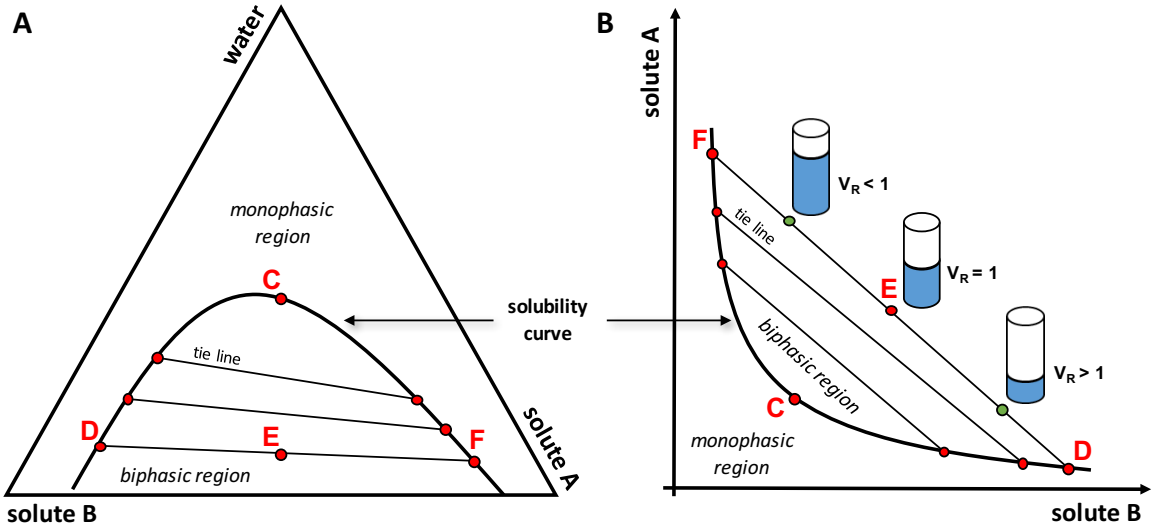

Figure 1.4. Ternary phase diagram for a hypothetical system composed of solute A + solute B + water: **(A)** triangular phase diagram; **(B)** orthogonal phase diagram.

Table 1.1. Examples of different types of ABS: usual phase-forming components, advantages (✓) and drawbacks (×).[41,42]

ABS	Component I	Component II	Advantages and drawbacks
Polymer-polymer	PEG; polyvinilpyrrolidone; ficoll	Dextran; poly(methyl vinyl ether)	✓Easy functionalization; ×high viscosity.
Polymer-salt	PEG	$(NH_4)_2SO_4$; Na_2SO_4; K_2HPO_4/KH_2PO_4; Na_2CO_3	✓Lower viscosity; ✓short phase-separation time; ✓large working range of pH values; ×high ionic strength environment.
Alcohol-salt	Ethanol; 1-propanol; 2-methyl-2-propanol	K_2HPO_4/KH_2PO_4; Na_2SO_4	✓Low cost; ✓low viscosity; ✓rapid two-phase formation; ✓recyclability of the alcohol; ×denaturation of labile biomolecules; ×high volatility of the alcohol.
Micellar	Octylphenol ethoxylate; *n*-decyl tetra(ethylene oxide); dioctanoyl phosphatidylcholine; dlkyltrimethylammonium bromide;	Nonionic and ionic surfactants, salts and/or low-molecular-weight solvents	✓High selectivity of biomolecules through solubilization; ✓recyclability of thermosensitive surfactants; ×high cost.
IL-based	$[C_nC_nim]^+$-, $[N_{nnnn}]^+$-, $[P_{nnnn}]^+$- and $[N_{111(2OH)}]^+$-based ILs	Organic and inorganic salts (K_3PO_4, K_2CO_3, $K_3C_6H_5O_7$,etc.), polymers (PEG 2000 and poly(propylene glycol) (PPG 400)), carbohydrates and amino acids	✓High solvation ability; ✓low viscosity; ✓high chemical and thermal stability; ✓high selectivity; ✓large hydrophobic-hydrophilic range; ×high cost (some ILs)

Due to the extremely low ionic strength of ABS composed of two polymers, this type of systems is preferentially used in the separation, recovery and purification of solutes extremely sensitive to ionic environments.[38,39] On the other hand, the use of salts as substitutes of polymers in ABS presents some advantages in terms of viscosity, separation time and pH working range.[40,43] However, and despite polymer-salt ABS being widely used for the extraction and separation of biomolecules, the high ionic strength of salt-rich phases presents some drawbacks, since it may

leads to the denaturation of extracted proteins and also to environmental concerns.[42] The less extensively studied ABS are those constituted by the mixture of low molecular weight alcohols (*e.g.* ethanol, propanol, among others) and salts.[44] This type of ABS presents some advantages when compared with polymer-based systems, namely the lower cost of its constituents (when compared with polymers), easy recovery and recycling of the system components, lower viscosity and faster separation of their phases. Nevertheless, the presence of alcohols may induce the denaturation of some biomolecules; thus, alcohol-salt ABS have been used mostly on the fractionation of low-molecular-weight products and suitable and less sensitive macromolecules.[45–49]

The number of studies regarding the development and application of micellar ABS has been increasing during the last years. These ABS are constituted by surfactants and present a remarkable ability of keeping the biomolecules native conformations and activities.[50] Micellar ABS are formed by heating a surfactant solution above their cloud-point temperature, resulting in separation into two phases, one micelle-rich phase and one micelle-poor phase.[50–53] Some parameters, such as the surfactant concentration, the temperature, pH and ionic strength can be used to control the size and shape of micelles, allowing also a control over the partition behavior of solutes in these systems.[41] Proteins, viruses, DNA and antibiotics are some examples of the types of molecules extracted with micellar ABS.[50,54-56]

IL-based ABS appeared in 2003, when Rogers and co-workers[57] reported the phase separation of aqueous mixtures of ILs and inorganic salts. Compared to polymer-based ABS, this new type of systems presents additional advantages, such as low viscosity, quick phase separation and high extraction efficiencies and selectivities,[20] contributing to more cost-effective processes if adequate ILs are chosen. Furthermore, pioneering studies have demonstrated the potential of IL-based ABS for the extraction of natural value-added compounds.[25] Since the study, characterization and application of IL-based ABS is the main subject of the present work, these systems are discussed in detail in the following section.

1.3. Ionic-liquid-based aqueous biphasic systems (IL-based ABS)

ABS composed of ILs combine all the advantages of these alternative solvents with the advantages of ABS, making these systems valuable in processes of extraction and separation of a wide range of compounds. After the pioneering work of Rogers and co-workers[57] in 2003, only in 2007 the interest of the scientific community has increased, and studies addressing the potential application of ILs as phase-forming compounds in ABS have appeared.[25]

1.3.1. Mechanisms of formation of IL-based ABS

ABS composed of ILs can be formed when salts, polymers, amino acids or carbohydrates are added to an IL aqueous solution. The capability of these compounds to induce the formation of an ABS is dependent of their nature. With the aim of finding trends able to explain the effect of the chemical nature of the phase-forming components in ABS formation, several authors studied the ability of different ILs – evaluating the cation and anion nature, as well as the alkyl chain length and functional groups effect – and other phase forming species to induce the phases demixing.[25] These effects are nowadays fairly well understood, being possible to know how to design and use the phase-forming components structures to induce ABS formation or to change the phases properties to obtain a better extraction and selectivity performance.

In all IL-based ABS, with the exception of IL-polymer systems, the formation mechanism is dominated by a salting-out effect over the IL. In **Figure 1.5** a schematic representation of the effects associated to the chemical structure of the phase-forming components for IL-salt, IL-amino-acid and IL-carbohydrate systems is presented. In these ABS, the IL is excluded to an IL-rich phase due to the preferential hydration of high charge density salts, amino acids or carbohydrates, which act as salting-out species. ILs are composed of low-symmetry charge-delocalized ions only capable of weak directional intermolecular interactions, and thus they are less prone to be hydrated than the mentioned salting-out inducing species.[25] In fact, the higher the capacity of salting-out species to form hydration complexes, the higher their ability to induce the demixing of the phases and ABS formation.

Studies comprising the inorganic and organic salts effect upon ABS formation show that the salt ions ability follows the Hofmeister series.[25] Since the Hofmeister series effect was traditionally explained based on the ordering of bulk water and ability of the ions to increase or decrease the water structure, the Gibbs free energy of hydration of the ions was used by several authors to explain the observed trends.[46,58–66] However, Shahriari et al.[60], based in a large compilation of systems involving different salts and a common IL, revealed a close correlation between the IL molality of the species necessary for the formation of a specific ABS and the molar entropy of hydration of the ions, and where the Gibbs free energy of hydration presented a poor correlation with the ABS formation ability. Based on this evidence and on previous works[67–69] on the water solubility of ILs, the authors[60] proposed that the IL-based ABS formation is an entropically driven process.

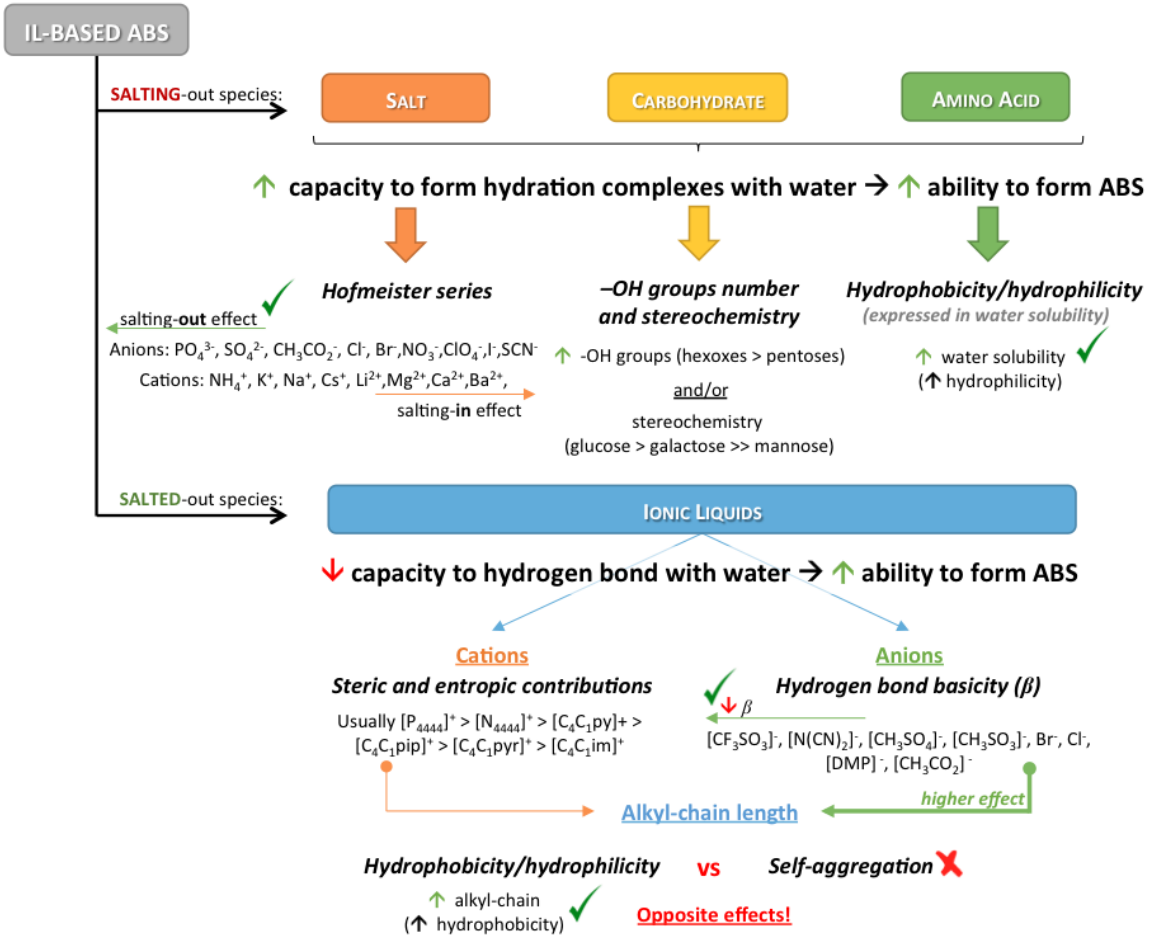

Figure 1.5. Effects of the several phase-forming components in IL-based ABS formation.

Carbohydrates and amino acids are weaker salting-out agents than conventional salts. On an extensive study concerning the effect of carbohydrates structures on ABS formation, Freire et al.[70] showed that hexoses are stronger salting-out agents than pentoses due to their larger number of -OH groups, and thus with a higher capacity to form hydrogen bonds with water. Furthermore, through the study of isomers (such as glucose and fructose), enantiomers (namely, D-(–)-arabinose and L-(+)-arabinose), and epimers – structures with opposite configurations of -OH groups at specific positions, such as D-glucose and D-mannose – the authors[70] concluded that the conformation, the relative position of the hydroxyl groups at C(2) and C(4), and the ratio between the axial and equatorial hydroxyl groups are also crucial factors in the saccharides facility to be hydrated and to induce ABS formation. Thus, the strength of the salting-out effect of carbohydrates is related with both the number of -OH groups and their stereochemistry.

The amino acids ability to induce ABS formation can be related with their hydrophobicity/hydrophilicity, expressed in terms of water solubility.[71] Thus, the higher is the

solubility of an amino acid in water, the greater its capacity to form hydrogen-bonds and consequently to salt-out the IL.

In all the ABS shown in **Figure 1.5**, the IL is the salted-out specie. Thus, the IL chemical structure effect on ABS formation presents an opposite behavior to the salting-out inducing species, *i.e.*, the lower is its capacity to hydrogen bond with water, the higher its ability to induce the formation of a two-phase system. Concerning the effect of the IL anions on ABS formation, Ventura et al.[72] suggested that the IL anions ability to produce ABS inversely correlates with their hydrogen-bond acceptor nature. Since the formation of an ABS is the result of a competition between the salting-out species and the IL ions for the formation of hydration complexes, anions with lower hydrogen bond basicity (β) have a lower ability to create these hydration complexes and, consequently, are more easily salted-out. Several other works supporting this interpretation have been reported.[73–76] Although as a less studied effect, Marrucho and co-workers[77] reported that the increase of the alkyl chain length in ILs anions presents a high effect through the IL hydrophobicity and consequently on the IL aptitude to undergo liquid-liquid demixing. Since the ILs hydration is mainly ruled by the interactions established between the ILs anions and water, the increase of the anions hydrophobicity presents a higher effect on the ILs ability to form ABS. However, in this study,[77] alkyl chains larger than hexyl were not studied, preventing the evaluation of the self-aggregation derived from the IL anion. Although some results suggest that the self-aggregation of anions has a smaller impact on ABS formation[62,78,79] a detailed analysis of this effect is still lacking in literature, although it has been well described for the IL cation.[80]

Concerning the cation core effect for a fixed anion, it is well known that the quaternary $[P_{4444}]^+$- and $[N_{4444}]^+$-based salts present the highest ability to phase separate. The charges, located mostly on the heteroatom, are shielded by four alkyl-chains, which turns more difficult their hydration leading to a higher tendency to be salted-out.[64] In contrast, the nitrogen-based cyclic ILs (imidazolium-, pyrrolidinium-, pyridinium-, and piperidinium-based, *cf*. **Figure 1.2**) present a less shielded charge. It was further reported[61] that 6-sided ring cations, such as pyridinium and piperidinium, are more able to induce ABS than the smaller 5-sided ring imidazolium and pyrrolidinium cations. This trend also correlates with the solubility of these ILs in water.[61] In summary, the influence of the IL cation core on IL-based ABS formation seems to be dominated by steric and entropic contributions.

The influence of the cation alkyl chain length was extensively studied. To evaluate the trends observed in the literature, two opposite effects need to be taken into consideration: i) the increase of the IL hydrophobicity (water solubility decrease) with the increase of the alkyl chain

length, and ii) the ability of ILs with aliphatic chains larger than hexyl to self-aggregate in aqueous solution.[25] As the alkyl chain length of the cation increases, the IL ability to induce ABS formation also increases. However, when self-aggregation starts to occur, a trendshift is observed and the ability to form ABS is reduced.[80]

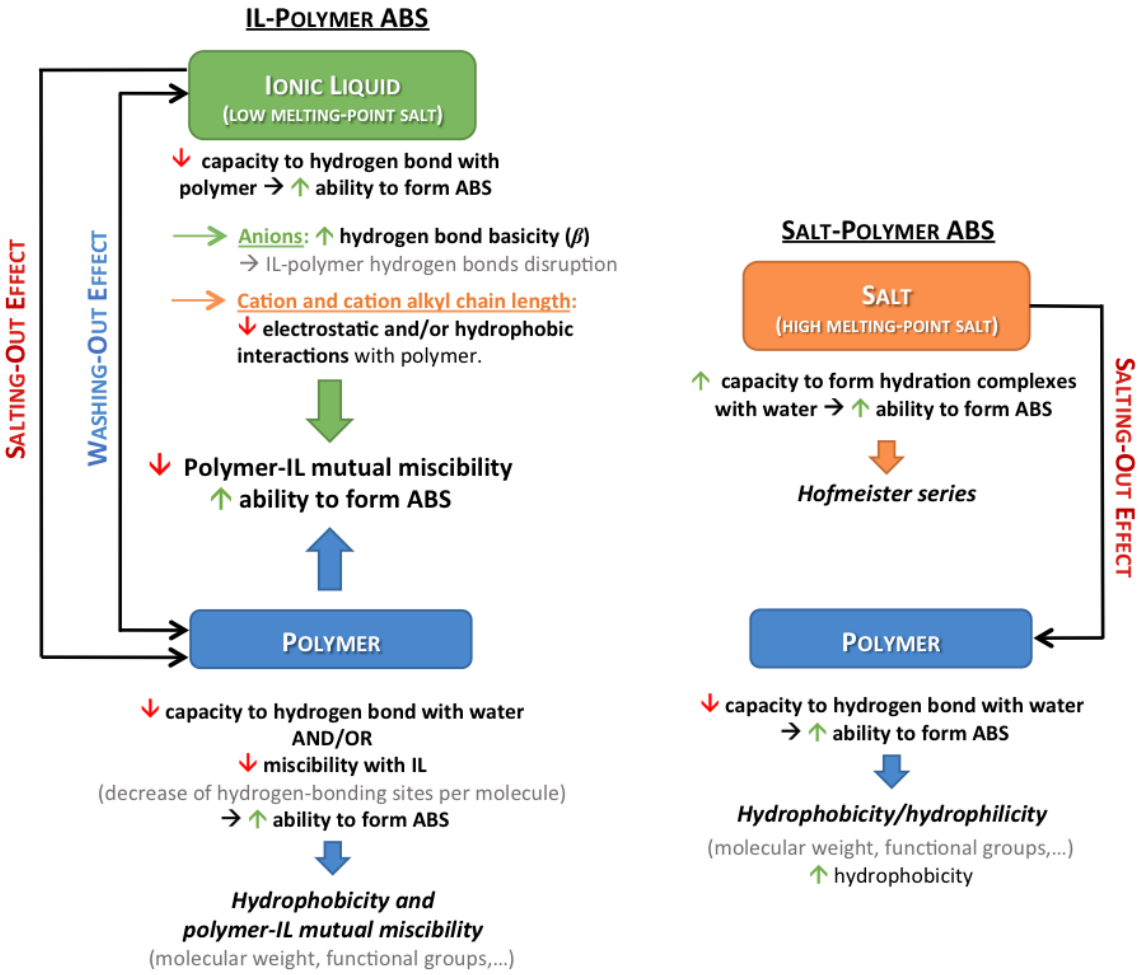

Figure 1.6. The effect of phase-forming components nature in IL-polymer and salt-polymer ABS formation.

Contrarily to the ABS formed by IL and salts, amino acids or carbohydrates, the formation of IL-based ABS with polymers seems to result from more complex mechanisms,[81,82] represented in **Figure 1.6**. As discussed above, since high melting point salts are composed of simple and high charge density ions, they present a high ability to be hydrated and, consequently, in salt-polymer ABS they also act as salting-out agents. However, it was demonstrated[81,82] that when these ions are substituted by more complex and/or organic ions (for example, IL ions), specific interactions are established with the polymer and not just with water, influencing the salting-in/-out effects observed. Coutinho and co-workers[81] were the first to propose that the IL-polymer ABS formation is not only ruled by the ions' ability to form hydration complexes, but also by the interactions that

occur between the IL and the polymer. The authors[81] observed that as the immiscibility between [C_4C_1im]-based ILs and PEG increases, the ability of the IL to form ABS with the polymer also increases. Later, the authors[83,84] complemented this study with molecular dynamics simulations studies, showing that when water is added to a binary mixture of an IL and a polymer, the hydrogen-bonds formed between the two compounds are replaced by more favorable and stronger water-IL anion and water-PEG terminal -OH hydrogen-bonds, inducing the separation and the formation of an ABS, being designated by a washing-out effect.

The polymer-IL mutual miscibility can be tuned to influence the ABS formation, by changing the IL and polymer natures – *cf.* **Figure 1.6**. It was demonstrated that the ILs anion effect is straightly related with their ability to be solvated by water.[81,82] If ILs are composed of anions with high hydrogen bonds basicities, the addition of water to IL-polymer mixtures will result in the destruction of the hydrogen bonds established between the IL and the polymer, and consequently in ABS formation. However, the IL cation influence showed to be more complex and specific interactions (electrostatic and/or hydrophobic) that could affect the ILs solubility in the polymer also need to be taken into consideration.[81,82]

Besides the ternary ABS composed of ILs, polymers and water, Pereira et al.[85] proposed the use of ILs as additives to control the polarity of the phases of conventional polymer-salt ABS, creating novel quaternary systems. Although the addition of a small amount of IL (5 wt %) does not induce significant changes in the phase diagrams of the original PEG 600 + Na_2SO_4 + H_2O ternary system, it was shown to have a significant impact on the tailoring of the extraction ability of these systems for some amino acids.[85] Other authors have also been adopting this methodology to tailor and improve the performance of different types of ABS for the extraction of other biomolecules, such as proteins/enzymes and antioxidants.[86–89]

1.3.2. pH and temperature dependency of IL-based ABS

The control of specific ABS conditions can be of high relevance for the extraction and purification of labile biomolecules, such as proteins. In this context, the effect of pH and temperature in the formation of ABS has been object of numerous publications.[25] Concerning the pH effect in IL-based ABS formation, it has been reported that acidic or neutral pH values are less favorable than alkaline solutions to induce the demixing of the phases.[25] In general, at acidic pH values the ability of the salts to induce phase separation is lower, since salts will be protonated and with a lower salting-out ability.[65,90,91] However, Kurnia et al.[92] showed that the mechanisms associated to the pH dependency of ABS formation is more complex than what was expected. The

authors[92] reported that the IL-based ABS formation is dominated by the ability of the higher valency, and completely dissociated salting-out ions to interact with water to form the hydration complexes inducing thus the phases demixing. This ability is connected to the speciation of the salts in aqueous solution, in particular with their pH dependency. The understanding of the speciation of the salts and its influence on ABS formation allowed explaining why some salts ions work better at alkaline pH, while others present better performances at acidic conditions. Thus, the tailoring of IL-based ABS phase diagrams can be adequately carried out if the speciation and the various species and their relative concentrations in solution are taken into consideration.

The temperature dependency of IL-based ABS is related with its impact upon the ABS components interactions with water. In ternary systems composed of IL + salt + water, IL + amino acid + water and IL + carbohydrate + water an increase of temperature reduces the biphasic region, *i.e.*, a large amount of both solutes is necessary to undergo phase separation – *cf.* **Figure 1.7 A**.[70,93–95] At higher temperatures, ILs and water are more soluble (upper critical solution temperature (UCST)-type phase behavior), decreasing thus their ability to form ABS.[93-95] On the other hand, IL-polymer binary mixtures typically follow a lower critical solution temperature (LCST)-type phase behavior, that is transposed to the respective ABS (**Figure 1.7 B**).[81,96,97] For PEG-salt ABS it was shown that the temperature influence is dominated by the hydrogen-bonding interactions between PEG and water.[82] Binary solutions of PEG and water present a LCST-type behavior, with the biphasic region increasing with an increase in temperature.[98] Based on these temperature dependencies, Kodama et al.[99] further showed that an increase in temperature is favorable for the creation of IL-polymer ABS since the hydrogen bonding between polyethers, such as PPG and PEG, and imidazolium cations breaks at higher temperatures, resulting thus in an easier phase separation of the mixture.

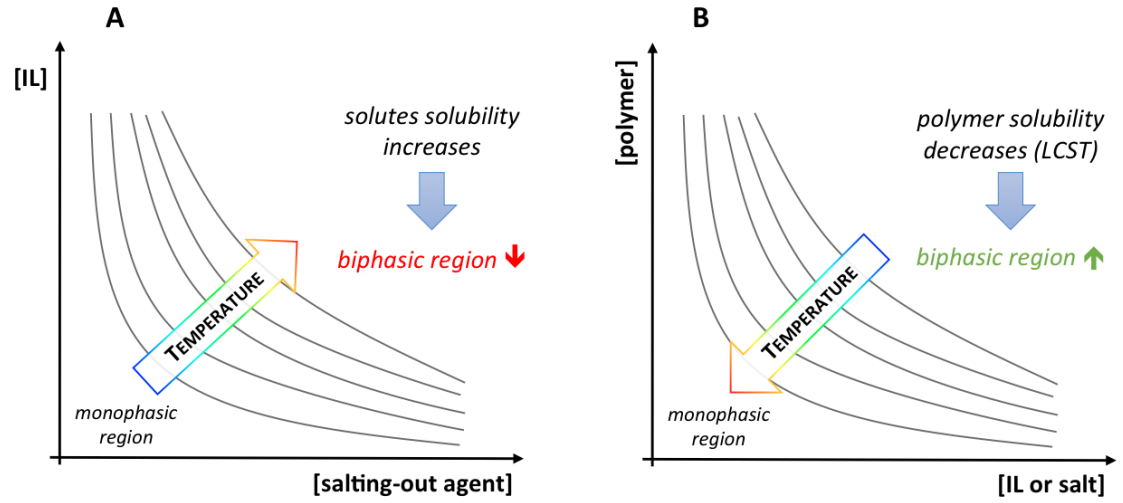

Figure 1.7. Temperature effect on ABS composed of **(A)** IL + salt/amino acid/carbohydrate + water and **(B)** IL/salt + polymer + water.

Despite the studied pH and temperature effects on IL-based ABS formation, the use of these dependencies for the development of tailored and cost-effective extraction and separation processes has not yet attracted a large attention from researchers. The ability to induce phase transitions between homogeneous and biphasic liquid-liquid systems, at pre-defined and suitable operating temperatures, is however of crucial relevance in the design of separation processes. The pH and temperature dependency of IL-based ABS could be used to switch between monophasic and biphasic regions and create reversible phase transitions. In this context, the thermoreversible behavior of IL-based ABS and their potential applications are object of study in this work.

1.3.3. Physicochemical characterization of IL-based ABS

Industrial applications of ABS have been plagued by a poor understanding of the mechanisms which rule their formation and of the partition of biomolecules between their phases. For this purpose, the physicochemical characterization of the ABS coexisting phases is of high relevance. In addition to the phase diagrams, thermophysical properties, such as density and viscosity, are pertinent for the design of IL-based ABS at a large scale. Low viscosities of the coexisting phases enhance mass transfer and reduce energy consumption, while densities are important for equipment design. However, and although a large number of publications reporting the phase diagrams of IL-based ABS can be found,[25] few of them report on the physical properties of their coexisting phases.[58,70,100,101]

Concerning the distribution of compounds in ABS, it seems clear that this is ruled by differences in solute-solvent interactions in the coexisting phases. There are not many approaches for the characterization of the differences in the solvation ability between the ABS phases. Several authors have been trying to assess their relative polarity by the measurement of the Gibbs free energy of transfer of a methylene group between the phases[57,59,102–107] or by the determination of the Kamlet-Taft solvatochromic parameters[104,108–114] of the coexisting phases – dipolarity/polarizability (π^*), hydrogen bond donor acidity (α), and hydrogen bond acceptor basicity (β) – in polymer-polymer and polymer-salt ABS. Unfortunately, there has been no attempts concerning the determination of these parameters in IL-based ABS.

Due to the lack of literature regarding the physicochemical characterization of IL-based ABS, this is a focus of the present work. The evaluation of the density and viscosity, as well as the determination of the Gibbs free energy of methylene transfer and Kamlet-Taft solvatochromic parameters of the coexisting phases in ABS composed of ILs, were considered.

1.3.4. Applications of IL-based ABS

Extraction processes. Several works have been published reporting to the application of IL-based ABS in the extraction, separation and purification of a wide range of solutes, from simple alcohols to complex enzymes.[25] Usually, the mechanisms which rule the partition of molecules between the coexisting phases are very complex, and controlled by solute-solvent interactions, such as van der Waals, hydrogen-bonding, and electrostatic forces. Steric and conformation effects may also play a role. These interactions are different in each phase resulting in the selective partition of the target-compound. The partition behavior depends thus on the coexisting phases and molecules properties and can be controlled in different ways. It is possible to control the target-compound affinity for one of the phases by: i) changing the nature of the system components; ii) changing the composition of the system by manipulation of the components concentration; and iii) by inserting additional co-solvents, anti-solvents or amphiphilic structures into the system.[25]

The partition coefficient (K) is frequently used as a measure of the IL-based ABS ability to extract a specific molecule to one of the phases. It is defined by the ratio of the concentration of the solute/molecule in the IL-rich phase to that in phase II (salt-, amino acid-, carbohydrate- or polymer-rich phase), according to **Equation (1.1)**:

$$K = \frac{[solute]_{IL}}{[solute]_{phase\ II}} \qquad \textbf{(1.1)}$$

The extraction efficiency ($EE\%$) is also used in the literature to determine the percentage ratio between the amount of a specific solute/molecule partitioned to the IL-rich phase and that present in the mixture – *cf.* **Equation (1.2)**

$$EE\% = \frac{w_{solute}^{IL}}{w_{solute}^{IL} + w_{solute}^{phase\ II}} \times 100 \qquad \textbf{(1.2)}$$

Amongst the compounds studied in liquid-liquid ABS extraction systems, it is possible to identify alkaloids (caffeine, nicotine, theophylline, etc.), pharmaceutical drugs (penicillin, morphine, papaverine, tetracycline, etc.), amino acids (L-tryptophan, L-phenylalanine, L-tyrosine, among others), proteins/enzymes (BSA, trypsin, cytochrome C, CaLC and CaLB, etc.), steroid hormones (testosterone and epitestosterone), short chain alcohols (from methanol to hexanol), aromatic and phenolic compounds (gallic acid, β-carotene, rhodamine 6G, etc.) and metals (Cr(IV), Cr(III) and Cd^{2+}).[25] When compared to conventional ABS, namely polymer-polymer and salt-polymer, IL-based ABS often present better performances, with partition coefficients and extraction efficiencies considerably higher, as well as a higher selectivity.

Pre-concentration of samples. In 2012 a new potential application of IL-based ABS was proposed. Freire and co-workers[115] proved the possibility of using ABS composed of ILs and inorganic salts as a pre-concentration step in the analysis of bisphenol A (BPA), an endocrine disruptor, in human fluids. These compounds present several drawbacks to the environment and human health; however, their low levels in biological fluids or in the soil, air and aqueous environments, make it difficult to detect them via conventional techniques, preventing thus their correct monitoring. Authors[115] showed that IL-based ABS could be used to successfully concentrate BPA up to 100-fold from human fluid samples, allowing its further identification and quantification by conventional analytical techniques, such as high performance liquid chromatography (HPLC).

Others endocrine disruptors are present in the environment at considerably lower concentrations than BPA. After showing the potential application of IL-based ABS as a pre-concentration step, it is proposed here to go further and to develop a system able to completely extract and concentrate up to 1000-fold the 17α-ethinylestradiol, EE2, the most potent estrogen found in sewage effluents.[116] The concentration of EE2 from ng·L^{-1} to µg·L^{-1} in waste water samples allows a simpler, yet correct, monitoring, and the evaluation of its environmental impact.

Recovery of hydrophilic ILs from aqueous solutions. Despite the ILs field movement towards more benign ILs, their environmental impact is still an important issue and their recovery or

removal from waste streams is very important when dealing with their application at large scales. Some authors[57,58,63] showed that the intrinsic nature of IL-based ABS makes of them a great option for the recovery and also to concentrate hydrophilic ILs from aqueous solutions aiming at their further recycling. Wu et al.[95,117] reported that 60 to 75 % of imidazolium-based ILs could be recovered through the formation of IL-carbohydrates ABS. Other authors[63,66] proposed the use of inorganic and organic salts, and considerably largest recoveries were attained (> 98 %) even with the addition of relatively small amounts of salts. The best results were reported by Neves et al.[58] using $Al_2(SO_4)_3$, a salt commonly applied in water treatment processes as a coagulant. The authors[58] reached IL recovery efficiencies ranging between 96 and 100 %, with the addition of salt amounts ranging between 2 to 16 %. These works show the potential of IL-based ABS in the recovery or removal of ILs from aqueous media, minimizing potential contamination and further promoting the industrial application of this alternative class of solvents.

1.3.5. IL-based ABS scale-up: economic and environmental analyses

ABS-based separations are attractive for industrial applications due to the easy scale-up and undemanding equipment required to their implementation – in some cases it is even possible the use of conventional extraction equipment already installed in the chemical plant.[118] However, and considering ABS composed of ILs, despite the large number of works highlighting their potential to be scaled-up, no relevant studies were yet reported with this purpose, being this normally attributed to economic and environmental factors, such as, the ILs' cost, toxicity, persistence and bioaccumulation.[6,119–125]

The lack of volatility in ILs is a major advance in the reduction of an environmental footprint. Nevertheless, this negligible volatile nature afforded by ILs also makes more complex the isolation and recovery of the compounds extracted/purified with IL-based ABS. Trying to overcome this issue some alternatives were already proposed,[126] as will be discussed below. On the other hand, a complete life cycle assessment of ILs' processes is crucial to support their suitability from a "greener" and sustainable perspective. For that purpose, the recovery and reusability of phase-forming components, specially the IL – the most expensive solute – are vital issues to minimize the cost and environmental footprint of IL-based processes.

The high production costs associated to ILs recurrently create a large controversy on the viability of their application at an industrial scale.[127] It is well known that the price of ILs is mainly dependent on the starting materials needed for their production and a rough estimation of their relative prices was already carried out and is presented in **Figure 1.8**. **A**.[127,128] The industrial price

of some commodities and specialty chemicals, along with the estimated cost of $[C_nC_1im]^+$- and ammonium-based ILs is presented in **Figure 1.8**. **B**.[129–133] Quaternary ammonium- (including cholinium-) based ILs are less expensive than their imidazolium-based counterparts and surely deserve to be further investigated. On the other hand, ILs composed of fluorinated anions are more expensive and should be substituted by carboxylate-, Cl- and Br-based ones.

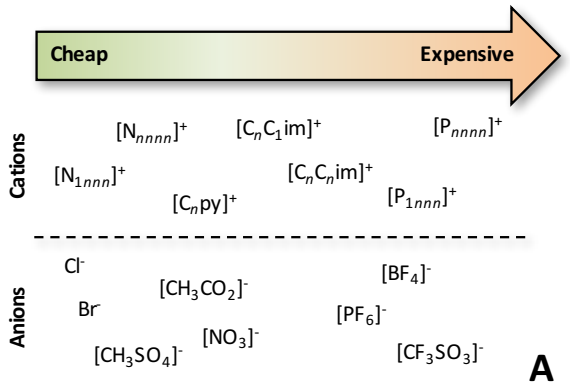

Organic Solvents / $US			Ionic Liquids / $US		
toluene	0.74 - 1.05	/L	$[C_nC_1im]$-based	14-34	/kg
ethanol	0.82 - 0.98	/L	$[C_1im][HSO_4]$	2.96-5.88	/kg
methanol	0.25 - 0.54	/L	$[N_{2220}][HSO_4]$	1.24	/kg
acetonitrile	1.06 - 1.12	/kg	$[N_{111(2OH)}]Cl$	1.21	/kg
n-butyl acetate	1.48 - 1.59	/kg	$[N_{(10)(10)11}]Cl$	8.71	/kg
chloroform	0.53 - 1.04	/kg	$[N_{11(13)(C7H7)}]Cl$	5.28	/kg
ethylene glycols	1.43	/kg	$[N_{1(2OH)(TH)(TH)}][CH_3SO_4]$	2.27	/kg
n-methyl pyrrolidone	4.08 - 4.19	/kg			
sulfolane	~3.7	/kg			

B

Figure 1.8. (A) Schematic illustration of the relative prices of ILs estimated based on the cost of the starting materials used in their synthesis.[127] **(B)** Industrial production price[129–133] of some organic solvents and ILs: $[C_nC_1im]^+$ – 1-alkyl-3-methylimidazolium cation; $[C_1im][HSO_4]$ – 1-methylimidazolium hydrogensulfate; $[N_{2220}][HSO_4]$ – triethylammonium hydrogensulfate; $[N_{111(2OH)}]Cl$ – cholinium chloride; $[N_{(10)(10)11}]Cl$ – didecyldimethylammonium chloride; $[N_{11(13)(C7H7)}]Cl$ – cocoalkonium chloride; $[N_{1(2OH)(TH)(TH)}][CH_3SO_4]$ – dihydrogenated tallowoylethyl hydroxyethylmonium methylsulfate.

Even if researchers optimize production processes for ILs, the price of an IL will be not comparable to that of a commodity solvent, but it would rather be comparable to specialty chemicals, class to which they would belong. Nevertheless, and as already mentioned, it should be remarked that the ILs field is slowly moving away from imidazolium-based ILs into an era of cheaper and more environmentally benign ILs, such as carboxylate-, amino acid-, carbohydrate- and cholinium-based ILs. Their raw materials are cheaper and can be obtained from renewable sources, and more work should be devoted on the study of these alternatives. Other aspects should also be considered regarding the advantages of ILs over common VOCs. It is well-known that the use of organic solvents has been restricted and strongly regulated by new legislations.[134] Nowadays, the costs connected to organic solvents applications should also cover the costs associated with, for instance, personal protective equipment, emission control hardware and monitoring equipment. Thus, non-volatile compounds, such as ILs, present some advantages and should not be discarded based only on the price of the solvent.

As stated before, the recovery and reusability of the phase-forming components of IL-based ABS are fundamental aspects to support the economic viability and to minimize the environmental footprint of these separation processes. However, the number of methodologies purposed to isolate the target compounds and recover and recycle the systems' phases is still scarce. Different types of strategies, such as the evaporation of water or other organic solvents used in the isolation of the target compounds,[135] their precipitation by anti-solvents,[136-138] and even the application of membrane processes,[139] have been reported. For instance, Almeida et al.[136] proposed a complete strategy to remove active pharmaceutical ingredients from aqueous media using IL-based ABS. These compounds are discarded into aqueous systems and are responsible for serious human health problems. Authors[136] reported extraction efficiencies of quinolones to the IL-rich phase up to 98 %, and proposed a complete methodology to recycle and reuse the system phases. As schematically presented in **Figure 1.9**, after the extraction of fluoroquinolones to the IL-rich phase, their recovery is attained by the addition of K_3PO_4 to this phase, which induces the precipitation of the target compounds through the modification of the system's pH and its strong salting-out effect. Finally, it was induced the formation of the crystal $AlPO_4$ by the addition of $Al_2(SO_4)_3$ to the IL-rich phase + K_3PO_4 mixture, allowing the regeneration of the IL-rich phase. Furthermore, the authors[136] showed that the capacity of, for instance, 1-ethyl-3-methylimidazolium trifluoromethanesulfonate ($[C_2C_1im][CF_3SO_3]$) to remove fluoroquinolones from water and concentrate them in the IL-rich phase is maintained during a total of four cycles, with low contamination of the phases and no significant losses of IL.

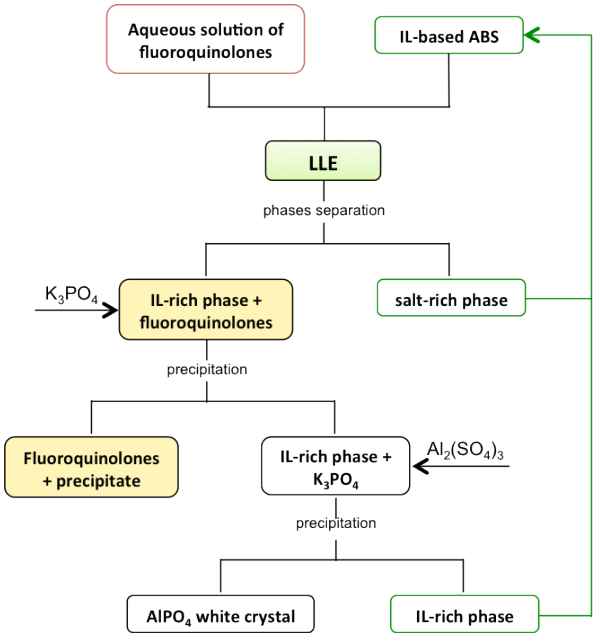

Figure 1.9. IL-based ABS application in the removal of fluoroquinolones.[136]

Recently, Ventura and co-workers[137] developed a sustainable process based on ABS composed of ILs, for the recovery of valuable drugs from pharmaceutical wastes. In this study, the authors' main goal was to recover the antidepressant drug amitriptyline hydrochloride, by its separation from the excipients present in the original formulation. The experimental study started with the optimization of the ABS used in the purification of the antidepressant, evaluating the

effect of the type of IL, the pH of the system and the composition of the mixture. This optimization allowed to extract and concentrate the amitriptyline in the IL-rich phase, with extraction efficiencies ranging between 93 and 100 %. Having demonstrated the potential of IL-based ABS for the extraction and concentration of the target molecule, the authors[137] proposed a three-step process, which is represented in **Figure 1.10**. The process starts with a solid-liquid extraction of the antidepressant from ADT 25 pills, using water as the extractive solvent. The obtained extract was centrifuged and filtrated to remove the insoluble excipients, and then an IL-based ABS was prepared using the antidepressant aqueous solution as the aqueous matrix of the system. After the drug extraction to the IL-rich phase, the molecule was recovered by the addition of an aqueous solution of KOH. The modification of the solution pH results in the decrease of the amitriptyline solubility and, consequently, its precipitation. Finally, the authors[137] proposed that both ABS phases could be recycled. For example, the IL-rich phase can be neutralized by the addition of phosphoric acid, and the high molecular weight excipients present in the salt-rich phase can be removed through an ultrafiltration step.

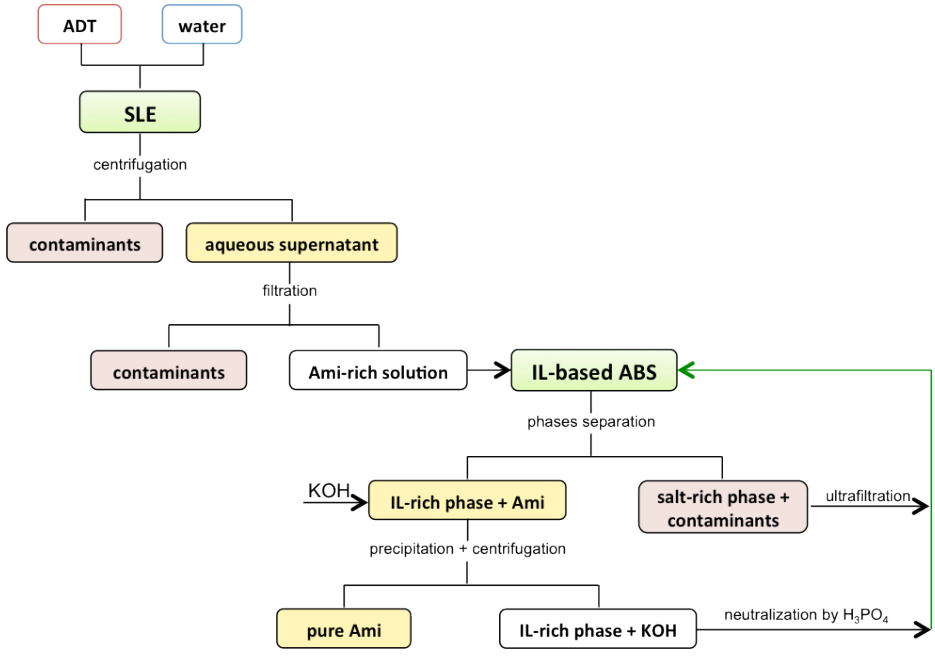

Figure 1.10. Integrated process developed for the recovery of amitriptyline (Ami) from pharmaceutical residuals.[137]

Among others, the results reported by Almeida et al[136] and Ventura and co-workers[137] show that the recovered IL or IL-rich phases can be regenerated and reintroduced in new cycles of extraction without losing the IL and target-compounds integrity, and the systems extraction ability. Nevertheless, the number of works concerning this topic is still scarce and there is a need for more studies where the purification of other types of (bio)molecules from different kinds of

relevant raw materials are integrated with the study of ILs and phase-forming components recyclability.

1.4. Scope and objectives

As stated before, the study and application of ILs as phase-forming components of ABS has been widely investigated during the past decade.[25] Several authors focused on a better understanding of the mechanisms which rule the IL-based ABS formation and the partition of solutes between the coexisting phases, and nowadays is possible to state with a high confidence level that the scientific community already has a good understanding of the basic principles governing the IL-based ABS formation and their properties tuning. Nevertheless, there are still several gaps in the knowledge of this type of systems and several possibilities of research on IL-based ABS. In particular, the development of novel, more efficient, target-specific and benign systems, as well as the study of new applications for these ABS, is of high relevance. In this context, the development of this thesis was according to three main purposes: **i) DEVELOPMENT** of new, tailored and better performing systems; **ii) CHARACTERIZATION** of the properties of the coexisting phases of IL-based ABS and **UNDERSTANDING** of the mechanisms which rule the formation of these systems and the partition of solutes; and **iii)** study on new potential **APPLICATIONS** of IL-based ABS. To a better understanding of this thesis organization, a schematic representation of its layout is given in **Figure 1.11.**

The ability to induce reversible phase transitions between homogeneous solutions and biphasic liquid-liquid systems, at pre-defined and suitable operating temperatures, is of crucial relevance in the design of separation processes. Since IL-based ABS have demonstrated superior performance as alternative extraction platforms, chapter 2 (**chapter 2.1**) starts with the study of the thermoreversible behavior of ABS by the use of protic ILs. Beyond their characterization, the temperature-induced phase transition was evaluated in the extraction of two proteins, namely azocasein and cytochrome C. In the second study (**chapter 2.2**), a self-buffering and more biocompatible liquid-liquid extraction system was developed by the application of Good's buffers – inert biological buffers commonly used in biochemical and biological studies – as phase-forming components of IL-based ABS. Furthermore, their application in the extraction of amino acids (L-phenylalanine and L-tryptophan) was also ascertained. In **chapter 2.3**, mixtures of two ILs with a common cation and different anions were investigated aiming the manipulation of the phases' polarities and ABS ability to undergo liquid-liquid demixing. Considering that in an IL-salt ABS the IL is salted-out by the salt, in a salt-polymer ABS the salt induces the salting-out of the polymer,

and in a polymer-IL ABS the components are washed-out by water, it was also evaluated the possibility of creating multiphase aqueous systems by mixing ILs, salts and polymers in aqueous media – fourth section of chapter 2 (**chapter 2.4**). Finally, on **chapter 2.5**, deep eutectic solvents (DES)-based ABS are addressed and the mechanisms associated to their phases demixing, as well as, the DES stability in aqueous solutions, were investigated. The use of DES to form ABS was recently proposed in the literature[140,141] and this study aims at comparing the performance of DES-based ABS with the corresponding IL-based ABS, and to address the critical question of whether DES-based ABS are in fact ternary or quaternary mixtures, *i.e.* whether the DES integrity is kept in aqueous solution. All these works not only comprise the study of new types of ABS but also attempted the exploitation of their potential application to the extraction and separation of a variety of solutes, from alkaloids to textile dyes.

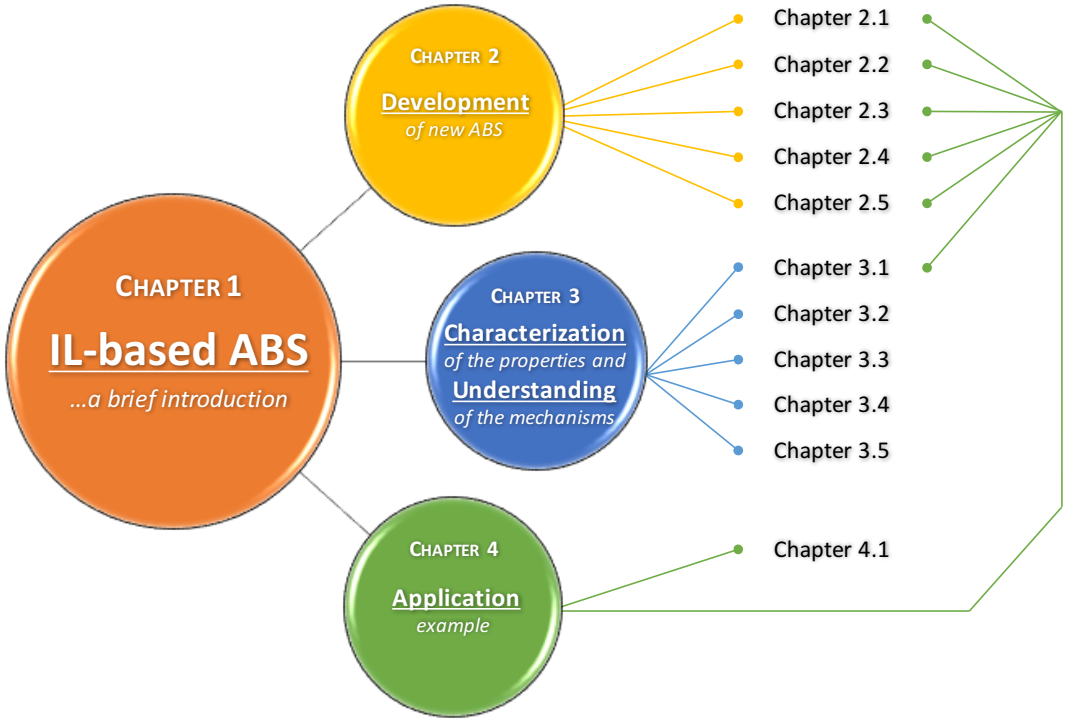

Figure 1.11. Current thesis layout.

One of the greatest barriers to the application of IL-based ABS at industrial level is the difficulty to predict their behavior without the need of an extensive characterization of their phase diagrams and partition behavior. The process design will eventually require the ability to model ABS using an equation of state (EoS) or a gE model so that a process can be simulated into a process simulator. For that reason, the Perturbed-Chain Statistical Associating Fluid Theory (PC-SAFT) was here (**chapter 3.1**) used to describe the vapor-liquid equilibria (VLE) of binary systems composed of water and imidazolium-based ILs as a first step towards the description of ABS. The

PC-SAFT EoS was evaluated for the estimation of water activity coefficients at infinite dilution in ILs. Furthermore, its potential application as a tool to predict the liquid-liquid equilibrium (LLE) behavior of ternary mixtures composed of IL, salt and water, based on IL/water binary mixtures experimental data, was also shown. Coutinho and co-workers[72–74] had previously suggested the existence of a relationship between the hydrogen bond acceptor basicity (β) of ILs and their ability to form ABS, but failed to quantify it. Thus, in **chapter 3.2,** this previously observed relationship was studied and the development of correlations that could be used to predict the IL-based ABS formation was attempted. Since the IL-based ABS phase diagrams and the physical properties of the coexisting phases are of relevance when envisaging their large-scale application, **chapter 3.3** is focused in the characterization of ABS composed of different ILs and acetate-based organic salts by reporting the experimental measurements of density and viscosity of the coexisting phases at several compositions and temperatures. Although highly relevant to an adequate selection of solvents for a given application, the determination of the hydrogen-bond donor acidity (α) of aqueous solutions of ILs is a difficult task due to the poor solubility of the common probes in aqueous media. In **chapter 3.4,** a new probe, pyridine-*N*-oxide, was investigated in the determination of hydrogen-bond acidity of both neat ILs and their aqueous solutions. The suitability of these values to predict the ability of ILs to form ABS was also evaluated. Since a deeper understanding on the mechanisms which rule the partition of the biomolecules between the coexisting phases is still missing, in the fifth part of chapter 3 (**chapter 3.5**), the determination of the relative hydrophobicity, as well as of the identification of new probes and approaches to assess the solvatochromic parameters (solvent dipolarity/polarizability, π^*, solvent hydrogen-bond donor acidity, α, and solvent hydrogen-bond acceptor basicity, β) of the coexisting phases of ABS composed of ILs and inorganic salts was carried out. The ILs investigated were selected to determine the IL anion impact on the relative hydrophobicities and solvatochromic properties displayed by IL-based ABS.

Potential applications of IL-based ABS were considered in more than half of the studies that constitute this thesis, as described above. The extraction of different types of molecules, namely dyes, alkaloids, amino acids and proteins by IL-based ABS was evaluated in several works (*cf.* **Figure 1.11**). One work here reported is focused however on an additional application – the use of these systems as a pre-concentration method for analytical purposes. As a main example of their applicability, a one-step extraction and concentration method based on IL-based ABS for estrogens, namely ethinylestradiol (EE2), was developed aiming an adequate monitoring of wastewaters, shown in chapter 4 (**chapter 4.1**).

In summary, the current thesis represents a deep study on IL-based ABS, ranging from a better understanding of the two-phase formation underlying mechanisms to the development of novel and more efficient systems. Furthermore, since the implementation of IL-based ABS depends on the ability to design these systems to a specific application, new methodologies that allow to predict the IL-based ABS behavior were also developed.

1.5. References

(1) P. T. Anastas and M. M. Kirchhoff, *Acc. Chem. Res.*, 2002, **35**, 686–694;
(2) C. Capello, U. Fischer and K. Hungerbühler, *Green Chem.*, 2007, **9**, 927–934;
(3) K. R. Seddon, *J. Chem. Technol. Biotechnol.*, 1997, **68**, 351–356;
(4) P. Wasserscheid and T. Welton, Eds., *Ionic Liquids in Synthesis*, Wiley-VCH Verlag GmbH & Co. KGaA, Weinheim, Germany, 2007;
(5) M. J. Earle and K. R. Seddon, *Pure Appl. Chem.*, 2000, **72**, 1391–1398;
(6) J. Ranke, S. Stolte, R. Störmann, J. Arning and B. Jastorff, *Chem. Rev.*, 2007, **107**, 2183–2206;
(7) T. Welton, *Chem. Rev.*, 1999, **99**, 2071–2084;
(8) P. Walden, *Bull. Russ. Acad. Sci.*, 1914, **8**, 405–422;
(9) F. H. Hurley, *Electrodeposition of Aluminium*, United States Pat, 2446331, 1948;
(10) T. P. Wier and F. H. Hurley, *Electrodeposition of Aluminium*, United States Pat, 2446349, 1948;
(11) C. Graenacher, *Cellulose solution*, United States Pat, 1943176, 1934;
(12) N. V. Plechkova and K. R. Seddon, *Chem. Soc. Rev.*, 2008, **37**, 123–150;
(13) C. R. Allen, P. L. Richard, A. J. Ward, L. G. A. van de Water, A. F. Masters and T. Maschmeyer, *Tetrahedron Lett.*, 2006, **47**, 7367–7370;
(14) K. Fukumoto, M. Yoshizawa and H. Ohno, *J. Am. Chem. Soc.*, 2005, **127**, 2398–2399;
(15) G. Tao, L. He, W. Liu, L. Xu, W. Xiong, T. Wang and Y. Kou, *Green Chem.*, 2006, **8**, 639–646;
(16) S. P. M. Ventura, M. Gurbisz, M. Ghavre, F. M. M. Ferreira, F. Gonçalves, I. Beadham, B. Quilty, J. A. P. Coutinho and N. Gathergood, *ACS Sustain. Chem. Eng.*, 2013, **1**, 393–402;
(17) D.-J. Tao, Z. Cheng, F.-F. Chen, Z.-M. Li, N. Hu and X.-S. Chen, *J. Chem. Eng. Data*, 2013, **58**, 1542–1548;
(18) D. Coleman and N. Gathergood, *Chem. Soc. Rev.*, 2010, **39**, 600–637;
(19) L. M. N. B. F. Santos, J. N. Canongia Lopes, J. A. P. Coutinho, J. M. S. S. Esperança, L. R. Gomes, I. M. Marrucho and L. P. N. Rebelo, *J. Am. Chem. Soc.*, 2007, **129**, 284–285;
(20) R. D. Rogers and K. R. Seddon, *Science*, 2003, **302**, 792–793;
(21) M. J. Earle, J. M. S. S. Esperança, M. A. Gilea, J. N. Canongia Lopes, L. P. N. Rebelo, J. W. Magee, K. R. Seddon and J. A. Widegren, *Nature*, 2006, **439**, 831–834;
(22) J. G. Huddleston, H. D. Willauer, R. P. Swatloski, A. E. Visser and R. D. Rogers, *Chem. Commun.*, 1998, 1765–1766;
(23) A. E. Visser, R. P. Swatloski and R. D. Rogers, *Green Chem.*, 2000, **2**, 1–4;
(24) R. P. Swatloski, S. K. Spear, J. D. Holbrey and R. D. Rogers, *J. Am. Chem. Soc.*, 2002, **124**, 4974–4975;
(25) M. G. Freire, A. F. M. Cláudio, J. M. M. Araújo, J. A. P. Coutinho, I. M. Marrucho, J. N. C. Lopes and L. P. N. Rebelo, *Chem. Soc. Rev.*, 2012, **41**, 4966–4995;
(26) S. P. M. Ventura, L. D. F. Santos, J. A. Saraiva and J. A. P. Coutinho, *Green Chem.*, 2012, **14**, 1620–1625;
(27) M. Martínez-Aragón, S. Burghoff, E. L. V Goetheer and A. B. de Haan, *Sep. Purif. Technol.*, 2009, **65**, 65–72;

(28) V. S. Kislik, *Solvent Extraction: Classical and Novel Approaches*, Elsevier, 1st edn., 2012;
(29) F. W. Fifield and D. Kealey, *Principles and practice of analytical chemistry*, Wiley-BlackwellScience, 5th edn., 2000;
(30) J. Rydberg, M. Cox, C. Musikas and G. R. Choppin, *Principles and Practices of Solvent Extraction*, CRC Press, 2nd edn., 2004;
(31) P. Å. Albertsson, *Nature*, 1958, **182**, 709–711;
(32) B. Zavlasky, *Aqueous Two-Phase Partitioning: Physical Chemistry and Bioanalytical Applications*, M. Dekker, New York, 1994;
(33) H. Walter, D. E. Brooks and D. Fisher, Eds., *Partitioning in Aqueous Two-Phase System*, Academic Press, 1985;
(34) H. D. Willauer, J. G. Huddleston and R. D. Rogers, *Ind. Eng. Chem. Res.*, 2002, **41**, 2591–2601;
(35) R. D. Rogers, A. H. Bond, S. T. Griffin and E. Philip Horwitz, *Solvent Extr. Ion Exch.*, 1996, **14**, 919–946;
(36) J. A. Asenjo and B. A. Andrews, *J. Chromatogr. A*, 2011, **1218**, 8826–8835;
(37) H. Cabezas, *J. Chromatogr. B Biomed. Sci. Appl.*, 1996, **680**, 3–30;
(38) P. Å. Albertsson, *Partition of cell particles and macromolecules*, Wiley, New York, 1986;
(39) P. Å. Albertsson, *Biochem. Pharmacol.*, 1961, **5**, 351–358;
(40) R. Hatti-Kaul, *Aqueous Two-Phase Systems: Methods and Protocols*, Humana Press, New Jersey, 2000, vol. 11;
(41) J. Benavides, M. Rito-Palomares and J. A. Asenjo, in *Comprehensive Biotechnology*, Academic Press, 2011, pp. 697–713;
(42) P.-L. Show, T.-C. Ling, J. C.-W. Lan, B.-T. Tey, R. N. Ramanan, S.-T. Yong and C.-W. Ooi, *Curr. Org. Chem.*, 2015, **19**, 19–29;
(43) M. Rito-Palomares, *J. Chromatogr. B*, 2004, **807**, 3–11;
(44) A. Greve and M.-R. Kula, *Fluid Phase Equilib.*, 1991, **62**, 53–63;
(45) B. Jiang, Z.-G. Li, J.-Y. Dai, D.-J. Zhang and Z.-L. Xiu, *Process Biochem.*, 2009, **44**, 112–117;
(46) Z. Li, B. Jiang, D. Zhang and Z. Xiu, *Sep. Purif. Technol.*, 2009, **66**, 472–478;
(47) W. Zhi and Q. Deng, *J. Chromatogr. A*, 2006, **1116**, 149–152;
(48) T. Tianwei, H. Qing and L. Qiang, *Biotechnol. Lett.*, 2002, **24**, 1417–1420;
(49) A. Louwrier, *Biotechnol. Tech.*, 1998, **12**, 363–365;
(50) C. Liu, D. T. Kamei, J. A. King, D. I. Wang and D. Blankschtein, *J. Chromatogr. B Biomed. Sci. Appl.*, 1998, **711**, 127–138;
(51) C. L. Liu, Y. J. Nikas and D. Blankschtein, *Biotechnol Bioeng.*, 1996, **52**, 185–192;
(52) C. O. Rangel-Yagui, A. Pessoa-Jr and D. Blankschtein, *Brazilian J. Chem. Eng.*, 2004, **21**, 531–544;
(53) H. Tani, T. Kamidate and H. Watanabe, *Anal. Sci.*, 1998, **14**, 875–888;
(54) C. Bordier, *J. Biol. Chem.*, 1981, **256**, 1604–1607;
(55) F. Mashayekhi, A. S. Meyer, S. A. Shiigi, V. Nguyen and D. T. Kamei, *Biotechnol. Bioeng.*, 2009, **102**, 1613–1623;
(56) V. C. Santos, F. A. Hasmann, A. Converti and A. Pessoa, *Biochem. Eng. J.*, 2011, **56**, 75–83;
(57) K. E. Gutowski, G. A. Broker, H. D. Willauer, J. G. Huddleston, R. P. Swatloski, J. D. Holbrey and R. D. Rogers, *J. Am. Chem. Soc.*, 2003, **125**, 6632–6633;
(58) C. M. S. S. Neves, M. G. Freire and J. A. P. Coutinho, *RSC Adv.*, 2012, **2**, 10882–10890;
(59) Y. Pei, J. Wang, K. Wu, X. Xuan and X. Lu, *Sep. Purif. Technol.*, 2009, **64**, 288–295;
(60) S. Shahriari, C. M. S. S. Neves, M. G. Freire and J. A. P. Coutinho, *J. Phys. Chem. B*, 2012, **116**, 7252–7258;
(61) S. P. M. Ventura, S. G. Sousa, L. S. Serafim, Á. S. Lima, M. G. Freire and J. A. P. Coutinho, *J. Chem. Eng. Data*, 2011, **56**, 4253–4260;

(62) F. J. Deive, A. Rodríguez, I. M. Marrucho and L. P. N. Rebelo, *J. Chem. Thermodyn.*, 2011, **43**, 1565–1572;
(63) Y. Deng, T. Long, D. Zhang, J. Chen and S. Gan, *J. Chem. Eng. Data*, 2009, **54**, 2470–2473;
(64) N. J. Bridges, K. E. Gutowski and R. D. Rogers, *Green Chem.*, 2007, **9**, 177–183;
(65) C. He, S. Li, H. Liu, K. Li and F. Liu, *J. Chromatogr. A*, 2005, **1082**, 143–149;
(66) C. Li, J. Han, Y. Wang, Y. Yan, J. Pan, X. Xu and Z. Zhang, *J. Chem. Eng. Data*, 2009, **55**, 1087–1092;
(67) L. I. N. Tome, R. Varanda, M. G. Freire and I. M. Marrucho, *J. Phys. Chem. B*, 2009, **113**, 2815–2825;
(68) M. G. Freire, P. J. Carvalho, A. M. S. Silva, L. M. N. B. F. Santos, L. P. N. Rebelo, I. M. Marrucho and J. A. P. Coutinho, *J. Phys. Chem. B B*, 2009, **113**, 202–211;
(69) M. G. Freire, C. M. S. S. Neves, A. M. S. Silva, M. N. B. F. Santos, I. M. Marrucho, P. N. Rebelo, J. K. Shah and E. J. Maginn, *J. Phys. Chem. B*, 2010, **114**, 2004–2014;
(70) M. G. Freire, C. L. S. Louros, L. P. N. Rebelo and J. A. P. Coutinho, *Green Chem.*, 2011, **13**, 1536–1545;
(71) M. Domínguez-Pérez, L. I. N. Tomé, M. G. Freire, I. M. Marrucho, O. Cabeza and J. A. P. Coutinho, *Sep. Purif. Technol.*, 2010, **72**, 85–91;
(72) S. P. M. Ventura, C. M. S. S. Neves, M. G. Freire, I. M. Marrucho, J. Oliveira and J. A. P. Coutinho, *J. Phys. Chem. B*, 2009, **113**, 9304–9310;
(73) A. F. M. Cláudio, A. M. Ferreira, S. Shahriari, M. G. Freire and J. A. P. Coutinho, *J. Phys. Chem. B*, 2011, **115**, 11145–11153;
(74) T. Mourão, A. F. M. Cláudio, I. Boal-Palheiros, M. G. Freire and J. A. P. Coutinho, *J. Chem. Thermodyn.*, 2012, **54**, 398–405;
(75) H. Passos, A. R. Ferreira, A. F. M. Cláudio, J. A. P. Coutinho and M. G. Freire, *Biochem. Eng. J.*, 2012, **67**, 68–76;
(76) S. P. M. Ventura, S. G. Sousa, L. S. Serafim, Á. S. Lima, M. G. Freire and J. A. P. Coutinho, *J. Chem. Eng. Data*, 2012, **57**, 507–512;
(77) D. J. S. Patinha, F. Alves, L. P. N. Rebelo and I. M. Marrucho, *J. Chem. Thermodyn.*, 2013, **65**, 106–112;
(78) Y. Xie, H. Xing, Q. Yang, Z. Bao, B. Su and Q. Ren, *ACS Sustain. Chem. Eng.*, 2015, **3**, 3365–3372;
(79) S. Malekghasemi, B. Mokhtarani, S. Hamzehzadeh, A. Sharifi and M. Mirzaei, *J. Mol. Liq.*, 2016, **219**, 95–103;
(80) M. G. Freire, C. M. S. S. Neves, J. N. C. Lopes, I. M. Marrucho, J. A. P. Coutinho and L. P. N. Rebelo, *J. Phys. Chem. B*, 2012, **116**, 7660–7668;
(81) M. G. Freire, J. F. B. Pereira, M. Francisco, H. Rodríguez, Luís, P. N. Rebelo, R. D. Rogers and J. A. P. Coutinho, *Chem. Eur. J.*, 2012, **18**, 1831–1839;
(82) J. F. B. Pereira, K. A. Kurnia, O. A. Cojocaru, G. Gurau, L. P. N. Rebelo, R. D. Rogers, M. G. Freire and J. A. P. Coutinho, *Phys. Chem. Chem. Phys.*, 2014, **16**, 5723–5731;
(83) L. I. N. Tomé, J. F. B. Pereira, R. D. Rogers, M. G. Freire, J. R. B. Gomes and J. A. P. Coutinho, *Phys. Chem. Chem. Phys.*, 2014, **16**, 2271–2274;
(84) L. I. N. Tomé, J. F. B. Pereira, R. D. Rogers, M. G. Freire, J. R. B. Gomes and J. A. P. Coutinho, *J. Phys. Chem. B*, 2014, **118**, 4615–4629;
(85) J. F. B. Pereira, Á. S. Lima, M. G. Freire and J. A. P. Coutinho, *Green Chem.*, 2010, **12**, 1661–1669;
(86) J. H. P. M. Santos, F. A. e Silva, J. A. P. Coutinho, S. P. M. Ventura and A. Pessoa, *Process Biochem.*, 2015, **50**, 661–668;
(87) R. L. Souza, S. P. M. Ventura, C. M. F. Soares, J. A. P. Coutinho and Á. S. Lima, *Green Chem.*, 2015, **17**, 3026–3034;

(88) R. L. de Souza, V. C. Campos, S. P. M. Ventura, C. M. F. Soares, J. A. P. Coutinho and Á. S. Lima, *Fluid Phase Equilib.*, 2014, **375**, 30–36;
(89) M. R. Almeida, H. Passos, M. M. Pereira, Á. S. Lima, J. A. P. Coutinho and M. G. Freire, *Sep. Purif. Technol.*, 2014, **128**, 1–10;
(90) M. T. Zafarani-Moattar and S. Hamzehzadeh, *Fluid Phase Equilib.*, 2011, **304**, 110–120;
(91) S. Li, C. He, H. Liu, K. Li and F. Liu, *J. Chromatogr. B*, 2005, **826**, 58–62;
(92) K. A. Kurnia, M. G. Freire and J. A. P. Coutinho, *J. Phys. Chem. B*, 2013, **118**, 297−308;
(93) J. Zhang, Y. Zhang, Y. Chen and S. Zhang, *J. Chem. Eng. Data*, 2007, **52**, 2488–2490;
(94) R. Sadeghi, R. Golabiazar and H. Shekaari, *J. Chem. Thermodyn.*, 2010, **42**, 441–453;
(95) B. Wu, Y. Zhang, H. Wang and L. Yang, *J. Phys. Chem. B*, 2008, **112**, 13163–13165;
(96) Z. P. Visak, J. N. Canongia Lopes and L. P. N. Rebelo, *Monatshefte für Chemie - Chem. Mon.*, 2007, **138**, 1153–1157;
(97) M. T. Zafarani-Moattar, S. Hamzehzadeh and S. Nasiri, *Biotechnol. Prog.*, 2012, **28**, 146–156;
(98) V. Fischer, W. Borchard and M. Karas, *J. Phys. Chem.*, 1996, **100**, 15992–15999;
(99) K. Kodama, R. Tsuda, K. Niitsuma, T. Tamura, T. Ueki, H. Kokubo and M. Watanabe, *Polym. J.*, 2011, **43**, 242–248;
(100) C. L. S. Louros, A. F. M. Cláudio, C. M. S. S. Neves, M. G. Freire, I. M. Marrucho, J. Pauly and J. A. P. Coutinho, *Int. J. Mol. Sci.*, 2010, **11**, 1777–1791;
(101) J. Gao, L. Chen, Y. Xin and Z. Yan, *J. Chem. Eng. Data*, 2014, **59**, 2150–2158;
(102) P. P. Madeira, A. Bessa, D. P. C. de Barros, M. A. Teixeira, L. Álvares-Ribeiro, M. R. Aires-Barros, A. E. Rodrigues, A. Chait and B. Y. Zaslavsky, *J. Chromatogr. A*, 2013, **1271**, 10–16;
(103) M. L. Moody, H. D. Willauer, S. T. Griffin, J. G. Huddleston and R. D. Rogers, *Ind. Eng. Chem. Res.*, 2005, **44**, 3749–3760;
(104) S. C. Silvério, P. P. Madeira, O. Rodríguez, J. A. Teixeira and E. A. Macedo, *J. Chem. Eng. Data*, 2008, **53**, 1622–1625;
(105) C. Wu, J. Wang, H. Wang, Y. Pei and Z. Li, *J. Chromatogr. A*, 2011, **1218**, 8587–93;
(106) B. Y. Zaslavsky, L. M. Miheeva and S. V. Rogozhin, *J. Chromatogr. A*, 1981, **212**, 13–22;
(107) B. Y. Zaslavsky, L. M. Miheeva and S. V. Rogozhin, *J. Chromatogr. A*, 1981, **216**, 103–113;
(108) J. G. Huddleston, H. D. Willauer and R. D. Rogers, *Phys. Chem. Chem. Phys.*, 2002, **4**, 4065–4070;
(109) P. P. Madeira, C. A. Reis, A. E. Rodrigues, L. M. Mikheeva, A. Chait and B. Y. Zaslavsky, *J. Chromatogr. A*, 2011, **1218**, 1379–84;
(110) O. Rodríguez, S. C. Silvério, P. P. Madeira, J. A. Teixeira and E. A. Macedo, *Ind. Eng. Chem. Res.*, 2007, **46**, 8199–8204;
(111) B. Y. Zaslavsky, V. N. Uversky and A. Chait, *Biochim. Biophys. Acta*, 2016, **1864**, 622–44;
(112) M. J. Kamlet and R. W. Taft, *J. Am. Chem. Soc.*, 1976, **98**, 377–383;
(113) M. J. Kamlet, J. L. Abboud and R. W. Taft, *J. Am. Chem. Soc.*, 1977, **99**, 6027–6038;
(114) R. W. Taft and M. J. Kamlet, *J. Am. Chem. Soc.*, 1976, **98**, 2886–2894;
(115) H. Passos, A. C. A. Sousa, M. R. Pastorinho, A. J. A. Nogueira, L. P. N. Rebelo, J. A. P. Coutinho and M. G. Freire, *Anal. Methods*, 2012, **4**, 2664–2667;
(116) A. C. Johnson and J. P. Sumpter, *Environ. Sci. Technol.*, 2001, **35**, 4697–4703;
(117) B. Wu, Y. M. Zhang and H. P. Wang, *J. Chem. Eng. Data*, 2008, **53**, 983–985;
(118) P. A. J. Rosa, I. F. Ferreira, A. M. Azevedo and M. R. Aires-Barros, *J. Chromatogr. A*, 2010, **1217**, 2296–2305;
(119) M. Matzke, J. Arning, J. Ranke, B. Jastorff, S. Stolte, M. Matzke, J. Arning, J. Ranke, B. Jastorff and S. Stolte, in *Handbook of Green Chemistry*, Wiley-VCH Verlag GmbH & Co. KGaA, Weinheim, Germany, 2010;

(120) B. Jastorff, K. Mölter, P. Behrend, U. Bottin-Weber, J. Filser, A. Heimers, B. Ondruschka, J. Ranke, M. Schaefer, H. Schröder, A. Stark, P. Stepnowski, F. Stock, R. Störmann, S. Stolte, U. Welz-Biermann, S. Ziegert and J. Thöming, *Green Chem.*, 2005, **7**, 362;
(121) S. P. M. Ventura, A. M. M. Gonçalves, T. Sintra, J. L. Pereira, F. Gonçalves and J. A. P. Coutinho, *Ecotoxicology*, 2013, **22**, 1–12;
(122) M. Petkovic, J. L. Ferguson, H. Q. N. Gunaratne, R. Ferreira, M. C. Leitão, K. R. Seddon, L. P. N. Rebelo and C. S. Pereira, *Green Chem.*, 2010, **12**, 643;
(123) T. P. Thuy Pham, C.-W. Cho and Y.-S. Yun, *Water Res.*, 2010, **44**, 352–372;
(124) L. Pisarova, S. Steudte, N. Dorr, E. Pittenauer, G. Allmaier, P. Stepnowski and S. Stolte, *Proc. Inst. Mech. Eng. Part J J. Eng. Tribol.*, 2012, **226**, 903–922;
(125) S. P. M. Ventura, R. L. Gardas, F. Gonçalves and J. A. P. Coutinho, *J. Chem. Technol. Biotechnol.*, 2011, **86**, 957–963;
(126) S. P. M. Ventura and J. A. P. Coutinho, Springer Berlin Heidelberg, 2016, pp. 285–315;
(127) R. D. Rogers, K. R. Seddon and S. Volkov, *Green Industrial Applications of Ionic Liquids*, Springer, 2003;
(128) M. C. Bubalo, K. Radošević, I. R. Redovniković, J. Halambek and V. G. Srček, *Ecotoxicol. Environ. Saf.*, 2014, **99**, 1–12;
(129) P. E. Rakita, in *Ionic Liquids as Green Solvents*, eds. R. D. Rogers and K. R. Seddon, American Chemical Society, 2003, pp. 32–40;
(130) G. Wytze Meindersma, L. M. Galán Sánchez, A. R. Hansmeier and A. B. de Haan, *Monatshefte für Chemie - Chem. Mon.*, 2007, **138**, 1125–1136;
(131) L. Chen, M. Sharifzadeh, N. Mac Dowell, T. Welton, N. Shah and J. P. Hallett, *Green Chem.*, 2014, **16**, 3098–3106;
(132) ICIS - *Trusted market intelligence for the global chemical, energy and fertilizer industries*, 2014, available from: https://www.icis.com/chemicals/channel-info-chemicals-a-z/;
(133) T. Zaiz, H. Lanez and B. Kechida, *Int. J. Chem. Pet. Sci.*, 2013, **2**, 10–19;
(134) *Regulation (EC) No. 1907/2006 of the European Parliament and of the Council of 18 December 2006 concerning the Registration, Evaluation, Authorisation and Restriction of Chemicals (REACH), establishing a European Chemicals Agency*;
(135) A. F. M. Cláudio, A. M. Ferreira, C. S. R. Freire, A. J. D. Silvestre, M. G. Freire and J. A. P. Coutinho, *Sep. Purif. Technol.*, 2012, **97**, 142–149;
(136) H. F. D. Almeida, M. G. Freire and I. M. Marrucho, *Green Chem.*, 2016, **18**, 2717–2725;
(137) M. Zawadzki, F. A. e Silva, U. Domańska, J. A. P. Coutinho and S. P. M. Ventura, *Green Chem.*, 2016, **18**, 3527–3536;
(138) A. M. Ferreira, J. A. P. Coutinho, A. M. Fernandes and M. G. Freire, *Sep. Purif. Technol.*, 2014, **128**, 58–66;
(139) M. M. Pereira, S. N. Pedro, M. V. Quental, Á. S. Lima, J. A. P. Coutinho and M. G. Freire, *J. Biotechnol.*, 2015, **206**, 17–25;
(140) Q. Zeng, Y. Wang, Y. Huang, X. Ding, J. Chen and K. Xu, *Analyst*, 2014, **139**, 2565–73;
(141) K. Xu, Y. Wang, Y. Huang, N. Li and Q. Wen, *Anal. Chim. Acta*, 2015, **864**, 9–20.

2. DEVELOPMENT
OF NEW ABS

2.1. Thermoreversible (ionic-liquid-based) aqueous biphasic systems

This chapter is based on the published manuscript

Helena Passos, Andreia Luís, João A. P. Coutinho and Mara G. Freire;[1]

"Thermoreversible (ionic-liquid-based) aqueous biphasic systems",

Scientific Reports 6 (2016) 20276.

2.1.1. Abstract

The ability to induce reversible phase transitions between homogeneous solutions and biphasic liquid-liquid systems, at pre-defined and suitable operating temperatures, is of crucial relevance in the design of separation processes. Ionic-liquid-based aqueous biphasic systems (IL-based ABS) have demonstrated superior performance as alternative extraction platforms, and their thermoreversible behavior is here disclosed by the use of protic ILs. The applicability of the temperature-induced phase switching is further demonstrated with the complete extraction of two value-added proteins, achieved in a single-step. It is shown that these temperature-induced mono(bi)phasic systems are significantly more versatile than classical liquid-liquid systems which are constrained by their critical temperatures. IL-based ABS allow to work in a wide range of temperatures and compositions which can be tailored to fit the requirements of a given separation process.

2.1.2. Introduction

Liquid-liquid extraction processes are technologically simple, of low cost and often highly effective for the separation of a large plethora of compounds or materials. Consequently, liquid-liquid extraction has regularly been a favored choice in process engineering. These systems can display a strong temperature dependence and be used as switchable systems, as attempted by Bergbreiter *et al.*[1], who proposed the use of thermomorphic catalysis, which allows both the product separation and the catalyst recovery. Other organic-organic or organic-aqueous systems have been used in the separation of catalysts, metals, organic and biological products.[2] However, the use of volatile and hazardous organic solvents in extraction processes presents major drawbacks. In this context, ionic liquids (ILs) represent a viable alternative due to their non-volatile nature coupled to a high and tailored solvation ability.

[1]**Contributions:** M.G.F. and J.A.P.C. conceived and directed this work. H.P. and A.L. acquired the experimental data. H.P., J.A.P.C. and M.G.F interpreted the experimental data. The manuscript was mainly written by H.P. and M.G.F. with significant contributions from the remaining authors.

In the past few years, the research on dynamic and reversible biphasic systems constituted by ILs has received a crucial attention towards the development of novel and more efficient separation processes.[3-5] It was demonstrated that phase transitions in mixtures involving ILs and other solvents can be induced by changes in temperature or by reversible reactions with CO_2.[6-15] Some IL/solvent mixtures display an upper critical solution temperature (UCST)[16] whereas others present a lower critical solution temperature (LCST).[17] These temperature-dependent phase transitions have shown to be highly advantageous in the selective separation of proteins,[18] metals[16] and catalysts.[1,9] However, most UCST and LCST in IL-containing systems often occur at temperatures away from room temperature and are confined to mixture compositions imposed by the critical point of each phase diagram. Therefore, the design of novel systems with UCST or LCST close to room temperature has been object of a great deal of work; yet, only a restricted number of systems has been identified.[3,8,17] Moreover, these systems are composed of an IL-rich phase (typically with hydrophobic characteristics) and a molecular-solvent-rich phase.[16,17] Reversible liquid-liquid systems have also been prepared with molecular solvents that react with CO_2 forming salts and/or ILs.[6-8,19] Nevertheless, this type of reversibility requires the flushing of the system with gases and the use of specific equipment.[6-8]

The research in liquid-liquid extractions using ILs focuses on two main approaches: (i) the direct use of hydrophobic ILs[11,12,18,20] which leads to the formation of an IL- and a water- or organic-solvent-rich phase (where the UCST and LCST reversible temperature-induced systems fall); and (ii) the use of aqueous biphasic systems (ABS) composed of ILs and organic/inorganic salts[21,22] that above given concentrations lead to the formation of two aqueous-rich phases. ABS are commonly seen as "greener" and more biocompatible options since they are mostly composed of water (up to 70 wt % in the overall system).[22] Furthermore, one of the most outstanding features of ILs – their tailoring capacity by appropriate cation/anion combinations – is transposable to IL-based ABS, and thus, these systems allow an efficient design for the selective extraction of a variety of compounds.[21-24]

The number of potential IL-based liquid-liquid extraction routes surpasses by far conventional polymer-salt or polymer-polymer ABS.[21,22] Typical ABS have been largely investigated in the extraction and purification of proteins, including value-added antibodies, cells organelles and viruses.[25,26] Nevertheless, these systems display restricted differences on their phases' polarities and affinities for target compounds which have been obstructing high selectivities and extraction efficiencies to be attained. Due to their tailoring ability, IL-based ABS have shown to be promising extraction/purification routes for a large plethora of biologically active compounds, *e.g.* proteins,

enzymes and biopharmaceuticals.[22,27-32] In most studies, the complete extraction of the biological compounds was attained in a single-step without denaturation or precipitation effects.[29-31] Moreover, the application of IL-based ABS to real matrices, *e.g.* bovine serum to extract bovine serum albumin,[33] and the recovery and reuse of the IL-rich phase was also demonstrated.[29] Nevertheless, imidazolium-,[28] cholinium-[33] and tetraalkylphosphonium-based ILs[29] have been the preferred choice as phase-forming components of ABS and no studies comprising protic ILs have been found.

In addition to the well-established outstanding extraction performances of IL-based ABS, their temperature dependent phase-behavior is a relevant aspect, though still scarcely explored.[21,22] Most studies were carried out at a fixed temperature since only ABS formed by aprotic ILs combined with salts or polymers were investigated, and these display a weak dependence on temperature.[21,22]

Herein, we reveal a novel class of thermoreversible ABS formed by protic ILs (PILs) and polymers, in particular poly(propylene glycol) (PPG) with an average molecular weight of 400 $g \cdot mol^{-1}$. PILs are formed in one-step reactions between a low-cost acid, such as acetic acid, and a base (*e.g.*, an amine).[34] Their easy synthesis is a major advantage that coupled to their lower cost and more benign character,[34] make of them viable candidates to replace the aprotic ILs used in ABS formulations. The biocompatible nature of PPG 400 is also well-established.[30] As shown below, the phase diagrams of PIL-based ABS are highly dependent on temperature, with small changes on temperature being enough to trigger the phase transition.

2.1.3. Experimental procedures

Materials. The determination of the liquid-liquid ternary phase diagrams was performed using aqueous solutions of PPG 400 (from Sigma-Aldrich) and individual aqueous solutions of the following PILs: *N*,*N*-dimethyl-*N*-ethylammonium acetate, $[N_{1120}][CH_3CO_2]$ (98 wt %); *N*,*N*-diethyl-*N*-methylammonium methane sulfonate, $[N_{1220}][CH_3SO_3]$ (> 97 wt %); *N*,*N*-dimethyl-*N*-(*N*´,*N*´dimethylaminoethyl)ammonium acetate, $[N_{11[2(N110)]0}][CH_3CO_2]$ (98 wt %); *N*,*N*-dimethyl-*N*-(*N*´,*N*´dimethylaminoethyl) ammonium chloride, $[N_{11[2(N110)]0}]Cl$ (97 wt %); *N*,*N*-dimethyl-*N*-ethylammonium phenylacetate, $[N_{1120}][C_7H_7CO_2]$ (> 98 wt %); and *N*,*N*-dimethyl-*N*-(*N*´,*N*´dimethylaminoethyl) ammonium octanoate, $[N_{11[2(N110)]0}][C_7H_{15}CO_2]$ (> 98 wt %). All ammonium-based ILs were purchased from Iolitec and their chemical structures are shown in **Figure 2.1**. To reduce the volatile impurities to negligible values, PIL individual samples were purified under constant agitation, vacuum, and at moderate temperature (323 K), for a minimum

of 24 h. After this procedure, the purity of each IL was further checked by ^{1}H nuclear magnetic resonance (NMR) spectra and found to be in accordance with the stated purity level provided by the suppliers (*cf.* **Appendix A**). The water used was double distilled, passed through a reverse osmosis system, and further treated with a Milli-Q plus 185 apparatus. Cytochrome c and azocasein were purchased from Sigma-Aldrich.

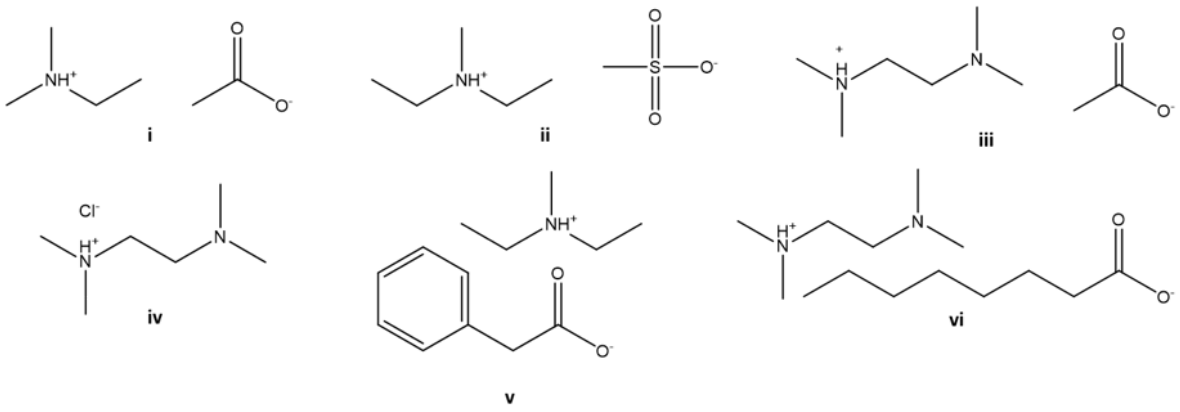

Figure 2.1. Chemical structure of the PILs studied: (i) $[N_{1120}][CH_3CO_2]$; (ii) $[N_{1220}][CH_3SO_3]$; (iii) $[N_{11[2(N11)]0}][CH_3CO_2]$; (iv) $[N_{11[2(N11)]0}]Cl$; (v) $[N_{1120}][C_7H_7CO_2]$; (vi) $[N_{11[2(N11)]0}][C_7H_{15}CO_2]$.

Phase diagrams and tie-lines. The solubility curves were determined through the cloud point titration method[22] at 298, 308, 318 and 328 K (± 1K) and atmospheric pressure. Aqueous solutions of PPG at circa 80 wt % and aqueous solutions of the different ILs (with concentrations ranging from 50 wt % to 90 wt %) were prepared and used for the determination of the binodal curves. Repetitive drop wise addition of the aqueous PIL solution to the aqueous solutions of PPG was carried out until the detection of a cloudy (biphasic) solution, followed by the drop wise addition of ultrapure water until the finding of a monophasic region (clear and limpid solution). The ternary system compositions were determined by weight quantification within $\pm 10^{-4}$ g.

The experimental binodal curves at 298 K were fitted by **Equation (2.1)**.[35]

$$[Y] = Aexp[(B[X]^{0.5}) - (C[X]^3)] \quad \textbf{(2.1)}$$

where $[Y]$ and $[X]$ are the salted-out and the salting-out species weight fraction percentages, respectively, and A, B, and C are constants obtained by the regression of the experimental binodal data (see **Appendix A**). In this work, it was observed that the PILs are the salting-out species while the PPG is salted-out compound.

The tie-lines were determined by a gravimetric method originally proposed by Merchuk *et al.*[35] for polymer-based ABS, and later on applied by Rogers and co-workers[21] to IL-based ABS. A ternary mixture composed of PPG + PIL + water at the biphasic region was gravimetrically

prepared within ±10^{-4} g, vigorously agitated, and left to equilibrate for at least 12 h at (298 ± 1) K, aiming at a complete separation of the coexisting phases. After such time, both phases were carefully separated and individually weighed. Each tie-line was determined by the lever-arm rule through the relationship between the salted-out specie rich-phase (the PPG-rich phase) and the overall system composition, and for which the following system of four equations (**Equation (2.2) to (2.5)**) and four unknown values ($[Y]_Y$, $[Y]_X$, $[X]_Y$, and $[X]_X$) was solved:[35]

$$[Y]_Y = Aexp\left[\left(B[X]_Y^{0.5}\right) - \left(C[X]_Y^3\right)\right] \quad \textbf{(2.2)}$$

$$[Y]_X = Aexp\left[\left(B[X]_X^{0.5}\right) - \left(C[X]_X^3\right)\right] \quad \textbf{(2.3)}$$

$$[Y]_Y = \frac{[Y]_M}{\alpha} - \frac{1-\alpha}{\alpha}[Y]_X \quad \textbf{(2.4)}$$

$$[X]_Y = \frac{[X]_M}{\alpha} - \frac{1-\alpha}{\alpha}[X]_X \quad \textbf{(2.5)}$$

where subscripts Y, X, and M designate the salted-out specie (PPG) rich phase, the salting-out specie (PIL) rich phase and the mixture, respectively. α is the ratio between the weight of the salting-out specie rich phase and the total weight of the mixture. The system solution results in the composition (wt %) of the PIL and PPG in the top and bottom phases.

For the calculation of each tie-line length (TLL) the following equation was used:

$$TLL = \sqrt{([X]_Y - [X]_X)^2 + ([Y]_Y - [Y]_X)^2} \quad \textbf{(2.6)}$$

pH and conductivity measurements. The pH values (± 0.02) of the PPG-rich and PIL-rich aqueous phases were measured at 298, 308, 318 and 328 K (± 1 K), and the electrical conductivity was measured at (298 ± 1) K, using a Mettler Toledo SevenMultiTMdual pH/conductivity meter.

Partition of cytochrome c and azocasein. Cytochrome c and azocasein were studied as representative examples of added-value proteins. Aqueous solutions of each biomolecule were prepared at the concentrations of 1, 2 and 3 g·L^{-1}. Aiming at studying the possibility of moving from monophasic to biphasic regimes in PIL-based ABS, by temperature changes, an initial ternary mixture at the monophasic region was chosen based on the phase diagram of $[N_{11[2(N11)]0}][CH_3CO_2]$-based ABS: 6 wt % $[N_{11[2(N11)]0}][CH_3CO_2]$ + 30 wt % PPG + 64 wt % aqueous solution of protein. The mixture was vigorously stirred and left to equilibrate at 318 K for 12 h to achieve the complete partition of cytochrome c and azocasein between the two phases. After a

careful separation of both phases, the quantification of cytochrome c and azocasein in each phase was carried out by UV-spectroscopy, using a BioTeck Synergy HT microplate reader, at a wavelength of 410 nm for cytochrome c and 342 nm for azocasein using calibration curves previously established. At least three individual samples were prepared and three samples of each phase were quantified in order to determine the average in the extractions efficiencies and respective standard deviations. Possible interferences of the PPG and PIL with the analytical method were controlled using blank control samples. The percentage extraction efficiency of cytochrome c and azocasein is defined as the percentage ratio between the amount of each protein in the PIL-aqueous-rich phase and that in the total mixture (*cf.* **Equation (1.2)**).

Thermal stability of protic ionic liquids. The PILs thermal stability, after the drying process and after being submitted at 328 K for 12 h, as well as of the PIL- and PPG-rich phases of some systems after being submitted at 328 K for 12 h, were evaluated by ^{1}H and ^{13}C NMR spectra using a Bruker Avance 300 at 300.13 and 75.47 MHz, respectively, with deuterium oxide (D_2O) as solvent and trimethylsilyl propanoic acid (TSP) as internal reference.

Proteins stability. The proteins stability in the PIL-rich phase after the extraction occurring at 318 K was evaluated by Fourier Transform Infrared Spectroscopy (FTIR). The spectrum of each protein in a buffer solution at pH 7 and 298 K and of the PIL-rich phases after the extraction of proteins at 318 K were recorded. Blank control samples containing the same composition but without protein were always used. FTIR spectra were determined by a Perkin Elmer BX spectrometer operating in the attenuated total reflection (ATR) mode (equipped with a single horizontal Golden Gate ATR cell) with a resolution of 4 cm^{-1}.

2.1.4. Results and discussion

Ionic-liquid-based aqueous biphasic systems at different temperatures. To study the thermoreversibility of PIL-based ABS, the respective phase diagrams at four temperatures (298, 308, 318 and 328 K), for the systems composed of water, PPG and six PILs – $[N_{1120}][CH_3CO_2]$, $[N_{1220}][CH_3SO_3]$, $[N_{11[2(N110)]0}][CH_3CO_2]$, $[N_{11[2(N110)]0}]Cl$, $[N_{1120}][C_7H_7CO_2]$, and $[N_{11[2(N110)]0}][C_7H_{15}CO_2]$ – were determined. ^{1}H and ^{13}C NMR spectra of pure PILs and of the water-rich phases after being submitted to 328 K are presented in **Appendix A**. Two examples of their liquid-liquid phase diagrams are depicted in **Figure 2.2**. The detailed experimental weight fraction data, as well as the representation of the phase diagrams for the remaining ILs are presented in the **Appendix A**, along with the compositions of the coexisting phases, *i.e.*, the respective tie-lines and tie-line lengths.

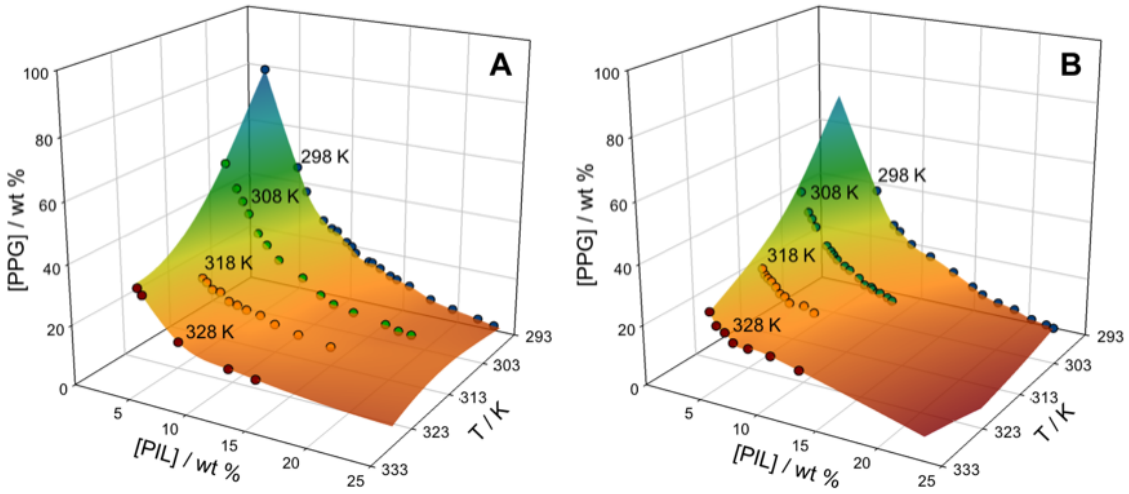

Figure 2.2. 3D representation of the temperature effect in the ternary phase diagrams composed of **(A)** $[N_{1120}][CH_3CO_2]$ + PPG + H_2O and **(B)** $[N_{11[2(N11)]0}][CH_3CO_2]$ + PPG + H_2O at 298 K (●), 308 K (●), 318 K (●) and 328 K (●).

For all phase diagrams, the biphasic region is located above the binodal curve while the monophasic region is localized below. In general, the larger the biphasic region, the higher is the capacity of the system to undergo liquid-liquid demixing. For a fixed temperature, *e.g.*, 298 K, and at 20 wt % of PPG, the PILs capability to form ABS follows the order: $[N_{1220}][CH_3SO_3] < [N_{1120}][CH_3CO_2]$ ~ $[N_{11[2(N11)]0}][CH_3CO_2] < [N_{11[2(N11)]0}]Cl$ – *cf.* the **Appendix A**. Amongst the studied ILs, $[N_{1120}][C_7H_7CO_2]$ and $[N_{11[2(N11)]0}][C_7H_{15}CO_2]$ were not able to induce ABS formation at any of the temperatures investigated. The presence of an aromatic ring and a long alkyl chain length at the anion and cation of $[N_{1120}][C_7H_7CO_2]$ and $[N_{11[2(N11)]0}][C_7H_{15}CO_2]$, respectively, increase the hydrophobicity of these PILs further preventing the formation of ABS with PPG. In summary, PILs constituted by more hydrophilic anions, *i.e.*, anions with higher affinity for water, are more favorable for ABS formation. These trends are in agreement with previous works,[36] for which the higher the IL ion's ability to create hydration complexes the easier is the formation of IL-polymer ABS. It should be highlighted that the differences between the binodal curves for the various ILs investigated are more significant at higher temperatures.

In the studied ABS at 298 K, the top phase corresponds to the PPG-rich phase, while the bottom phase is enriched in PIL and water, with the exception of the $[CH_3CO_2]$-based PILs for which the opposite behavior was observed. Curiously, at 318 K it was observed an inversion on the phases' densities for the $[N_{11[2(N11)]0}][CH_3CO_2]$-based ABS, where the PIL-rich phase corresponds to the bottom layer as confirmed by conductivity measurements presented in **Appendix A**.

Figure 2.2 shows the effect of temperature on the ternary phase diagrams of the systems composed of $[N_{1120}][CH_3CO_2]$ + PPG + H_2O and $[N_{11[2(N11)]0}][CH_3CO_2]$ + PPG + H_2O. The depicted surfaces represent the limit between the monophasic and biphasic regions revealing that a temperature increase enhances the ability of PILs to form ABS – at higher temperatures lower amounts of IL or PPG are required for phase demixing. Albeit the phase diagrams depicted in **Figure 2.2** are presented at intervals of 10 K, it should be remarked that the differences observed are large enough to trigger the reversible behavior by changes in temperature as small as 1 K.

Thermoreversible behavior. Upon the establishment of the temperature dependency of the studied ABS, their reversible behavior was further ascertained. For that purpose, a monophasic ternary mixture was prepared at 298 K, with a composition within the hatched region of **Figure 2.3**, and the temperature was then increased to 318 K resulting in the phase separation. As the systems is cooled down to 298 K the system becomes monophasic again. This reversible behavior can be applied as many times as desired without changes in the composition of the coexisting phases for a given initial mixture. Even so, one of the major advantages of these reversible IL-based ABS is that the temperature range of operation can be selected based on the ternary mixture composition to fit the requirements of a specific process (stability of the biomolecule being purified or optimization of the extraction efficiencies) and is not restricted to fixed temperatures imposed by the thermodynamic nature of binary liquid-liquid systems (UCST or LCST).[16,17,37-39] Surfactant-based aqueous two-phase systems are also thermoreversible systems and have been extensively explored in the past decades for (bio)separation approaches.[40] Nevertheless, mostly aqueous two-phase micellar systems are binary systems, and thus, only one solubility curve exists, *i.e.*, for a given concentration of surfactant, a given temperature has to be reached to allow the liquid-liquid demixing. In ABS, while being ternary systems, the temperature at which the phase separation is carried out can be

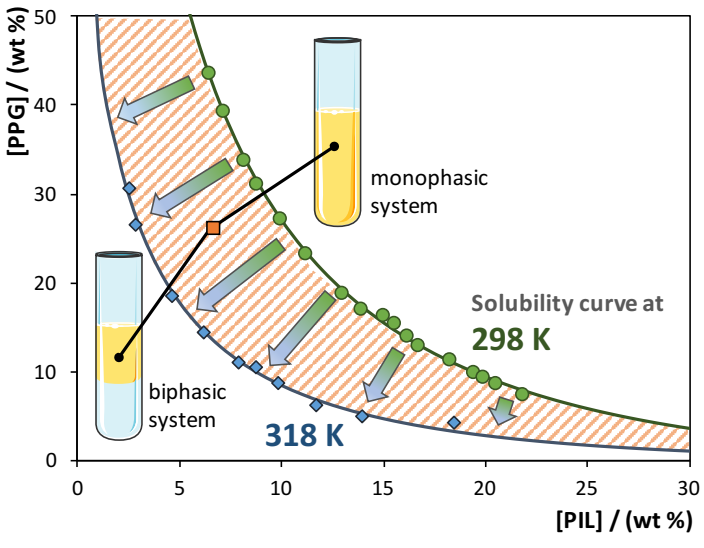

Figure 2.3. Schematic representation of PIL-based ABS thermoreversibility: binodal curve of the ternary system composed of $[N_{11[2(N11)]0}]Cl$ + PPG + H_2O at 298 K (●) and 318 K (◆); initial mixture composition (■).

tuned by a simple manipulation of the concentration of the phase-forming components. In summary, thermoreversible IL-based ABS allow the design of their operating temperatures by defining the mixture compositions, resulting thus on more flexible and tailored liquid-liquid extraction processes.

Applicability of protic-ionic-liquid-based aqueous biphasic systems. The applicability of the investigated thermoreversible IL-based ABS was further evaluated for separation processes, using two added-value proteins, namely cytochrome c and azocasein. For this purpose, homogeneous ternary mixtures composed of 6 wt % of $[N_{11[2(N11)]0}][CH_3CO_2]$ + 30 wt % of PPG + 64 wt % of aqueous solutions containing the proteins at 1, 2 and 3 $g{\cdot}L^{-1}$ were prepared at 298 K. Certainly, other points could be selected within this region and which allow the reversible cycles among monophasic and biphasic regimes to be achieved, by simple changes in temperature. Even so, a point using a small amount of IL was selected while attempting the demonstration of low-cost and biocompatible thermoreversible ABS. The temperature was then increased up to 318 K to induce the phase separation and the proteins partition between the coexisting phases.

Remarkably, the two proteins, and at the three concentrations investigated, almost completely migrate for the PIL-aqueous-rich phase in a single-step (**Figure 2.4**). The coexisting phases of the $[N_{11[2(N11)]0}][CH_3CO_2]$-based ABS display a pH value of circa 7.9 (see **Appendix A**), and according to the proteins isoelectric points (10.2 for cytochrome c[18] and 4.8 for casein[41]), both macromolecules are charged – cytochrome c is positively charged while azocasein is negatively charged – and both preferentially partition for the phase with the higher ionic strength. Moreover, the PIL-rich phase also corresponds to the most "hydrated" layer – higher

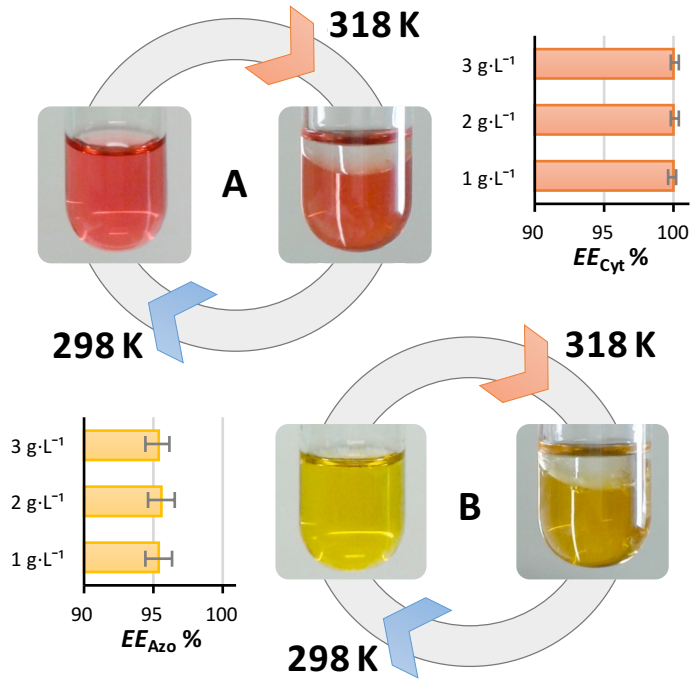

Figure 2.4. Partition of cytochrome c and azocasein at three different concentrations (1, 2 and 3 $g{\cdot}L^{-1}$) in PIL-based ABS formed at 318 K. Extraction efficiency of **(A)** cytochrome c (EE_{Cyt}%) **(B)** azocasein (EE_{Azo}%). The extraction efficiency data are presented in **Appendix A**.

water content as revealed by the tie-lines data shown in the **Appendix A**. Pure ILs have almost no ability to solubilize proteins without denaturation.[42] In these, the modification of proteins is usually carried out with amphiphilic polymers.[43] The chemical modification involves multi-step treatments and further purification steps, which may cause the denaturation of proteins. However, some "hydrated ILs" or ILs aqueous solutions have demonstrated to be extraordinary media for solubilizing and stabilizing proteins.[18] LCST-type phase diagrams of IL-water mixtures were previously proposed by Ohno and co-workers[3,18] for the separation of proteins. These systems are mostly composed of an IL-rich phase, for which the proteins partition, and an almost pure water phase. Nevertheless, the authors[18] demonstrated that cytochrome c was not extracted into the IL-phase for water contents below 13 wt %. In this work, taking advantage of two aqueous-rich phases formed by ternary mixtures, in particular of an IL-rich phase with high amounts of water that can be properly tuned by variations either in the initial mixture composition or in temperature, the complete extraction of proteins in a single-step was observed. Furthermore, the cyclic reversibility between monophasic and biphasic regimes, driven by a decrease/increase in temperature, was demonstrated with 3 cooling-heating cycles, with no losses on the extraction efficiencies obtained for the two proteins. Although several promising approaches have been proposed for the recovery of the most diverse value-added compounds from the IL-rich phase,[44-46] the recovery of both proteins from the PIL-rich phase can be simple attained by a dialysis process.[29]

The proteins stability at 318 K in the PIL-rich phase was also ascertained by FTIR spectroscopy. The proteins secondary structure can be studied through the analysis of amine I and II bands. The amide I band represents primarily the C = O stretching vibration of the amide groups and occurs near 1650 cm^{-1}, while the amide II band represents the C—N stretching vibrations and occurs close to 1550 cm^{-1}.[47] Through the results shown in **Appendix A** it is possible to conclude that both proteins maintain their native structures in the PIL-rich phase after the extraction being conducted at 318 K. Fujita et al.[48] and Ohno and co-workers[18,49] reported that hydrophilic ILs having carboxyl residues are effective for dissolving and maintaining the structure of proteins. In this context, the PILs derived from carboxylic acids used in this work seem to be an appropriate option to form ABS envisaging their use in downstream processes, namely on the extraction and purification of proteins, enzymes and antibodies.

2.1.5. Conclusions

The results here presented disclose that IL-based ABS can be highly temperature dependent, allowing to trigger reversible phase separations by small changes in temperature. Furthermore, the working temperature range is not restricted to fixed temperatures imposed by the thermodynamic nature of binary liquid-liquid systems. Instead, not only the phase behavior but also the water content and extraction performance of IL-based ABS could be controlled by selecting a suitable triad (nature of the phase-forming components, mixture compositions and temperature). The temperature-driven reversible behavior of IL-based ABS allows them to be used as novel separation platforms and boosts the potential applicability of ILs in biomedical and pharmaceutical fields.

2.1.6. References

(1) D. E. Bergbreiter, P. L. Osburn, A. Wilson, and E. M. Sink, *J. Am. Chem. Soc.*, 2000, **122**, 9058–9064;
(2) A. Behr, G. Henze, and R. Schomäcker, *Adv. Synth. Catal.*, 2006, **348**, 1485–1495;
(3) Y. Kohno and H. Ohno, *Chem. Commun.*, 2012, **48**, 7119–7130;
(4) P. G. Jessop, S. M. Mercer, and D. J. Heldebrant, *Energy Environ. Sci.*, 2012, **5**, 7240–7253;
(5) J. Luo, T. Xin, and Y. Wang, *New J. Chem.*, 2013, **37**, 269–273;
(6) Y. Kohno, H. Arai, and H. Ohno, *Chem. Commun.*, 2011, **47**, 4772–4774;
(7) D. Xiong, H. Wang, Z. Li, and J. Wang, *Chem. Sus. Chem.*, 2012, **5**, 2255–2261;
(8) S. Saita, Y. Kohno, N. Nakamura, and H. Ohno, *Chem. Commun.*, 2013, **49**, 8988–8990;
(9) A. Behr and C. Fängewisch, *J. Mol. Catal. A: Chem.*, 2003, **197**, 115–126;
(10) A. Riisager, R. Fehrmann, R. W. Berg, R. van Hal, and P. Wasserscheid, *Phys. Chem. Chem. Phys.*, 2005, **7**, 3052–3058;
(11) P. Nockemann, K. Binnemans, B. Thijs, T. N. Parac-Vogt, K. Merz, A.-V. Mudring, P. C. Menon, R. N. Rajesh, G. Cordoyiannis, J. Thoen, J. Leys, and C. Glorieux, *J. Phys. Chem. B*, 2009, **113**, 1429–1437;
(12) Z.-L. Xie and A. Taubert, *ChemPhysChem*, 2011, **12**, 364–368;
(13) W. Zhu, Y. Yu, H. Yang, L. Hua, Y. Qiao, X. Zhao, and Z. Hou, *Chem. Eur. J.*, 2013, **19**, 2059–2066;
(14) T. V. Hoogerstraete, B. Onghena, and K. Binnemans, *J. Phys. Chem. Lett.*, 2013, **4**, 1659–1663;
(15) B. Onghena, T. Opsomer, and K. Binnemans, *Chem. Commun.*, 2015, **51**, 15932–15935;
(16) P. Nockemann, B. Thijs, S. Pittois, J. Thoen, C. Glorieux, K. Van Hecke, L. Van Meervelt, B. Kirchner, and K. Binnemans, *J. Phys. Chem. B*, 2006, **110**, 20978–20992;
(17) K. Fukumoto and H. Ohno, *Angew. Chem. Int. Ed.*, 2007, **46**, 1852–1855;
(18) Y. Kohno, S. Saita, K. Murata, and N. Nakamura, H. Ohno, *Polym. Chem.*, 2011, **2**, 862–867;
(19) P. G. Jessop, D. J. Heldebrant, X. Li, C. A. Eckert, and C. L. Liotta, *Nature*, 2005, **436**, 1102–1102;
(20) G. J. Huddleston and R. D. Rogers, *Chem. Commun.*, 1998, 1765–1766;
(21) K. E. Gutowski, G. A. Broker, H. D. Willauer, J. G. Huddleston, R. P. Swatloski, J. D. Holbrey, and R. D. Rogers, *J. Am. Chem. Soc.*, 2003, **125**, 6632–6633;
(22) M. G. Freire, A. F. M. Cláudio, J. M. M. Araújo, J. A. P. Coutinho, I. M. Marrucho, J. N. Canongia Lopes, and L. P. N. Rebelo, *Chem. Soc. Rev.*, 2012, **41**, 4966–4995;
(23) M. G. Freire, C. M. S. S. Neves, I. M. Marrucho, J. N. Canongia Lopes, L. P. N. Rebelo, and J. A. P. Coutinho, *Green Chem.*, 2010, **12**, 1715–1718;

(24) M. G. Freire, C. L. S. Louros, L. P. N. Rebelo, and J. A. P. Coutinho, *Green Chem.*, 2011, **13**, 1536–1545;
(25) P.-A. Albertsson, *Nature*, 1958, **182**, 709–711;
(26) J. A. Asenjo and B. A. Andrews, *J. Chromatogr. A*, 2011, **1218**, 8826–8835;
(27) P. Selvakumar, T. C. Ling, S. Walker, and A. Lyddiatt, *Sep. Pur. Technol.*, 2012, **90**, 182–188;
(28) J.-K. Yan, H.-L. Ma, J.-J. Pei, Z.-B. Wang, and J.-Y. Wu, *Sep. Pur. Technol.*, 2014, **135**, 278–284;
(29) M. M. Pereira, S. N. Pedro, M. V. Quental, Á. S. Lima, J. A. P. Coutinho, and M. G. Freire, *J. Biotechnol.*, 2015, **206**, 17–25;
(30) M. Taha, M. R. Almeida, F. A. e. Silva, P. Domingues, S. P. M. Ventura, J. A. P. Coutinho, and M. G. Freire, *Chem. Eur. J.*, 2015, **21**, 4781–4788;
(31) M. Taha, F. A. e Silva, M. V. Quental, S. P. M. Ventura, M. G. Freire, and J. A. P. Coutinho, *Green Chem.*, 2014, **16**, 3149–3159;
(32) S. P. M. Ventura, R. L. F. de Barros, J. M. de Pinho Barbosa, C. M. F. Soares, A. S. Lima, and J. A. P. Coutinho, *Green Chem.*, 2012, **14**, 734–740;
(33) M. G. Freire, J. F. B. Pereira, M. Francisco, H. Rodríguez, L. P. N. Rebelo, R. D. Rogers, and J. A. P. Coutinho, *Biotechnol. J.*, 2015, **10**, 1457–1466;
(34) T. L. Greaves and C. J. Drummond, *Chem. Rev.*, 2008, **108**, 206–237;
(35) J. C. Merchuk, B. A. Andrews, and J. A. Asenjo, *J. Chromatogr. B*, Biomed.Sci. Appl., 1998, **711**, 285–293;
(36) M. G. Freire, J. F. B. Pereira, M. Francisco, H. Rodríguez, L. P. N. Rebelo, R. D. Rogers, and J. A. P. Coutinho, *Chem. Eur. J.*, 2012, **18**, 1831–1839;
(37) M. G. Freire, C. M. S. S. Neves, K. Shimizu, C. E. S. Bernardes, I. M. Marrucho, J. A. P. Coutinho, J. N. Canongia Lopes, and L. P. N. Rebelo, *J. Phys. Chem. B*, 2010, **114**, 15925–15934;
(38) J. Łachwa, J. Szydłowski, A. Makowska, K. R. Seddon, J. M. S. S. Esperança, H. J. R. Guedes, and L. P. N. Rebelo, *Green Chem.*, 2006, **8**, 262–267;
(39) S. Saita, Y. Kohno, and H. Ohno, *Chem. Commun.*, 2013, **49**, 93–95;
(40) H. Tani, T. Kamidate, and H. Watanabe, *Anal. Sci.*, 1998, **14**, 875–888;
(41) Y. Liu and R. Guo, *Biomacromolecules*, 2007, **8**, 2902–2908;
(42) M. B. Turner, S. K. Spear, J. G. Huddleston, J. D. Holbrey, and R. D. Rogers, *Green Chem.*, 2003, **5**, 443–447;
(43) K. Shimojo, K. Nakashima, N. Kamiya, and M. Goto, *Biomacromolecules*, 2006, **7**, 2–5;
(44) A. F. Cláudio, C. F. C. Marques, I. Boal-Palheiros, M. G. Freire, and J. A. P. Coutinho, *Green Chem.*, 2014, **16**, 259–268;
(45) A. F. M. Cláudio, A. M. Ferreira, M. G. Freire, and J. A. P. Coutinho, *Green Chem.*, 2013, **15**, 2002–2010;
(46) A. M. Ferreira, J. A. P. Coutinho, A. M. Fernandes, and M. G. Freire, *Sep. Pur. Technol.*, 2014, **128**, 58–66;
(47) A. Barth, *Biochim. Biophys. Acta*, 2007, **1767**, 1073–1101;
(48) K. Fujita, D. R. MacFarlane, and M. Forsyth, *Chem. Commun.*, 2005, 4804–4806;
(49) K. Fujita, D. R. MacFarlane, M. Forsyth, M. Yoshizawa-Fujita, K. Murata, N. Nakamura, and H. Ohno, *Biomacromolecules*, 2007, **8**, 2080–2086.

2.2. Good's buffers as novel phase-forming components of ionic-liquid-based aqueous biphasic systems

This chapter is based on the published manuscript

Andreia Luís, Teresa B. V. Dinis, Helena Passos, Mohamed Taha, Mara G. Freire; [1]

"Good's buffers as novel phase-forming components of ionic-liquid-based aqueous biphasic systems", Biochemical Engineering Journal 101 (2015) 142–149.

2.2.1. Abstract

Aiming at the development of self-buffering and benign extraction/separation processes, this work reports a novel class of aqueous biphasic systems (ABS) composed of ionic liquids (ILs) and organic biological buffers (Good's buffers, GBs). A large array of ILs and GBs was investigated, revealing than only the more hydrophobic and fluorinated ILs are able to form ABS. For these systems, the phase diagrams, tie-lines, tie-line lengths, and critical points were determined at 298 K. The ABS were then evaluated as alternative liquid-liquid extraction strategies for two amino acids (L-phenylalanine and L-tryptophan). The single-step extraction efficiencies for the GB-rich phase range between 22.4 and 100.0 % (complete extraction). Contrarily to the most conventional IL-salt ABS, in most of the systems investigated, the amino acids preferentially migrate to the more biocompatible and hydrophilic GB-rich phase. Remarkably, in two of the studied ABS, L-phenylalanine completely partitions to the GB-rich phase while L-tryptophan shows a preferential affinity for the opposite phase. These results show that the extraction efficiencies of similar amino acids can be tailored by the design of the chemical structures of the phase-forming components, creating thus new possibilities for the use of IL-based ABS in biotechnological separations.

2.2.2. Introduction

The development of benign separation techniques has been a hot topic of research envisaging the extraction and purification of added-value compounds from biological media.[1,2] Biocompatibility is a crucial feature in the design of these platforms, particularly when dealing with biologically active products.[3] Typical organic solvents employed in liquid-liquid extractions from aqueous media are usually highly volatile and toxic. In this context, aqueous biphasic

[1] **Contributions:** M.G.F. and H.P. conceived and directed this work. A.L. and T.B.V.D. acquired the experimental data. All authors contributed to the interpretation of the experimental data. A.L., H.P. and M.G.F. wrote the final manuscript.

systems (ABS) – liquid–liquid systems mostly composed of water – are potential alternatives for extraction and purification processes. These systems consist in two aqueous-rich phases and can be created by the mixture of two polymers, a polymer with a salt or two salts. Liquid-liquid extractions by ABS have been intensively explored and used to separate and purify several biological products[4–6] and also to recover metal ions, radiochemicals, drugs molecules, dyes, among others, from complex mixtures.[7,8]

In the last decade, it was demonstrated that ionic liquids (ILs) can be also employed as phase-forming components of ABS.[9] In general, ILs are organic salts with a melting temperature below 373 K. Due to their ionic nature, ILs display exceptional properties, such as a negligible vapor pressure, a wide liquid temperature range, a high solvating ability for a wide variety of compounds or materials, and high thermal and chemical stabilities.[10] ILs are also good extraction solvents, both neat and in aqueous solutions, and are able to increase the stability of added-value biomolecules, namely proteins, enzymes and DNA.[11–15] Taking into account these features, IL-based ABS have been extensively investigated as alternative liquid-liquid extraction processes, allowing enhanced and selective extractions.[16] These ternary systems consist of two immiscible aqueous-rich phases, and could be designed by IL + salt, IL + carbohydrate, IL + amino acid or IL + polymer pairs dissolved in aqueous solution.[12] However, most of the investigations carried out with IL-based ABS are focused on combinations of ILs and high charge density salts.[16] The major reason behind such a selection is related to the large ability of high-charge density salts, and thus to their salting-out nature, to create IL-based ABS. The salting-out effect is mostly a result of the formation of water-ion complexes that results on the "dehydration" of the IL.[17–19] Nevertheless, these systems suffer from major drawbacks resulting from the use of inorganic salts, namely their high charge-density and the creation of solutions of high ionic strength and extreme pH values that may damage the biological products, such as proteins, if buffers combinations or mixtures of salts are not employed. Moreover, the high concentration of these salts may be deleterious when discharged into aqueous effluents.[20] Even so, most studies regarding IL-based ABS comprised inorganic salts based on phosphate, carbonate and sulfate anions.[14,21–23] Most of the systems investigated lead to the formation of alkaline aqueous salt solutions (*e.g.*, with the use of K_2HPO_4, K_3PO_4, K_2CO_3, KOH, Na_2HPO_4 and NaOH).[9,21,23,24] On the other hand, the use of salt mixtures and buffered solutions with pH close to biological values has been less explored.[25,26] In this context, the phase-forming ability of IL-based ABS by the addition of non-electrolytes, self-buffering and biocompatible salting-out agents (Good's buffers, GBs) was here investigated for the first time.

GBs, recognized as inert biological buffers for biochemical and biological studies, were developed by Good and co-workers.[27–29] GBs are zwitterionic compounds consisting of *N*-substituted taurine and glycine derivatives. Most of these buffers display pK_a values between 6 and 8, have a good solubility in water, do not readily permeate through cell membranes, do not chelate with metal-ions, are chemically stable and resist to enzymatic degradation, and are easily prepared and purified from low-cost materials.[27,29,30] Taking into account the collective benefits of GBs and ILs, we propose here their combined use as phase-forming components of ABS. Among the available GBs, *N*-tris(hydroxymethyl) methylglycine (Tricine), 4-(2-hydroxyethyl)-1-piperazineethanesulfonic acid (HEPES), *N*-tris(hydroxymethyl)methyl-2-aminoethanesulfonic acid (TES), *N*-cyclohexyl-2-aminoethanesulfonic acid (CHES), and 2-(*N*-morpholino)ethanesulfonic acid (MES) were selected because they are suitable buffers for pH control in the physiological pH region (although an alkaline species needs to be added for this purpose).[29,30] Novel ternary phase diagrams for ABS composed of GBs and ILs were determined at 298 K, and their ability as novel liquid-liquid systems for extraction/purification purposes was evaluated by partition studies carried out with standard aqueous solutions of two amino acids that can be produced in fermentative medium (L-tryptophan and L-phenylalanine).[31,32]

2.2.3. Experimental procedures

Materials. The GBs investigated were Tricine (purity > 99 wt %), HEPES (purity > 99.5 wt %), TES (purity > 99 wt %), CHES (purity > 99 wt %), and MES (purity > 99 wt %), all purchased from Sigma-Aldrich. The ILs studied for ABS formation were 1-butyl-3-methylimidazolium trifluoromethanesulfonate ($[C_4C_1im][CF_3SO_3]$, purity ≥ 99 wt %), 1-butyl-3-methylimidazolium tetrafluoroborate ($[C_4C_1im][BF_4]$, purity ≥ 99 wt%), 1-butyl-3-methylimidazolium dicyanamide ($[C_4C_1im][N(CN)_2]$, purity > 98 wt%), 1-butyl-3-methylimidazolium thiocyanate ($[C_4C_1im][SCN]$, purity > 98 wt%), 1-butyl-3- methylimidazolium tosylate ($[C_4C_1im][TOS]$, purity 99 wt%), 1-ethyl-3-methylimidazolium trifluoromethanesulfonate ($[C_2C_1im][CF_3SO_3]$, purity 99 wt%), 1-ethyl-1-methylpyrrolidinium trifluoromethanesulfonate ($[C_2C_1pyr][CF_3SO_3]$, purity 99 wt%), all purchased from Iolitec. Tetrabutylphosphonium bromide ($[P_{4444}]Br$, purity > 95 wt%), kindly supplied by Cytec Industries Inc. was also investigated. To reduce the volatile impurities to negligible values, IL samples were purified under constant agitation, under vacuum, and at moderate temperature (333 K), for a minimum of 24 h. After this procedure, the purity of each IL was further checked by ^{1}H, ^{13}C and ^{19}F NMR spectra (whenever applicable) and found to be in accordance with the stated purity level provided by the suppliers. L-Tryptophan (purity > 99.0 wt %) and L-phenylalanine

(purity 99.0 wt %) were acquired from Sigma-Aldrich and Merck, respectively. Although several combinations of ILs and GBs were tested to create novel ABS, only aqueous mixtures composed of the more hydrophobic ILs ($[C_4C_1im][CF_3SO_3]$ and $[C_4C_1im][BF_4]$) and the GBs Tricine, HEPES and TES were able to form ABS. The chemical structures of the GBs and ILs able to undergo liquid-liquid demixing toward the formation of ABS, and of the amino acids used in the extraction experiments, are shown in **Figure 2.5**. The water used was double distilled, passed through a reverse osmosis system, and additionally treated with a Milli-Q plus 185 purification apparatus.

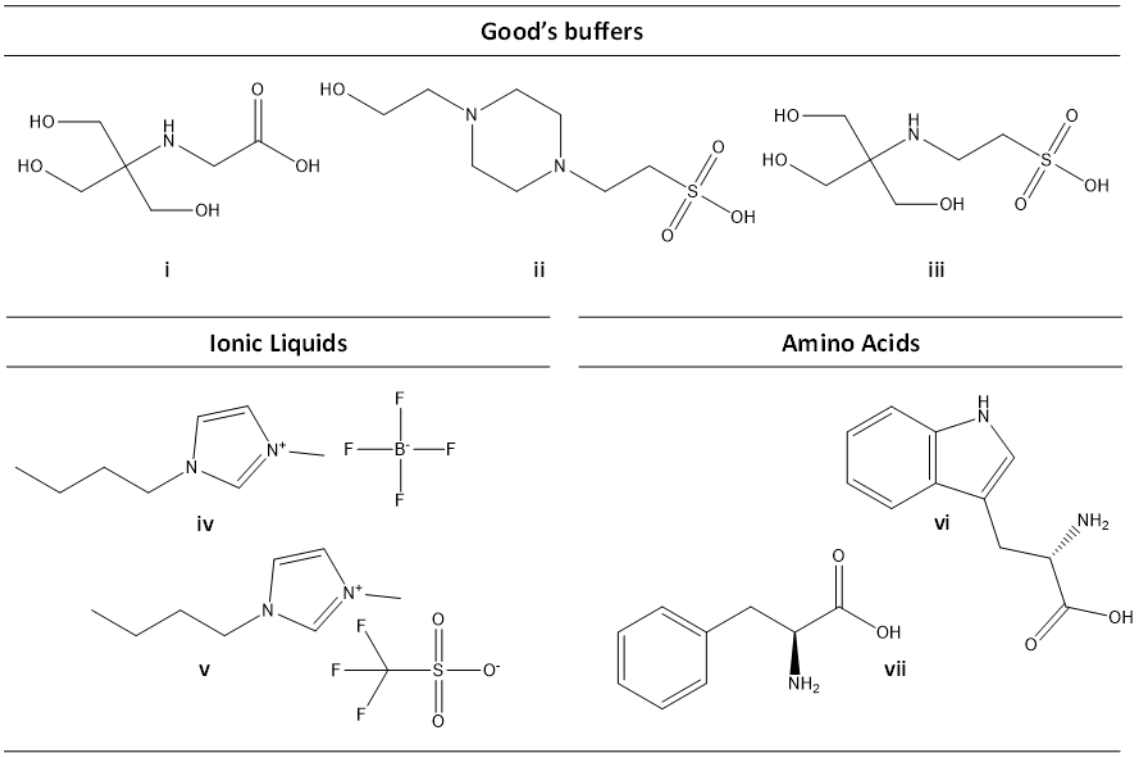

Figure 2.5. Chemical structure of the GBs, ILs and amino acids studied: (i) Tricine; (ii) HEPES; (iii) TES; (iv) $[C_4C_1im][CF_3SO_3]$; (v) $[C_4C_1im][BF_4]$; (vi) L-tryptophan; (vii) L-phenylalanine.

Phase diagrams, tie-lines and critical points. The solubility (saturation) curves were determined through the cloud point titration method[33] at (298 ± 1) K and atmospheric pressure. The experimental procedure adopted in this work follows the method already validated by us and described in **chapter 2.1**. Aqueous solutions of ILs at 80-90 wt % and aqueous solutions of the different GBs at concentrations below, yet close, to their saturation values in water (Tricine at 20 wt %, HEPES at 50 wt % and TES at 55 wt %) were prepared gravimetrically and used for the determination of the binodal curves. Repetitive drop wise addition of the aqueous IL solution to the aqueous solution of each GB was carried out until the detection of a cloudy (biphasic) mixture, followed by the drop wise addition of ultrapure water until the observation of the monophasic region (clear and limpid solution). The ternary system compositions were determined by weight

quantification within ± 10^{-4} g. The experimental binodal curves were fitted by least-squares regression according to **Equation (2.1)** presented in **chapter 2.1**.

For the determination of each tie-line (TL), a ternary mixture composed of IL + GB + water at the biphasic region was gravimetrically prepared as indicated in **chapter 2.1**, and determined through the relationship between the weight of the salted-out specie rich phase and the overall weight by the lever-arm rule using **Equations (2.2) to (2.5)**. Moreover, the tie-line length (TLL) was determined using **Equation (2.6)**.

The critical point of each system (the mixture composition at which the composition of the two aqueous phases becomes equal) was also estimated. The critical point was determined by extrapolating the TLs' slopes of distinct systems by the fitting provided by **Equation (2.7)**.[34]

$$[\mathrm{IL}] = f[\mathrm{GB}] + g \qquad \textbf{(2.7)}$$

where f and g are fitting parameters.

The pH values (±0.02) were measured at (298 ± 1) K using a Mettler Toledo SevenMultiTMdual pH meter.

Partition of amino acids. Aqueous solutions of amino acids were prepared at the concentration of 0.73 g·dm^{-3} (3.6 × 10^{-3} mol·dm^{-3}) for L-tryptophan and 0.60 g·dm^{-3} (3.6 × 10^{-3} mol dm^{-3}) for L-phenylalanine. At these concentrations, amino acids can be considered at infinite dilution and completely solvated in aqueous media, avoiding thus specific interactions between the biomolecules. The ternary mixtures compositions were chosen based on the phase diagrams determined before for each IL-GB ABS. To avoid discrepancies in the results which could arise from the different compositions of the phases, all the partition studies were performed at a constant TLL (*ca.* 50) and weight ratio (~ 0.5). Each mixture was vigorously stirred and left to equilibrate for at least 12 h (a time established in previous optimizing experiments), to achieve the complete partition of each amino acid between the coexisting phases. After a careful separation of both phases, the quantification of each amino acid in each phase was carried by UV-spectroscopy, using a BioTeck Synergy HT microplate reader, at a wavelength of 279 nm for L-tryptophan and 257 nm for L-phenylalanine using calibration curves previously established. At least three individual biphasic systems were prepared in order to determine the average in the amino acids partition coefficients and extraction efficiencies, as well as the respective standard deviations. Possible interferences of the GBs and ILs with the analytical method were taking into account, and control samples were always prepared at the same weight fraction composition, using pure water instead of the amino acid aqueous solution. The partition coefficients of L-

tryptophan (K_{Trp}) and L-phenylalanine (K_{Phe}) are defined as the ratio of the concentration of each amino acid in the GB-rich phase to that in the IL-rich phase – **Equation (2.8)**,

$$K_{\mathrm{AA}} = \frac{[AA]_{\mathrm{GB}}}{[AA]_{\mathrm{IL}}} \quad \textbf{(2.8)}$$

where $[AA]_{\mathrm{GB}}$ and $[AA]_{\mathrm{IL}}$ are the concentration of each amino acid (AA) in the GB- and in the IL-rich aqueous phases, respectively. The percentage extraction efficiency of L-tryptophan ($EE_{Trp}\%$) and L-phenylalanine ($EE_{Phe}\%$) are defined as the percentage ratio between the amount of amino acid in the GB-rich aqueous phase and that in the total mixture, according to **Equation (2.9)**.

$$EE_{\mathrm{AA}}\% = \frac{w_{AA}^{GB}}{w_{AA}^{GB} + w_{AA}^{IL}} \quad \textbf{(2.9)}$$

where w_{AA}^{GB} and w_{AA}^{IL} are the weight of amino acid in the GB-rich and in the IL-rich aqueous phase, respectively.

2.2.4. Results and discussion

Phase diagrams, tie-lines and critical points. Novel ternary phase diagrams were determined in this work, and the respective solubility curves are illustrated in **Figure 2.6**. The detailed experimental weight fraction data are given in the **Appendix A**. In the studied ABS, the bottom phase corresponds to the IL-rich phase, while the top phase is mainly composed of GB and water. The only exception was observed with the ABS composed of $[C_4C_1im][BF_4]$ + TES + H_2O. The identification of the IL-rich phase in each system was carried out by UV-spectroscopy.

Although a large range of ILs was investigated, only those composed of $[CF_3SO_3]$- and $[BF_4]$-anions coupled to the imidazolium cation with a longer alkyl side chain (at least butyl) were able to form ABS with GBs. This is a result of the weak salting-out ability of the GBs for instance when compared with high-charge density salts,[16] and agrees with previous results on the formation of IL-based ABS with weaker salting-out species, such as carbohydrates[35] or amino acids.[36] The GBs seem to be preferentially hydrated and lead to the "dehydration" of the IL and to the formation of a second liquid phase taking into account that only the most hydrophobic ILs are able to form ABS. In **Figure 2.6**, the solubility curves are presented in weight fraction, whereas their representation in molality units is provided in the **Appendix A**. However, it should be highlighted that the same trend on the ILs and GBs ability to form ABS is observed in both units. In all phase diagrams, the biphasic region is localized above the solubility curve whereas the monophasic

region corresponds to compositions described below the solubility curve. The larger the biphasic region, the higher the ability of the IL or GB to undergo liquid-liquid demixing.

For the studied systems, the experimental binodal data were further fitted by the empirical relationship described by **Equation (2.1)**. The regression parameters A, B and C were estimated by the least squares regression method, and their values and corresponding standard deviations (σ) are provided in **Table 2.1**. In general, good correlation coefficients were obtained for all systems, indicating that these fittings can be used to estimate the phase diagram in a region where no experimental results are available. The representation of the fitting by **Equation (2.1)** is also depicted in **Figure 2.6**. Additionally, the critical point of each system was determined and is represented in **Figure 2.6** – detailed data are given in the **Appendix A**. The compositions of the coexisting phases become equal at concentrations of GB ranging between 3.87 and 22.35 wt % and at concentrations of IL ranging from 41.12 to 51.07 wt %. The critical point is more dependent on the concentration of the GB than on the IL composition and, in general, the concentration of IL at the critical point is higher for systems with less ability to form ABS.

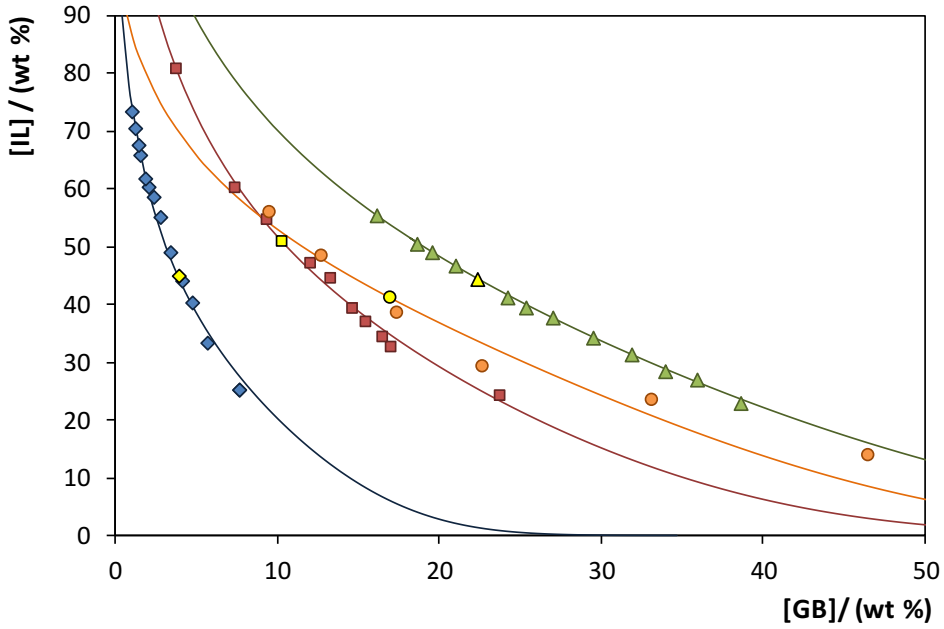

Figure 2.6. Phase diagrams at 298 K for the ABS composed of $[C_4C_1im][BF_4]$ + Tricine + H_2O (◆); $[C_4C_1im][BF_4]$ + HEPES + H_2O (■); $[C_4C_1im][BF_4]$ + TES + H_2O (●); and $[C_4C_1im][CF_3SO_3]$ + HEPES + H_2O (▲). The lines represent the fitting of the experimental data by **Equation (2.1)** (–) and the yellow symbols represent the critical point of each system.

Table 2.1. Correlation parameters used to describe the experimental binodal data by **Equation (2.1)** and respective standard deviation (σ).

GB	$A \pm \sigma$	$B \pm \sigma$	$10^5(C \pm \sigma)$	R^2
$[C_4C_1im][BF_4]$ + GB				
Tricine	125.6 ± 4.8	-0.517 ± 0.027	18.48 ± 9.28	0.9922
HEPES	159.3 ± 8.0	-0.351 ± 0.019	1.60 ± 0.68	0.9941
TES	108.6 ± 40.7	-0.224 ± 0.107	1.00 ± 0.70	0.9535
$[C_4C_1im][CF_3SO_3]$ + GB				
HEPES	158.0 ± 8.1	-0.256 ± 0.013	5.50 ± 0.59	0.9992

The experimental TLs, along with their respective length (TLL), as well as the pH values of both phases in each ABS, and for the compositions for which the TLs were determined, are given in **Table 2.2**. An example of the TLs obtained is depicted in **Figure 2.7**, while the TLs for the remaining systems are depicted in the **Appendix A**.

Table 2.2. Experimental data for TLs, TLLs and pH of the coexisting phases of the investigated ABS.

GB	Weight fraction composition / wt %								TLL
	$[IL]_{IL}$	$[GB]_{IL}$	pH_{IL}	$[IL]_{M}$	$[GB]_{M}$	$[IL]_{GB}$	$[GB]_{GB}$	pH_{GB}	
$[C_4C_1im][BF_4]$ + GB									
Tricine	52.70	2.79	5.09	39.73	5.98	15.11	12.04	4.82	38.71
	56.15	2.41	3.72	38.19	7.54	6.62	16.56	3.62	51.52
	60.47	1.99	3.77	38.21	9.05	2.56	20.36	3.65	60.76
HEPES	71.60	5.16	5.00	49.07	13.39	26.38	21.68	5.21	48.14
	85.67	3.12	5.56	38.06	19.94	19.31	26.57	5.13	70.38
	88.89	2.76	5.53	37.87	21.93	14.18	30.82	5.48	79.80
TES	58.80	7.42	2.05	43.51	17.04	28.66	26.38	2.00	35.61
	65.50	5.08	4.37	43.67	18.56	22.48	31.65	3.94	50.56
	72.26	3.31	2.34	43.44	19.97	21.12	32.88	1.95	59.08
$[C_4C_1im][CF_3SO_3]$ + GB									
HEPES	69.49	10.19	5.21	51.14	20.96	28.18	34.44	5.15	47.90
	82.58	6.42	6.08	49.72	24.88	20.85	41.21	5.95	70.86
	90.64	4.72	5.87	43.88	30.26	17.60	44.61	5.81	83.22

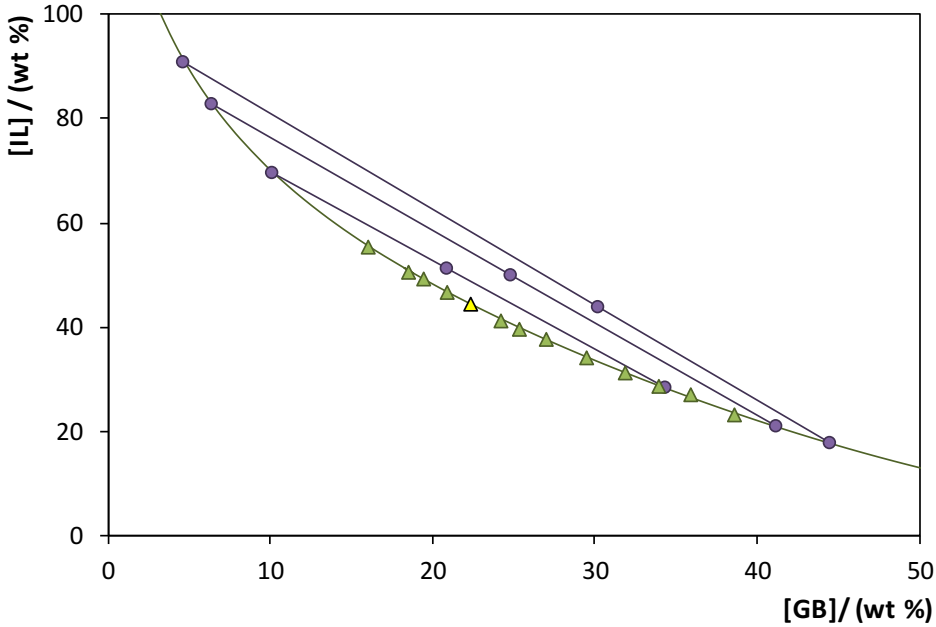

Figure 2.7. Phase diagram for the ternary system composed of $[C_4C_1im][CF_3SO_3]$ + HEPES + H_2O: binodal data (▲); TL data (●); critical point (▲); adjusted binodal data through **Equation (2.1)** (–).

The pH values of these systems are in the acidic region due to the acidic nature of the pure GBs (aqueous solutions of 30 wt % of HEPES, TES, and Tricine present pH values from 3 to 5 as determined by us). The pH values determined for the coexisting phases of the IL-based ABS range between 2 and 6, with an average pH value of circa 4.9. Although not attempted in this work, it should be stressed that the pH of these systems can be adjusted to the physiological pH range by the addition of an alkaline species.[26] However, acidic ABS are particularly valuable for the extraction of high-value compounds with low acidic dissociation constants to guarantee their neutral form.[37] The ABS studied in this work are also a particular class of acidic systems, since most works in the literature on IL-based ABS display alkaline coexisting phases that may be deleterious to a number of pH sensitive biomolecules.[21,38]

Figure 2.6 depicts the effect of different GBs in the formation of ABS. For instance, at 40 wt % of $[C_4C_1im][BF_4]$, the ability of the GBs to undergo liquid-liquid demixing follows the trend: Tricine » HEPES > TES. Overall, a decrease on the hydrophobicity of the GB was expected to facilitate the creation of ABS. The log(K_{OW}) values of each buffer are, respectively, -3.11 for HEPES, -4.48 for TES, and -5.25 for Tricine.[39] Although all the GBs investigated are quite hydrophilic, the trend observed for the ABS formation does not follow the K_{ow} values. Moreover, if Tricine is the GB with the highest ability to form ABS with $[C_4C_1im][BF_4]$, the same should be observed with $[C_4C_1im][CF_3SO_3]$. Instead, with $[C_4C_1im][CF_3SO_3]$, only the most hydrophobic GB (HEPES) revealed to be able to induce liquid-liquid demixing. It should be highlighted that more hydrophobic GBs,

namely MES ($\log(K_{OW})$ = -2.49) and CHES ($\log(K_{OW})$ = -0.59),[39] were also tested with both ILs, although no phase separation was observed. Even so, and since only highly hydrophobic and fluorinated ILs were able to form ABS, the overall results seem to indicate that GBs display a higher affinity for water compared to the ILs, and thus, there is the preferential exclusion of the IL from the aqueous solution leading to the formation of ABS. However, and in general, it seems that more complex interactions between the GBs and the ILs, in addition to preferential hydration of the GBs, are taking place.

The formation of ABS depends also on the type of IL. In the studied phase diagrams it is possible to observe that the IL $[C_4C_1im][BF_4]$ is more able to form ABS than $[C_4C_1im][CF_3SO_3]$. $[C_4C_1im][CF_3SO_3]$ was only able to form ABS with HEPES, while solid-liquid equilibrium was observed when this IL is mixed with aqueous solutions of Tricine or TES in the whole composition range. It should be remarked that although $[C_4C_1im][BF_4]$ is not the best candidate to form ABS, since it may suffers hydrolysis when in aqueous media,[40] the pH values presented in **Table 2.2** support that if hydrolysis occurs, it is very limited – at least within the 12 h of equilibrium used for the determination of the TLs. In fact, the pH values of the coexisting phases corresponding to the system formed by $[C_4C_1im][BF_4]$ + HEPES are very similar to those displayed by the water-stable IL $[C_4C_1im][CF_3SO_3]$. Even though other ILs should be more adequate to form ABS, and as attempted and explored in this work with $[C_4C_1im][N(CN)_2]$, $[C_4C_1im][SCN]$, $[P_{4444}]Br$, $[C_4C_1im][TOS]$, $[C_2C_1im][CF_3SO_3]$ and $[C_2C_1pyr][CF_3SO_3]$, these were not able to form ABS with GBs, and thus IL-GBs ABS are confined to highly hydrophobic and fluorinated ILs.

It was already demonstrated that $[C_4C_1im][CF_3SO_3]$ could form IL-based ABS with others salting-out agents, such as salts, *e.g.* NaCl,[41] carbohydrates,[35] amino acids (L-lysine, D,L-lysine HCl and L-proline)[36] and polymers.[42] **Figure 2.8** depicts the comparison on the capacity of GBs to induce liquid-liquid demixing of $[C_4C_1im][CF_3SO_3]$ aqueous solutions against the previously reported salting-out agents.[35,36,41,42] The results are shown in molality units to avoid distortions on the ability of the phase forming components to create ABS as a result of their different molecular weights. The ability of HEPES to induce ABS is quite similar to that afforded by a weak salting-out salt such as NaCl (the solubility curves almost overlap). On the other hand, the polymer PEG 2000, L-lysine or D-(+)-glucose display a higher ability to form ABS (larger biphasic regions above the solubility curves), whereas L-proline and D-(+)-xylose are weaker salting-out species than HEPES (smaller biphasic regions).

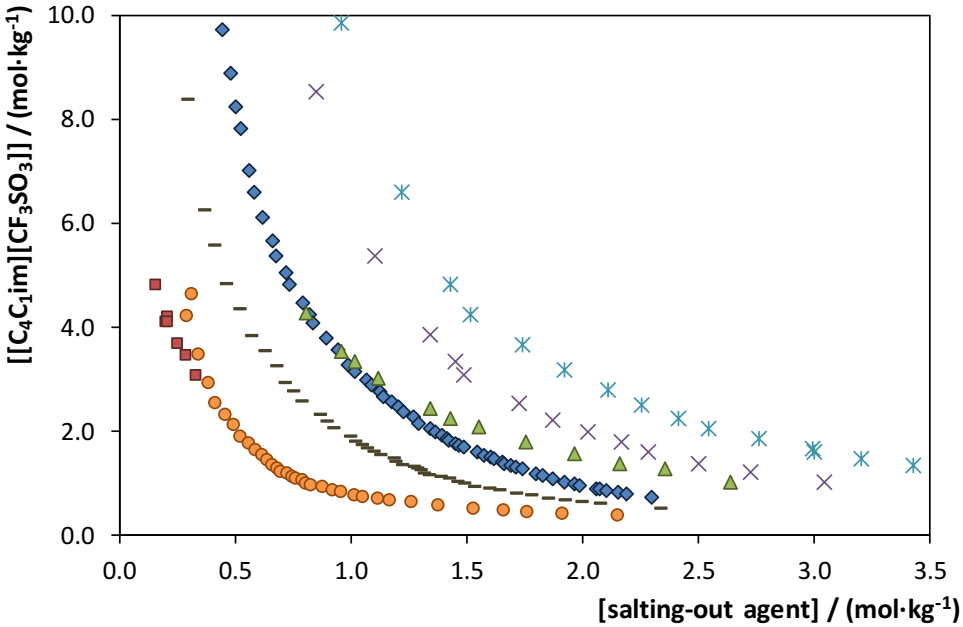

Figure 2.8. Phase diagrams for ABS composed of $[C_4C_1im][CF_3SO_3]$ and different salting-out agents: PEG 2000 (■); L-lysine (●); D-(+)-glucose (–); NaCl (◆); HEPES (▲); D-(+)-xylose (×); and L-proline (✳).

Although a few number of GBs and ILs presented the capacity to create ABS, it should be highlighted that their characteristics, such as the possibility of adjusting the pH of the systems to the physiological pH range, make of these systems a potential route for the recovery and purification of value-added biomolecules.

Extraction of amino acids. **Figure 2.9** depicts the percentage extraction efficiencies of L-tryptophan and L-phenylalanine in several IL-based ABS for the GB-rich phase. The results obtained for the partition coefficients of L-tryptophan and L-phenylalanine are illustrated in the **Appendix A**. The composition of the coexisting phases corresponding to the initial mixtures of $[C_4C_1im][CF_3SO_3]$ + HEPES (36 wt % of HEPES, 30 wt % of IL, and 34 wt % of water), $[C_4C_1im][BF_4]$ + HEPES (13.5 wt % of HEPES, 49 wt % of IL, and 37.5 wt % of water), $[C_4C_1im][BF_4]$ + TES (19 wt % of TES, 43 wt % of IL, and 38 wt % of water) and for $[C_4C_1im][BF_4]$ + Tricine (9 wt % of Tricine, 38 wt % of IL, and 53 wt % of water) used in the partition experiments are provided in **Table 2.2**. All the experiments were performed at a constant TLL (*ca.* 50) and weight ratio ($\alpha \sim 0.5$). The extraction efficiencies of L-tryptophan (EE_{Trp}%) and L-phenylalanine (EE_{Phe}%) for the GB-rich phase range between 22.4 and 100.0 %. These results reveal that the partition of the two amino acids depends either on the IL or on the GB that compose a given ABS.

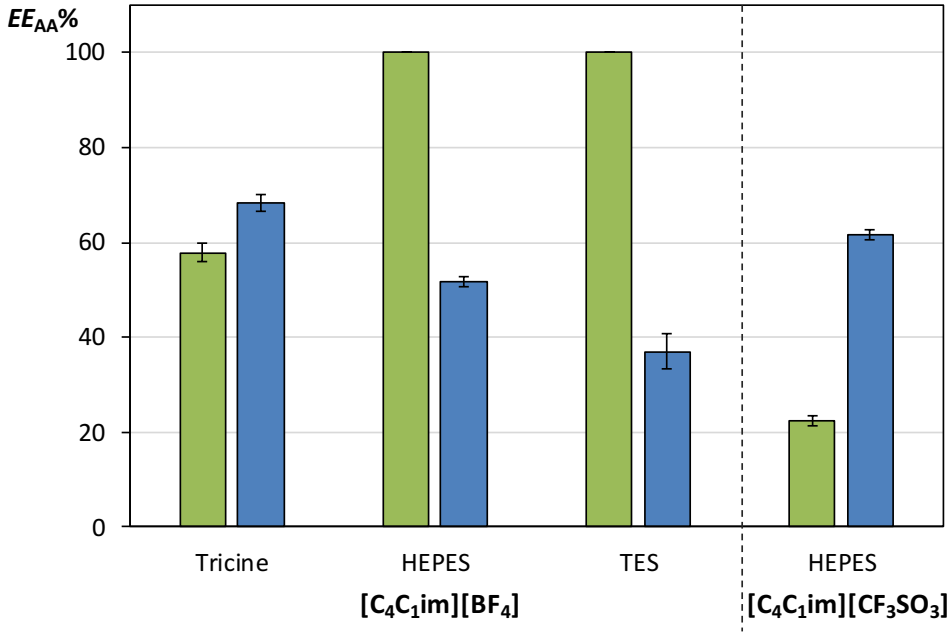

Figure 2.9. Percentage extraction efficiencies of amino acids between the IL- and GB-rich aqueous phases at 298 K: L-phenylalanine (green bars) and L-tryptophan (blue bars).

The octanol-water partition coefficients (K_{ow}) of both amino acids are very similar and their values translate their hydrophilic character ($\log(K_{ow})_{Trp}$ = -1.06 and $\log(K_{ow})_{Phe}$ = -1.38).[43] In most situations, there is a preferential partition of both amino acids for the GB-rich phase – the most hydrophilic phase as can be ascertained by the water content in the coexisting phases given in **Table 2.2**. The extraction efficiency of L-tryptophan for the GB-rich phase follows the trend: $[C_4C_1im][BF_4]$–Tricine > $[C_4C_1im][CF_3SO_3]$–HEPES > $[C_4C_1im][BF_4]$–HEPES > $[C_4C_1im][BF_4]$–TES. On the other hand, the trend observed for L-phenylalanine is: $[C_4C_1im][BF_4]$–HEPES $[C_4C_1im][BF_4]$–TES > $[C_4C_1im][BF_4]$–Tricine > $[C_4C_1im]$ $[CF_3SO_3]$–HEPES.

At the pH of the coexisting phases of the ABS studied, both amino acids are predominately on their zwitterionic form (with no net charge) – for L-tryptophan: pK_a^1 = 2.38 and pK_a^2 = 9.39; and for L-phenylalanine: pK_a^1 = 2.13 and pK_a^2 = 8.62.[43] Consequently, the partition results obtained in this work are related with the affinity of each amino acid for the coexisting phases ruled by H-bonding and dispersive forces. Aqueous biphasic systems composed of polymer + salt, polymer + IL and salt + IL were already evaluated for the extraction of amino acids. For instance, partition coefficients for tryptophan of ≈1 in conventional polymer–polysaccharides,[44] between 1 and 7 in polymer–salt[22] and between 10 and 120 in IL–salt[45] ABS were already reported.

Zafarani-Moattar and Hamzehzadeh[46] also determined the partition coefficients of several amino acids in ABS composed of 1-butyl-3-methylimidazolium bromide ($[C_4C_1im]Br$) and potassium citrate at 298 K as a function of the pH of the aqueous media. The authors[46] concluded

that dispersive interactions were the main driving force for the amino acids partition, although salting-out effects and electrostatic interactions also play a role. Nevertheless, in ABS composed of IL and salts, *e.g.* potassium citrate or potassium phosphate, aromatic amino acids always preferentially migrate for the IL-rich phase.[33,38,45] It was previously suggested that hydrophilic imidazolium-based ILs are good at extracting aromatic amino acids due to preferential $\pi \cdots \pi$ and H-bonding interactions.[33,38,45] In this work, and though in presence of imidazolium-based ILs, both phenylalanine and tryptophan do not always preferentially partition toward the IL-rich phase. Therefore, in previous works,[33,38,45] the salting-out effect afforded by the high-charge density salt must play a major role whereas, in this work, there is a more delicate balance between the favorable $\pi \cdots \pi$ interactions with the IL-rich phase and H-bonding interactions that can occur between the amino acids and all the phases components. Even though the chemical structure of carbohydrates was found to be negligible in the extraction of L-tryptophan with ABS formed by $[C_4C_1im][CF_3SO_3]$ and a wide range of monosaccharides, disaccharides and polyols,[35] in IL-GB-based ABS the chemical structure of the GB seems to be an important factor.

Outstanding results were achieved with ABS composed of $[C_4C_1im][BF_4]$ and HEPES or TES, where the total recovery of L-phenylalanine to the GB-rich phase was observed in a single-step ($EE_{Phe}\%$ = 100 %). These two systems have the additional interest of L-tryptophan showing a preferential affinity for the IL-rich phase. Based on these results, it can be envisaged that these systems can be optimized to reach a complete selective extraction, in a single-step, by the optimization of the mixture composition and pH of the coexisting phases. Furthermore, successive extractions can be applied to improve the separation of both amino acids, as well as by the use of more complex technologies, such as centrifugal partition chromatography (CPC).[47] In summary, these systems open the possibility to deal with the selective separation of complex mixtures of amino acids, for instance from a fermentation broth or from hydrolyzed peptide mixtures.

Although the preferential migration of aromatic amino acids was not observed for the IL-rich phase, as observed before with IL + salt[33,38,45,48] and IL + carbohydrate[35] ABS, it should be remarked that partition coefficients of L-tryptophan and L-phenylalanine similar to those observed in polymer-salt-based ABS[22] have been obtained, and up to complete extraction, in a single-step. Moreover, the IL-GB ABS studied here allow a tailoring on the extraction of similar amino acids by an adequate manipulation of the chemical structure of either the IL or GB. Finally, the amino acids can be enriched in a benign and biocompatible GB-rich phase instead of the usual IL-rich phase.

The scalability of ABS is a well-known feature. For instance, Kroner *et al.*[49] reported the application of polymer-based ABS on the purification of formate dehydrogenase from *Candida boidinii*, while Selber *et al.*[50] showed the application of detergent-based ABS on the purification of a fusion protein. The easiness in scaling-up and the almost non-existence of instrumental complexity supports the high potential of ABS as integrated extraction and purification strategies.

2.2.5. Conclusions

The extraction and purification of (bio)molecules by means of ABS is a promising approach due their water-rich environment and inherent biocompatibility. In the past decade, IL-based ABS have been studied as novel extraction routes while being able to demonstrate an outstanding performance on the extraction and purification of a large variety of compounds; yet, most of the IL-based ABS investigated are formed with high-charge density inorganic salts. Aiming at developing self-buffering and more biocompatible liquid-liquid extraction systems, in this work, we proposed the use of GBs as novel phase-forming components of IL-based ABS. A large array of ILs and GBs was investigated and, for the systems able to form ABS, the respective ternary phase diagrams, TLs, TLLs and critical points were determined. In general, only highly hydrophobic and fluorinated ILs are able to undergo liquid-liquid demixing with GBs in aqueous media.

The applicability of these ABS was also evaluated through the determination of the extraction efficiencies of two amino acids (L-tryptophan and L-phenylalanine) usually produced by fermentation processes. Contrarily to the most previously investigated IL-salt ABS, in most situations, the amino acids preferentially partition to the more hydrophilic GB-rich phase. The extraction efficiencies obtained range between 22 % and 100 %, and are highly dependent on the IL and GB chemical structures. Outstanding results were obtained with the systems formed by $[C_4C_1im][BF_4]$ and HEPES or TES, where the complete extraction of L-phenylalanine for the GB-rich phase was observed in a single-step, while L-tryptophan preferentially migrates for the opposite phase. These results confirm a tailoring ability of the novel IL-GB ABS which can be useful in the selective extraction of mixtures of amino acids in biotechnological separations.

2.2.6. References

(1) M. Rito-Palomares, *J. Chromatogr. B*, 2004, **807**, 3–11;
(2) R.M. Banik, A. Santhiagu, B. Kanari, C. Sabarinath, and S.N. Upadhyay, *World J. Microb. Biot.*, 2003, **19**, 337–348;
(3) D.E. Gloria, K. Regina, and R.M. Douglas, *Ionic Liquids: From Knowledge to Application*, 2009, Chapter 6, pp. 95–105;
(4) P.A. Albertsson, *Partitioning of cell particles and macromolecules*, 3rd ed., New York, 1986;

(5) H. Walter, D.E. Brooks, and D. Fisher, *Partitioning in Aqueous Two-Phase System*, Academic Press, 1985;
(6) B.Y. Zaslavsky, *Aqueous Two-phase Partitioning*, *Physical Chemistry and Bioanalytical Applications*, CRC, Press, New York, 1995;
(7) R.D. Rogers, J. Zhang, New T*echnologies for Metal Ion Separations Polyethylene Glycol Based-aqueous Biphasic Systems and Aqueous Biphasic Extraction Chromatography*, in: J.A. Marinsky, Y. Marcus (Eds.), Dekker, New York, 1997, pp. 141–193;
(8) H.D. Willauer, J.G. Huddleston, and R.D. Rogers, *Ind. Eng. Chem. Res.*, 2002, **41**, 2591–2601;
(9) K.E. Gutowski, G.A. Broker, H.D. Willauer, J.G. Huddleston, R.P. Swatloski, J.D. Holbrey, and R.D. Rogers, *J. Am. Chem. Soc.*, 2003, **125**, 6632–6633;
(10) P. Wasserscheid and T. Welton, *Ionic Liquids in Synthesis*, Wiley-VCH Verlag GmbH & Co. KGaA, Weinheim, 2002;
(11) N. Debeljuh, C.J. Barrow, L. Henderson, and N. Byrne, *Chem. Commun.*, 2011, **47**, 6371–6373;
(12) I. Khimji, K. Doan, K. Bruggeman, P.-J.J. Huang, P. Vajha, and J. Liu, *Chem. Commun.*, 2013, **49**, 4537–4539;
(13) A. Kumar and P. Venkatesu, *Chem. Rev.*, 2012, **112**, 4283–4307;
(14) M. Taha, F.A. e Silva, M.V. Quental, S.P.M. Ventura, M.G. Freire, and J.A.P. Coutinho, *Green Chem.*, 2014, **16**, 3149–3159;
(15) R.M. Vrikkis, K.J. Fraser, K. Fujita, D.R. MacFarlane, and G.D. Elliott, *J. Biomech. Eng.*, 2009, **131**, 074514–074518;
(16) M.G. Freire, A.F.M. Cláudio, J.M.M. Araújo, J.A.P. Coutinho, I.M. Marrucho, J.N.C. Lopes, and L.P.N. Rebelo, *Chem. Soc. Rev.*, 2012, **41**, 4966–4995;
(17) M.G. Freire, P.J. Carvalho, A.M.S. Silva, L.M.N.B.F. Santos, L.P.N. Rebelo, I.M. Marrucho, and J.A.P. Coutinho, *J. Phys. Chem. B*, 2009, **113**, 202–211;
(18) M.G. Freire, C.M.S.S. Neves, A.M.S. Silva, M.N.B.F. Santos, I.M. Marrucho, P.N. Rebelo, J.K. Shah, and E.J. Maginn, *J. Phys. Chem. B*, 2010, **114**, 2004–2014;
(19) L.I.N. Tomé, R. Varanda, M.G. Freire, and I.M. Marrucho, *J. Phys. Chem. B*, 2009, **113**, 2815–2825;
(20) S. Abdolrahimi, B. Nasernejad, and G. Pazuki, *Phys. Chem. Chem. Phys.*, 2015, **17**, 655–669;
(21) T. Mourão, A.F.M. Cláudio, I. Boal-Palheiros, M.G. Freire, and J.A.P. Coutinho, *J. Chem. Thermodyn.*, 2012, **54**, 398–405;
(22) A. Salabat, M.H. Abnosi, and A. Motahari, *J. Chem. Eng. Data*, 2008, **53**, 2018–2021;
(23) Y. Wang, X. Xu, Y. Yan, J. Han, and Z. Zhang, *Thermochim. Acta*, 2010, **501**, 112–118;
(24) C. He, S. Li, H. Liu, K. Li, and F. Liu, *J. Chromatogr. A*, 2005, **1082**, 143–149;
(25) S.P.M. Ventura, S.G. Sousa, L.S. Serafim, Á.S. Lima, M.G. Freire, and J.A.P. Coutinho, *J. Chem. Eng. Data*, 2011, **56**, 4253–4260;
(26) S.P.M. Ventura, S.G. Sousa, L.S. Serafim, Á.S. Lima, M.G. Freire, and J.A.P. Coutinho, *J. Chem. Eng. Data*, 2012, **57**, 507–512;
(27) W.J. Ferguson, K.I. Braunschweiger, J.R. Smith, J.J. McCormick, and C.C. Wasmann, *Anal. Biochem.*, 1980, **104**, 300–310;
(28) E. Good and S. Izawa, *Methods Enzymol.*, 1972, **24**, 53–68;
(29) N.E. Good, G.D. Winget, W. Winter, T.N. Connolly, S. Izawa, and R.M.M. Sing, *Biochemistry*, 1966, **5**, 467–477;
(30) A.A. Shah and I.B. Henson, *J. Chem. Eng. Data*, 2011, **56**, 4126–4132;
(31) K. Nakayama, L. Hagino. *Process for producing l-tryptophan*. US3849251A, 1974.
(32) T. Tsuchida, K. Sano. *Method for producing l-phenylalanine by fermentation*. US4407952 A, 1983.
(33) C.M.S.S. Neves, S.P.M. Ventura, M.G. Freire, I.M. Marrucho, and J.A.P. Coutinho, *J. Phys. Chem. B*, 2009, **113**, 5194–5199;

(34) J.C. Merchuk, B.A. Andrews, and J.A. Asenjo, *J. Chromatogr. B. Biomed. Sci. Appl.*, 1998, **711**, 285–293;
(35) M.G. Freire, C.L.S. Louros, L.P.N. Rebelo, and J.A.P. Coutinho, *Green Chem.*, 2011, **13**, 1536–1545;
(36) M. Domínguez-Pérez, L.I.N. Tomé, M.G. Freire, I.M. Marrucho, O. Cabeza, and J.A.P. Coutinho, *Sep. Purif. Technol.*, 2010, **72**, 85–91;
(37) A.F.M. Cláudio, A.M. Ferreira, S. Shahriari, M.G. Freire, and J.A.P. Coutinho, *J. Phys. Chem. B*, 2011, **115**, 11145–11153;
(38) H. Passos, A.R. Ferreira, A.F.M. Cláudio, J.A.P. Coutinho, and M.G. Freire, *Biochem. Eng. J.*, 2012, **67**, 68–76;
(39) ChemSpider – The free chemical database, 2012, www.chemspider.com;
(40) M.G. Freire, C.M.S.S. Neves, I.M. Marrucho, J.A.P. Coutinho, and A.M. Fernandes, *J. Phys. Chem. A*, 2010, **114**, 3744–3749;
(41) S. Shahriari, C.M.S.S. Neves, M.G. Freire, and J.A.P. Coutinho, *J Phys Chem B.*, 2012, **116**, 7252–7258;
(42) M.G. Freire, J.F.B. Pereira, M. Francisco, H. Rodríguez, L.P.N. Rebelo, R.D. Rogers, and J.A.P. Coutinho, *Chemistry*, 2012, **18**, 1831–1839;
(43) J. Wang, Y. Pei, Y. Zhao, and Z. Hu, *Green Chem.*, 2005, **7**, 196–202;
(44) M. Lu and F. Tjerneld, *J. Chromatogr. A*, 1997, **766**, 99–108;
(45) S.P.M. Ventura, C.M.S.S. Neves, M.G. Freire, I.M. Marrucho, J. Oliveira, and J.A.P. Coutinho, *J. Phys. Chem. B*, 2009, **113**, 9304–9310;
(46) M.T. Zafarani-Moattar and S. Hamzehzadeh, *Biotechnol. Prog.*, 2011, **27**, 986–997;
(47) I.A. Sutherland, *J. Chromatogr. A*, 2007, **1151**, 6–13;
(48) J.F.B. Pereira, A.S. Lima, M.G. Freire, and J.A.P. Coutinho, *Green Chem.*, 2010, **12**, 1661–1669;
(49) K.H. Kroner, H. Schütte, W. Stach, and M.R. Kula, *J. Chem. Technol. Biotechnol.*, 1982, **32**, 130–137;
(50) K. Selber, F. Tjerneld, A. Collén, T. Hyytiä, T. Nakari-Setälä, M. Bailey, R. Fagerström, J. Kan, J. van der Laan, M. Penttilä, and M.-R. Kula, *Process Biochem.*, 2004, **39**, 889–896.

2.3. Ionic liquids mixtures as an alternative approach to enhance the tunability of aqueous biphasic systems

This chapter is based on an ongoing work with the following authors involved: Helena Passos, Teresa B. V. Dinis, Mara G. Freire and João A. P. Coutinho.[1]

2.3.1. Abstract

With the aim of manipulating the coexisting phases' polarities and aqueous biphasic systems (ABS) ability to undergo liquid-liquid demixing, mixtures of two ILs with a common cation and different anions were investigated in this work. In a first attempt, novel phase diagrams were determined and characterized for systems composed of K_2CO_3, water and mixtures of 1-butyl-3-methylimidazolium trifluoromethanesulfonate ($[C_4C_1im][CF_3SO_3]$) and 1-butyl-3-methylimidazolium chloride ($[C_4C_1im]Cl$) at different mole fractions. The behavior of these new systems was compared to that of the ABS composed of pure ILs. The partition and extraction behavior of L-tryptophan and L-tyrosine were also evaluated to infer on the tunability of the systems selective extraction through the use of ILs mixtures at different molar proportions. The results suggest that, depending on the inorganic salt concentration in a quaternary mixture, each IL anion has a region where its effect prevails over the other. Furthermore, this behavior makes ABS composed of ILs mixtures a promising strategy for developing more selective separation platforms.

2.3.2. Introduction

Ionic liquids (ILs) are salts with low melting points that found application in several areas, such as in organic and inorganic synthesis,[1,2] catalysis,[3] energy applications,[4] separations,[5] among others. Despite their unique properties, one of the main reasons behind the increased interest on ILs resides in the ability of tuning the ILs physical and chemical properties to fulfill a specific application, through an appropriate ion selection, and with more than 10^6 different possibilities. This characteristic gave to ILs the denomination of "designer solvents".[6] However, in the last few years, an extension of this concept has been addressed – the use of IL-IL mixtures to fine-tuning their properties.[7]

Several authors proposed the use of IL-IL mixtures to improve ILs target properties while, at the same time, expand their favorable characteristics.[7,8] The application of some of these IL

[1]**Contributions:** M.G.F. and J.A.P.C. conceived and are directing this work. H.P. and T.B.V.D. acquired the experimental data. H.P., J.A.P.C. and M.G.F interpreted the experimental data obtained up to date.

mixtures already showed promising results in areas such as liquid-liquid extraction,[9-11] gas solubility,[12,13] batteries,[14] solar cells,[15,16] solvent reaction media,[17,18] and as gas chromatography stationary phases.[19] Furthermore, the IL mixtures characterization has been addressed and physicochemical properties such as the excess volume and enthalpy, density, viscosity, conductivity, diffusivity, surface tension and refractive index were already evaluated.[20-25] It was observed that, for most of these properties, IL mixtures present a "simple" mixing behavior, with a quasi-linear trend of each property as a function of the concentration between the two pure ILs.[20,21,23-25] However, not only nearly ideal mixing behaviors were found, but also non-ideal mixing behaviors were observed,[20,25] to the extent that some of these mixtures prove to be mutual insoluble,[25,26] suggesting that IL-IL mixtures are a new and broad research area.

In the past decade, ILs were introduced as phase-forming components and as promising replacements of polymers in aqueous biphasic systems (ABS).[27] Due to the wide variety of their chemical structures, the introduction of ILs in ABS allows to overcome the narrow hydrophilic-hydrophobic range of polymer-based ABS. As a result, IL-based ABS have shown to provide higher extractions performance and increased selectivity for a wide variety of compounds.[28] Phase diagrams and possible applications of ABS composed of ILs and salts were extensively investigated and it is now accepted that the phases' demixing ability and polarities of the coexisting phases are largely dependent on the IL anion hydrogen-bond basicity.[28] Thus, the tuning of ABS phases properties is frequently achieved by the IL anion change. In this context, and taking into account the potential of IL-IL mixtures already demonstrated in the literature, the present work has as main goal the evaluation on the use of mixtures of two imidazolium-based ILs, in the upper and lower range limit of hydrogen-bond basicities, in the preparation of ABS for the fine tuning of their phases polarities.

2.3.3. Experimental procedures

Materials. The ABS studied in this work were established by using aqueous solutions of potassium carbonate, K_2CO_3 (99 wt % pure from Sigma-Aldrich), and different aqueous solutions of the following hydrophilic imidazolium-based ILs: 1-butyl-3-methylimidazolium trifluoromethanesulfonate, $[C_4C_1im][CF_3SO_3]$ (99 wt %), 1-butyl-3-methylimidazolium thiocyanate, $[C_4C_1im][SCN]$ (>98 wt %), 1-butyl-3-methylimidazolium tosylate, $[C_4C_1im][TOS]$ (99 wt %), 1-butyl-3-methylimidazolium dicyanamide, $[C_4C_1im][N(CN)_2]$ (>98 wt %) 1-butyl-3-methylimidazolium ethylsulfate, $[C_4C_1im][C_2H_5SO_4]$ (98 wt %), 1-butyl-3-methylimidazolium methylsulfate, $[C_4C_1im][CH_3SO_4]$ (99 wt %), 1-butyl-3-methylimidazolium bromide, $[C_4C_1im]Br$ (99 wt %), 1-butyl-

3-methylimidazolium dimethylphosphate, $[C_4C_1im][DMP]$ (>98 wt %), 1-butyl-3-methylimidazolium methylacetate, $[C_4C_1im][CH_3CO_2]$ (>98 wt %), 1-butyl-3-methylimidazolium methanesulfonate, $[C_4C_1im][CH_3SO_3]$ (98 wt %), and 1-butyl-3-methylimidazolium chloride, $[C_4C_1im]Cl$ (99 wt %) from Iolitec. The chemical structure of the cation and the different anions that compose the studied ILs are represented in **Figure 2.10**. To reduce the water and volatile compounds content to negligible values, ILs individual samples were dried under constant stirring at vacuum and moderate temperature (≈ 323 K) for a minimum of 48 h. After this step, the purity of each IL was checked by ^1H and ^{13}C NMR spectra and found to be in accordance with the purity given by the suppliers. The water used was double distilled, passed through a reverse osmosis system, and further treated with a Milli-Q plus 185 apparatus. L-Tryptophan and L-tyrosine with a purity of >99.0 wt % were supplied by Sigma and Fluka, respectively.

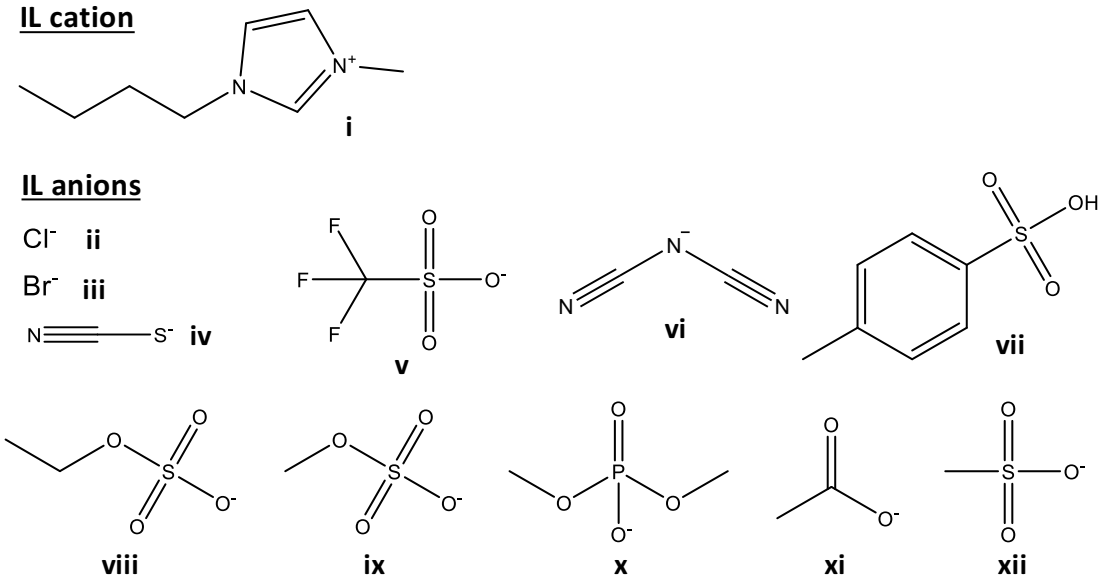

Figure 2.10. ILs cation and anions chemical structures: (i) $[C_4C_1im]^+$; (ii) Cl^-; (iii) Br^-; (iv) $[SCN]^-$; (v) $[CF_3SO_3]^-$; (vi) $[N(CN)_2]^-$; (vii) $[TOS]^-$; (viii) $[C_2H_5SO_4]^-$; (ix) $[CH_3SO_4]^-$; (x) $[DMP]^-$; (xi) $[CH_3CO_2]^-$; (xii) $[CH_3SO_3]^-$.

Phase diagrams. The experimental procedure used in this work to determine the binodal curves was previously described in **chapter 2.1**. The solubility curves were determined at (298 ± 1) K and atmospheric pressure. Aqueous solutions of K_2CO_3 at 50 wt % and aqueous solutions of ILs at variable concentrations were prepared gravimetrically and used to determine the binodal curves. The binodal curves of quaternary mixtures were determine using mixtures of $[C_4C_1im]Cl$ and $[C_4C_1im][CF_3SO_3]$ at the following $[C_4C_1im]Cl$ mole fractions: 0.12, 0.27, 0.50, 0.64, 0.74, 0.81, 0.89. Repetitive drop wise addition of the aqueous solution of each IL or IL-IL mixture to the K_2CO_3 aqueous solution was carried out until the detection of a cloudy (biphasic) mixture, followed by

the drop wise addition of ultrapure water until the observation of the monophasic region (clear and limpid solution). The ternary system compositions were determined by weight quantification within ± 10^{-4} g.

Partition of amino acids. L-Tryptophan and L-tyrosine aqueous solutions were prepared at the concentrations of 0.73 g dm^{-3} (3.6 × 10^{-3} mol·dm^{-3}) and 0.33 g·dm^{-3} (1.8 × 10^{-3} mol dm^{-3}), respectively, guaranteeing that both amino acids are at infinite dilution and completely solvated in aqueous media, avoiding thus specific interactions between the biomolecules. The quaternary mixtures compositions were chosen based on the phase diagrams determined before for $[C_4C_1im]Cl$ + $[C_4C_1im][CF_3SO_3]$ + K_2CO_3 + H_2O ABS. All the partition studies were performed at the same mixture point, 1.80 mol·kg^{-1} of IL-IL mixture + 1.80 mol·kg^{-1} of K_2CO_3. Each mixture was vigorously stirred and left to equilibrate for at least 12 h (a time established in previous optimizing experiments), to achieve the complete partition of each amino acid between the coexisting phases. After a careful separation of both phases, the quantification of each amino acid in each phases was carried by UV-spectroscopy, using a BioTeck Synergy HT microplate reader, at a wavelength of 279 nm for L-tryptophan and 292 nm for L-tyrosine using calibration curves previously established. Possible interferences of the salt and ILs with the analytical method were taken into account, and control samples were always prepared at the same weight fraction composition, using pure water instead of the amino acid aqueous solutions. The partition coefficients of L-tryptophan (K_{Trp}) and L-tyrosine (K_{Tyr}) are defined as the ratio of the concentration of each amino acid in the IL-rich phase to that in the salt-rich phase (*cf.* **Equation (2.8)**), while the extraction efficiency ($EE\%$) was calculated as the percentage ratio between the amount of each amino acid in the IL-rich aqueous phase and that in the total mixture, according to **Equation (2.9)**.

2.3.4. Results and discussion

Aiming at evaluating the behavior of ABS composed by the inorganic salt K_2CO_3 and different $[C_4C_1im]$-based ILs, as well as to study the effect of IL anion in ABS formation, the phase diagrams of these ternary systems were determined at 298 K and atmospheric pressure. The respective solubility curves are illustrated in **Figure 2.11** and the experimental weight fraction data of each system are given at **Appendix A**. The solubility curves are represented in molality units for a better understanding of the IL anion structure impact on the phase diagrams behavior, avoiding thus differences that could result from different molecular weights. In all phase diagrams the biphasic region is located above the solubility curve and, the larger this region the higher the

ability of IL to undergo liquid-liquid demixing, *i.e.*, the easier the IL is salted-out by potassium carbonate salt.

For the studied systems, at 1.0 mol·kg^{-1} of K_2CO_3, the IL anion ability to form ABS is as follows: $Cl^- \approx [CH_3SO_3]^- < [CH_3CO_2]^- < [DMP]^- < [Br]^- \approx [CH_3SO_4]^- < [C_2H_5SO_4]^- << [TOS]^- < [N(CN)_2]^- < [SCN]^- < [CF_3SO_3]^-$ – *cf.* **Figure 2.11**. This rank is in close agreement with previous works where the use of different organic and inorganic salts was reported.[29-31] In fact, the IL anion effect on ABS formation is nowadays well understood. The anions of IL compete with the salt ions for the formation of hydration complexes. This competition is usually dominated by the ions with higher charge density, *i.e.*, ions that are capable of stronger interactions with water. Therefore, when a group of ILs with a common cation is under study, the ILs composed of anions with lower hydrogen bond basicity (β) are more able to form ABS. In this context, it was already identified a dependency between the ILs ability to induce phase demixing and their hydrogen bond basicity values determined by solvatochromic probes.[32]

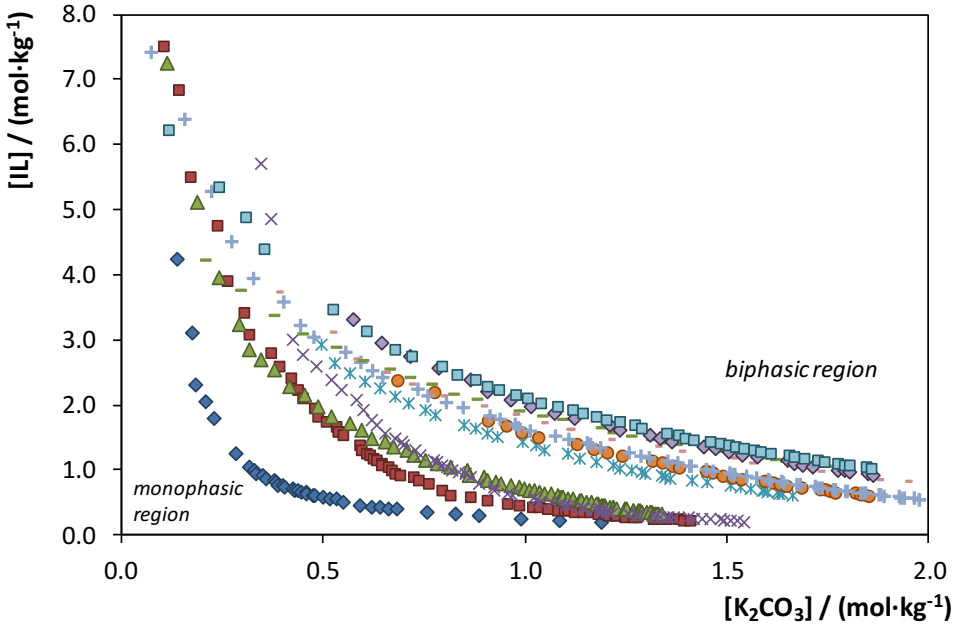

Figure 2.11. Ternary phase diagrams composed of $[C_4C_1im]$-based ILs + K_2CO_3 + H_2O: $[C_4C_1im][CF_3SO_3]$ (◆); $[C_4C_1im][SCN]$ (■); $[C_4C_1im][TOS]$ (▲); $[C_4C_1im][N(CN)_2]$ (×); $[C_4C_1im][C_2H_5SO_4]$ (✳); $[C_4C_1im][CH_3SO_4]$ (●); $[C_4C_1im]Br$ (+); $[C_4C_1im][DMP]$ (-); $[C_4C_1im][CH_3CO_2]$ (–); $[C_4C_1im][CH_3SO_3]$ (◆); and $[C_4C_1im]Cl$ (■).

The IL anion nature not only influences the IL ability to form ABS, but also changes the physical-chemical properties of the ABS coexisting phases, allowing a proper tailoring of the phases' polarities. In this context, and similarly to other studies concerning the use of ILs mixtures to fine tuning their properties, a question remains: is it possible to use only two ILs with very

distinct hydrogen bond basicities to cover all the polarity range that is attained using different IL anions, and consequently, to increase the design ability of IL-based ABS?

Through the inspection of **Figure 2.11**, it is possible to conclude that amongst the ILs investigated the ILs $[C_4C_1im][CF_3SO_3]$ and $[C_4C_1im]Cl$ present, respectively, the higher and lower ability to form an ABS when mixed with the inorganic salt K_2CO_3, *i.e.*, the lower and higher hydrogen bond basicity values. Thus, and in a first attempt to answer to the question stated above, the phase diagrams of quaternary mixtures composed of $[C_4C_1im]Cl$ + $[C_4C_1im][CF_3SO_3]$ + K_2CO_3 + H_2O were determined at different $[C_4C_1im]Cl$:$[C_4C_1im][CF_3SO_3]$ molar fractions, at room temperature and atmospheric pressure. The obtained results are presented in **Figure 2.12**, while the experimental weight fraction data of each system are given at **Appendix A.**

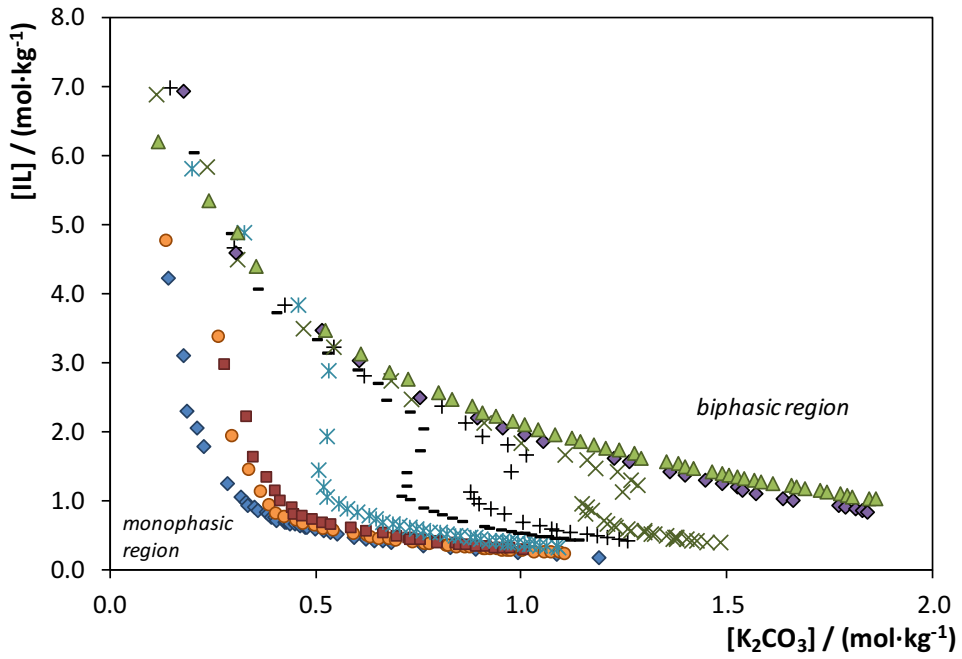

Figure 2.12. Phase diagrams of ternary and quaternary mixtures composed of $[C_4C_1im]Cl$, $[C_4C_1im][CF_3SO_3]$, K_2CO_3 and H_2O at different IL-IL mixture molar fractions: $x_{[C4C1im]Cl}$ = 0.0 (◆, $[C_4C_1im][CF_3SO_3]$ + K_2CO_3 + H_2O ABS), 0.12 (●), 0.27 (■), 0.50 (✳), 0.64 (▬), 0.74 (+), 0.81 (×), 0.89 (◆) and 1.0 (▲, $[C_4C_1im]Cl$ + K_2CO_3 + H_2O ABS).

The quaternary systems composed of $[C_4C_1im]Cl$, $[C_4C_1im][CF_3SO_3]$, K_2CO_3 and water are represented as pseudo-ternary systems in **Figure 2.12**, with [IL] in the yy axis representing the sum of both ILs molality. However, the phase diagrams obtained by changing the ions proportion in the mixtures follow a different pattern from that observed for one IL cation-anion pair (**Figure 2.11**). It is possible to observe the existence of a dominant effect ruled by the anion composition in the mixture. By decreasing the inorganic salt concentration and increasing the $[C_4C_1im]Cl$ molar fraction, the phase diagrams tend to be controlled by the Cl^- anion, while for higher

concentrations of K_2CO_3, the $CF_3SO_3^-$ anion effect starts to prevail. These results suggest that these type of ABS cannot be considered as pseudo-ternary systems, and the composition of the four components should be take into account, as represented in **Figure 2.13**.

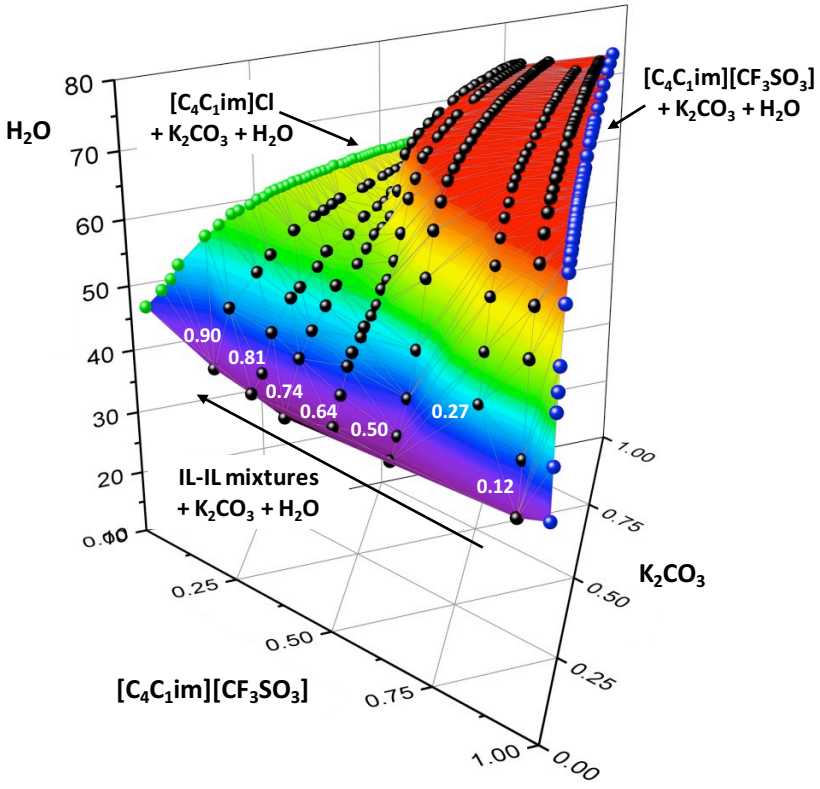

Figure 2.13. Quaternary phase diagrams composed of $[C_4C_1im]Cl$ + $[C_4C_1im][CF_3SO_3]$ + K_2CO_3 + H_2O.

In **Figure 2.13** it is possible to distinguish the binodal curves of the ternary systems composed of $[C_4C_1im]Cl$ + K_2CO_3 + H_2O and $[C_4C_1im][CF_3SO_3]$ + K_2CO_3 + H_2O, in the left and right face of the prism. Through this representation it is clear that the quaternary systems composed of $[C_4C_1im]Cl$ + $[C_4C_1im][CF_3SO_3]$ + K_2CO_3 + H_2O cover the region in the space between these two binodal curves, which is represented by an equilibrium surface. Similarly to a binodal curve, this surface represents the limit between the biphasic and the monophasic regions of the quaternary system under study. In this particular case, below the surface is the biphasic region, while above the surface all the mixture points result in homogenous solutions – monophasic region.

In the last years, the scientific community involved in ILs mixtures research started a deep discussion on how these mixtures should be considered. Rogers and co-workers[33] proposed that mixtures of pure ILs should be considered as double salts instead of simple mixtures of ILs or solutions of a salt in an IL. By definition, a double salt is a salt composed of more than one cation or anion and which presents different physicochemical properties than of its component single

salts. This means that authors[33] are proposing that a new and pure IL is formed when two pure ILs are mixed. Through a deep revision and discussion of the literature concerning physicochemical properties of IL-IL mixtures, Rogers and co-workers[33] supported the concept of double salt ILs. However, the behavior of ILs mixtures in aqueous solutions remains unexplored.

The results obtained in this work show that the mixture of two ILs, constituted by the same cation but different anions, presents a complex behavior in ABS formation when mixed with a salt. In fact, as discussed above, it seems clear that there is not the formation of a double salt IL (composed of three different ions), but a different partition extent of the starting ILs, $[C_4C_1im]Cl$ and $[C_4C_1im][CF_3SO_3]$, occurs between the coexisting phases. This also suggests that the properties of the phases that compose this quaternary system may not be between the properties of the ternary systems composed of each individual IL, or present a direct relation with the molar fraction of IL-IL mixtures. However, it is still needed to characterize the biphasic region of this system through the determination of the respective TLs – which will allow to know how both ILs are distributed in the phases – and to study the physicochemical properties of the coexisting phases to understand the real behavior and the formation mechanisms of ABS composed by ILs mixtures.

In order to get a broader vision on the IL-IL mixtures effect on the respective ABS extraction performance, the partition behavior of two model amino acids, L-tryptophan and L-tyrosine, was determined. The results obtained for the partition coefficients and extraction efficiencies are shown in **Figure 2.14**. Further details are given in the **Appendix A**.

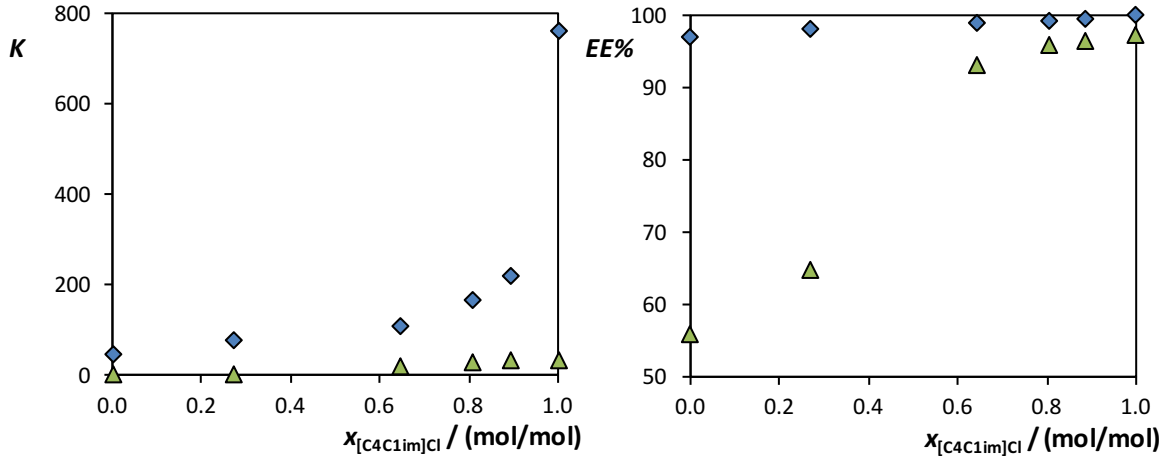

Figure 2.14. L-Tryptophan (blue diamons) and L-tyrosine (green triangules) partition coefficients (*K*) and extraction efficiencies (*EE*%) in function of the $[C_4C_1im]Cl$ molar fraction ($x_{[C4C1im]Cl}$) in the quaternary system composed of $[C_4C_1im]Cl$ + $[C_4C_1im][CF_3SO_3]$ + K_2CO_3 + H_2O.

The results obtained show that L-tryptophan and L-tyrosine present a higher affinity to the IL-rich phase – *cf.* **Figure 2.14**. In the studied systems the pH of the phases ranges between 12.1 and 12.7 (*cf.* **Appendix A**), without significant differences observed between the coexisting phases, meaning that both amino acids are in their anionic forms (pK_a1^{Trp} =2.54, pK_a2^{Trp} = 9.40, and pK_a1^{Tyr} = 2.00, pK_a2^{Tyr} = 9.19)[34], and thus with no contributions of the presence or not of additional electrostatic interactions within all systems investigated. Furthermore, the partition and extraction of both solutes follow the $[C_4C_1im]Cl$ mole fraction, proving the higher affinity of these amino acids for IL-rich phases with a high hydrophilic character (the best and worst partition coefficient and extraction efficiency of both solutes are obtained with pure $[C_4C_1im]Cl$ and pure $[C_4C_1im][CF_3SO_3]$, respectively), which is in good agreement with their octanol-water partition coefficients: $\log(K_{OW})_{Trp}$ = -1.09 and $\log(K_{OW})_{Tyr}$ = -1.49.[34] However, it is important to highlight the very distinct partition patterns that are observed with these two amino acids, where partition coefficient values are significantly higher for L-tryptophan. Furthermore, it is relevant to remark that the partition coefficients and extraction efficiencies do not follow an ideal behavior according to one of the ILs mole fraction, further supporting the different dominant effects of the different IL anions up to given concentrations, as observed with the phase diagrams behavior.

To better understand the different patterns observed, in **Figure 2.15** is represented the selectivity of quaternary systems under study in the extraction of L-tryptophan and L-tyrosine ($S_{Trp/Tyr}$),. It seems that when pure ILs are used there is no effect on the preferential partition of L-tryptophan over L-tyrosine; however, if ILs mixtures are applied, very distinct selectivities are observed, with the best result obtained at a $[C_4C_1im]Cl$ molar fraction of 0.27. These results clearly

show that the ion composition of the mixture is an important factor for the ability of these ABS to preferentially partition the solutes between the phases. However, and despite these preliminary results, further studies to understand the nature of the interactions involved are still needed.

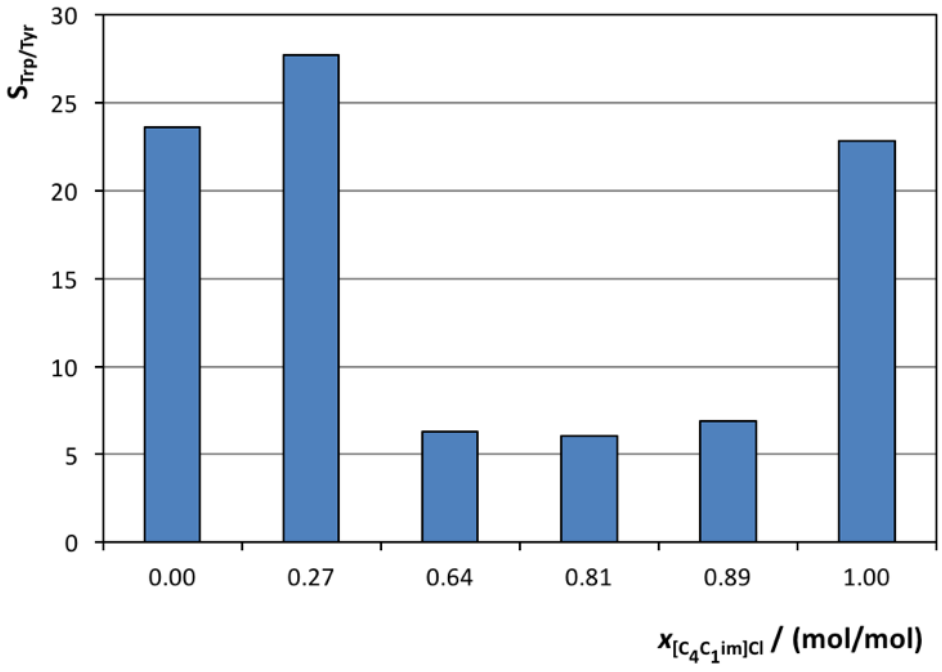

Figure 2.15. Selectivity ($S_{Trp/Tyr}$) of quaternary systems composed of $[C_4C_1im]Cl$ + $[C_4C_1im][CF_3SO_3]$ + K_2CO_3 + H_2O for L-tryptophan and L-tyrosine as a function of the $[C_4C_1im]Cl$ mole fraction ($x_{[C4C1im]Cl}$).

2.3.5. Conclusions

In this work, novel phase diagrams for ABS composed of IL-IL mixtures, a salt and water were determined. The obtained results show that these new quaternary systems cannot be considered as pseudo-ternary systems, and that the use of IL-IL mixtures has a high potential in the tuning of the ABS phases properties. Furthermore, it was demonstrated that ABS composed of mixtures of ILs display a higher selectivity and can be properly tailored by playing around the two ILs composition.

2.3.6. References

(1) J. P. Hallett and T. Welton, *Chem. Rev.*, 2011, **111**, 3508–3576;
(2) V. I. Pârvulescu and C. Hardacre, *Chem. Rev.*, 2007, **107**, 2615–2665;
(3) M. Armand, F. Endres, D. R. MacFarlane, H. Ohno and B. Scrosati, *Nat. Mater.*, 2009, **8**, 621–629;
(4) D. R. MacFarlane, N. Tachikawa, M. Forsyth, J. M. Pringle, P. C. Howlett, G. D. Elliott, J. H. Davis, M. Watanabe, P. Simon and C. A. Angell, *Energy Environ. Sci.*, 2014, **7**, 232–250;
(5) X. Han and D. W. Armstrong, *Acc. Chem. Res.*, 2007, **40**, 1079–1086;
(6) M. Freemantle, *Chem. Eng. News*, 1998, **76**, 32–37;

(7) H. Niedermeyer, J. P. Hallett, I. J. Villar-Garcia, P. A. Hunt and T. Welton, *Chem. Soc. Rev.*, 2012, **41**, 7780–7802;
(8) M. Y. Lui, L. Crowhurst, J. P. Hallett, P. A. Hunt, H. Niedermeyer and T. Welton, *Chem. Sci.*, 2011, **2**, 1491–1496;
(9) S. García, M. Larriba, J. García, J. S. Torrecilla and F. Rodríguez, *Chem. Eng. J.*, 2012, **180**, 210–215;
(10) S. Katsuta, N. Yamaguchi, R. Ogawa, Y. Kudo and Y. Takeda, *Anal. Sci.*, 2008, **24**, 1261–1267;
(11) S. García, M. Larriba, J. García, J. S. Torrecilla and F. Rodríguez, *J. Chem. Thermodyn.*, 2012, **53**, 119–124;
(12) A. M. Pinto, H. Rodríguez, Y. J. Colón, A. Arce, A. Arce and A. Soto, *Ind. Eng. Chem. Res.*, 2013, **52**, 5975–5984;
(13) A. Finotello, J. E. Bara, S. Narayan, A. D. Camper and R. D. Noble, *J. Phys. Chem. B*, 2008, **112**, 2335–2339;
(14) T. Kakibe, J. Hishii, N. Yoshimoto, M. Egashira and M. Morita, *J. Power Sources*, 2012, **203**, 195–200;
(15) Z. Yu, N. Vlachopoulos, A. Hagfeldt and L. Kloo, *RSC Adv.*, 2013, **3**, 1896–1901;
(16) M. Zistler, P. Wachter, C. Schreiner, M. Fleischmann, D. Gerhard, P. Wasserscheid, A. Hinsch, and H. J. Gores, *J. Electrochem. Soc.*, 2007, **154**, B925–B930;
(17) C. C. Weber, A. F. Masters and T. Maschmeyer, *J. Phys. Chem. B*, 2012, **116**, 1858–1864;
(18) A. R. Khosropour, I. Mohammadpoor-Baltork and F. Kiani, *Comptes Rendus Chim.*, 2011, **14**, 441–445;
(19) Q. Q. Baltazar, S. K. Leininger and J. L. Anderson, *J. Chromatogr. A*, 2008, **1182**, 119–127;
(20) Paloma Navia, J. Troncoso and L. Romaní, *J. Chem. Eng. Data*, 2007, **52**, 1369–1374;
(21) M. B. Oliveira, M. Domínguez-Pérez, O. Cabeza, J. A. Lopes-da-Silva, M. G. Freire and J. A. P. Coutinho, *J. Chem. Thermodyn*., 2013, **64**, 22–27;
(22) G. Annat, D. R. MacFarlane and M. Forsyth, *J. Phys. Chem. B*, 2007, **111**, 9018–9024;
(23) A. Stoppa, R. Buchner and G. Hefter, *J. Mol. Liq.*, 2010, **153**, 46–51;
(24) M. Larriba, S. García, P. Navarro, J. García and F. Rodríguez, *J. Chem. Eng. Data*, 2012, **57**, 1318–1325;
(25) G. Annat, M. Forsyth and D. R. MacFarlane, *J. Phys. Chem. B*, 2012, **116**, 8251–8258;
(26) A. Arce, M. J. Earle, S. P. Katdare, H. Rodríguez and K. R. Seddon, *Chem. Commun.*, 2006, 2548–2550;
(27) K. E. Gutowski, G. A. Broker, H. D. Willauer, J. G. Huddleston, R. P. Swatloski, J. D. Holbrey and R. D. Rogers, *J. Am. Chem. Soc.*, 2003, **125**, 6632–6633;
(28) M. G. Freire, A. F. M. Cláudio, J. M. M. Araújo, J. A. P. Coutinho, I. M. Marrucho, J. N. C. Lopes and L. P. N. Rebelo, *Chem. Soc. Rev.*, 2012, **41**, 4966–4995;
(29) A. F. M. Cláudio, A. M. Ferreira, S. Shahriari, M. G. Freire and J. A. P. Coutinho, *J. Phys. Chem. B*, 2011, **115**, 11145–11153;
(30) S. P. M. Ventura, C. M. S. S. Neves, M. G. Freire, I. M. Marrucho, J. Oliveira and J. A. P. Coutinho, *J. Phys. Chem. B*, 2009, **113**, 9304–9310;
(31) H. Passos, A. R. Ferreira, A. F. M. Cláudio, J. a. P. Coutinho and M. G. Freire, *Biochem. Eng. J.*, 2012, **67**, 68–76;
(32) R. Lungwitz and S. Spange, *New J. Chem.*, 2008, **32**, 392–394;
(33) G. Chatel, J. F. B. Pereira, V. Debbeti, H. Wang and R. D. Rogers, *Green Chem.*, 2014, **16**, 2051–2083;
(34) *ChemSpider – The free chemical database*, 2015, www.chemspider.com.

2.4. Ionic liquids as phase-forming components of aqueous multiphase systems

This chapter is based on the submitted manuscript:

Helena Passos, Sara Costa, Ana M. Fernandes, Mara G. Freire, Robin D. Rogers and João A.P. Coutinho;[1] "Triple salting-out effect: a required phenomenon in the formation of ionic-liquid-based aqueous multiphase systems", Chemical Communications (2017).

2.4.1. Abstract

Novel aqueous multiphase systems (MuPS) formed by quaternary mixtures composed of cholinium-based ionic liquids (ILs), polymers, inorganic salts and water are here reported. The influence of several ILs was studied, demonstrating that triple salting-out is a required phenomenon to prepare MuPS. The respective phase diagrams and "tie-surfaces" were determined, followed by the evaluation of the effect of temperature. Finally, it was shown the remarkable ability of IL-based MuPS to selectively separate a complex mixture of dyes.

2.4.2. Introduction

Separation processes based on three-liquid-phase systems are promising approaches for the isolation of different compounds present in complex mixtures, allowing their simultaneous separation amongst the different phases in a single-step.[1-8] These systems are usually prepared by the addition of an organic solvent to a polymer-salt-based aqueous biphasic system (ABS), resulting in the formation of an organic-solvent-rich top phase, a polymer-rich middle phase and a salt-rich bottom phase. Furthermore, due to their compositions and the chemical nature of each phase, the coexisting phases present a wide range of polarities and highly distinct chemical properties. This is one of the main reasons behind the considerably higher selectivities displayed by three-liquid phase systems when compared to conventional water-oil liquid-liquid systems and ABS.[9]

In 2012, Mace et al.[10] introduced the concept of aqueous multiphase systems (MuPS), *i.e.*, systems composed of three or more aqueous-rich phases, without organic solvents employed. The authors[10] reported the formation of more than 300 MuPS by mixing different polymers and surfactants in aqueous solutions. Following their approach, Liang et al.[11] presented an in-depth study on an aqueous four-phase system constituted by sodium dodecyl sulphate (SDS),

[1]**Contributions:** R.D.R., M.G.F. and J.A.P.C. conceived and directing this work. H.P. and S.C. acquired the experimental data. A.M.F. supervised the mass spectrometer mesurements. H.P., R.D.R., M.G.F and J.A.P.C. interpreted the experimental data obtained until now.

dodecyltrimethylammonium bromide (DTAB), polyethylene glycol (PEG) with a molecular weight of 6000 mol·g^{-1}, and NaBr. In this work, the phase compositions and their properties, as well as the partition of xylenol orange between the coexisting phases, were studied and reported.[11] Other authors demonstrated that MuPS present characteristics useful for specific applications, such as in the separation of nanoparticles by rate-zonal centrifugation,[12] or even in the treatment of cellular components of human blood for medical purposes.[13] Nevertheless, the molecular-level knowledge behind the formation of MuPS is still very limited, and the mechanisms associated with the multiple phases' separation were not fully disclosed in these pioneering works.[10-13] Furthermore, the phase-forming components proposed for the creation of MuPS were always polymers, surfactants and polysaccharides of high molecular weights, resulting in highly viscous aqueous phases and further difficulties in the phases' separation and mass transfer phenomena.

The application of ionic liquids (ILs) as phase-forming components of ABS has been a hot topic of research in the past years.[14,15] Their unique properties, such as their high solvation ability for a large range of compounds and the possibility of tuning their properties by the correct choice of both the cation and anion, makes IL-based ABS valuable in processes of extraction and separation of a wide range of compounds. Furthermore, these types of systems present additional and outstanding advantages when compared to the more traditional polymer-based systems, such as low viscosity, quick phase separation, and high extraction efficiencies for the most diverse biomolecules,[14] contributing to the development of more cost-effective processes. Although not investigated to date, these advantages could be transposed to MuPS if ILs could be used as phase-forming components. Thus, in this work, we evaluate the possibility of using ILs for the formation of MuPS, address their phase diagrams and the molecular-level mechanisms behind the observed phase transitions, and evaluate their efficacy in separation processes.

2.4.3. Experimental procedures

Materials. The determination of the liquid-liquid quaternary phase diagrams was performed using tri-potassium phosphate, K_3PO_4, (98 wt % pure) from Sigma, poly(ethylene glycol), with an average molecular weight of 600 g·mol^{-1} (PEG 600) from Sigma-Aldrich, and the following cholinium ([$N_{111(2OH)}$])-based ILs: cholinium butanoate, [$N_{111(2OH)}$][But], cholinium propanoate, [$N_{111(2OH)}$][Pro], cholinium lactate, [$N_{111(2OH)}$][Lac], cholinium acetate, [$N_{111(2OH)}$][Ace] (98 wt % pure), cholinium glycolate, [$N_{111(2OH)}$][Gly], cholinium dihydrogenphosphate, [$N_{111(2OH)}$][DHP] (99 wt % pure) and cholinium chloride, [$N_{111(2OH)}$]Cl (≥ 98 wt %). The chemical structures of investigated ILs are presented in **Figure 2.16**. [$N_{111(2OH)}$][Ace] and [$N_{111(2OH)}$][DHP] were supplied by Iolitec while

$[N_{111(2OH)}]Cl$ were provided by Sigma. $[N_{111(2OH)}][But]$, $[N_{111(2OH)}][Pro]$, $[N_{111(2OH)}][Lac]$ and $[N_{111(2OH)}][Gly]$ were synthesized in our lab according to well established procedures.[16,17] To reduce the volatile impurities to negligible values and remove traces of water, individual samples of each IL were dried at moderate temperature (≈ 323 K) and at high vacuum (≈ 10^{-5} Pa), under constant stirring, and for a minimum period of 24 h. After this procedure, the purity of each IL was further checked by ^{1}H and ^{13}C NMR spectra and found to be > 98 wt %. The textile dyes sudan III and pigment blue (PB) 27 were acquired from Merck and Daicolor and Holliday Pigment, respectively. The food additive used was a dye composed of water, tartrazine (E102) and acetic acid from Globo. The water used was double distilled, passed through a reverse osmosis system, and further treated with a Milli-Q plus 185 apparatus.

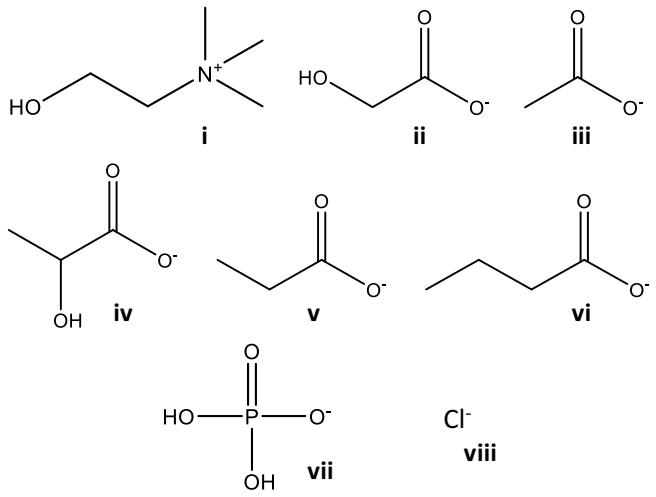

Figure 2.16. Chemical structure of the cation and anions that constitute the studied ILs: (i) $[N_{111(2OH)}]^{+}$; (ii) $[Gly]^{-}$; (iii) $[Ace]^{-}$; (iv) $[Lac]^{-}$; (v) $[Prop]^{-}$; (vi) $[But]^{-}$; (vii) $[DHP]^{-}$; (viii) Cl^{-}.

Determination of aqueous biphasic systems phase diagrams. The experimental phase diagrams investigated in this work were determined by the cloud-point titration method[18,19] at (298 ± 1) K and atmospheric pressure. Aqueous solutions of K_3PO_4 at 50 wt % and aqueous solutions of $[N_{111(2OH)}]Cl$ and PEG at several mole fractions (0.08, 0.31, 0.49, 0.55, 0.82 and 0.95 moles of $[N_{111(2OH)}]Cl$ *per* total moles) were prepared gravimetrically (± 10^{-4} g) and used to determine the binodal curves. Repetitive drop wise addition of the aqueous inorganic salt solution to each aqueous solution of $[N_{111(2OH)}]Cl$/PEG was carried out until the detection of a cloudy solution, followed by the drop wise addition of ultra-pure water until the detection of a single and limpid phase. The whole procedure was performed under constant stirring and the quaternary system compositions were determined by the weight quantification of all the components added. The same procedure was executed to determine the solubility curves of the ternary systems composed of PEG 600 + K_3PO_4 + H_2O and $[N_{111(2OH)}][Lac]$ + K_3PO_4 + H_2O.

For the system composed of $[N_{111(2OH)}][Gly] + K_3PO_4 + H_2O$ and $[N_{111(2OH)}][DHP] + K_3PO_4 + H_2O$ the turbidimetric method was used.[20] Several mixtures of the system at the biphasic region were initially prepared. Under constant stirring, ultra-pure water was added until the detection of a clear and limpid solution (monophasic region). Each mixture corresponds to one point of the binodal curve. The mixture compositions were gravimetrically determined within $\pm 10^{-4}$ g and at (298 ± 1) K. The same procedure was used to determine the limit between the three phases region and the biphasic region, and the solid-liquid region and the three phases region. The 3D representations of $[N_{111(2OH)}]Cl$-based MuPS were carried out using the Origin Pro 9.1.0 software, from Origin Lab Corporation.

Characterization of coexisting phases composition. Mixtures at the ternary regions were gravimetrically prepared with $[N_{111(2OH)}]$-based ILs + PEG + K_3PO_4 + H_2O, vigorously stirred, and allowed to equilibrate for at least 12 h at (298 ± 1) K. After the separation, all the three phases were weighted. The coexisting phases' composition of the $[N_{111(2OH)}]Cl$ + PEG + K_3PO_4 + H_2O system were analytically determined. The water content was determined gravimetrically by evaporation until constant weight of the dried phase in an air oven and at constant temperature (± 378 K). The $[N_{111(2OH)}]^+$ cation quantification was carried out by a Micromass Quattro LC triple quadrupole mass spectrometer using a calibration curve previously established. The operating conditions of the mass spectrometer were the following: source and desolvation temperatures of 353 K and 423 K, respectively; capillary voltage of 3000 V; and cone voltage of 30 V. N_2 was used as the nebulization gas and the diluted samples (50:1000, v/v) were introduced at a 10 $mL \cdot min^{-1}$ flow rate using the methanol–water (1:1, v/v) mixture as the eluent solvent. For the measurement of peak abundances, an average of 100 scans for each mass spectrum was used. Triplicate independent sampling measurements were performed for both standards and samples. The chloride anion content was determined through a chloride ion selective electrode. The potassium and phosphonium content was quantified by inductively coupled plasma-optical emission spectrometry (ICPOES) using a Jobin Yvon 70 plus, power 880 W, under a plasma gas flow of 16 $mL \cdot min^{-1}$ and pressure of 2.6 bar. For the remaining $[N_{111(2OH)}]$-based MuPSs the coexisting phases were identified through the measure of their electrical conductivity at (298 ± 1) K, using a Mettler Toledo SevenMultiTMdual pH/conductivity meter.

Selective extraction of dyes. Three dyes, sudan III, PB27 and E102, were studied as model molecules to demonstrate the potential application of MuPSs. Quaternary mixtures with a common composition and within the triphasic regions of the phase diagrams investigated, were prepared: 23 wt % of PEG + 23 wt % of $[N_{111(2OH)}]$-based IL + 23 wt % K_3PO_4 + 31 wt % of H_2O and

20 wt % of PEG + 19 wt % of $[N_{111(2OH)}][DHP]$ + 33 wt % K_3PO_4 + 28 wt % of H_2O. In each system, a small amount of each dye (≈ 0.30 mg) was added to glass tubes containing the quaternary mixtures with a total weight of 3 g. All mixtures were centrifuged during 10 min at 2000 rpm to achieve complete phase separation. After a careful separation of the phases, the quantification of each dye was carried by UV-spectroscopy using a synergy/HT microplate reader at a wavelength of 510 nm for sudan III, 600 nm for PB27 and 400 nm for E102. The interference of the salt, PEG and ILs was also taken into account and blank control samples were always employed. The extraction efficiencies of sudan III is defined as the ratio between the amount of dye in the PEG-aqueous-rich phase and in the total mixture. Similarly, the extraction efficiencies of PB 29 and E102 are defined as the ratio between the amount of dye in the salt- and IL-aqueous-rich phases, respectively, and in the total mixture – *cf.* **Equation (1.2)**.

2.4.4. Results and discussion

Quaternary mixtures of cholinium ($[N_{111(2OH)}]$)-based ILs, PEG with a molecular weight of 600 $mol \cdot g^{-1}$ (PEG 600), potassium phosphate (K_3PO_4), and water were used to prepare MuPS. The mixtures able to form three-phase systems (or not) are identified in **Table 2.3**, complemented with the information on the ability of the same ILs to form ABS (two-phase systems) with PEG 600 or K_3PO_4. It should be remarked that $[N_{111(2OH)}]Cl$ and $[N_{111(2OH)}][DHP]$ do not fall within the IL category if their melting temperatures are considered as a threshold (> 373 K). However, when dealing with IL-based ABS and related aqueous systems the phenomenon is more intricate and does not depend only on the melting temperature of each salt.[21,22] Therefore, and for a matter of simplicity, all the investigated cholinium-based salts will be described as ILs and K_3PO_4 as the (inorganic) salt.

Table 2.3. Identification of mixtures able (✓) or not able (×) to form ABS or MuPS with aqueous solutions of PEG 600 and/or K_3PO_4.

	ABS		MuPS
[$N_{111(2OH)}$]-based IL	**PEG 600**[21]	**K_3PO_4**	**PEG 600 + K_3PO_4**
[$N_{111(2OH)}$]Cl	✓	✓[23]	✓
[$N_{111(2OH)}$][Ace]	✓	✓[23]	✓
[$N_{111(2OH)}$][Lac]	✓	✓[a]	✓
[$N_{111(2OH)}$][Gly]	✓	✓[a]	✓
[$N_{111(2OH)}$][DHP]	✓	✓[a]	✓
[$N_{111(2OH)}$][Pro]	×	✓[24]	×
[$N_{111(2OH)}$][But]	×	✓[24]	×

[a]Phase diagrams determined in this work (experimental data are provided in the **Appendix A**).

With the exception of [$N_{111(2OH)}$][Pro] and [$N_{111(2OH)}$][But], all the studied [$N_{111(2OH)}$]-based ILs are able to form three-phase systems when mixed (in correct proportions) with aqueous solutions of PEG 600 and K_3PO_4 – *cf.* **Table 2.3**. These data reveal that the ability of an IL to form a three-phase system is related with its ability to form ABS with the other two solutes, *i.e.*, with the salt or the polymer. These results are in good agreement with the criteria used by previous authors,[10-13] who suggested that if the aqueous mixtures composed of the solutes A/B, B/C and A/C are able to form ABS, aqueous mixtures composed of A/B/C will result in the formation of three-phase systems. However, and despite the apparent validity of this criterion, its application requires previous knowledge on the pairs of solutes able to form ABS, resulting in a hard and time-consuming procedure. To overcome this drawback, it is crucial to understand the molecular-level mechanisms behind the formation of MuPS to be able to predict which mixtures allow their formation.

The demixing of two aqueous phases, and consequent formation of an ABS, occurs when two water-soluble solutes are mixed above certain concentrations and/or temperature in an aqueous solution. These solutes compete for the formation of hydration complexes and the phase-separation occurs.[14,21,25] Several pairs of solutes, such as polymers, salts, ILs, carbohydrates, amino acids, among others, can be used in ABS formation and, depending on the selected pair, the same solute can act as the salting-out or the salting-in species. For example, in systems constituted by [$N_{111(2OH)}$]-based ILs and K_3PO_4, the liquid-liquid demixing results from the salting-out effect of the salt over the IL, *i.e.*, high-charge density salt ions are preferentially hydrated leading to the exclusion of the less hydrophilic IL to a second liquid phase.[18,19] Similarly, for systems composed of polymers and salts, such as PEG 600 + K_3PO_4 + H_2O and PEG 600 + [$N_{111(2OH)}$]-based ILs + H_2O, there

is a salting-out effect of the salt (or IL) over the polymer and the phases demixing occurs.[21] Thus, when a quaternary mixture is prepared using three solutes able to induce ABS formation when mixed as pairs, all these interactions and preferential hydration will occur, resulting in the formation of three distinct aqueous phases: an IL-rich phase, a salt-rich phase and a polymer-rich phase.

A schematic representation of the salting-out effects identified in the quaternary mixtures under study is presented in **Figure 2.17**. The vertices of the triangles represent the three solutes that compose the aqueous quaternary mixture, while the edges represent the ternary mixtures (two solutes and water) that are, or not, able to form an ABS. In the cases where phase separation occurs, the arrows indicate the direction of the salting-out effect. As discussed above, and as represented in **Figure 2.17 A**, when all solutes that compose the quaternary system are able to induce a two-phase separation when mixed in pairs in aqueous media, three salting-out effects occur simultaneously in the mixture – the K_3PO_4 salting-out effect over $[N_{111(2OH)}]Cl$ and PEG 600, and the $[N_{111(2OH)}]Cl$ salting-out over PEG 600 – and a MuPS is obtained. This behavior is transversal to the quaternary mixtures composed of all the $[N_{111(2OH)}]$-based ILs able to form MuPS – *cf.* **Table 2.3**. However, for the cases where there is only two salting-out effect occurring – K_3PO_4 salting-out effect over both PEG 600 and $[N_{111(2OH)}][Pro]$, and no salting-out effect of the IL over the polymer – it is impossible to from a MuPS (**Figure 2.17 B**). This last example occurs for the ILs $[N_{111(2OH)}][Pro]$ and $[N_{111(2OH)}][But]$ which present favorable IL–PEG interactions,[21] not allowing their exclusion to different phases and further formation of a MuPS. It is thus clear that a triple salting-out effect is the crucial phenomenon which rules the formation of three-phase systems.

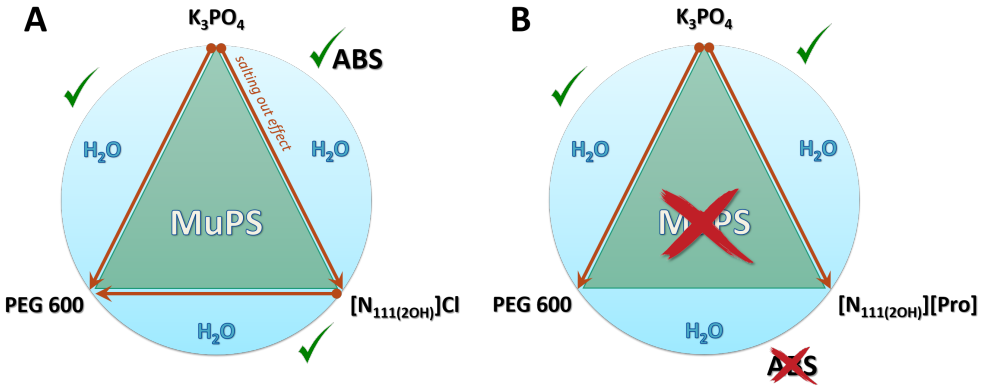

Figure 2.17. Schematic representation of the salting-out effect in quaternary mixtures composed of K_3PO_4, PEG 600, water and **(A)** $[N_{111(2OH)}]Cl$ or **(B)** $[N_{111(2OH)}][Pro]$.

To gather a better understanding on the three phases separation in IL-based MuPS, the system composed of $[N_{111(2OH)}]Cl$ + PEG 600 + K_3PO_4 + H_2O was studied in detail. First, the surfaces

limiting the monophasic, biphasic, triphasic, and solid-liquid regions were established (**Figure 2.18**). In **Figure 2.18 A** it is possible to distinguish a surface connecting the binodals of the ternary phase diagrams composed of $[N_{111(2OH)}]Cl + K_3PO_4 + H_2O$ (blue dots) and PEG 600 + K_3PO_4 + H_2O (green dots), limited in the bottom by the $[N_{111(2OH)}]Cl$ + PEG 600 + H_2O system (red dots). All quaternary mixtures prepared at concentrations above this surface will result in homogeneous solutions – monophasic region – while, below the surface, all mixtures are within the multiphasic region. Thus, this surface is the phase boundary, whereas the three-phase region is within the multiphase region delimited by the phase boundary. In **Figure 2.18 B** it is shown that the three-phase region is considerably smaller than the biphasic region. To obtain a system with three phases in equilibrium, the water amount in the quaternary mixture should be between ~40 and 25 wt %, while the concentration of K_3PO_4 and $[N_{111(2OH)}]Cl$ cannot be higher than 30-40 wt %, otherwise precipitation will occur. On the other hand, it is possible to prepare a three-phase system with a high polymer content (> 60 wt %) if the salt concentration is considerably low. In fact, the triphasic region is limited in the bottom by the solid-liquid region, in which the solutes are not completely soluble and a solid-phase appears – *cf.* **Figure 2.18 B**.

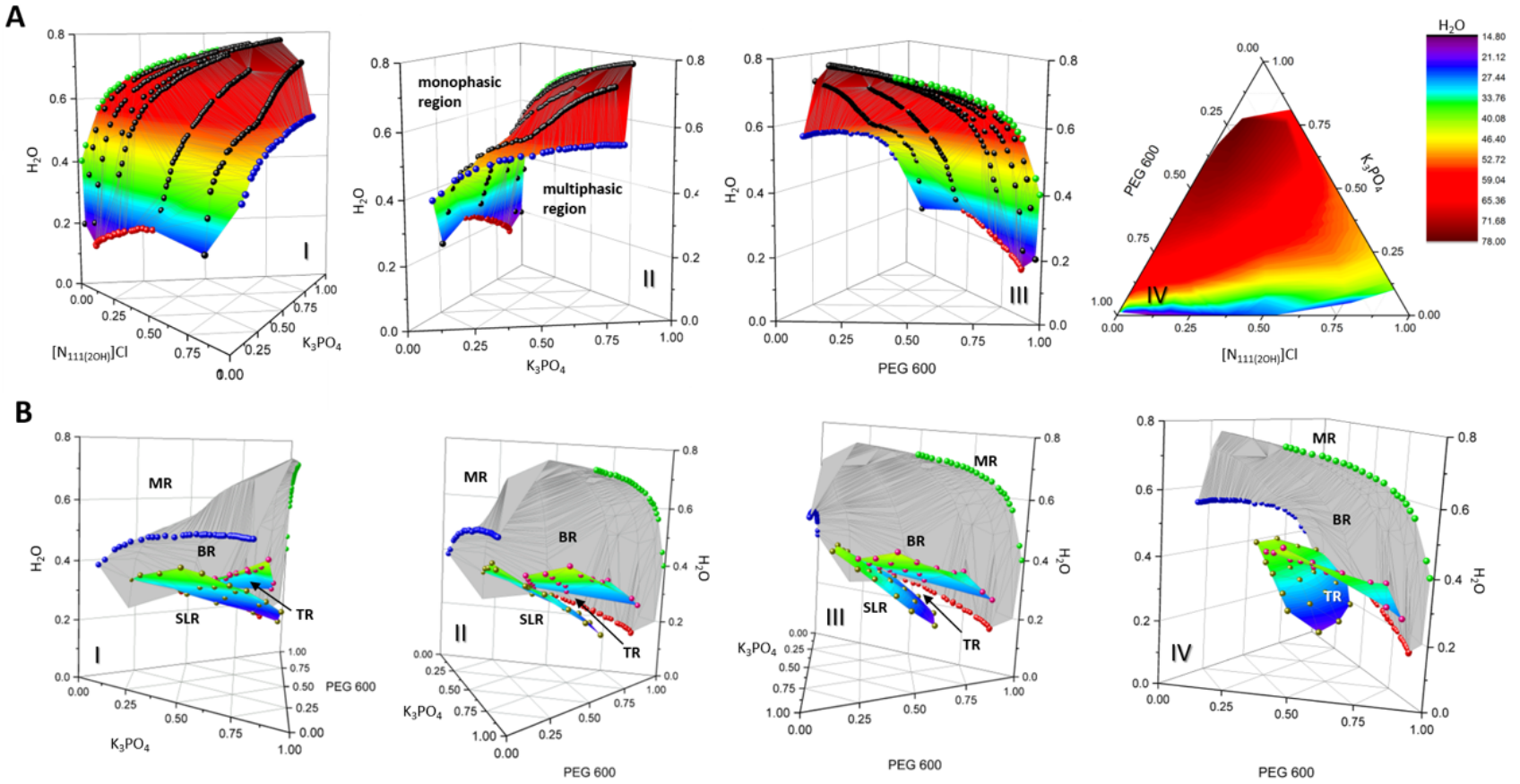

Figure 2.18. The phase diagram of the MuPS composed of $[N_{111(2OH)}]Cl$ +PEG 600 + K_3PO_4 + H_2O. **(A)** The phase boundary between the monophasic and multiphasic regions from different perspectives – ternary phase diagrams composed of $[N_{111(2OH)}]Cl$ + K_3PO_4 + H_2O (blue points), PEG 600 + K_3PO_4 + H_2O (green points), and $[N_{111(2OH)}]Cl$ + PEG 600 + H_2O (red points), and quaternary mixtures composed of $[N_{111(2OH)}]Cl$ +PEG 600 + K_3PO_4 + H_2O (black points). **(B)** The limits between the biphasic and triphasic regions (pink points) and the triphasic and solid-liquid regions (yellow points) from different perspectives. Legend: MR – monophasic region, BR – biphasic region, TR – triphasic region, SLR – solid-liquid region.

The composition of the coexisting phases of two quaternary mixtures were analytically determined, namely 30.70 wt % of $[N_{111(2OH)}]Cl$ + 29.64 wt % of PEG 600 + 9.86 wt % of K_3PO_4 + 29.81 wt % of H_2O and 22.61 wt % of $[N_{111(2OH)}]Cl$ + 21.36 wt % of PEG 600 + 22.63 wt % of K_3PO_4 + 33.40 wt % of H_2O, mainly to infer the phase composition and if ions exchange between the phases occurs. The obtained results are depicted in **Figure 2.19** through the representation of "tie surfaces".

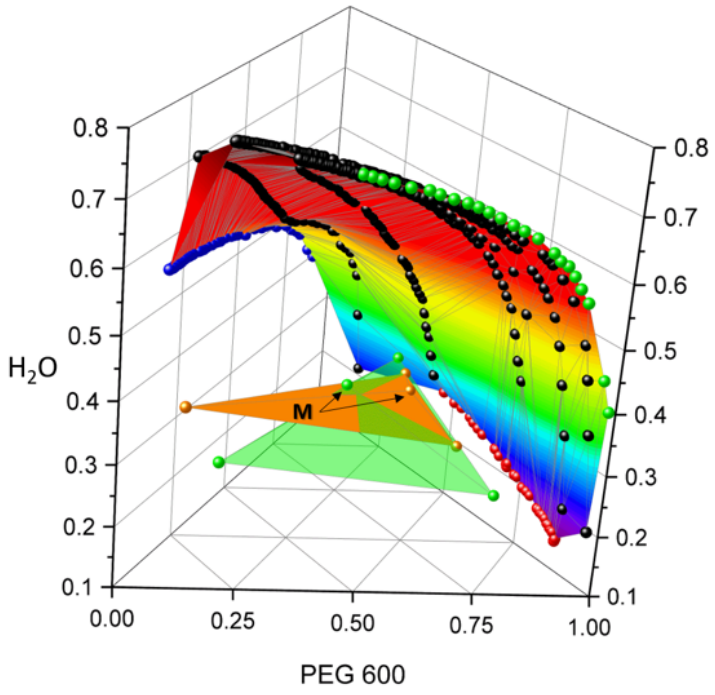

Figure 2.19. Quaternary phase diagram composed of $[N_{111(2OH)}]Cl$ + PEG 600 + K_3PO_4 + H_2O and "tie surfaces" determined in the mixture points 30.70 wt % of $[N_{111(2OH)}]Cl$ + 29.64 wt % of PEG 600 + 9.86 wt % of K_3PO_4 + 29.81 wt % of H_2O ("tie surface" 1 - orange) and 22.61 wt % of $[N_{111(2OH)}]Cl$ + 21.36 wt % of PEG 600 + 22.63 wt % of K_3PO_4 + 33.40 wt % of H_2O ("tie surface" 2 - green). Legend: M – mixture point.

The detailed composition of the coexisting phases is given in **Table 2.4**. As expected, each phase is composed of water, $[N_{111(2OH)}]Cl$, PEG 600 and K_3PO_4. However, each aqueous phase is richer in one of these three components. In the two mixture points studied, the top phases are rich in $[N_{111(2OH)}]Cl$, the middle phases are mostly composed of PEG 600, and the bottom phases are mainly constituted by the inorganic salt. The quantification of each ion (of the salt and IL) in each phase was also carried out, demonstrating that the ion exchange between the phases is negligible in these systems – detailed data are given in the **Appendix A**.

Table 2.4. Composition of the coexisting phases of the MuPS composed of 30.70 wt % of $[N_{111(2OH)}]Cl$ + 29.64 wt % of PEG 600 + 9.86 wt % of K_3PO_4 + 29.81 wt % of H_2O ("tie surface" 1) and 22.61 wt % of $[N_{111(2OH)}]Cl$ + 21.36 wt % of PEG 600 + 22.63 wt % of K_3PO_4 + 33.40 wt % of H_2O ("tie surface" 2).

	MuPSs rich phases		
	$[N_{111(2OH)}]Cl$	**PEG 600**	**K_3PO_4**
	"tie surface" 1		
$[N_{111(2OH)}]Cl$ (wt %)	41.72 ± 2.00	29.89 ± 0.48	0.56 ± 0.02
PEG 600 (wt %)	25.52 ± 1.40	43.36 ± 3.63	7.92 ± 0.32
K_3PO_4 (wt %)	4.36 ± 0.35	4.67 ± 0.31	53.00 ± 4.9
H_2O (wt %)	28.40 ± 0.07	22.08 ± 0.32	39.08 ± 0.18
	"tie surface" 2		
$[N_{111(2OH)}]Cl$ (wt %)	45.31 ± 1.34	20.46 ± 0.83	1.21 ± 0.01
PEG 600 (wt %)	22.28 ± 0.53	56.82 ± 3.21	14.02 ± 0.02
K_3PO_4 (wt %)	3.00 ± 0.08	4.60 ± 0.51	55.72 ± 5.43
H_2O (wt %)	29.41 ± 0.14	18.10 ± 0.10	30.29 ± 0.04

The temperature effect on the formation of MuPS was also evaluated. The surface that limits the biphasic and the triphasic regions was determined at 318 and 338 K, and compared to the surface previously determined at 298 K. The obtained results are represented in **Figure 2.20** for a phase diagram cut at 0.85 mol of $[N_{111(2OH)}]Cl$ *per* mol of $[N_{111(2OH)}]Cl$ + PEG 600, where it is shown that an increase in the temperature leads to an increase of the three phases region, *i.e.*, is favorable for the phase demixing. This behavior is observed in the entire range of the phase diagram – *cf.* the **Appendix A**. The reported behavior is similar to that observed in polymer-salt-based ABS in which the systems temperature dependency is dominated by hydrogen-bonding interactions occurring between the polymer and water.[26,27]

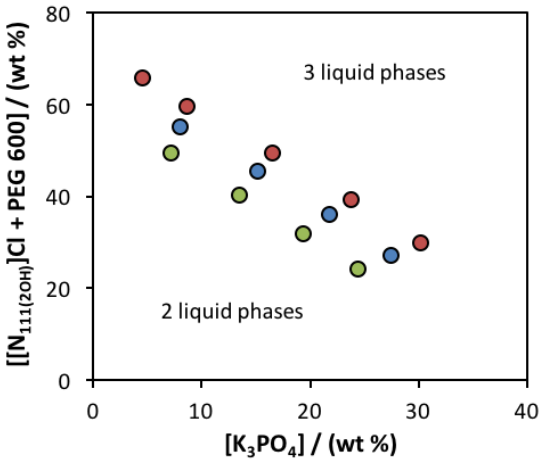

Figure 2.20. Temperature effect in the three phase region of the MuPS composed of $[N_{111(2OH)}]Cl$ + PEG 600 + K_3PO_4 + H_2O - phase diagram cut at 0.85 mol of $[N_{111(2OH)}]Cl$ *per* mol of $[N_{111(2OH)}]Cl$ + PEG 600: 298 K (red dots), 318 K (blue dots), and 338 K (green dots).

Aiming at assessing the application of the studied systems in separation processes, the ability of IL-based MuPS for the selective separation of a mixture of three dyes – sudan III, pigment blue (PB) 27 and tartrazine (E102) – was evaluated. The macroscopic appearance, as well as the

extraction efficiencies of the $[N_{111(2OH)}][Ace]$-based MuPS for dyes, are presented in **Figure 2.21 A**. Remarkably, the investigated system allows the separation of the three dyes by the three phases with an extraction efficiency of 93% for one of the dyes and complete separation of the other two. Sudan III, which has a less polar character ($\log(K_{OW}) = 7.47$),[28] is completely extracted to the more hydrophobic PEG 600-rich phase (purple-dyed phase). On the other hand, charged species, such as PB27 and E102 ($\log(K_{OW}) < 0$)[28] partition preferentially to the more charged and polar phases, such as the IL- (yellow dyed phase) and salt-rich phases (blue dyed phase). The extraction efficiencies of the remaining MuPS for the three dyes are shown in **Figure 2.21 B**. The same remarkable separation ability was obtained, with the complete extraction of sudan to the PEG-rich phase, the complete extraction of PB27 to the salt-rich phase, and a more dependent extraction efficiency for the E102 dye according to the IL chemical nature (decreasing with the IL hydrophilic character).

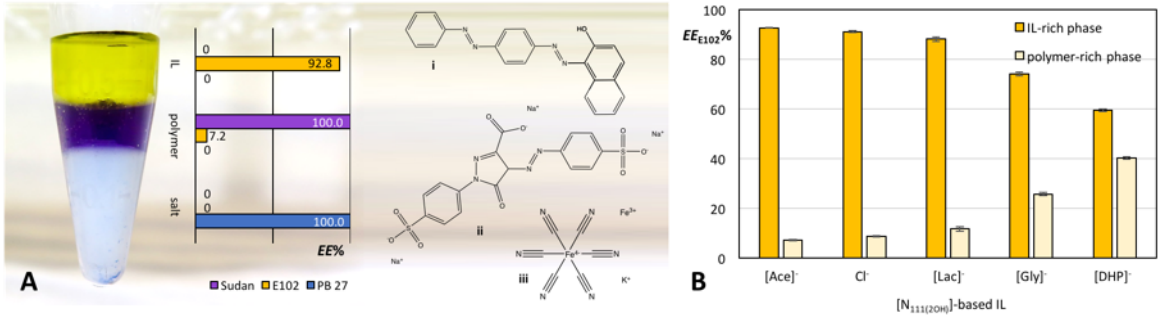

Figure 2.21. Dyes mixture separation in MuPS composed of $[N_{111(2OH)}]$-based IL + PEG 600 + K_3PO_4 + H_2O. **(A)** Selective extraction of (i) sudan, (ii) E102 and (iii) PB 27 in $[N_{111(2OH)}][Ace]$-based MuPS; **(B)** IL anion effect on the selective extraction of E102 dye between the IL- and polymer-rich phases.

2.4.5. Conclusions

The formation of novel IL-based MuPS was here demonstrated. A large number of novel MuPS composed of cholinium-based ILs, K_3PO_4, PEG 600, and water were investigated, allowing the conclusion that the formation of three aqueous phase systems is ruled by a triple salting-out effect. Moreover, an increase in temperature is favorable for the formation of IL-based MuPS. Due to the use of ILs as phase-forming components, these systems are of low viscosity and display an improved separation performance, as demonstrated here with a mixture of three dyes.

2.4.6. References

(1) S. Shen, Z. Chang and H. Liu, *Sep. Purif. Technol.*, 2006, **49**, 217–222;
(2) M. Mojski and I. Glyukh, *J. Anal. Chem.*, 1996, **51**, 329–342;
(3) L. Liu, Y. Dong and Z. Xiu, *Process Biochem.*, 2010, **45**, 752–756;
(4) S. Shen, Z. Chang, J. Liu, X. Sun, X. Hu and H. Liu, *Sep. Purif. Technol.*, 2007, **53**, 216–223;

(5) J. Chen, H. Z. Liu, B. Wang, Z. T. An and Q. F. Liu, in *Proceedings of the International Solvent Extraction Conference (ISEC2002)*, Johannesburg, 2002, pp. 602–606;
(6) Xian-Dong Tan, Ji Qing and Zhi-Dong Chang, *Chinese J. Process Eng.*, 2006, **6**, 363–368;
(7) J. L. Womack, J. C. Lichter and D. J. Wilson, *Sep. Sci. Technol.*, 1982, **17**, 897–924;
(8) K. Xie, J. Zhao, L. Yang, P. Yu and H. Liu, *Sep. Purif. Technol.*, 2010, **76**, 191–197;
(9) H. Cabezas, *J. Chromatogr. B Biomed. Sci. Appl.*, 1996, **680**, 3–30;
(10) C. R. Mace, O. Akbulut, A. A. Kumar, N. D. Shapiro, R. Derda, M. R. Patton and G. M. Whitesides, *J. Am. Chem. Soc.*, 2012, **134**, 9094–9097;
(11) Y. Liang, S. Xu, Y. Shang, C. Peng and H. Liu, *Colloids Surfaces A Physicochem. Eng. Asp.*, 2014, **454**, 152–158;
(12) O. Akbulut, C. R. Mace, R. V. Martinez, A. A. Kumar, Z. Nie, M. R. Patton and G. M. Whitesides, *Nano Lett.*, 2012, **12**, 4060–4064;
(13) A. A. Kumar, C. Lim, Y. Moreno, C. R. Mace, A. Syed, D. Van Tyne, D. F. Wirth, M. T. Duraisingh and G. M. Whitesides, *Am. J. Hematol.*, 2015, **90**, 31–36;
(14) M. G. Freire, A. F. M. Cláudio, J. M. M. Araújo, J. A. P. Coutinho, I. M. Marrucho, J. N. C. Lopes and L. P. N. Rebelo, *Chem. Soc. Rev.*, 2012, **41**, 4966–4995;
(15) M. G. Freire, Ed., *Ionic-Liquid-Based Aqueous Biphasic Systems*, Springer Berlin Heidelberg, Berlin, Heidelberg, 2016;
(16) N. Muhammad, M. I. Hossain, Z. Man, M. El-Harbawi, M. A. Bustam, Y. A. Noaman, N. B. Mohamed Alitheen, M. K. Ng, G. Hefter and C.-Y. Yin, *J. Chem. Eng. Data*, 2012, **57**, 2191–2196;
(17) J. Pernak, A. Syguda, I. Mirska, A. Pernak, J. Nawrot, A. Pradzyńska, S. T. Griffin and R. D. Rogers, *Chem. - A Eur. J.*, 2007, **13**, 6817–6827;
(18) S. P. M. Ventura, C. M. S. S. Neves, M. G. Freire, I. M. Marrucho, J. Oliveira and J. a P. Coutinho, *J. Phys. Chem. B*, 2009, **113**, 9304–9310;
(19) C. M. S. S. Neves, S. P. M. Ventura, M. G. Freire, I. M. Marrucho and J. a P. Coutinho, *J. Phys. Chem. B*, 2009, **113**, 5194–5199;
(20) B. Zavlasky, *Aqueous Two-Phase Partitioning: Physical Chemistry and Bioanalytical Applications*, M. Dekker, New York, 1994;
(21) J. F. B. Pereira, K. A. Kurnia, O. A. Cojocaru, G. Gurau, L. P. N. Rebelo, R. D. Rogers, M. G. Freire and J. A. P. Coutinho, *Phys. Chem. Chem. Phys.*, 2014, **16**, 5723–5731;
(22) F. A. e Silva, J. F. B. Pereira, K. A. Kurnia, S. P. M. Ventura, A. M. S. Silva, R. D. Rogers, J. A. P. Coutinho and M. G. Freire, *Chem. Commun.*, 2017, DOI: 10.1039/C7CC02294H;
(23) S. Shahriari, L. C. Tomé, J. M. M. Araújo, L. P. N. Rebelo, J. A. P. Coutinho, I. M. Marrucho and M. G. Freire, *RSC Adv.*, 2013, **3**, 1835–1843;
(24) Pedro D. O. Esteves, *Extraction and Purification of Theobromine using Ionic Liquids*. Master Thesis. University of Aveiro, Aveiro, Portugal, 2015;
(25) S. Shahriari, C. M. S. S. Neves, M. G. Freire and J. A. P. Coutinho, *J. Phys. Chem. B*, 2012, **116**, 7252–7258;
(26) D. Fontana and G. Ricci, *J. Chromatogr. B Biomed. Sci. Appl.*, 2000, **743**, 231–234;
(27) H. D. Willauer, J. G. Huddleston, M. Li and R. D. Rogers, *J. Chromatogr. B Biomed. Sci. Appl.*, 2000, **743**, 127–135;
(28) *ChemSpider – The free chemical database*, 2017, www.chemspider.com.

2.5. Are aqueous biphasic systems composed of deep eutectic solvents ternary or quaternary systems?

This chapter is based on the published manuscript

Helena Passos, Daniel J. P. Tavares, Ana M. Ferreira, Mara G. Freire, and João A. P. Coutinho;[1]

"Are aqueous biphasic systems composed of deep eutectic solvents ternary or quaternary systems?", ACS Sustainable Chemistry and Engineering 4 (2016) 2881–2886.

2.5.1. Abstract

Deep eutectic solvents (DES) have emerged in the past few years as a new class of solvents with promising applications in several fields. In the present work, the application of DES (formed by binary mixtures of cholinium chloride and carboxylic acids or urea) as phase-forming components of aqueous biphasic systems (ABS) is investigated. The mechanisms associated with the phases demixing of ABS composed of DES, as well as the DES stability in aqueous solutions, are investigated to address the critical question whether DES-based ABS are in fact ternary or quaternary mixtures. It is shown that the DES integrity is destroyed in ABS by the disruption of the hydrogen-bonding interactions of the complex (a result of the isolated components preferential solvation by water), and as confirmed by a nonstoichiometric partition of the DES components between the coexisting phases. As a result, there are no "real" DES-based ABS; instead, there is the formation of ABS composed of four components, where the carboxylic acid used as the hydrogen-bond donor species seems to act as an additive. Finally, it is shown that these ABS have an outstanding potential to be used in extraction processes, as it is here demonstrated with the complete separation of two dyes. However, the volatile nature of short chain carboxylic acids and the nonstoichiometric partition of the DES components in ABS make the development of recovery and recycling steps more difficult to accomplish.

2.5.2. Introduction

Deep eutectic solvents (DES) were introduced in 2003, when Abbott and co-workers[1] demonstrated the possibility of producing a liquid solvent at room temperature by mixing two solid starting materials with considerably higher melting points (*e.g.*, urea and cholinium chloride ($[N_{111(2OH)}]Cl$), with melting temperatures of 406 and 575 K, respectively). After this proof of

[1]**Contributions:** M.G.F. and J.A.P.C. conceived and directed this work. H.P. and D.J.P.T. acquired the experimental data. A.M.F. worked on the selective extraction of the dyes. H.P., M.G.F and J.A.P.C. interpreted the experimental data and wrote the final manuscript, with significant contributions of the remaining authors.

concept, the number of works concerning the understanding of the underlying molecular-level scenario, their physical and chemical properties, as well as their applications as alternative solvents, increased significantly.[2–4]

The formation of DES results from the formation of strong hydrogen bonds between the two starting materials, namely, a hydrogen-bond donor (HBD) and a hydrogen-bond acceptor (HBA). The formation of ion-HBD complexes leads to a lower entropic difference of the phase transition and to the further depression of the freezing temperature.[5–7] The first reported DES (composed of $[N_{111(2OH)}]Cl$ and urea)[1] remains the most widely investigated. However, DES can be formed by mixing other substituted tetraalkylammonium or phosphonium salts with a HBD, such as amines, carboxylic acids, and carbohydrates, among others.[8–10]

Many DES share some of the unique characteristics of ionic liquids (ILs), namely, a low volatility, high conductivity, wide liquid temperature range, and high solvation ability for a large number of compounds.[3,4] DES are also able to overcome some of the disadvantages related to ILs. They are easier to prepare, by a simple mixture of the starting materials at moderate temperatures, without requiring a reaction step. Furthermore, the addition of an agent able to disrupt hydrogen-bonding interactions can lead to the recovery of at least one of the initial compounds.[3,4,11,12] The starting materials are usually cheaper, toxicologically well-characterized, and often derived from renewable resources, which results in low-cost and more environmentally friendly products.[3,4,11,12] As in ILs, innumerous combinations of the starting materials can be attempted, and therefore, DES may also be classified as "designer solvents". Since DES have fewer restrictions in terms of stoichiometry, their properties and phase behavior can be tuned by changing the ratio of their components, thus adding one more degree of freedom to their design.[3,4,11,12] Although reports regarding the applications of DES are still limited, a reasonable number of studies have shown the potential of DES as alternative solvents in electrochemistry, catalysis, synthesis, and separation processes.[3,4,13–15]

In the past decade, aqueous biphasic systems (ABS) composed of ILs and a wide number of salts, carbohydrates, polymers, or amino acids have been extensively studied for the extraction and purification of bioactive compounds.[16] IL-based ABS lead to remarkable extraction efficiencies and selectivities by a proper tailoring of their phases' polarities and affinities.[16] Albeit scarcely investigated, the potential of DES as phase forming components of ABS was recently reported by Xu and co-workers.[17,18] Yet, those pioneering phenomenological results did not comprise the mechanisms associated with the coexisting phases demixing and the stability of the HBD:HBA complex in aqueous media. Only "ternary" phase diagrams for each ABS were reported, and their

applications to the extraction of proteins were presented.[17,18] Whether DES in the form of a HBD:HBA complex will form a ternary system, as in common ABS, or the alleged DES-based ABS is a quaternary system that phase separates with a nonstoichiometric partition of the HBD and HBA species between the two phases remains an open question. In this context, the present work aims at shedding light on this subject. For this purpose, novel ABS composed of water, poly(propylene glycol) with an average molecular weight of 400 g·mol^{-1} (PPG 400), and several DES formed by [$N_{111(2OH)}$]Cl and carboxylic acids or urea were investigated. PPG 400 was selected for its good ability to form ABS[19,20] and because the use of polymers instead of ILs or salts to form DES-based ABS prevents the introduction of other ionic species into solution and possible ion exchange between the two phases. The studied DES allow the analysis of the effect of the urea or carboxylic acid:[$N_{111(2OH)}$]Cl ratio and the impact of the HBD species on their ability for the creation of ABS, as well as to infer on their nonstoichiometric partition between the coexisting phases. The phase-formation capability of these systems is also herein compared with ABS formed by [$N_{111(2OH)}$]-based ILs, with anions corresponding to the investigated acids, and PPG 400. Finally, the application of these systems for the selective separation of dyes is investigated to ascertain on their potential applicability.

2.5.3. Experimental procedures

Materials. The determination of the liquid−liquid phase diagrams was performed using aqueous solutions of PPG with an average molecular weight of 400 g·mol^{-1} (from Sigma-Aldrich, Germany) and individual aqueous solutions of DES, prepared by us, using the following components: [$N_{111(2OH)}$]Cl (98 wt % pure from Sigma-Aldrich, Germany), glycolic acid (>99 wt % pure from Sigma-Aldrich, Germany), acetic acid (>99 wt % pure from Sigma-Aldrich, Germany), lactic acid (88−92 wt % pure from Riedel-de Haen, Germany), citric acid tetrahydrated (100 % pure from Fisher Scientific, USA), and urea (99.0 − 100.5 % pure from Panreac, Spain). All components used on the DES preparation were dried under vacuum (10 Pa) at room temperature for a minimum of 24 h. The cholinium-based ILs used on the dyes' selective extraction were [$N_{111(2OH)}$]Cl, cholinium dihydrogen citrate, [$N_{111(2OH)}$][DHC] (98 wt % pure from Sigma-Aldrich, Germany), cholinium acetate, [$N_{111(2OH)}$][Ace] (98 wt % pure from Iolitec, Germany), cholinium glycolate, [$N_{111(2OH)}$][Gly] (97 wt % pure and synthesized by us), and cholinium lactate, [$N_{111(2OH)}$][Lac] (99 wt % pure and synthesized by us). The ILs synthesized by us were prepared according to well-established protocols.[21,22] The required precursors were commercially acquired, namely, cholinium hydroxide [$N_{111(2OH)}$][OH] (40 wt % in methanol) from Sigma-Aldrich (Germany)

and glycolic acid and lactic acid as described before. After the synthesis and before use, all ILs were purified and dried for a minimum of 24 h at constant agitation, at a moderate temperature (~343 K) under vacuum (10 Pa). The extracted dyes were sudan III (>99 wt % pure) from Merck (Germany) and pigment blue-29 (PB 29) obtained from Holliday Pigments (France). The chemical structures of studied DES, ILs, PPG, and dyes are presented in the **Figure 2.22**. The water used was double distilled, passed through a reverse osmosis system, and further treated with a Milli-Q plus 185 apparatus.

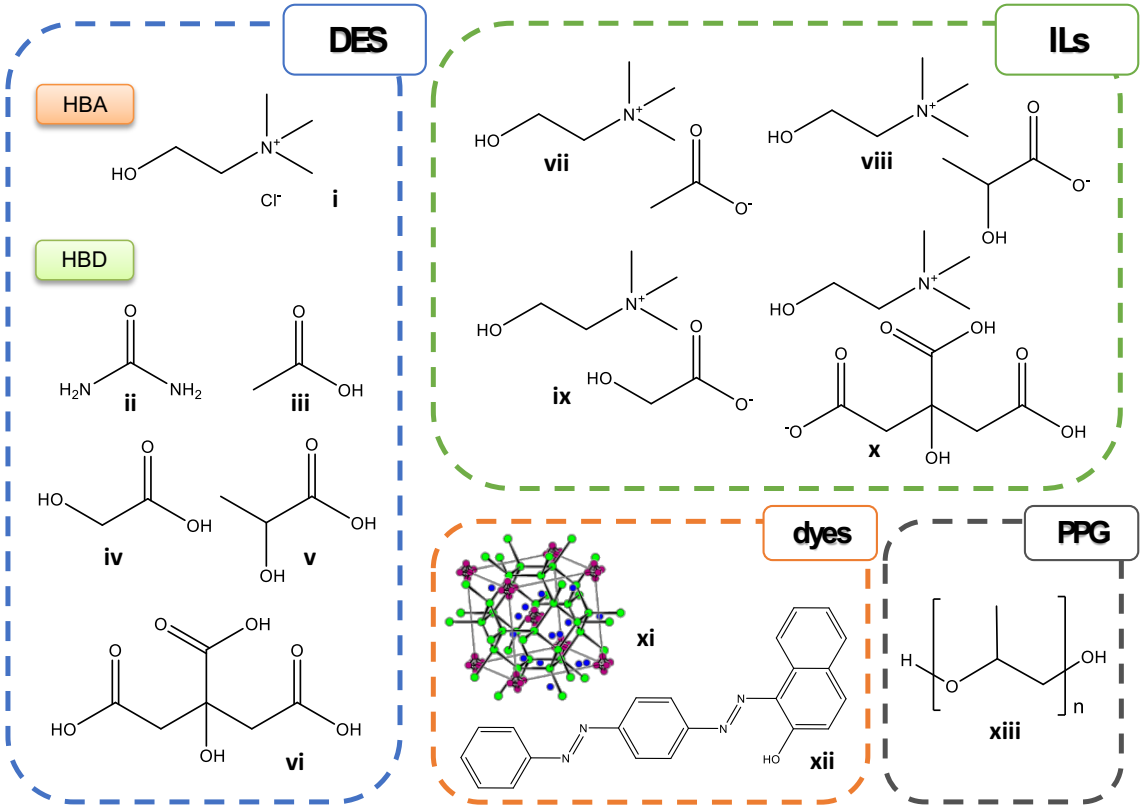

Figure 2.22. Chemical structure of the investigated DES constituents (hydrogen bond acceptor (HBA) and hydrogen bond donor (HBD)), ILs, dyes and PPG: (i) $[N_{111(2OH)}]Cl$; (ii) urea; (iii) acetic acid; (iv) glycolic acid; (v) lactic acid; (vi) citric acid; (vii) $[N_{111(2OH)}][Ace]$; (viii) $[N_{111(2OH)}][Lac]$; (ix) $[N_{111(2OH)}][Gly]$; (x) $[N_{111(2OH)}][DHC]$; (xi) PB 29; (xii) sudan III; (xiii) PPG.

DES preparation. For the preparation of DES, both the hydrogen-bond donor (carboxylic acids or urea) and acceptor ($[N_{111(2OH)}]Cl$) species were added gravimetrically within $\pm 10^{-4}$ g to closed vials, at three different mole ratios, 1:2, 1:1, and 2:1 of carboxylic acid:$[N_{111(2OH)}]Cl$ and urea:$[N_{111(2OH)}]Cl$, and heated in an oil bath with constant agitation. The maximum temperature reached was 333 K for the DES composed of acetic acid and 373 K for DES composed of glycolic acid, lactic acid, and urea. For the preparation of the citric-acid-based DES, higher temperatures, close to 393 K, were required until the formation of a transparent liquid. After the formation of a

liquid, the mixture was maintained for 1 h at the final temperature and was then cooled down to room temperature. All the procedure was executed under an inert atmosphere. The water content of the DES constituents was measured using a Metrohm 831 Karl Fischer coulometer that was taken into consideration during the preparation of each mixture. The final physical state (liquid or wet solid) and composition of the synthesized DES at room temperature are described in the **Appendix A**.

Phase diagrams and tie-lines. The solubility curves were determined through the cloud point titration method[23,24] at 298 K (± 1 K) and atmospheric pressure. The experimental procedure adopted in this work follows the method already validated by us and described in **chapter 2.1**. Aqueous solutions of PPG at approximately 80 wt % and aqueous solutions of the different DES at 75 wt % were prepared and used for the determination of the binodal curves. Repetitive dropwise addition, under constant stirring, of the aqueous DES solution to the aqueous solutions of PPG was carried out until the detection of a cloudy (biphasic) solution, followed by the dropwise addition of ultrapure water until the finding of a monophasic region (clear and limpid solution). The ternary system compositions were determined by weight quantification within $\pm 10^{-4}$ g. The experimental binodal curves were fitted by least-squares regression according to **Equation (2.1)**.

For the determination of each tie-line (TL), a ternary mixture composed of DES + PPG + water at the biphasic region was gravimetrically prepared as indicated in **chapter 2.1**, and determined through the relationship between the weight of the salted-out specie ("DES") rich phase and the overall weight by the lever-arm rule using **Equations (2.2)** to **(2.5)**. The tie-line length (TLL) was determined using **Equation (2.6)**.

The pH values (±0.02) of the PPG- and "DES"-rich aqueous phases were measured at (298 ± 1) K using a Mettler Toledo SevenMulti dual pH meter.

DES stability in aqueous media. To evaluate if the HBD-[$N_{111(2OH)}$]Cl hydrogen-bonding interactions are maintained when DES are dissolved in water or in the ABS formation, the mole ratio between each carboxylic acid or urea and the cholinium cation in each phase of the corresponding ABS was determined by ^{1}H nuclear magnetic resonance (NMR), in solution and neat, respectively, using a Bruker Avance 300 at 300.13 MHz, with deuterium oxide (D_2O) as solvent and trimethylsilyl propanoic acid (TSP) as the internal reference. For this, individual ABS composed of PPG + DES + water at the biphasic region were gravimetrically prepared within $\pm 10^{-4}$ g, vigorously agitated, and centrifuged at 3500 rpm for 30 min at (298 ± 1) K, in order to reach the equilibrium and a complete separation of the coexisting phases. Samples of each phase were then taken for the quantification of each carboxylic acid or urea and the cholinium cation by ^{1}H NMR.

Selective extraction of textile dyes. Two textile dyes, sudan III and PB 29, were studied as model molecules to demonstrate the potential application of DES-based ABS. A ternary mixture with a common composition, and within the biphasic region, was prepared with 21 wt % of DES, 40 wt % of PPG, and 39 wt % of water with the exception of the ABS constituted by the following DES: 1:1 and 2:1 of citric acid:$[N_{111(2OH)}]Cl$. With these two systems, the following mixture point was used: 25 wt % of DES + 50 wt % of PPG + 25 wt % of H_2O. In each system, with a total weight of 3 g, a small amount of each dye (≈0.30 mg) was added. After the total dissolution of both dyes, each mixture was centrifuged at 1500 rpm for 10 min at (298 ± 1) K to achieve the complete partition of each dye between the two phases.

After a careful separation of both phases, the quantification of each dye in the two phases was carried by UV-vis spectroscopy, using a synergy/HT microplate reader, at a wavelength of 348 nm for sudan III and 725 nm for PB 29. At least three individual experiments were performed in order to determine the average in the extraction efficiency, as well as the respective standard deviations. The interference of the polymer and DES with the quantification method was also taken into account, and blank control samples were always employed. The percentage extraction efficiency of sudan III is defined as the percentage ratio between the amount of dye in the PPG aqueous-rich phase and that in the total mixture. Similarly, the percentage extraction efficiency of PB 29 is defined as the percentage ratio between the amount of dye in the "DES"-aqueous-rich phase and that in the total mixture.

2.5.4. Results and discussion

A total of 15 DES formed by $[N_{111(2OH)}]Cl$, as the HBA, and four carboxylic acids as the HBD, namely, lactic, glycolic, citric and acetic acids, or urea, at three mole composition ratios (2:1, 1:1, and 1:2), were prepared. The liquid−liquid phase diagrams of some ABS composed of DES + PPG 400 + H_2O are depicted in **Figure 2.23**. For all phase diagrams, the biphasic region is located above the binodal curve, and the monophasic region is localized below. The detailed experimental weight fraction data and the representation of the phase diagrams for the remaining DES-based ABS are presented in the **Appendix A**, along with the compositions of the coexisting phases (tie-lines). In the studied ABS, the top phase corresponds to the PPG-rich phase, while the bottom phase is mainly composed of an aqueous solution enriched in DES.

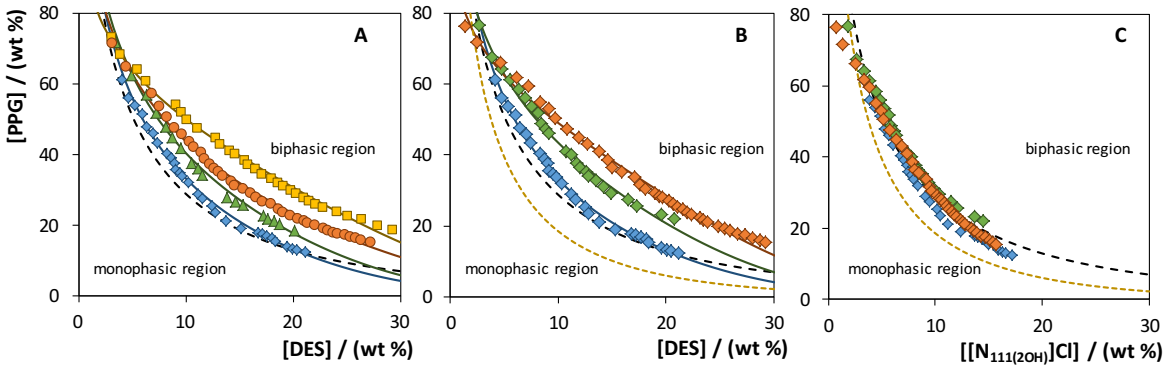

Figure 2.23. Phase diagrams of DES-based ABS at 298 K. **(A)** Carboxylic acid nature effect on ABS formation: DES constituted by 1:2 mole proportion of acetic acid:[$N_{111(2OH)}$]Cl (◆), glycolic acid:[$N_{111(2OH)}$]Cl (▲), lactic acid:[$N_{111(2OH)}$]Cl (●) and citric acid:[$N_{111(2OH)}$]Cl (■); fitting of the binodal data by **Equation (2.1)** (–); [$N_{111(2OH)}$]Cl-based ABS binodal curve (---). **(B)** Carboxylic acid concentration effect on ABS formation: DES composed of acetic acid:[$N_{111(2OH)}$]Cl mole proportion of 1:2 (◆), 1:1 (◆) and 2:1 (◆); fitting of the binodal data by **Equation (2.1)** (–); [$N_{111(2OH)}$]Cl-based ABS binodal curve (---); [$N_{111(2OH)}$][Ace]-based ABS binodal curve (---). **(C)** Representation of the binodal curves of acetic acid:[$N_{111(2OH)}$]Cl-based ABS as function of the [$N_{111(2OH)}$]Cl concentration: DES composed of acetic acid:[$N_{111(2OH)}$]Cl mole proportion of 1:2 (◆), 1:1 (◆) and 2:1 (◆); [$N_{111(2OH)}$]Cl-based ABS binodal curve (---); [$N_{111(2OH)}$][Ace]-based ABS binodal curve (---).

Figure 2.23 **A** allows the evaluation of the effect of the carboxylic acid nature on the ABS formation ability. It is well-established that the higher the ion's ability to create hydration complexes is the easier the formation of salt-polymer or IL-salt ABS is.[16,25] The DES ability to form ABS is in the following order: acetic acid:[$N_{111(2OH)}$]Cl > glycolic acid:[$N_{111(2OH)}$]Cl > lactic acid: [$N_{111(2OH)}$]Cl > citric acid:[$N_{111(2OH)}$]Cl. In a comparison of the DES capability to form ABS with the corresponding [$N_{111(2OH)}$]-based ILs ([$N_{111(2OH)}$][Gly] ~ [$N_{111(2OH)}$][Ace] > [$N_{111(2OH)}$][Lac] ~ [$N_{111(2OH)}$]Cl > [$N_{111(2OH)}$][DHC]),[26] it is possible to identify a similar trend. According to the [$N_{111(2OH)}$]Cl position in this trend, it is however evident that there is a stronger aptitude of the [$N_{111(2OH)}$]-based ILs to form ABS (*cf.* the **Appendix A**). In general, and as represented in **Figure 2.23 A**, it seems that carboxylic acids with shorter alkyl side chains have a higher liquid-liquid demixing ability. Nevertheless, when the weight fraction of the several acids is not considered, a different scenario emerges, with a nonsignificant impact of the acid nature as discussed below.

Figure 2.23 B depicts the carboxylic acid concentration effect, where an increase of the acid content leads to a decrease on the area of the biphasic regime. This behavior is always observed and appears to be independent of the acid nature. Furthermore, with consideration of the eutectic point of the DES studied (~2:1 for acetic and lactic-acid-based DES, 1:1 for glycolic acid: [$N_{111(2OH)}$]Cl DES, and 1:2 for citric acid:[$N_{111(2OH)}$]Cl DES),[11] it is clear that the application of an eutectic mixture does not change this trend. It was previously reported that [$N_{111(2OH)}$]Cl is the salting-out agent in PPG-based ABS.[26] As shown in **Figure 2.23 A**, the presence of a non-salting-out

species, such as a carboxylic acid, seems to decrease the ability of ABS formation by $[N_{111(2OH)}]Cl$. However, when the binodal curves are presented as a function of the isolated $[N_{111(2OH)}]Cl$ concentration, **Figure 2.23 C**, there is an almost complete superposition of the solubility curves. This pattern supports the vision of a mechanism of salting-out of $[N_{111(2OH)}]Cl$ over PPG in aqueous media, with the carboxylic acid contributing with a minor effect on the ability of ABS formation.

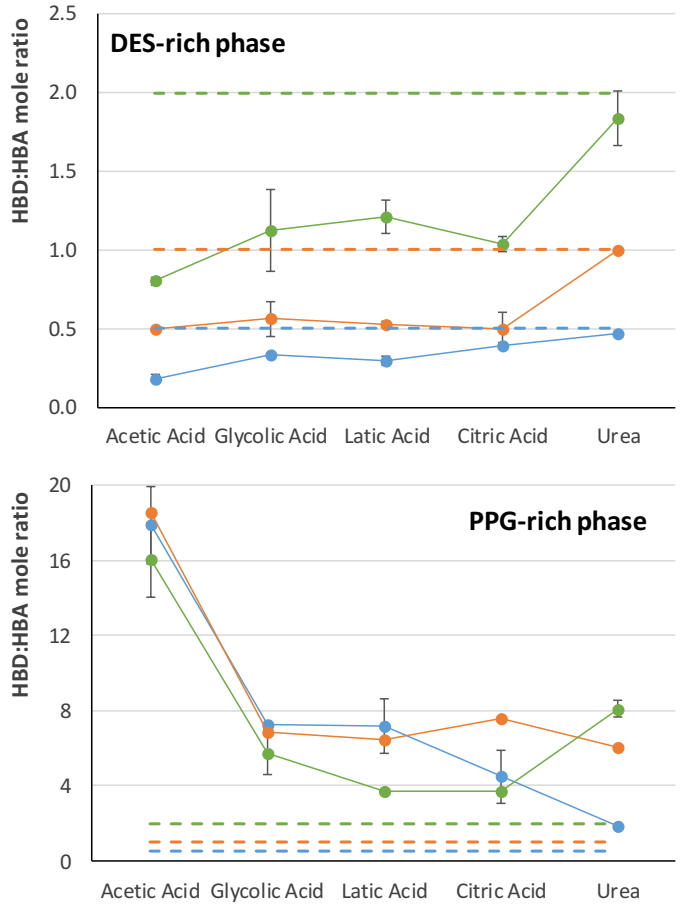

Figure 2.24. Mole ratio between the HBD and $[N_{111(2OH)}]Cl$ (HBA) in the coexisting phases of ABS composed of DES + PPG + H_2O (solid lines) and in DES initial composition (dashed lines): 1:2 (blue); 1:1 (orange); 2:1 (green).

Although the formation of ABS using DES is unquestionable, there remains the major question of whether the carboxylic acid:$[N_{111(2OH)}]Cl$ DES complexes are maintained when dissolved in aqueous media (for ABS formation). To gather novel insights on this matter, ^1H NMR spectra of both phases were acquired to evaluate the content and ratio between each acid and $[N_{111(2OH)}]Cl$. Examples of these spectra are provided in the **Appendix A.**

Figure 2.24 depicts the HBD:$[N_{111(2OH)}]Cl$ mole ratio obtained for both "DES"- and PPG-rich phases. The number of moles of each DES component in each phase, as well as mole ratio between the HBD and HBA species, are presented in the **Appendix A**. These results reveal that the carboxylic acid:$[N_{111(2OH)}]Cl$ complexes are destroyed, since the ratio used on DES preparation is not maintained in the coexisting phases of DES-based ABS. This nonstoichiometric partition of the DES components also reinforces the hypothesis that these ABS are formed by the salting-out effect exerted by $[N_{111(2OH)}]Cl$ over the polymer in aqueous media, since the formation of two-phase systems was always observed. As previously highlighted, carboxylic acids slightly affect the solubility curves; however, they partition in different amounts between the coexisting phases. The extent of their partition is presented in

the **Appendix A**. Although more than 40% of carboxylic acids remain in the "DES"-rich phase, in the PPG-rich phase the amount of carboxylic acids is considerably higher than that of $[N_{111(2OH)}]Cl$. In summary, there are no "real" DES-based ABS. There are, on the other hand, ABS formed by $[N_{111(2OH)}]Cl$ and PPG, where carboxylic acids seem to act as additives and tend to partition to different extents (according to the acid nature) between the coexisting phases.

The water effect on the DES integrity is one of the major gaps in the DES research field. The observed nonstoichiometric partition of the DES components between the coexisting phases reveals that the DES integrity is destroyed in an ABS by the disruption of the hydrogen-bonding interactions within the HBD:HBA complex. These results are further corroborated by some recent works[27–31] which demonstrated that the dilution of DES in water results in a progressive rupture of the hydrogen bonds between the starting materials. For each DES, there seems to exists a maximum amount of water that can be added before the complete disruption of the DES complex followed by the formation of an aqueous solution containing the solvated individual components.

On the basis of the results reported here, it can be concluded that ABS composed of carboxylic-acid-based DES are indeed quaternary systems and not ternary systems as other types of ABS. The formation of the ABS seems to be controlled by PPG 400 and $[N_{111(2OH)}]Cl$, with a minor effect of the carboxylic acids. There are no "real" DES-based ABS; instead, these systems are ABS formed by $[N_{111(2OH)}]Cl$ and PPG 400, as previously reported,[26] where the carboxylic acid acts as a fourth compound or additive in the ABS.[32–34]

The interactions between carboxylic acids and $[N_{111(2OH)}]Cl$ are weaker than those observed in DES constituted by urea and $[N_{111(2OH)}]Cl$.[1] As a further confirmation test, ABS composed of the DES formed by urea:$[N_{111(2OH)}]Cl$ (at the mole composition ratios of 1:2, 1:1, and 2:1) and PPG 400 were also studied. The detailed experimental weight fraction data, respective phase diagrams, and compositions of the phases are presented in the **Appendix A**. As observed with the ABS formed by carboxylic acids:$[N_{111(2OH)}]Cl$ DES, PPG is salted-out by $[N_{111(2OH)}]Cl$, while urea has a negligible effect on the phase diagram behavior. However, unlike for the other systems discussed above, the urea:$[N_{111(2OH)}]Cl$ mole ratio in the "DES"-rich phase depicted in **Figure 2.24** is the same as the initial mole ratio used in the DES preparation. The question of the stability of this particular DES complex is thus not settled by the results reported here. A finer analysis of these results is thus in order. From all HBD species studied in this work, urea presents the lowest octanol–water partition coefficient (K_{ow}), thus presenting a higher affinity for salt-aqueous-rich phases when compared with the carboxylic acids. Contrary to that observed for carboxylic acids, the extraction efficiency of urea is higher than 90% meaning that most urea on the system remains in the

cholinium-rich phase; the number of moles of each species in each phase is provided in the **Appendix A**. Since PPG aqueous-rich phases are composed of a large amount of polymer (>70 wt % from tie-lines data, *cf.* **Appendix A**), with only a small amount of water and other components, the distribution data obtained by ^{1}H NMR spectroscopy for the coexisting phases of the urea: [$N_{111(2OH)}$]Cl-based ABS could be a result of the almost total partition of both the [$N_{111(2OH)}$]Cl and urea to the most hydrophilic phase, which would explain the results obtained (*cf.* **Appendix A**). In fact, literature results[27–31] support the idea that this complex is not stable at water concentrations higher than 50 wt % (*cf.* **Appendix A**), as those observed in the "DES"-rich phase of our systems. Overall, the obtained results suggest that DES-based ABS are quaternary systems composed of [$N_{111(2OH)}$]Cl, PPG 400, and water, with carboxylic acids or urea acting as additives.

Although ABS composed of DES are quaternary instead of ternary systems, their applicability may not be conditioned by the DES nonstoichiometric partition. To demonstrate their potential in separation processes, the selective extraction of two textile dyes, namely, pigment blue (PB 29) and sudan III, was evaluated, **Figure 2.25**. Mixture compositions and extraction efficiencies (EE_{dye}%) are described in detail in the **Appendix A**. In all DES-based ABS, sudan III preferentially partitions to the PPG-rich phase, while PB 29 completely migrates to the opposite phase. Sudan III has a less polar character (log(K_{OW}) = 7.74)[35] than PB 29 and therefore preferentially partitions to the more hydrophobic PPG-rich phase, while the inorganic pigment partitions to the more polar salt-rich phase.

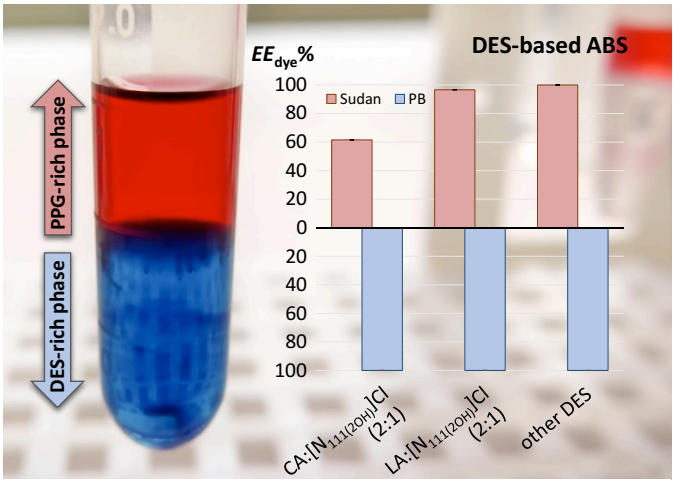

Figure 2.25. Selective extraction of the textile dyes sudan III and PB 29 with ABS composed of DES.

Remarkably, for 10 of the 12 studied systems, the complete separation of the two dyes was achieved; *i.e.*, they are completely enriched in one of the phases. Only the systems composed of citric acid:[$N_{111(2OH)}$]Cl (2:1) and lactic acid: [$N_{111(2OH)}$]Cl (2:1) display lower extraction efficiencies for sudan III, 61.6% and 96.6%, respectively (**Figure 2.25**). The worst performance of these two systems seems to be related to their lower ability to create ABS. Furthermore, the extraction performance of DES-based ABS is identical to that of IL-based ABS formed by [$N_{111(2OH)}$]-based ILs, [$N_{111(2OH)}$]Cl, [$N_{111(2OH)}$][Ace], [$N_{111(2OH)}$][Gly], [$N_{111(2OH)}$][Lac], and [$N_{111(2OH)}$][DHC], and PPG 400 (*cf.*

the **Appendix A**), which means that DES-based ABS are able to compete in terms of extraction performance with IL-based systems. Nevertheless, contrary to IL-based ABS, the presence of volatile acids and the nonstoichiometric partition of the DES isolated components between the coexisting phases makes the design of a sustainable process more difficult, particularly when the recovery and recycling of the phase-forming components is envisaged. For instance, two approaches were previously proposed by Ferreira et al.[36] for the recovery of textile dyes (by induced precipitation) from the coexisting phases of ABS composed of ILs and salts by a reduction in temperature or by water evaporation, which further permits the recycling of the phase-forming components. In DES-based ABS, the presence of volatile acids and the nonstoichiometric partition of the DES isolated components between the coexisting phases require the design of more complex recovery processes.

2.5.5. Conclusions

The results reported here demonstrate that the DES integrity is destroyed in ABS by the disruption of the DES hydrogen-bond complex and preferential solvation of the isolated components by water. This is confirmed by the nonstoichiometric partition of the HBD and HBA species between the coexisting phases supporting the idea that DES-based ABS are in fact quaternary instead of ternary systems. These ABS are formed by $[N_{111(2OH)}]Cl$ and PPG 400 in water, where the carboxylic acids or urea act as the fourth component or as an additive in the overall system. It was also shown that DES-based ABS have potential to be used in extraction and purification processes, as it is here demonstrated with the complete separation of two dyes for opposite phases in a single-step. However, it should be kept in mind that the nonstoichiometric partition of the DES components and the volatile nature of short chain carboxylic acids make the design of an integrated and sustainable separation process more complex than that required, for instance, with IL-based ABS.[36]

2.5.6. References

(1) A.P. Abbott, G. Capper, D.L. Davies, R.K. Rasheed, and V. Tambyrajah, *Chem. Commun.*, 2003, 70–71;
(2) A. Paiva, R. Craveiro, I. Aroso, M. Martins, R.L. Reis, and A.R.C. Duarte, *ACS Sustainable Chem. Eng.*, 2014, **2**, 1063-1071;
(3) M. Francisco, A. van den Bruinhorst, and M.C. Kroon, *Angew. Chem. Int. Ed.*, 2013, **52**, 3074–3085;
(4) E.L. Smith, A.P. Abbott, and K.S. Ryder, *Chem. Rev.*, 2014, **114**, 11060–11082;
(5) A.P. Abbott, G. Capper, D.L. Davies, H.L. Munro, R.K. Rasheed, and V. Tambyrajah, *Chem. Commun.*, 2001, 2010–2011;
(6) P. Wasserscheid and W. Keim, *Angew. Chem. Int. Ed.*, 2000, **39**, 3772–3789;

(7) T. Welton, *Chem. Rev.*, 1999, **99**, 2071–2084;
(8) C. Florindo, F.S. Oliveira, L.P.N. Rebelo, A.M. Fernandes, and I.M. Marrucho, *ACS Sustainable Chem. Eng.*, 2014, **2**, 2416-2425;
(9) Y.H. Choi, J.V. Spronsen, Y. Dai, M. Verberne, F. Hollmann, I.W.C.E. Arends, G.-J. Witkamp, and R. Verpoorte, *Plant Physiol.*, 2011, **156**, 1701–1705;
(10) M.A. Kareem, F.S. Mjalli, M.A. Hashim, and I.M. AlNashef, *J. Chem. Eng. Data*, 2010, **55**, 4632–4637;
(11) A.P. Abbott, D. Boothby, G. Capper, D.L. Davies, and R.K. Rasheed, *J. Am. Chem. Soc.*, 2004, **126**, 9142–9147;
(12) M. Francisco, A. van den Bruinhorst, and M.C. Kroon, *Green Chem.*, 2012, **14**, 2153–2157;
(13) I. Gállego, M.A. Grover, and N.V. Hud, *Angew. Chem.*, 2015, **127**, 6869–6873;
(14) C. Vidal, J. García-Álvarez, A. Hernán-Gómez, A.R. Kennedy, and E. Hevia, *Angew. Chem. Int. Ed.*, 2014, **53**, 5969–5973;
(15) H. Wang, G. Gurau, J. Shamshina, O.A. Cojocaru, J. Janikowski, D.R. MacFarlane, J.H. Davis, and R.D. Rogers, *Chem. Sci.*, 2014, **5**, 3449–3456;
(16) M.G. Freire, A.F.M. Cláudio, J.M.M. Araújo, J.A.P. Coutinho, I.M. Marrucho, J.N. Canongia Lopes, and L.P.N. Rebelo, *Chem. Soc. Rev.*, 2012, **41**, 4966–4995;
(17) K. Xu, Y. Wang, Y. Huang, N. Li, and Q. Wen, *Anal. Chim. Acta*, 2015, **864**, 9–20;
(18) Q. Zeng, Y. Wang, Y. Huang, X. Ding, J. Chen, and K. Xu, *Analyst*, 2014, **139**, 2565–2573;
(19) C. Wu, J. Wang, Y. Pei, H. Wang, and Z. Li, *J. Chem. Eng. Data*, 2010, **55**, 5004-5008;
(20) M.T. Zafarani-Moattar, S. Hamzehzadeh, and S. Nasiri, *Biotechnol. Prog.*, 2012, **28**, 146-156;
(21) N. Muhammad, M.I. Hossain, Z. Man, M. El-Harbawi, M.A. Bustam, Y.A. Noaman, N.B. Mohamed Alitheen, M.K. Ng, G. Hefter, and C.-Y. Yin, *J. Chem. Eng. Data*, 2012, **57**, 2191–2196;
(22) J. Pernak, A. Syguda, I. Mirska, A. Pernak, J. Nawrot, A. Prądzyńska, S.T. Griffin, and R.D. Rogers, *Chem. Eur. J.*, 2007, **13**, 6817–6827;
(23) C.M.S.S. Neves, S.P.M. Ventura, M.G. Freire, I.M. Marrucho, and J.A.P. Coutinho, *J. Phys. Chem. B*, 2009, **113**, 5194–5199;
(24) S.P.M. Ventura, C.M.S.S. Neves, M.G. Freire, I.M. Marrucho, J. Oliveira, and J.A.P. Coutinho, *J. Phys. Chem. B*, 2009, **113**, 9304–9310;
(25) T. Mourão, A.F.M. Cláudio, I. Boal-Palheiros, M.G. Freire, and J.A.P. Coutinho, *J. Chem. Thermodynamics*, 2012, **54**, 398–405;
(26) M.V. Quental, M. Caban, M.M. Pereira, P. Stepnowski, J.A.P. Coutinho, and M.G. Freire, *Biotechnol. J.*, 2015, **10**, 1457–1466;
(27) C. D'Agostino, L.F. Gladden, M.D. Mantle, A.P. Abbott, E.I. Ahmed, A.Y.M. Al-Murshedi, and R.C. Harris, *Phys. Chem. Chem. Phys.*, 2015, **17**, 15297–15304;
(28) Y. Dai, J. van Spronsen, G.-J. Witkamp, R. Verpoorte, and Y.H. Choi, *Anal. Chim. Acta*, 2013, **766**, 61–68;
(29) Y. Dai, G.-J. Witkamp, R. Verpoorte, and Y.H. Choi, *Food Chem.*, 2015, **187**, 14–19;
(30) M.C. Gutiérrez, M.L. Ferrer, C.R. Mateo, and F. del Monte, *Langmuir*, 2009, **25**, 5509–5515;
(31) D. Shah and F.S. Mjalli, *Phys. Chem. Chem. Phys.*, 2014, **16**, 23900-23907;
(32) M.R. Almeida, H. Passos, M.M. Pereira, Á.S. Lima, J.A.P. Coutinho, and M.G. Freire, *Sep. Purif. Technol.*, 2014, **128**, 1–10;
(33) R.L. de Souza, V.C. Campos, S.P.M. Ventura, C.M.F. Soares, J.A.P. Coutinho, and Á.S. Lima, *Fluid Phase Equilibr.*, 2014, **375**, 30–36;
(34) J.F.B. Pereira, A.S. Lima, M.G. Freire, and J.A.P. Coutinho, *Green Chem.*, 2010, **12**, 1661–1669;
(35) *ChemSpider – The free chemical database*, 2015, www.chemspider.com;
(36) A.M. Ferreira, J.A.P. Coutinho, A.M. Fernandes, and M.G. Freire, *Sep. Pur. Tech.*, 2014, **128**, 58-66.

3. CHARACTERIZATION OF THE PROPERTIES AND UNDERSTANDING OF THE MECHANISMS RESPONSIBLE FOR THE TWO-PHASE FORMATION

3.1. Vapor-liquid equilibria of water + alkylimidazolium-based ionic liquids: measurements and Perturbed-Chain Statistical Associating Fluid Theory modeling

This chapter is based on the published manuscript

Helena Passos, Imran Khan, Fabrice Mutelet, Mariana B. Oliveira, Pedro J. Carvalho, Luís M. N. B. F. Santos, Christoph Held, Gabriele Sadowski, Mara G. Freire, and João A. P. Coutinho;[1]

"Vapor–liquid equilibria of water + alkylimidazolium-based ionic liquids: measurements and Perturbed-Chain Statistical Associating Fluid Theory modeling", Industrial and Engineering. Chemistry Research 53 (2014) 3737–3748.

3.1.1. Abstract

The industrial application of ionic liquids (ILs) requires the knowledge of their physical properties and phase behavior. This work addresses the experimental determination of the vapor–liquid equilibria (VLE) of binary systems composed of water + imidazolium-based ILs. The ILs under consideration are 1-butyl-3-methylimidazolium trifluoromethanesulfonate, 1-butyl-3-methylimidazolium thiocyanate, 1-butyl-3-methylimidazolium tosylate, 1-butyl-3-methylimidazolium trifluoroacetate, 1-butyl-3-methylimidazolium bromide, 1-butyl-3-methylimidazolium chloride, 1-butyl-3-methylimidazolium methanesulfonate, and 1-butyl-3-methylimidazolium acetate, which allows the evaluation of the influence of the IL anion through the phase behavior. Isobaric VLE data were measured at 0.05, 0.07, and 0.1 MPa for IL mole fractions ranging between 0 and 0.7. The observed increase in the boiling temperatures of the mixtures is related with the strength of the interaction between the IL anion and water. The Perturbed-Chain Statistical Associating Fluid Theory (PC-SAFT) was further used to describe the obtained experimental data. The ILs were treated as molecular associating species with two association sites per IL. The model parameters for the pure fluids and the binary interaction parameter k_{ij} between water and ILs were determined by a simultaneous fitting to pure-IL densities, water activity coefficients at 298.15 K and VLE data at 0.1 MPa. Pure-IL densities, water activity coefficients, and VLE data were well described by PC-SAFT in broad temperature, pressure, and composition ranges. The PC-SAFT parameters were applied to predict the water

[1]**Contributions:** This work was developed in collaboration between the research groups of J.A.P.C. and G.S from University of Aveiro, Portugal, and Technical University of Dortmund, Germany, respectively. J.A.P.C., G.S., C.H. and M.B.O. conceived and directed this work. I.K. and P.J.C. acquired the VLE experimental data. F.M. determined the experimental water activity coefficients at infinity dilution. H.P., C.H. and M.B.O worked on the thermodynamic modelling. H.P., I.K., C.H, M.B.O. and J.A.P.C. interpreted the experimental data and wrote the final manuscript, with significant contributions of the remaining authors.

activity coefficients at infinite dilution in ILs, and a satisfactory prediction of experimental data was observed. Finally, PC-SAFT potential for be used as tool to predict the LLE of ternary mixtures composed of IL + salt + water was also demonstrated.

3.1.2. Introduction

The absorption refrigeration is widely used in many fields, such as in military, air conditioning, electric power, steelmaking, chemical industry, and drugs manufacturing.[1] This technology requires a working pair of fluids composed of refrigerant and absorbent. Many working fluid pairs are suggested in literature[2–5] for absorption refrigeration, but there is still no ideal working fluid pair by now. The performance of absorption cycles depends on the thermodynamic properties of the working pair. Currently, the binary systems water + NH_3 and water + LiBr are applied as working fluid pairs in absorption refrigerators,[2] but these systems have some disadvantages such as corrosion, crystallization, or toxicity. Therefore, the finding of more advantageous working pairs with good thermal stability without corrosive and crystallization effects has become a research focus in recent years. Several researchers[3–5] demonstrated that the extreme values of the excess Gibbs function (G^E_{max}) can be used to evaluate the performance of the absorption cycle working pairs. Mixtures with negative deviation from the Raoult's law usually exhibit a strong absorption performance. The G^E_{max} of such mixtures are negative as the activity coefficients of the respective components are lower than unity. This causes large vapor pressure depressions and/or high boiling-point elevations.

Ionic liquids (ILs) have recently attracted increased attention because of their potential for absorption refrigeration.[6] Due to their physical properties, ILs can be used as new cooling absorbents for absorption chillers or absorption heat pumps where one possible working pair might be composed of water (refrigerant) and IL (absorber). Thus, knowledge about thermodynamic properties and phase equilibria of water + IL solutions is fundamental to determine their applicability as absorption refrigeration systems[7,8] and for a correct design and application of absorption processes.

A good working fluid pair for absorption refrigeration processes should show a large boiling-temperature elevation and/or vapor pressure depression. The boiling-temperature elevation of water depends on the kind of IL, on the IL concentration in the mixture and on temperature. For absorption systems using water + ILs, numerous literature works have been reported.[8–12] Experimental activity coefficients of water at infinite dilution in ILs, γ_w^∞, have also been extensively published.[13–34] Such data are an appropriate indicator for the evaluation of the

performance of a working pair for absorption refrigeration processes. For this application, low γ_w^∞ values are desired, meaning strong water-IL interactions.

Yokozeki and Shiflett stated that an optimized water + IL system could compete with the existing water + LiBr system[35] for absorption refrigeration processes. Zuo et al.[8] suggested the system water + 1-ethyl-3-methylimidazolium ethylsulfate ($[C_2C_1im][C_2H_5SO_4]$) as a new working pair. Wang *et al.*[36] proposed the application of the system constituted by water + 1,3-dimethylimidazolium chloride ($[C_1C_1im]Cl$) as an alternative working pair for absorption cycles based on the measurement of the binary vapor-liquid equilibrium (VLE) data. Kim et al.[37] showed broad theoretical work on various mixtures of refrigerants and ILs as working pairs for the absorption refrigeration system, and Zhang et al.[9] simulated a single-effect absorption cycle using the water + 1,3-dimethylimidazolium dimethylphosphate ($[C_1C_1im][DMP]$) and water + 1-ethyl-3-methylimidazolium dimethylphosphate ($[C_2C_1im][DMP]$) systems. Wu et al.[38] measured vapor pressures and the VLE of water + 1,3-dimethylimidazolium tetrafluoroborate ($[C_1C_1im][BF_4]$) mixtures and suggested them as promising working pairs on a comparison basis with $[C_1C_1im]Cl$[38] and 1- butyl-3-methylimidazolium tetrafluoroborate ($[C_4C_1im][BF_4]$).[39] Kim et al.[39] measured the vapor pressures of water + 1-butyl-3-methylimidazolium bromide ($[C_4C_1im]Br$), water + $[C_4C_1im][BF_4]$ and water + 1-(2-hydroxyethyl)-3-methylimidazolium tetrafluoroborate ($[OHC_2C_1im][BF_4]$) systems in broad concentration and temperature ranges. Nie et al.[10] suggested water + 1-(2-hydroxyethyl)-3-methylimidazolium chloride ($[OHC_2C_1im]Cl$) as a novel alternative working pair for the absorption heat pump cycle. The vapor pressure and specific heat capacity of binary solutions of 1-ethyl-3-ethylimidazolium diethylphosphate ($[C_2C_2im][DEP]$),[40] $[C_1C_1im][DMP]$,[41] $[C_2C_1im][DMP]$,[42] and 1-butyl-3-methylimidazolium dibutylphosphate ($[C_4C_1im][DBP]$)[41] with water, ethanol, or methanol were also investigated as new working pairs. Recently, Carvalho et al.[43] measured the VLE of 1-ethyl-3-methylimidazolium chloride ($[C_2C_1im]Cl$), 1-butyl-3-methylimidazolium chloride ($[C_4C_1im]Cl$), 1-hexyl-3-methylimidazolium chloride ($[C_6C_1im]Cl$), and choline chloride ($[N_{111(2OH)}]Cl$) with water and ethanol using a new isobaric microebulliometer at pressures ranging from 0.05 to 0.1 MPa. These binary systems present negative deviations from Raoult's Law and negative excess enthalpies, suggesting that some of them could be appropriate working pairs for absorption chillers or absorption heat pumps.

Several thermodynamic models have been applied to describe thermodynamic properties and phase equilibria of IL aqueous solutions, namely activity-coefficient models, equations of state (EoS), and unimolecular quantum chemistry calculations. For instance, Domańska and Marciniak described the liquid-liquid equilibrium (LLE) and the solid−liquid equilibrium (SLE) of the 1-butyl-3-

methylimidazolium bis-(trifluoromethylsulfonyl)amide ($[C_4C_1im][NTf_2]$) aqueous system with the Non-Random Two-Liquid (NRTL) and the Wilson models.[44] The VLE of the same system was also described with the modified UNIversal Functional Activity Coefficients (UNIFAC) by Nebig et al.[45] Li et al.[46] applied the Square-Well Chain Fluid with Variable Range EoS (SWCF-VR) to model thermodynamic properties of aqueous solutions of ILs, and Wang et al.[47] used the same EoS to describe the VLE of several systems constituted by water + $[NTf_2]$-based ILs. Banarjee et al.[48] applied the COnductor-like Screening MOdel for Realistic Solvation (COSMO-RS) – a predictive model based on unimolecular quantum chemistry calculations – to predict the VLE of water + alkylimidazolium-based ILs. Freire et al.[49–51] also studied the VLE and LLE of a large range of water + IL mixtures using COSMO-RS. Carvalho et al.[43] recently applied the NRTL model to correlate VLE data of binary mixtures of water + IL and ethanol + IL and the nonideal behavior of the liquid phase solutions.

In recent years, a physically grounded theoretical approach, the Statistical Associating Fluid Theory (SAFT), has been shown to be able to describe thermophysical properties and phase behaviors of ILs as well as their mixtures. Within this framework, the strong interactions between anions and cations are represented through specific association sites. Vega et al.[52] used soft-SAFT to describe the LLE of water + imidazolium-based ILs,[53] using three maximum association sites mimicking the strong interactions between the anion and the cation. Paduszyński and Domańska used the Perturbed-Chain Statistical Associating Fluid Theory (PC-SAFT) to calculate the LLE and the SLE of water + ILs. The authors modeled the ILs using ten association sites to represent the cation-anion interactions.[54] Nann et al.[55] modeled 1-butanol + IL mixtures with the 2B association approach for ILs in order to predict the LLE of water + 1-butanol + IL systems accurately with PC-SAFT. Ji et al.[56] used ePC-SAFT to predict the CO_2 solubilities in ILs with pure-IL parameters obtained from the fitting to pure-IL liquid densities.

In this work, the VLE (T,x) of several systems composed of water + imidazolium-based ILs, covering different families of anions, were experimentally measured at different pressures and in a broad composition range. In addition, the PC-SAFT EoS, using two association sites per molecular IL, was used to describe the experimental data. PC-SAFT parameters for the molecular ILs were regressed to pure-IL density data, VLE and water activity coefficient data of the studied mixtures. In a second step, these parameters were applied to predict the water infinite dilution activity coefficients of some water + IL systems and a comparison with literature and experimental data measured in this work is presented and discussed. Furthermore, and because the main aim of this thesis is the study of IL-based aqueous biphasic systems (ABS), the ability of

PC-SAFT to predict the formation of LLE in ternary mixtures composed of ILs, water and the inorganic salt K_3PO_4, was also evaluated by the PC-SAFT.

The physical properties of pure ILs and the phase behavior of water + IL mixtures strongly depend on the IL cation and anion.[57] In this work, new insights regarding IL-water interactions were inferred through the new experimental data and the respective PC-SAFT modeling.

3.1.3. Experimental procedures

Materials. Eight imidazolium-based ILs were investigated, namely 1-butyl-3-methylimidazolium trifluoromethanesulfonate ($[C_4C_1im][CF_3SO_3]$), 1-butyl-3-methylimidazolium thiocyanate ($[C_4C_1im][SCN]$), 1-butyl-3-methylimidazolium tosylate ($[C_4C_1im][TOS]$), 1-butyl-3-methylimidazolium trifluoroacetate ($[C_4C_1im][CF_3CO_2]$), 1-butyl-3-methylimidazolium bromide ($[C_4C_1im]Br$), 1-butyl-3-methylimidazolium chloride ($[C_4C_1im]Cl$), 1-butyl-3-methylimidazolium methanesulfonate ($[C_4C_1im][CH_3SO_3]$), and 1-butyl-3-methylimidazolium acetate ($[C_4C_1im][CH_3CO_2]$). The chemical structures of these ILs are shown in **Figure 3.1** The ILs were obtained from IoLiTec (Germany), with mass fraction purities higher than 98 wt %. To reduce the content of water and volatile organics to negligible values, high vacuum (103 Pa) and stirring at moderate temperature (303 K), for a period of at least 48 h, were applied prior to the measurements. The final water content of the ILs was determined with a Metrohm 831 Karl Fischer coulometer (Switzerland), using the Hydranal-Coulomat E from Riedel-de Haen as analyte, indicating a water mass fraction percentage lower than 30×10^{-6} wt %. The purity of each IL was further confirmed by ^{1}H and ^{13}C NMR using a Bruker Avance 300 spectrometer (Germany). The water used was double distilled and deionized.

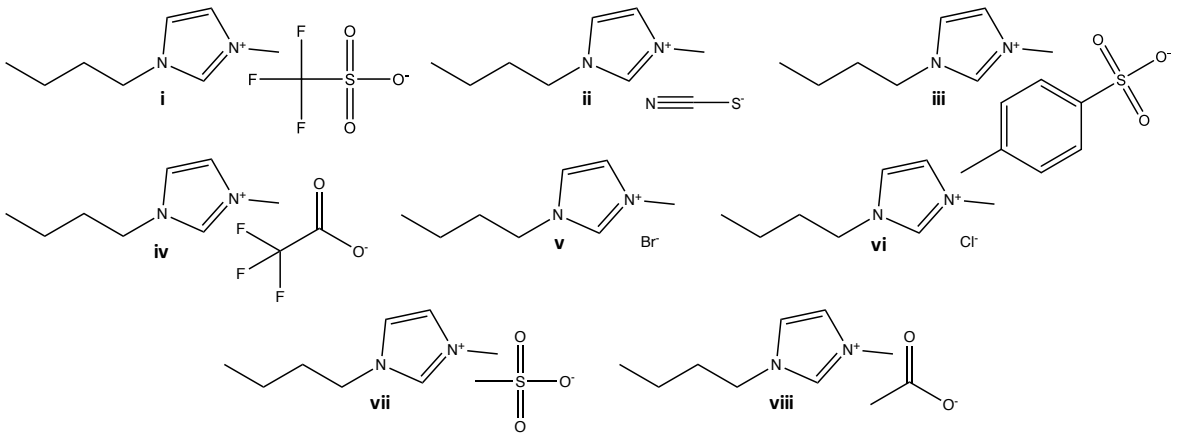

Figure 3.1. Chemical structures of the studied ILs: (i) $[C_4C_1im][CF_3SO_3]$; (ii) $[C_4C_1im][SCN]$); (iii) $[C_4C_1im][TOS]$; (iv) $[C_4C_1im][CF_3CO_2]$; (v) $[C_4C_1im]Br$; (vi) $[C_4C_1im]Cl$; (vii) $[C_4C_1im][CH_3SO_3]$ and (viii) $[C_4C_1im][CH_3CO_2]$.

Vapor-liquid equilibria. The VLE studies were carried out in an isobaric microebulliometer at different fixed pressures of 0.05, 0.07, and 0.1 MPa. The isobaric microebulliometer apparatus used, and methodology is described in detail elsewhere.[43]

The equilibrium temperature of the liquid phase was measured, with an uncertainty of 0.05 K, with a fast response glass-sealed Pt100 class 1/10, which was calibrated prior to the measurements by comparison with a NIST-certified Fluke RTD25 standard thermometer (U.S.A.). The internal pressure of the ebulliometer was kept constant through a vacuum pump Büchi V-700 and a V-850 Büchi (Switzerland), for pressure monitoring and pressure controller unit. Pressure was measured with a Baratron type capacitance Manometer, MKS model 728A (U.S.A.), with an accuracy of 0.5 %. This equipment was placed in the vacuum line away from the microebulliometer. Equilibrium was assumed after 30 min of constant and smooth boiling (reflux) at constant pressure. The mixture composition was determined with an Anton Paar Abbemat 500 Refractometer (Austria), with an uncertainty of 2×10^{-5} nD, using a calibration curve established prior to the measurements. The adequacy of the apparatus to measure this type of systems was previously confirmed.[43] Additionally, the apparatus was applied to measure the VLE of pure compounds (ethanol, water, *p*-xylene, and decane) covering the temperature range of interest for the water + IL systems studied in this work. An uncertainty of the boiling temperatures of 0.1 K was observed. The IL was kept under moderate vacuum (1 Pa) for at least 30 min before the measurements to ensure no water absorption from atmosphere during equilibration.

Activity coefficients at infinite dilution. Inverse chromatography experiments were carried out using a Bruker 450-GC gas chromatograph equipped with a heated on-column injector and a TCD detector. The injector and detector temperatures were kept constant at 523 K during all experiments. To obtain adequate retention times, the helium flow rate was adjusted. Air was used

to determine the column hold-up time. Exit gas flow rates were measured with a soap bubble flow meter. The temperature of the oven was determined with a Pt100 probe and controlled with an uncertainty of 0.1 K. A computer directly recorded the detector signals and the corresponding chromatograms were generated using the Galaxie Chromatography Software. Using a rotary evaporation preparatory technique, 1.0 m length columns were packed with a stationary phase, consisting of 0.20 to 0.35 mass fraction of IL on Chromosorb WHP (60−80 mesh) sorbent media. After the solvent (ethanol) evaporation, under vacuum, the support was left to equilibrate, at 333 K during 6 h. Prior to the measurements, each packed column was conditioned for 12 h at 363 K with a helium flow rate of 20 $cm^3 \cdot min^{-1}$. The packing level was calculated from the masses of the packed and empty columns and was checked throughout experiments. The weight of the stationary phase was determined with a precision of ±0.0003 g. A headspace sample volume of (1−5) × 10^{-3} cm^3 was injected to satisfy infinite dilution conditions. In order to confirm reproducibility, each experiment was repeated at least thrice. Retention times were rigorously reproducible with an uncertainty of 0.5−2 s. To verify the stability under these experimental conditions, ruling out elution of the stationary phase by the helium stream, measurements of retention time were repeated systematically each day for three solutes. No changes in the retention times were observed during this study.

The retention data garnered by inverse chromatography experiments were used to calculate partition coefficients of water in the different ILs. The standardized retention volume, V_N, was calculated following the relationship:[58,59]

$$V_N = J U_0 t'_R \frac{T_{col}}{T_{rt}} \left(1 - \frac{p^0_w}{p_{out}}\right) \quad \textbf{(3.1)}$$

where the adjusted retention time, t'_R, was taken as the difference between the retention time of water and that of air, T_{col} is the column temperature, U_0 is the flow rate of the carrier gas measured at room temperature (T_{rt}), p^0_w is the vapor pressure of water at T_{rt}, and p_{out} is the outlet pressures.

The factor J in **Equation (3.1)** corrects for the influence of the pressure drop along the column and is given through the relation:[58,59]

$$J = \frac{3}{2} \frac{\left[\left(\frac{p_{in}}{p_{out}}\right)^2 - 1\right]}{\left[\left(\frac{p_{in}}{p_{out}}\right)^3 - 1\right]} \quad \textbf{(3.2)}$$

where p_{in} is the inlet pressure.

Activity coefficients at infinite dilution of water in each IL, γ_w^∞, were calculated with the following equation:[58,59]

$$ln(\gamma_{\mathrm{w}}^{\infty}) = ln\left(\frac{n_2 RT}{V_N p_{\mathrm{w}}^0}\right) - p_{\mathrm{w}}^0\left(\frac{B_{\mathrm{ww}} - V_{\mathrm{w}}^0}{RT}\right) + \left(\frac{2B_{\mathrm{w3}} - V_{\mathrm{w}}^{\infty}}{RT}\right) \cdot Jp_{out} \qquad \textbf{(3.3)}$$

where n_2 is the number of moles of stationary phase component within the column, R is the ideal gas constant, T is the oven temperature, B_{ww} is the second virial coefficient of the solute in the vapor state at temperature T, B_{w3} is the mutual virial coefficient between water and the carrier gas (helium, denoted by "3"), and p_w^0 is the probe's vapor pressure at temperature T. The values of p_w^0 result from correlated experimental data. The molar volume of the water, V_w^0 , was determined from experimental densities, and the partial molar volumes of the water at infinite dilution, V_w^∞, were assumed to be equal to V_w^0. The values required for the calculation of these parameters were taken from previous works.[60]

Degree of dissociation. The degree of dissociation of the $[C_4C_1im]Br$ and $[C_4C_1im]Cl$ aqueous mixtures was determined through electrical conductivity with a Mettler Toledo S47 SevenMultiTMdual meter pH/conductivity, coupled with an InLab741 Conductivity Probe as electrode. Aqueous solutions of $[C_4C_1im]Br$ and $[C_4C_1im]Cl$ with concentration ranging between 0.5 and 2.5 mol·L^{-1} were prepared and used to measure the electrical conductivities (*cf.* **Appendix B**). Finally, the degree of dissociation was determined using the following equation:

$$\alpha = \frac{\Lambda}{\Lambda_0} \qquad \textbf{(3.4)}$$

where Λ is the molar conductivity and Λ_0 is the molar conductivity at infinite dilution. The molar conductivity at infinite dilution was extrapolated through the representation of molar conductivity in function of IL concentration.

3.1.4. Thermodynamic modeling

PC-SAFT. In this work, PC-SAFT[61,62] was applied to describe experimental pure-IL and water + IL mixture data. The PC-SAFT EoS is based on the first-order thermodynamic perturbation theory[63–66] that uses a system of freely jointed hard spheres as reference, designated as hard-chain system. PC-SAFT, as other SAFT approaches, is especially suited to treat chain molecules, and it is hence appropriate to consider IL systems.

In PC-SAFT the dimensionless residual Helmholtz energy, a^{res}, is defined as

$$a^{res} = a^{hc} + a^{disp} + a^{assoc} + a^{polar} \quad \textbf{(3.5)}$$

where the superscripts refer to the terms accounting for the residual, hard-chain fluid, dispersive, associative, and polar interactions, respectively. The polar term was not considered in this work as previous studies reported that the polar term has only a slight influence on the PC-SAFT description of IL systems, even for non-negligible dipole moments.[67]

In PC-SAFT, a nonassociating component i is provided with three pure-component parameters, namely the segment number, m_i^{seg}, the segment diameter, σ_i, and the van der Waals interaction (dispersion) energy parameter between two segments, u_i/k_B, in which k_B is the Boltzmann constant. For associating molecules, PC-SAFT requires two additional parameters, which are the association-energy parameter, $\varepsilon^{A_iB_i}/k_B$, and the association-volume parameter, $k^{A_iB_i}$. For each IL two association sites (the 2B association scheme) were applied.[68]

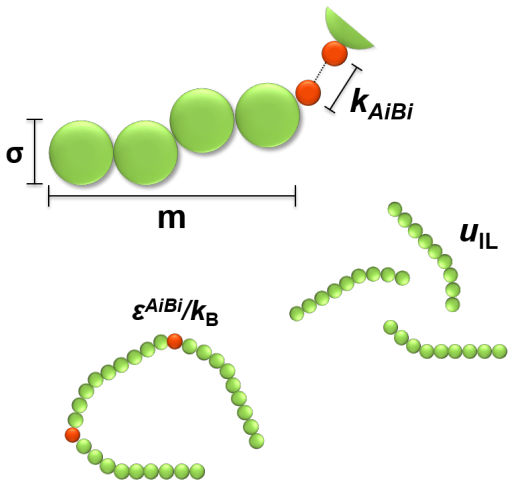

Figure 3.2. Schematic representation of PC-SAFT parameters: segment number, m_i^{seg}; segment diameter, σ_i; dispersion energy parameter of IL, u_{IL}; association-energy parameter, $\varepsilon^{A_iB_i}/k_B$; and association-volume parameter, $k^{A_iB_i}$.

The conventional Lorenz−Berthelot combining rules are used for mixtures and described according to

$$\sigma_{ij} = \frac{1}{2}(\sigma_i + \sigma_j) \quad \textbf{(3.6)}$$

$$u_{ij} = \sqrt{u_i u_j}(1 - k_{ij}) \quad \textbf{(3.7)}$$

where k_{ij} is a binary parameter between two components i and j for the correction of the cross-dispersion energy. In this work, the ILs were considered to be present as ion pairs and thus

dispersion among IL molecules was taken into account. In contrast, charge-charge interactions among the ILs were neglected.

Simple combining rules for cross-association interactions between two substances were suggested by Wolbach and Sandler[69] and used in this work:

$$\varepsilon^{A_iB_j} = \frac{1}{2}\left(\varepsilon^{A_iB_i} + \varepsilon^{A_jB_j}\right) \quad \textbf{(3.8)}$$

$$k^{A_iB_j} = \sqrt{k^{A_iB_i}k^{A_jB_j}}\left(\frac{\sqrt{\sigma_i\sigma_j}}{\frac{1}{2}(\sigma_i + \sigma_j)}\right)^3 \quad \textbf{(3.9)}$$

Calculation of activity coefficients and VLE with PC-SAFT. The water activity coefficient, γ_w, is the ratio of the water fugacity coefficient, φ_w^L, at the mole fraction x_w in a mixture, and the fugacity coefficient of the pure water, φ_{0w}^L:

$$\gamma_{\mathrm{w}}(T,p,x_{\mathrm{w}}) = \frac{\varphi_{\mathrm{w}}^L(T,p,x_{\mathrm{w}})}{\varphi_{0\mathrm{w}}^L(T,p,x_{\mathrm{w}}=1)} \quad \textbf{(3.10)}$$

where T and p represent a fixed temperature and pressure, respectively. The water fugacity coefficients can be calculated with PC-SAFT, and the exact relationship is given elsewhere.[70] The water activity coefficient at infinite dilution is calculated using the following equation:

$$\gamma_{\mathrm{w}}^{\infty}(T,p,x_{\mathrm{w}}) = \frac{\varphi_{\mathrm{w}}^{\infty,L}(T,p,x_{\mathrm{w}}\to 0)}{\varphi_{0\mathrm{w}}^L(T,p,x_{\mathrm{w}}=1)} \quad \textbf{(3.11)}$$

where $\varphi_w^{\infty,L}$ is the water fugacity coefficient at infinite dilution, which can be determined using PC-SAFT.

Calculation of LLE with PC-SAFT. LLE calculations of a multicomponent system are based on equal fugacity values, f_i, of all components i in the different phases I and II and were performed using the following relation

$$\varphi_i^I \cdot x_i^I = \varphi_i^{II} \cdot x_i^{II} \quad \textbf{(3.12)}$$

where x_i and φ_i are the mole fraction and fugacity coefficient, respectively, of component i. PC-SAFT was applied for calculating the fugacity coefficients, which depend on the components, mixture composition, density, and temperature.

3.1.5. Results and discussion

Experimental results. The boiling temperatures of seven water + IL systems were measured at three different pressures (0.05, 0.07, and 0.1 MPa) in a broad composition range using a microebulliometer designed by us for studying IL mixtures and previously validated and described elsewhere.[43] For the systems studied here, only the binary mixture formed by water + $[C_4C_1im][CF_3SO_3]$ was previously reported by Orchilles et al.[71] A good agreement between our data and literature was observed with an average relative deviation, ARD (**Equation (3.16)**), between the two data sets, of only 0.22%. The boiling temperatures of the water + $[C_4C_1im]Cl$ system used in this work were previously reported.[43]

The experimental VLE data for the systems measured in this work at 0.05, 0.07, and 0.1 MPa are listed in **Appendix B**. The results obtained at 0.1 MPa are depicted in **Figure 3.3**. The data show that all the ILs studied increase the boiling temperature of the related aqueous mixtures in different extents. The influence of ILs through the boiling temperatures follows the order: $[C_4C_1im][CF_3SO_3]$ < $[C_4C_1im][SCN]$ < $[C_4mim][CF_3CO_2]$ < $[C_4C_1im][TOS]$ < $[C_4C_1im]Br$ < $[C_4C_1im]Cl$ < $[C_4C_1im][CH_3SO_3]$ < $[C_4C_1im][CH_3CO_2]$. Since all the ILs studied have a common cation, the observed differentiation is essentially related to the effect of the anion on the water-IL interaction. In fact, a close agreement was identified between the IL's ability to increase the boiling temperature of water + IL binary solutions, and their hydrogen-bond basicity values determined by solvatochromic probes.[72] ILs with higher hydrogen-bond basicity values interact more strongly with water and stronger IL-water interactions difficult the evaporation of the water molecules, yielding thus higher boiling-point elevations and vapor pressure depressions. The observed behavior is in agreement with previous VLE data by Zhao et al.[41] and by Heym et al.[12] The researchers[12,41] found that the ILs with higher ionic hydration ability cause a higher boiling-point elevation than other solutes, such as glycols. As an example, it can be observed in **Figure 3.3**, that the boiling-point elevation observed for a water mole fraction of 0.72 is *ca.* 6.2 K for $[C_4C_1im][CF_3SO_3]$ and 27.2 K for $[C_4C_1im][CH_3SO_3]$. The fluorination of the methanesulfonate anion is responsible for this effect, supported by the fact that fluorinated anions are only able to form weak hydrogen bonds with water.[73] This effect can also be observed by comparing the boiling temperature elevation caused by ILs containing the anion acetate with trifluoroacetate where the same trend was observed.

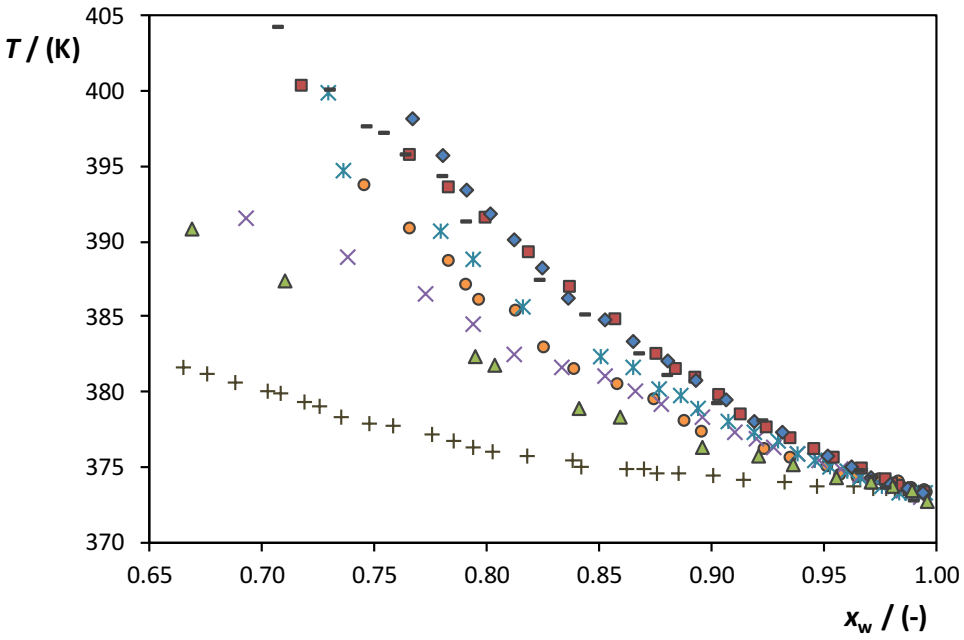

Figure 3.3. Experimental VLE in binary solutions of water + IL at 0.1 MPa: $[C_4C_1im][CF_3SO_3]$ (┼), $[C_4C_1im][SCN]$ (▲), $[C_4C_1im][CF_3CO_2]$ (×), $[C_4C_1im][TOS]$ (●), $[C_4C_1im]Br$ (✳), $[C_4C_1im]Cl$ (-), $[C_4C_1im][CH_3SO_3]$ (■) and $[C_4C_1im][CH_3CO_2]$ (◆).

From **Figure 3.3** it is also visible that the boiling-point elevation increases almost linearly for those ILs that weakly interact (low boiling-point elevations) with water, namely $[C_4C_1im][CF_3SO_3]$ and $[C_4C_1im][SCN]$. In contrast, ILs such as $[C_4C_1im][CH_3SO_3]$ and $[C_4C_1im][CH_3CO_2]$, which present stronger interactions with water by hydrogen-bonding (high boiling-point elevation), display a nonlinear boiling-point elevation.

Figure 3.4 and **Figure 3.5** depict the VLE of several water + IL systems as a function of composition and pressure. It can be seen that pressure does not have a strong influence on the concentration dependence of the boiling-point elevations as the *T*–*x* curves at different pressures are almost parallel to each other.

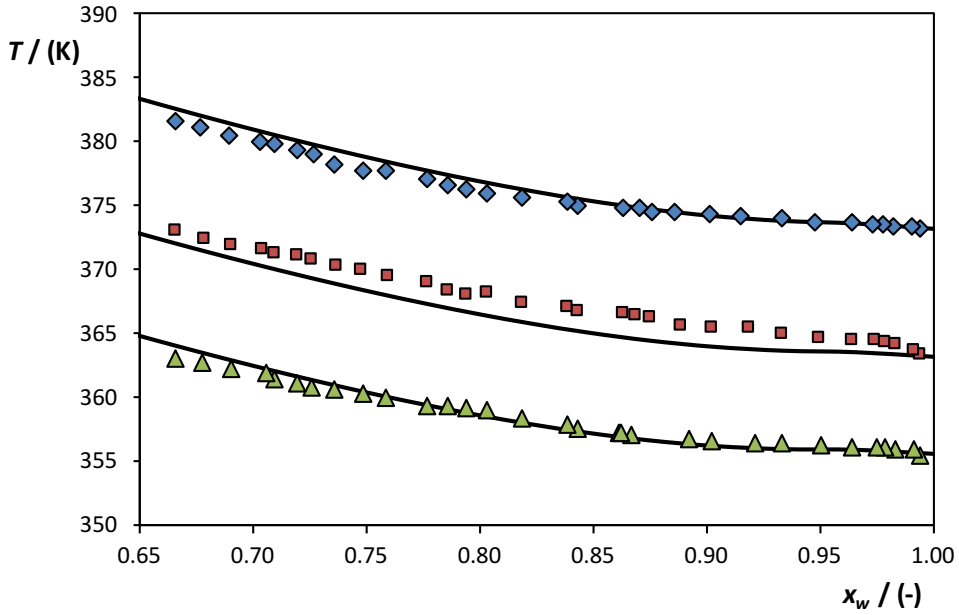

Figure 3.4. Experimental VLE data for the water + $[C_4C_1im][CF_3SO_3]$ system at 0.1 (◆), 0.07 (■) and 0.05 (▲) MPa. PC-SAFT correlation results are presented by the solid lines and parameters values can be found in **Table 3.1**.

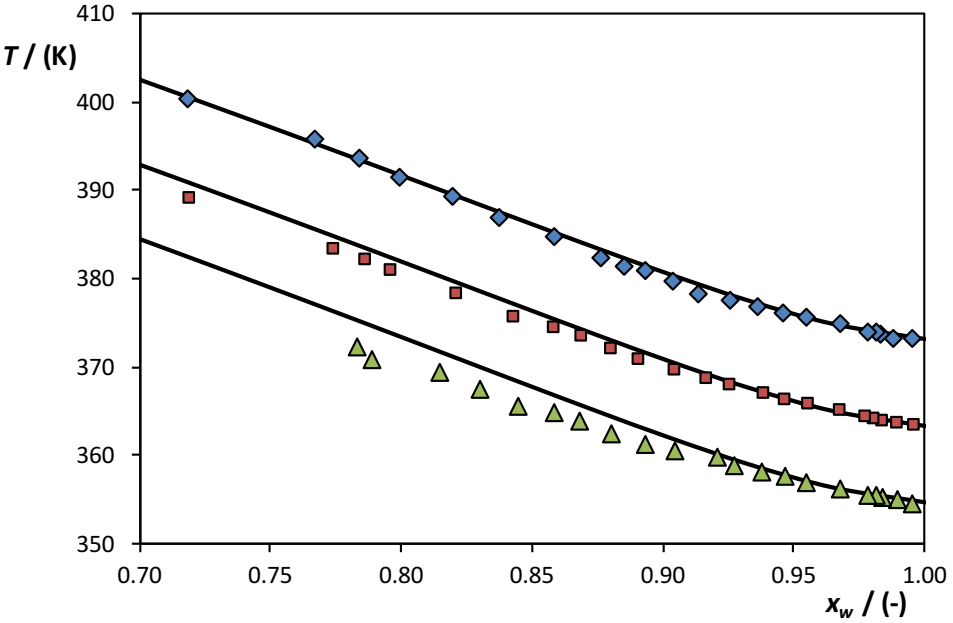

Figure 3.5. Experimental VLE data for water + $[C_4C_1im][CH_3SO_3]$ system at 0.1 (◆), 0.07 (■) and 0.05 (▲) MPa. PC-SAFT correlation results are presented by the solid lines and parameters values can be found in **Table 3.1**.

It is well-know that the volatility of an aprotic IL is negligible, and thus, the vapor phase of a binary mixture containing an IL and a molecular and volatile solvent is only constituted by the latter. Moreover, at the pressure and temperatures studied, the vapor phase fugacity coefficients

are very close to unity for the compounds studied, and therefore, **Equation (3.10)** can be simplified to

$$\gamma_{\mathrm{w}} = \frac{p}{x_{\mathrm{w}} p_{\mathrm{w}}^{\sigma}} \qquad \textbf{(3.13)}$$

where p is the system total pressure, x_i the mole fraction of the liquid phase and p_{w}^{σ} is the water vapor pressure.[74,75] Using Equation **(3.13)**, the water activity coefficients can be estimated and are presented in **Figure 3.6** at 0.1 MPa.

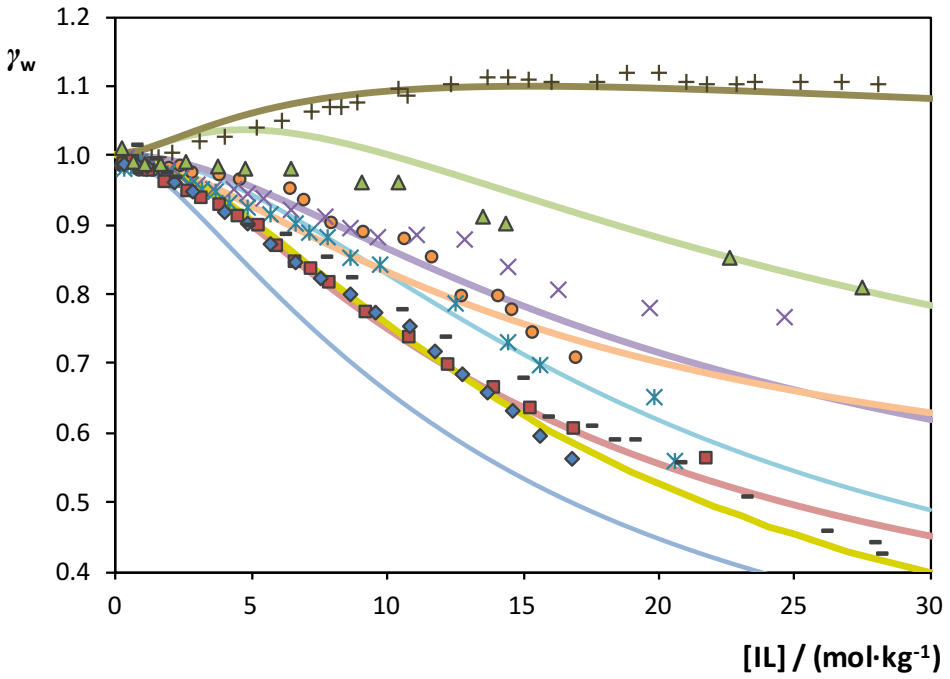

Figure 3.6. Water activity coefficients, γ_{w}, as function of the IL molality in binary solutions of water + IL at 0.1 MPa: [C_4C_1im][CF_3SO_3] (+), [C_4C_1im][SCN] (▲), [C_4C_1im][CF_3CO_2] (×), [C_4C_1im][TOS] (•), [C_4C_1im]Br (∗), [C_4C_1im]Cl (-), [C_4C_1im][CH_3SO_3] (■) and [C_4C_1im][CH_3CO_2] (◆). PC-SAFT correlation results are presented by the solid lines and parameters values can be found in **Table 3.1**.

Negative deviation to the ideal, which translates into activity coefficients lower than unity, results from the stronger IL- water interactions than the water-water. These stronger interactions force to retain the water molecules in the liquid phase, and higher potential is required to transfer water molecules into the vapor phase. Thus, the water boiling temperature will increase as observed in the VLE experimental data. Moreover, this effect is stronger for the ILs with higher interactions with water (higher hydrogen-bond basicity). In fact, the same trend observed before for the VLE is observed for the water activity coefficients: [C_4C_1im][CF_3SO_3] < [C_4C_1im][SCN] < [C_4C_1im][CF_3CO_2] ≈ [C_4C_1im][TOS] < [C_4C_1im] Br < [C_4C_1im]Cl < [C_4C_1im][CH_3SO_3] < [C_4C_1im][CH_3CO_2].

The water activity coefficient may be related with the solvent hydrophobicity.[76] All the studied ILs are considered hydrophilic since they are fully water-soluble. However, their hydrophilicity is not the same. For ILs with pronounced hydrophilic character (for example, $[C_4C_1im][CH_3CO_2]$ and $[C_4C_1im][CH_3SO_3]$) the interactions between IL and water are very strong resulting in very low water activity coefficients. In general, the less hydrophilic the IL the higher is the water activity coefficient. On the other hand, for the ILs with the weakest hydrophilic character ($[C_4C_1im][CF_3SO_3]$ and $[C_4C_1im][SCN]$), the water activity coefficients are slightly positive at low IL concentrations reflecting the weaker IL-water interaction. The influence of ions in an aqueous system is usually well described by the Hofmeister series or their ability to form hydration complexes.[77] ILs with higher affinity for water, that is, ILs with a higher charge density or higher propensity to form hydration complexes tend to the salting-out regime. The trend observed for the water activity coefficients is also in good agreement with the Hofmeister series[78] or their ability rank to interact with water by hydrogen-bonding, as expected. In fact, the observed trend correlates well with previous data where the influence of the IL anion to be salted-out by an inorganic salt was analyzed.[79] ILs with higher affinity for water are less prone for phase separation in aqueous media.[79]

An irregular behavior was observed for the ILs $[C_4C_1im]Br$ and $[C_4C_1im]Cl$. The water activity coefficients on $[C_4C_1im]Br$ and $[C_4C_1im]Cl$ are opposite to the observed for the chloride and bromide common salt–water systems.[80,81] Nevertheless, considering the Gibbs energy of ion hydration (ΔG_{hyd}) for both Br^- and Cl^- anions the Cl^- is expected to have a higher interaction with water, since it presents a lower ΔG value (ΔG_{hyd} (Br^-) = −321 kJ·mol^{-1} and ΔG_{hyd} (Cl^-) = −347 kJ·mol^{-1}),[82] which is in agreement with the results obtained in this work for the water activity coefficients. Moreover, at the very high IL concentrations that are studied in this work the formation of ion pairs can occur,[83] causing a lower IL interaction with water. This phenomenon can be observed and quantified through the degree of dissociation represented in **Figure 3.7** for both $[C_4C_1im]Br$ and $[C_4C_1im]Cl$.

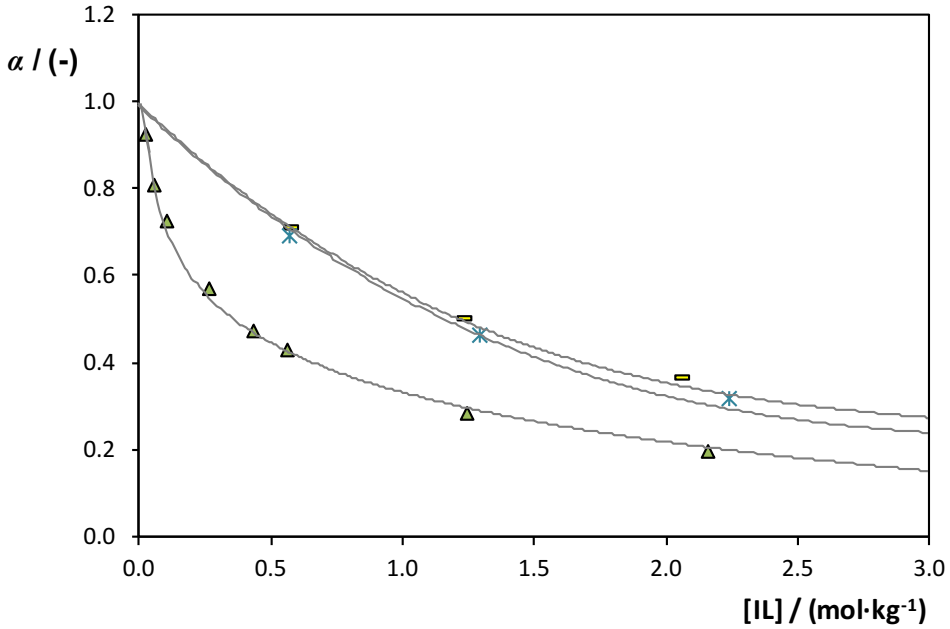

Figure 3.7. Degree of dissociation, α, as function of the IL molality in binary solutions of water + IL at 298.15 K and atmospheric pressure: $[C_4C_1im][SCN]$ (▲), $[C_4C_1im]Br$ (✳) and $[C_4C_1im]Cl$ (-).

At 2 mol·kg^{-1} the degree of dissociation is 0.336 for $[C_4C_1im]Br$ and 0.361 for $[C_4C_1im]Cl$. As expected, due to the similarities in structure and size of the ions composing these compounds, the differences observed between both ILs degree of dissociation are not very large. However, the differences observed are in agreement with the results obtained in this work for the water activity coefficients. $[C_4C_1im]Cl$ has a higher dissociation degree consequently meaning a higher interaction with water.

Held et al.[84] reported a similar behavior in the water activity coefficients of aqueous solutions of electrolytes containing the anions hydroxides, fluorides, and acetates. For these salts, the water activity coefficients presented a reverse sequence compared to the alkali salts trend. This behavior was justified by the possibility of occurring a localized hydrolysis[85] in presence of anions with strong ability to accept protons, which results in the decreasing of the number of ions in the solution.

In **Figure 3.7**, it is also represented the degree of dissociation for $[C_4C_1im][SCN]$, one of the less hydrophilic ILs studied in this work. As expected, a lower degree of dissociation (0.218 at 2 mol·kg^{-1}) compared to both $[C_4C_1im]Br$ and $[C_4C_1im]Cl$ was obtained for this IL, which is in agreement with the results obtained by Yee et al.,[83] showing that the tendency for dissociation decreases with the anion hydrophobicity.

Modeling results. Ji et al.[56] and Nann et al.[55] already used PC-SAFT to model IL solutions. The authors treated ILs as molecules with a distinctive association behavior by using the 2B

association scheme, where each IL was assigned two association sites, and association interaction was allowed between two different sites of two IL molecules. This approach was also applied in this work. Thus, within this framework, IL molecules can interact with each other and with water via hard-chain repulsion, dispersion, and association. Furthermore, according to the findings of Köddermann et al.,[86] the ILs were assumed to be nondissociated and nonaggregated for the PC-SAFT modeling in this work. This approach is justified through the results presented in **Figure 3.7**, where it is possible to see that ILs only present an extensive dissociation in dilute solutions and that at the concentration range studied in this work assuming ion pairs instead of dissociated ions is an acceptable approach.

The PC-SAFT parameters for the ILs were determined by a simultaneous regression of pure-IL densities,[87–92] water activity coefficients at 298.15 K,[93] and the VLE data of the water + IL binary mixtures at 0.1 MPa (determined in this work) using the following objective function:

$$OF = \sum_{i}^{NP}\left(\frac{\rho_i^{exp} - \rho_i^{calc}}{\rho_i^{exp}}\right)^2 + \sum_{i}^{NP}\left(\frac{\gamma_i^{exp} - \gamma_i^{calc}}{\gamma_i^{exp}}\right)^2 + \sum_{i}^{NP}\left(\frac{T_i^{b,exp} - T_i^{b,calc}}{T_i^{b,exp}}\right)^2 \qquad \textbf{(3.14)}$$

All the PC-SAFT parameters for the ILs considered in this work are summarized in **Table 3.1**, including the parameters of water that were taken from literature.[94]

As a result of the parameter estimation, the association energy parameters were found to be zero for all ILs with negative deviations to ideality. Since all these ILs are strongly hydrophilic, this result may be related with the possibility of each IL molecule to be completely surrounded by water molecules and thereby hindering direct IL-IL hydrogen bonds. In contrast, for $[C_4C_1im][CF_3SO_3]$, a nonzero association energy parameter was obtained. $[C_4C_1im][CF_3SO_3]$ is less hydrophilic, presenting positive deviation to ideality. The association-volume parameters seem to follow a very specific order, as presented in **Table 3.1**: $[C_4C_1im][CH_3CO_2]$ > $[C_4C_1im][CH_3SO_3]$ > $[C_4C_1im]Cl$ > $[C_4C_1im]Br$ > $[C_4C_1im][TOS]$ > $[C_4C_1im][CF_3CO_2]$ > $[C_4C_1im][SCN]$ > $[C_4C_1im][CF_3SO_3]$. This order clearly shows that the PC-SAFT association strength is in agreement with the experimentally observed sequence of water activity coefficients, meaning that the water-IL interactions due to hydrogen bonding are correctly being taken into account within the PC-SAFT framework.

Table 3.1. PC-SAFT parameters for water and ILs, as well as ARD values (calculated with **Equation (3.16)**), for pure and mixture properties.

IL	$[C_4C_1im][CF_3SO_3]$	$[C_4C_1im][SCN]$	$[C_4C_1im][CF_3CO_2]$	$[C_4C_1im][TOS]$	$[C_4C_1im]Br$	$[C_4C_1im]Cl$	$[C_4C_1im][CH_3SO_3]$	$[C_4C_1im][CH_3CO_2]$	water
***T* range[a] (K)**	[293.15 - 393.15]	[278.15 - 363.15]	[278.15 - 338.15]	[333.15 - 353.15]	[293.22 - 373.08]	[372.66 - 430.10]	[298.15 - 373.15]	[278.15 - 363.15]	---
x_{IL} **range**[a]	[0.006 - 0.820]	[0.010 - 0.969]	[0.006 - 0.861]	[0.004 - 0.335]	[0.005 - 0.410]	[0.012 – 0.415]	[0.005 - 0.376]	[0.006 - 0.961]	---
σ_i **(Å)**	3.3037	3.0300	3.0845	3.1681	3.6000	3.5000	2.7482	2.9504	*T* dependent[b]
m_i^{seg}	8.1368	10.3743	9.5000	10.0000	5.6851	5.1737	12.8442	10.0000	1.2047
u_{IL} **(K)**	206.85	246.95	224.30	175.62	447.15	294.38	214.78	251.90	353.95
ε^{AiBi}/k_B **(K)**	189.21	0.00	0.00	0.00	0.00	0.00	0.00	0.00	2425.67
k^{AiBi}	0.144	0.548	0.600	0.700	0.800	0.844	0.950	1.000	0.045
k_{ij}	-0.0741	-0.0173	-0.0725	-0.1461	0.0354	-0.0375	-0.0827	-0.0960	---
ARD % in ρ_{IL}	1.37	0.78	0.94	0.90	0.42	1.00	0.78	2.53	---
ARD % in γ_w	2.59	2.97	4.61	2.20	1.61	2.52	1.59	5.28	---
ARD % in VLE	1.47	2.89	3.07	2.93	2.11	3.95	1.01	7.85	---

[a] range of temperatures and IL mole fraction considering for the PC-SAFT parameters modeling;
[b] $\sigma = 2.7927 + 10.11 \cdot \exp(-0.01775 \cdot T/\mathrm{K}) - 1.417 \cdot \exp(-0.01146 \cdot T/\mathrm{K})$;
Segment number, m_i^{seg}; segment diameter, σ_i; dispersion energy parameter of IL, u_{IL}; association-energy parameter, $\varepsilon^{A_iB_i}/k_B$; and association-volume parameter, $k^{A_iB_i}$.

The results obtained for the segment number (m_i^{seg}) and the segment diameter (σ_i) are within reasonable ranges. The segment diameter varies between 2.75 Å for [C_4C_1im][CH_3SO_3] and 3.60 Å for [C_4C_1im]Br. The segment numbers oscillate considerably with the anion that constitutes the IL. The segment number and the segment diameter parameters of the ILs depend linearly on the molecular weight (M_w) according to the following equation:

$$m_i^{seg}\sigma_i^3 = 0.582 \cdot M_{\mathrm{w}} + 133.09\ (\text{Å}^3) \qquad \textbf{(3.15)}$$

The values for the dispersion-energy parameters of the ILs are also reasonable, ranging between 175.62 K for [C_4C_1im][TOS] and 447.15 K for [C_4C_1im]Br. This parameter does not depend linearly on the molecular weight.

The fitting errors of the pure-IL density, water activity coefficient, and VLE of water + IL binary mixtures are expressed as the average relative deviation (ARD) between modeled and experimental data:

$$ARD = 100\frac{1}{NP}\sum_{k=1}^{NP}\left|\left(1-\frac{Z_k^{mod}}{Z_k^{exp}}\right)\right| \qquad \textbf{(3.16)}$$

where NP is the number of experimental data points and the superscripts “mod” and “exp” are the modeled results and experimental data, respectively. These values are listed in **Table 3.1**.

PC-SAFT pure-IL densities are in good agreement with the experimental data with small deviations. To give an example, the ARD values range between 0.42 % for the pure-IL densities of [C_4C_1im]Br and 2.53% for [C_4C_1im][CH_3CO_2], as depicted in **Figure 3.8**.

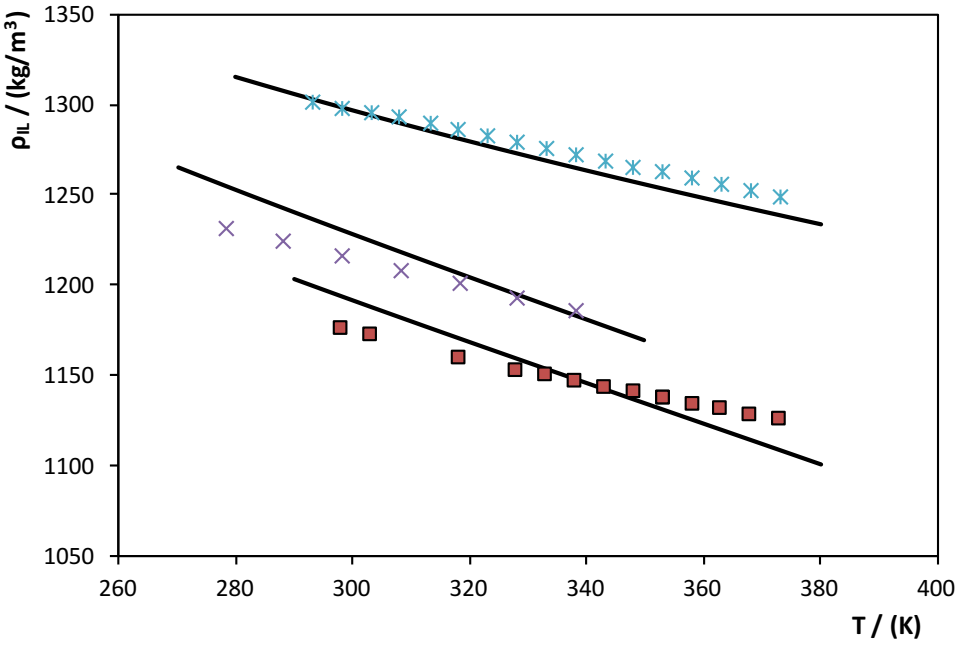

Figure 3.8. Experimental pure-IL density data, ρ_{IL}, as a function of temperature at atmospheric pressure: $[C_4C_1im]Br$ (✳), $[C_4C_1im][CF_3CO_2]$ (×), $[C_4C_1im][CH_3SO_3]$ (■). PC-SAFT correlation results are presented by the solid lines and the pure compound parameters values can be found in **Table 3.1**.

The modeling results obtained with the PC-SAFT for the water + IL binary systems are presented hereafter. A temperature-independent binary interaction parameter (k_{ij}), fitted to VLE data at 0.1 MPa and water activity coefficients at 298.15 K,[93] was used for each binary system. Some of the results obtained are illustrated in **Figure 3.9**, where the activity coefficients are shown as function of the molality of the IL (*i.e.*, mole of IL *per* kg of water solvent). It can be observed, from **Figure 3.9**, that PC-SAFT provides a good description of the behavior of both the more and the less hydrophobic ILs. The ARD values range between 1.59% for $[C_4C_1im][CH_3SO_3]$ and 5.28% for $[C_4C_1im][CH_3CO_2]$.

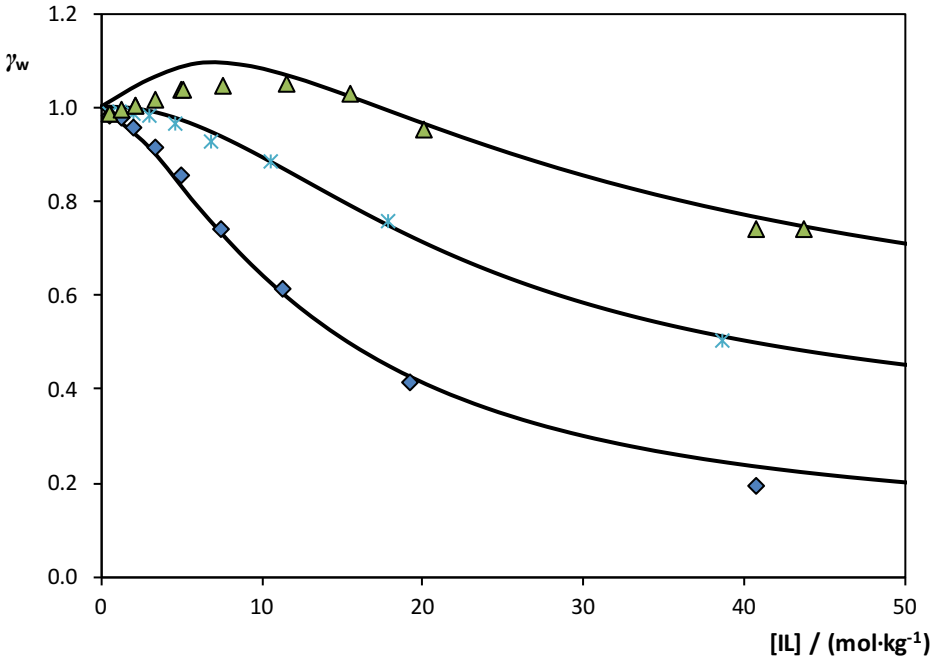

Figure 3.9. Experimental water activity coefficients, γ_w,[93] as a function of the IL molality in binary solutions of water + IL at 298.15 K: $[C_4C_1im][SCN]$ (▲), $[C_4C_1im]Br$ (✳), $[C_4C_1im][CH_3CO_2]$ (◆). PC-SAFT correlation results are presented by the solid lines and parameters values can be found in **Table 3.1**.

The PC-SAFT modeling of the VLE for the systems measured in this work are presented in **Figure 3.4** and **Figure 3.5** for the ILs $[C_4C_1im][CF_3SO_3]$ and $[C_4C_1im][C_1SO_3]$, respectively. The results are in good agreement with the experimental data: 0.1 MPa with an overall ARD of 3.04%. As expected, the water activity coefficients at 0.1 MPa for the binary systems are also well described by PC-SAFT, as observed in **Figure 3.6**. It is also shown that PC-SAFT can successfully be used to predict the VLE data at 0.07 and 0.05 MPa with an overall ARD of 3.82% and 5.20%, respectively. It should be emphasized that all IL pure-component PC-SAFT parameters and binary interaction parameters are temperature independent.

PC-SAFT was applied to predict the water activity coefficients at infinite dilution in ILs. In fact, for the ILs studied in this work, the experimental data for the water activity coefficients cover very large concentration ranges in most cases. However, data at such high IL molalities are difficult (and sometimes impossible depending on the IL) to experimentally determine due to solubility, viscosity, or decomposition concerns. Thus, it is strongly desirable to have a model that is able to estimate the water activity coefficients at infinite dilution either predicting them or by extrapolation of the available data. **Table 3.2** lists experimental water activity coefficients at infinite dilution for the ILs under study. For those for which no data were available in literature,[14,23,28] they were measured in this work. The absolute deviation (AD) and the average

absolute deviation (AAD) between the experimental data and PC-SAFT predicted values were calculated through Equations **(3.17)** and **(3.18)** and are presented in **Table 3.2**.

$$AD = \left| z_k^{exp} - z_k^{mod} \right| \quad \textbf{(3.17)}$$

$$AAD = \frac{1}{NP} \sum_{k=1}^{NP} \left| z_k^{exp} - z_k^{mod} \right| \quad \textbf{(3.18)}$$

Table 3.2. Experimental water activity coefficients at infinite dilution and predicted with PC-SAFT, as well as AD and AAD values (calculated with **Equations (3.17)** and **(3.18)**)

	γ_w^∞		
IL	**experimental data**	**PC-SAFT**	**AD**
$[C_4C_1im][CF_3SO_3]$	0.929 [14]	1.098	0.169
$[C_4C_1im][SCN]$	0.302 [23]	0.371	0.069
$[C_4C_1im][TOS]$	0.167 [28]	0.288	0.121
$[C_4C_1im][CF_3CO_2]$	0.133	0.231	0.098
$[C_4C_1im]Br$	0.045	0.248	0.203
$[C_4C_1im]Cl$	0.025	0.162	0.137
$[C_4C_1im][CH_3SO_3]$	0.097	0.136	0.039
$[C_4C_1im][CH_3CO_2]$	0.013	0.070	0.057
AAD			0.112

The PC-SAFT modeling used the model parameters presented in **Table 3.1** fitted to VLE and water activity coefficients at finite concentrations and not to activity coefficients at infinite dilution. The results appear to be quite promising as the model provides a satisfactorily prediction of the experimental water activity coefficients at infinite dilution. While PC-SAFT slightly overestimates the experimental data, the sequence of the experimental and predicted γ_w^∞ values are in good agreement except for $[C_4C_1im]Br$ and $[C_4C_1im]Cl$. Availability of activity coefficients in a minimum concentration range seems thus to be required for an adequate prediction of the infinite dilution activity coefficients. For $[C_4C_1im]Br$ and $[C_4C_1im]Cl$, this range seems to be insufficient.

Finally, and because the aim of this thesis is the study of IL-based ABS, the ability of PC-SAFT to predict the LLE behavior of ternary systems composed of ILs, water, and the inorganic salt K_3PO_4,[95] was evaluated. The previously determined pure component and binary interaction parameters between ILs and water (**Table 3.1**) were used. Additionally, different binary interaction parameters between IL and both the cation and anion of the salt were evaluated.

Figure 3.10 compare the predicted and the experimental[95] LLE data of ternary systems composed of IL + K_3PO_4 + water, for the ILs $[C_4C_1im][CF_3CO_2]$, $[C_4C_1im]Br$ and $[C_4C_1im][CH_3CO_2]$. The obtained results are very distinct between the ILs that compose the ternary system. The best

result was obtained for $[C_4C_1im]Br$ (**Figure 3.10 B**), with a very good prediction of experimental data; however, for the remaining ILs is clear that the predictive model needs to be improved. For the ILs $[C_4C_1im][CF_3SO_3]$ and $[C_4C_1im][SCN]$ demixing regions in the LLE of binary mixtures of IL and water in a temperature range of 270 to 330 K were identified, suggesting that new model parameters need to be determined to allow the evaluation of ternary mixtures LLE.

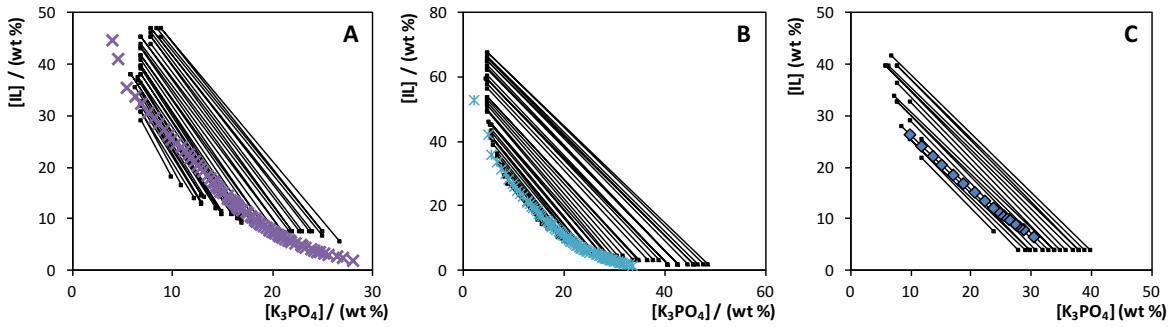

Figure 3.10. LLE of ternary mixtures composed of IL + K_3PO_4 + water at 298.15 K and atmospheric pressure (in weight fractions).[95] PC-SAFT predictions (black lines and squares): **(A)** $[C_4C_1im][CF_3CO_2]$ (k_{ij} = 0.35); **(B)** $[C_4C_1im]Br$ (k_{ij} = 0.50); **(C)** $[C_4C_1im][CH_3CO_2]$ (k_{ij} = 0.59).

Despite the unsatisfactory results presented in **Figure 3.10** for some ILs here studied, it is demonstrated that PC-SAFT presents the potential to be used as a tool to predict the formation of ABS composed of ILs by using only IL-water binary mixture experimental data.

3.1.6. Conclusions

VLE data for seven water + imidazolium-based IL systems covering different families of anions at three different pressures were measured in this work. The results indicate that the imidazolium-based ILs studied cause boiling-point elevations of different degrees according to the interaction strengths between water and the IL that mainly depends on the nature of the IL anion.

The PC-SAFT equation of state was used for the description of the experimental data. The PC-SAFT pure-component parameters and the binary interaction parameter were determined by a simultaneous fitting to pure-IL densities, water activity coefficients at 298.15 K, and VLE data at 0.10 MPa. The binary interaction parameters were considered to be temperature independent. This set of parameters allowed for quantitative modeling the pure-IL density, water activity coefficients at 298.15 K, and the VLE at 0.10 MPa for the water + IL binary mixtures. VLE at pressures different from 0.10 MPa can be predicted reasonably with PC-SAFT by using binary interaction parameters fitted to VLE data at 0.10 MPa. Moreover, PC-SAFT is capable to satisfactorily predict water activity coefficients at infinite dilution for systems where model parameters were adjusted to water activity coefficients at low IL molalities.

PC-SAFT showed to be a potential tool for the description of LLE of ternary mixtures composed of ILs, salts and water using only experimental data of IL-water binary mixtures. Despite work is still needed to be carried out in this subject, the preliminary results here reported open a line of research attempting the development of a predictive model that can be used to predict the IL-based ABS formation.

3.1.7. References

(1) S. Liang, W. Chen, K. Cheng, Y. Guo, and X. Gui, *The Latent Application of Ionic Liquids in Absorption Refrigeration. In Applications of Ionic Liquids in Science and Technology*; P.S. Handy, Eds.; InTech: Croatia, 2011; pp 467−494;
(2) C.Z. Zhuo and C.H.M. Machielsen, *Int. J. Refrig.*, 1993, **16**, 357−363;
(3) V. Tufano, *Appl. Therm. Eng.*, 1998, **18**, 171−177;
(4) D. Zheng, P. Ji, and J. Qi, *Int. J. Refrig.*, 2001, **24**, 834−840;
(5) M. Kernen, L.L. Lee, and H. Perez-Blanco, *Int. J. Refrig.*, 1995, **18**, 42−50;
(6) P. Srikhirin, S. Aphornratana, and S. Chungpaibulpatana, *Renewable Sustainable Energy Rev.*, 2001, **5**, 343−372;
(7) A. Yokozeki and M.B. Shiflett, *Ind. Eng. Chem. Res.*, 2008, **47**, 8389−8395;
(8) G. Zuo, Z. Zhao, S. Yan, and X. Zhang, *Chem. Eng. J.*, 2010, **156**, 613−617;
(9) X. Zhang and D. Hu, *Appl. Therm. Eng.*, 2012, **37**, 129−135;
(10) N. Nie, D. Zheng, L. Dong, and Y. Li, *J. Chem. Eng. Data*, 2012, **57**, 3598−3603;
(11) L. Dong, D. Zheng, N. Nie, and Y. Li, *Appl. Energy,* 2012, **98**, 326−332;
(12) F. Heym, J. Haber, W. Korth, B.J.M. Etzold, and A. Jess, *Chem. Eng. Technol.,* 2010, **33**, 1625−1634;
(13) U. Domańska and A. Marciniak, *J. Phys. Chem. B*, 2007, **111**, 11984−11988;
(14) U. Domańska and A. Marciniak, *J. Phys. Chem. B*, 2008, **112**, 11100−11105;
(15) U. Domańska and A. Marciniak, *J. Chem. Thermodyn.*, 2008, **40**, 860−866;
(16) M. Krummen, P. Wasserscheid, and J. Gmehling, *J. Chem. Eng. Data*, 2002, **47**, 1411−1417;
(17) M. Diedenhofen, F. Eckert, and A. Klamt, *J. Chem. Eng. Data*, 2003, **48**, 475−479;
(18) M. Ge, J. Xiong, and L. Wang, *Chin. Sci. Bull.*, 2009, **54**, 2225−2229;
(19) U. Domańska and M. Krolikowski, *J. Chem. Thermodyn.*, 2012, **54**, 20−27;
(20) R. Kato and J. Gmehling, *J. Chem. Thermodyn.*, 2005, **37**, 603−619;
(21) R. Kato and J. Gmehling, *Fluid Phase Equilib.*, 2004, **226**, 37−44;
(22) U. Domańska, G.G. Redhi, and A. Marciniak, *Fluid Phase Equilib.*, 2009, **278**, 97−102;
(23) U. Domańska and M. Laskowska, *J. Chem. Thermodyn.*, 2010, **42**, 947−948;
(24) U. Domańska, A. Marciniak, M. Krolikowski, and M. Arasimowicz, *J. Chem. Eng. Data*, 2010, **55**, 2532−2536;
(25) U. Domańska, M. Krolikowski, and W.E. Acree Jr., *J. Chem. Thermodyn.*, 2011, **43**, 1810−1817;
(26) U. Domańska, M. Krolikowski, and W.E. Acree Jr., G.A. Baker, *J. Chem. Thermodyn.*, 2011, **43**, 1050−1057;
(27) U. Domańska, E.V. Lukoshko, and M. Wlazło, *J. Chem. Thermodyn.*, 2012, **47**, 389−396;
(28) U. Domańska and M. Krolikowski, *J. Chem. Eng. Data*, 2010, **55**, 4817−4822;
(29) U. Domasńka and M. Krolikowski, *J. Chem. Eng. Data*, 2010, **56**, 124−129;
(30) U. Domańska and A. Marciniak, *J. Phys. Chem. B*, 2010, **114**, 16542−16547;
(31) U. Domańska and M. Krolikowski, *J. Phys. Chem. B*, 2011, **115**, 7397−7404;
(32) A. Marciniak and M. Wlazło, *J. Chem. Thermodyn.*, 2013, **57**, 197−202;
(33) M. Wlazło and A. Marciniak, *J. Chem. Thermodyn.*, 2012, **54**, 366−372;

(34) A. Marciniak and M. Wlazło, *J. Chem. Thermodyn.*, 2012, **54**, 90−96;
(35) A. Yokozeki and M.B. Shiflett, *Ind. Eng. Chem. Res.*, 2010, **49**, 9496−9503;
(36) J. Wang, D. Zheng, L. Fan, and L. Dong, *J. Chem. Eng. Data*, 2010, **55**, 2128−2132;
(37) Y.J. Kim, S. Kim, Y.K. Joshi, A.G. Fedorov, and P.A. Kohl, *Energy,* 2012, **44**, 1005−1016;
(38) X. Wu, J. Li, L. Fan, D. Zheng, and L. Dong, *Chin. J. Chem. Eng.*, 2011, **19**, 473−477;
(39) K.-S. Kim, S-Y. Park, S. Choi, and H. Lee, *J. Chem. Eng. Data*, 2004, **49**, 1550−1553;
(40) X.-C. Jiang, J.-F. Wang, C.-X. Li, L.-M. Wang, and Z.-H. Wang, *J. Chem. Thermodyn.*, 2007, **39**, 841−846;
(41) J. Zhao, X.-C. Jiang, C.-X. Li, and Z.-H. Wang, *Fluid Phase Equilib.*, 2006, **247**, 190−198;
(42) J.-F. Wang, C.-X. Li, Z.-H. Wang, Z.-J. Li, and Y.-B. Jiang, *Fluid Phase Equilib.*, 2007, **255**, 186−192;
(43) P.J. Carvalho, I. Khan, A. Morais, J.F.O. Granjo, N.M.C. Oliveira, L.M.N.B.F. Santos, and J.A.P. Coutinho, *Fluid Phase Equilib.*, 2013, **354**, 156−165;
(44) U. Domańska and A. Marciniak, *Fluid Phase Equilib.*, 2007, **260**, 9−18;
(45) S. Nebig, R. Bölts, and J. Gmehling, *Fluid Phase Equilib.*, 2007, **258**, 168−178;
(46) J. Li, C. He, C. Peng, H. Liu, and Y. Hu, *Ind. Eng. Chem. Res.*, 2011, **50**, 7027−7040;
(47) T. Wang, C. Peng, H. Liu, Y. Hu, and J. Jiang, *Ind. Eng. Chem. Res.*, 2007, **46**, 4323−4329;
(48) T. Banerjee, M.K. Singh, and A. Khanna, *Ind. Eng. Chem. Res.*, 2006, **45**, 3207−3219;
(49) M.G. Freire, C.M.S.S. Neves, P.J. Carvalho, R.L. Gardas, A.M. Fernandes, I. M. Marrucho, L.M.N.B.F. Santos, and J.A.P. Coutinho, *J. Phys. Chem. B*, 2007, **111**, 13082−13089;
(50) M.G. Freire, S.P.M. Ventura, L.M.N.B.F. Santos, I.M. Marrucho, and J.A.P. Coutinho, *Fluid Phase Equilib.* 2008, **268**, 74−84;
(51) M.G. Freire, P.J. Carvalho, R.L. Gardas, L.M.N.B.F. Santos, I.M. Marrucho, and J.A.P. Coutinho, *J. Chem. Eng. Data*, 2008, **53**, 2378−2382;
(52) F. Llovell, E. Valente, O. Vilaseca, and L.F. Vega, *J. Phys. Chem. B*, 2011, **115**, 4387−4398;
(53) L.F. Vega, O. Vilaseca, F. Llovell, and J.S. Andreu, *Fluid Phase Equilib.*, 2010, **294**, 15−30;
(54) K. Paduszyński and U. Domańska, *J. Phys. Chem. B*, 2012, **116**, 5002−5018;
(55) A. Nann, J. Mündges, C. Held, S.P. Verevkin, and G. Sadowski, *J. Phys. Chem. B*, 2013, **117**, 3173−3185;
(56) X. Ji, C. Held, and G. Sadowski, *Fluid Phase Equilib.*, 2012, **335**, 64−73;
(57) L. Dong, D.X. Zheng, Z. Wei, and X.H. Wu, *Int. J. Thermophys*, 2009, **30**, 1480−1490;
(58) A.J.B. Cruickshank, M.L. Windsor, and C.L. Young, *Proc. R. Soc. London*, *Ser. A*, 1966, **295**, 259−270;
(59) A.J.B. Cruickshank, M.L. Windsor, and C.L. Young, *Proc. R. Soc. London, Ser. A*, 1966, **295**, 271−287;
(60) A.-L. Revelli, L.M. Sprunger, J. Gibbs, W.E. Acree, G.A. Baker, and F. Mutelet, *J. Chem. Eng. Data*, 2009, **54**, 977−985;
(61) J. Gross and G. Sadowski, *Ind. Eng. Chem. Res.*, 2001, **40**, 1244−1260;
(62) J. Gross and G. Sadowski, *Ind. Eng. Chem. Res.*, 2002, **41**, 5510−5515;
(63) M.S. Wertheim, *J. Stat. Phys.*, 1984, **35**, 19−34;
(64) M.S. Wertheim, *J. Stat. Phys.*, 1984, **35**, 35−47;
(65) M.S. Wertheim, *J. Stat. Phys.*, 1986, **42**, 459−476;
(66) M.S. Wertheim, *J. Stat. Phys.*, 1986, **42**, 477− 492;
(67) K. Paduszyński, J. Chiyen, D. Ramjugernath, and T.M. Letcher, U. Domańska, *Fluid Phase Equilib.*, 2011, **305**, 43−52;
(68) S.H. Huang and M. Radosz, *Ind. Eng. Chem. Res.*, 1990, **29**, 2284−2294;
(69) J.P. Wolbach and S.I. Sandler, *Ind. Eng. Chem. Res.*, 1998, **37**, 2917−2928;
(70) C. Held, T. Neuhaus, and G. Sadowski, *Biophys. Chem.*, 2010, **152**, 28−39;

(71) A.V. Orchilles, P.J. Miguel, V. González-Alfaro, E. Vercher, and A. Martínez-Andreu, *J. Chem. Eng. Data*, 2011, **56**, 4454−4460;
(72) R. Lungwitz and S.A. Spange, *New J. Chem.*, 2008, **32**, 392−394;
(73) H. Passos, A.R. Ferreira, A.F.M. Cláudio, J.A.P. Coutinho, and M.G. Freire, *Biochem. Eng. J.*, 2012, **67**, 68−76;
(74) R.L. Rowley, W.V. Wilding, J.L. Oscarson, N.A. Zundel, T.L. Marshall, T.E. Daubert, and R.P. Danner, *DIPPR Data Compilation of Pure Compound Properties; Design Institute for Physical Properties*; AIChE: New York, 2002.
(75) H.Y. Afeefy and J.F. Liebman, S.E. Stein, Neutral Thermochemical Data in *NIST Chemistry WebBook*, NIST Standard Reference Database Number 69; Linstrom, P. J., Mallard, W. G., Eds.; National Institute of Standards and Technology, Gaithersburg, MD, June, 2005; p. 20899 (http://webbook.nist.gov);
(76) C. Held, *Measuring and Modeling Thermodynamic Properties of Biological Solutions.* Ph.D. Thesis, Technische Universitat Dortmund, Dortmund, Germany, Dec., 2011;
(77) M.G. Freire, P.J. Carvalho, A.M.S. Silva, L.M.N.B.F. Santos, L.P.N. Rebelo, I.M. Marrucho, and J.A.P. Coutinho, *J. Phys. Chem. B*, 2009, **113**, 202−211;
(78) F. Hofmeister, *Arch. Exp. Pathol. Pharmakol.*, 1888, **24**, 247−260;
(79) T. Mourão, A.F.M. Cláudio, I. Boal-Palheiros, M.G. Freire, and J.A.P. Coutinho, *J. Chem. Thermodyn.*, 2012, **54**, 398−405;
(80) R.A. Robinson and R.H. Stokes, *Electrolyte Solutions*, 2nd ed.; Courier Dover Publications: New York, 1970;
(81) V.M.M. Lobo and J.L. Quaresma, *Handbook of Electrolyte Solutions*; Elsevier: Amsterdam, 1989; Parts A and B;
(82) Y. Marcus, *Ion Properties*; Marcel Dekker, Inc.: New York, 1997; Vol. 1, pp. 124−125;
(83) P. Yee, J.K. Shah, and E.J. Maginn, *J. Phys. Chem. B*, 2013, **117**, 12556−12566;
(84) C. Held, L.F. Cameretti, and G. Sadowski, *Fluid Phase Equilib.*, 2008, **270**, 87−96;
(85) R.A. Robinson and H.S. Harned, *Chem. Rev.*, 1941, **28**, 419−476;
(86) T. Köddermann, C. Wertz, A. Heintz, and R. Ludwig, *ChemPhysChem*, 2006, **7**, 1944−1949;
(87) H.F.D. Almeida, H. Passos, J.A. Lopes-da-Silva, A.M. Fernandes, M.G. Freire, and J.A.P. Coutinho, *J. Chem. Eng. Data*, 2012, **57**, 3005− 3013;
(88) U. Domańska and M. Krolikowski, *J. Chem. Thermodyn.*, 2010, **42**, 355−362;
(89) R.L. Gardas, M.G. Freire, P.J. Carvalho, I.M. Marrucho, I.M.A. Fonseca, A.G.M. Ferreira, and J.A.P. Coutinho, *J. Chem. Eng. Data*, 2006, **52**, 80−88;
(90) C.M.S.S. Neves, K.A. Kurnia, J.A.P. Coutinho, I.M. Marrucho, J.N.C. Lopes, M.G. Freire, and L.P.N. Rebelo, *J. Phys. Chem. B*, 2013, **117**, 10271− 10283;
(91) P.N. Tshibangu, S.N. Ndwandwe, and E.D. Dikio, *Int. J. Electrochem. Sci.*, 2011, **6**, 2201−2213;
(92) O. Zech, A. Stoppa, R. Buchner, and W. Kunz, *J. Chem. Eng. Data*, 2010, **55**, 1774−1778;
(93) I. Khan, K.A. Kurnia, J.A. Saraiva, S.P. Pinho, and J.A.P. Coutinho, *J. Phys. Chem. B*, 2014, **118**, 1848−1860;
(94) D. Fuchs, J. Fischer, F. Tumakaka, and G. Sadowski, *Ind. Eng. Chem. Res.*, 2006, **45**, 6578−6584;
(95) S.P.M. Ventura, C.M.S.S. Neves, M.G. Freire, I.M. Marrucho, J. Oliveira, and J.A.P. Coutinho, *J. Phys. Chem. B*, 2009, **113**, 9304−9310.

3.2. The hydrogen bond basicity of ionic liquids as a tool for predicting the formation of aqueous biphasic systems

This chapter is based on the manuscript under preparation

Helena Passos, Teresa B. V. Dinis, Ana Filipa M. Cláudio, Mara G. Freire and João A. P. Coutinho[1]

"The hydrogen bond basicity of ionic liquids as a tool for predicting the formation of aqueous biphasic systems", 2017.

3.2.1. Abstracts

Systematic studies on aqueous biphasic systems (ABS) composed of ionic liquids (ILs) and conventional salts are useful for the design of extraction processes. However, due the large number of ILs that can be prepared and their high structural versatility, it is impossible to experimentally cover and characterize all the possible combinations of ILs and salts, turning the development of tools for the design of IL-based ABS a crucial requirement. To this end, an effective predictive model for predicting the formation ability of IL-based ABS was successfully established. A strong correlation between the hydrogen-bonding interaction energies of ILs, obtained by the COnductor-like Screening MOdel for Real Solvents (COSMO-RS), and the ILs ability to form ABS was established, and the predictive ability of this correlation further demonstrated. Considering the salt ions molar entropy of hydration, it was possible to additionally expand the predictive model to the salts ability to form ABS.

3.2.2. Introduction

Aqueous biphasic systems (ABS) composed of ionic liquids (ILs) offer several advantages over typical polymer-based ABS.[1] These include lower viscosities, higher thermal stability, and a wider hydrophilic/hydrophobic range that can lead to enhanced selectivities and tailored extraction efficiencies. Moreover, these systems provide higher density differences between the coexisting phases, which enable a faster and easier phase separation.[2]

The complexity of ILs structures, with non-polar, polar and charged moieties, confers them a high solvation ability for a wide range of biological compounds, both in neat form or in aqueous solution.[3-5] Since Gutowski *et al.*[6] prepared the first ABS composed of an hydrophilic IL – 1-buthyl-

[1]**Contributions:** M.G.F. and J.A.P.C. conceived and directed this work. H.P., T.B.V.D. and A.F.M.C. compilated and analised the experimental data from literature. T.B.V.D. determined the necessary binodal curves to complement this study. H.P., M.G.F. and J.A.P.C. developed the methodology here proposed, with significant contributions of the remaining authors.

3-methylimidazolium, $[C_4C_1im]Cl$ – combined with K_3PO_4, a large array of ILs and conventional salts have been combined in order to form IL-based ABS, and their extraction ability for a large number of biomolecules has been investigated.[1] Most of the studies and phase diagrams reported for IL-based ABS have been focused on imidazolium-based ILs.[1] However, given the large number of ILs that can be prepared and their high structural versatility, tools for the design of IL-based ABS are required for the development of more selective extraction processes.

From the many studies[1,7,8] on IL-based ABS, a molecular model for their formation has been proposed suggesting that it is driven by the competition between the IL and salt ions for the formation of hydration complexes. This competition is dominated by the ions with a higher charge density and, consequently, capable of stronger interactions with water.[1,7,8] Thus, ILs with a more hydrophobic character are better at inducing the phases demixing in presence of a high-charge density salt. In this context, Coutinho and co-workers[9-11] suggested the existence of a relationship between the hydrogen bond acceptor basicity (β) of ILs and their ability to form ABS. However, they[9-11] failed to quantify it.

The hydrogen bond acceptor basicity is actually one of the most important descriptors of the solvation capability of ILs,[3,12-14] and a great deal of efforts has been made to establish polarity scales capable of ranking ILs to explain the solvation of specific solutes. Furthermore, it was already shown that the polarity of ILs reflects also their own solvation in water, which is intrinsically associated to their capability to form ABS.[1] A polarity-scale of ILs is thus of high importance as it allows the development of a framework to, at least qualitatively, predict the solubility of a given solute in ILs and also of the ILs in a set of solvents.

Several dyes have been used as solvatochromic probes to experimentally determine the polarity of molecular solvents, including ILs.[15-25] The multiparametric approach proposed by Kamlet-Taft[26-29] is able to characterize a given fluid in terms of polarity, by the determination of specific parameters, namely β, and other useful parameters, such as the hydrogen-bond donating ability (α), and the dipolarity/polarizability (π^*) being one of the best established and accepted polarity scales in literature. Several researchers have determined these parameters in neat ILs.[16-25] However, the determination of the solvatochromic parameters consisting on the measurement of specific solute (probe dye)-solvent interactions is probe dependent, meaning that different solvatochromic probes will result in different values for the same parameter. Lungwitz et al.[18-20] and Welton and co-workers[21-25] are the two research groups that have more extensively studied the determination of solvatochromic parameters of pure ILs. For the β determination, Lungwitz et al.[19] used 3-(4-amino-3-methylphenyl)-7-phenyl-benzo-[1,2-*b*:4,5-*b'*]-difuran-2,6-di-one dye (1) as

solvatochromic probe, while Welton and co-workers[21-25] employed the *N*,*N*-diethyl-4-nitroaniline (2) and 4-nitroaniline (3) probes pair – **Figure 3.11**. Although the tendencies observed by both groups, concerning the ILs nature effect in the solvatochromic parameters, are similar, the absolute values obtained are considerably distinct. For example, for the ILs $[C_4C_1im][CH_3CO_2]$ and $[C_4C_1im][CF_3SO_3]$ the β values obtained are, respectively, 0.85 and 0.57[19] when 3-(4-amino-3-methylphenyl)-7-phenyl-benzo-[1,2-*b*:4,5-*b'*]-difuran-2,6-di-one is used, and 1.20 and 0.49[21] when the probe pair *N*,*N*-diethyl-4-nitroaniline/4-nitroaniline is used. Furthermore, the Kamlet-Taft parameters are highly sensitive to impurities and the presence of water,[26-31] which represents an experimental drawback in defining solvatochromic parameters for many of the existent ILs.

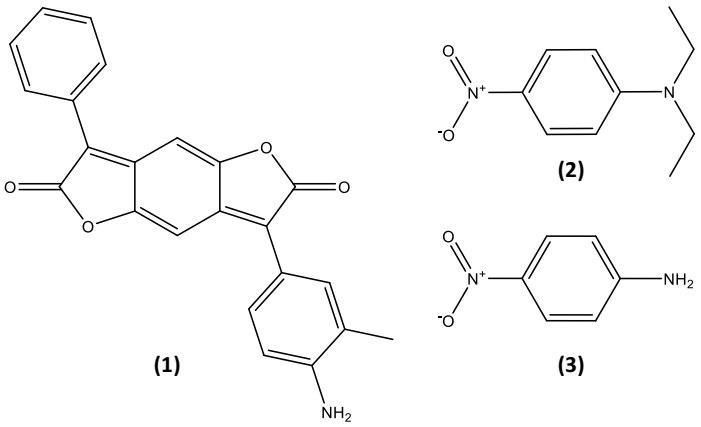

Figure 3.11. Chemical structures of the solvatochromic probes used by Lungwitz et al.[19] and Tom Welton and co-workers[21]: **(1)** 3-(4-amino-3-methylphenyl)-7-phenyl-benzo-[1,2-*b*:4,5-*b'*]-difuran-2,6-di-one dye; **(2)** *N*,*N*-diethyl-4-nitroaniline; **(3)** 4-nitroaniline.

The development of a generalized and coherent polarity β-scale for ILs is a major challenge. Furthermore, with the never-ending reports on the synthesis of new ILs – a result of their structural versatility – finding simple computational tools that can provide this assessment, based only on their cation and anion, is today of utmost importance. To overcome the drawbacks observed above with experimental approaches, several attempts have been made on developing predictive methods for solvatochromic parameters.[32-35] Hunt et al.[34] used computational simulations for predicting the Kamlet-Taft parameters α and β in neat ILs. However, this approach demands a high computational cost and expert knowledge, being unfeasible for a routine screening. A simpler and alternative computational method, based on COnductor-like Screening MOdel for Real Solvents (COSMO-RS), has been successfully applied for predicting solvatochromic parameters.[36,37] The COSMO-RS is an important computational approach well established in the literature.[38-40] Important solvation effects of pure and mixed fluids have been assessed by using only the chemical structure information of the molecules. Several authors have demonstrated the

ability of COSMO-RS to evaluate and correlate the polarity of ILs.[36,37,41,42] Of particular relevance is the work by Cláudio et al.[36] that reported the successful correlation of the experimental β parameters with the COSMO-RS hydrogen-bonding interaction energies in the IL cation-anion pairs (E_{HB} in kJ·mol^{-1}). They proposed a new and extended scale of polarities based on E_{HB}, for a variety of ILs composed of $[C_4C_1im]^+$ and a large number of anions.[36]

In this work, the solvatochromic parameter scales available for the hydrogen-bond basicity parameter – Lungwitz et al.[19], and Welton and co-workers[21] scales – are used to correlate the ABS binodal curves. However, due the reduced number of data reported in literature, the COSMO-RS hydrogen-bonding interaction energies were evaluated as potential substitutes of β in these correlations, attempting the development of a model that can be used to predict the IL-based ABS formation.

3.2.3. Experimental procedures

Phase diagrams. IL-based ABS experimental data considered in this work were already reported. Due the size of the database used, the values of IL molality at saturation of each ABS and respective reference are presented in **Appendix B**.

COSMO-RS. The IL hydrogen-bonding interaction energies, E_{HB}, were calculated using the COSMO-RS thermodynamic model that combines quantum chemistry, based on the dielectric continuum model known as COSMO (COnductor-like Screening MOdel for Real Solvents), with statistical thermodynamic calculations. The standard process of COSMO-RS calculations employed in this work was previously described by Kurnia et al.[37] The quantum chemical COSMO calculation was performed with the TURBOMOLE 6.1 program package on the density functional theory (DFT) level, applying the BP functional B88-P86 with a triple-ζ valence polarized basis set (TZVP) and the resolution of identity standard (RI) approximation.[43] The COSMO*thermX* program using the parameter file BP_TZVP_C20_0111 (COSMOlogic GmbH & Co KG, Leverkusen, Germany) was used in all calculations.[44]

3.2.4. Results and discussion

Based on the notion that the ABS formation results from a competition for the hydration of the ions present in the system, it was used the point of each binodal curve where the molality of the IL equals the molality of the salt, hereafter named "saturation solubility", and as proposed by Shahriari et al.[7], as a relative measure of the ABS formation ability. Based on the gathered data, when the IL molality at saturation solubility, $[IL]_{SS}$, is represented as function of the hydrogen

bond acceptor ability of pure ILs that compose the ABS in study, a linear correlation was found, according to the following equation:

$$[IL]_{SS} = A \cdot \beta + B \quad \textbf{(3.19)}$$

where A and B are constants that depend on the salt used in the preparation of the ABS.

In **Figure 3.12** are shown the correlations obtained for ABS composed of $[C_4C_1im]^+$-based ILs and the following salts: K_3PO_4,[11,45-50] $K_3C_6H_5O_7$,[51] K_2HPO_4,[10,45,52] Na_2CO_3,[7,53-56] Na_2SO_4,[11,48,57] and $KNaC_4H_4O_6$.[2] Two different correlations for each salt are obtained, depending on the set of β values used - β values determined with the solvatochromic probe (1) by Lungwitz et al.[19] (β_{Lung}), or with the pair (2)/(3) by Welton and co-workers[21] (β_{TW}). The preferential formation of ion-water interactions depends on the IL hydrogen bond accepting ability. This parameter is highly dependent on the IL anion nature.[36] Thus, ILs anions with lower β values have less capacity to interact with water being more prone to be salted-out by the salt ions, and thus an easier liquid-liquid demixing is achieved at lower $[IL]_{SS}$ values.

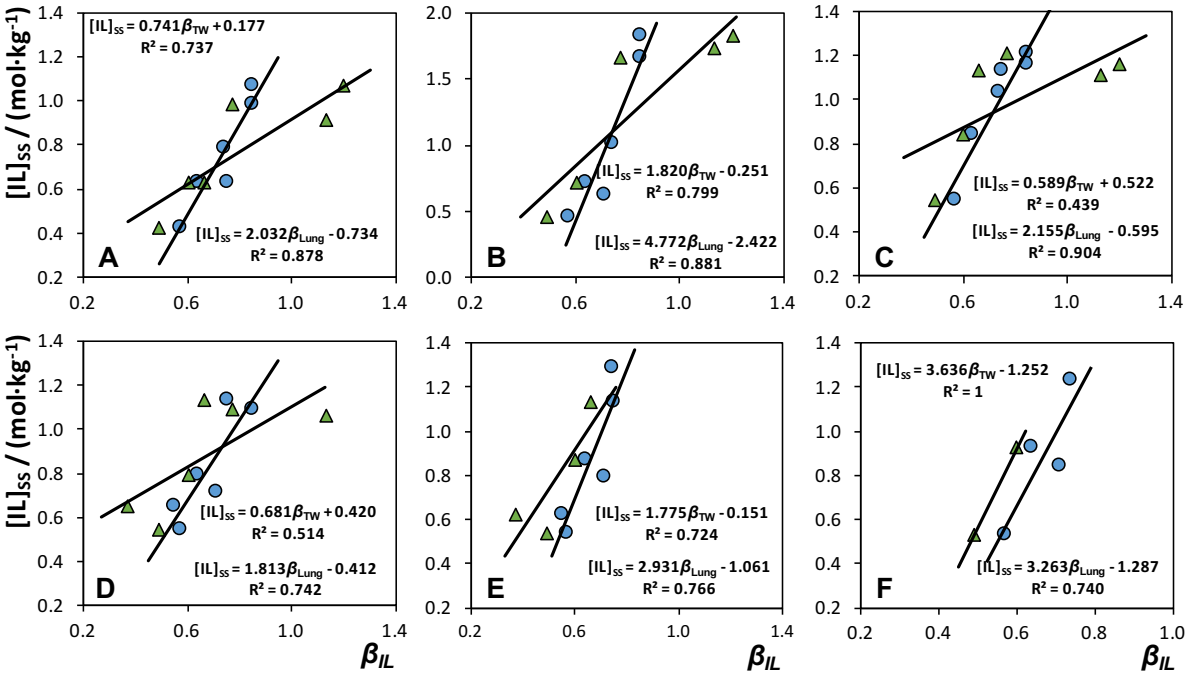

Figure 3.12. Relationship between the molality of the IL at saturation solubility ($[IL]_{SS}$) and the hydrogen-bond acceptor basicity (β) of $[C_4C_1im]^+$-based ILs determined with the solvatochromic probes (1) by Lungwitz et al.[19] (β_{Lung}, blue circles) and the pair (2)/(3) by Welton and co-workers[21] (β_{TW}, green triangles) for IL-based ABS composed of: **(A)** K_3PO_4;[11,45-50] **(B)** $K_3C_6H_5O_7$;[51] **(C)** K_2HPO_4;[10,45,52] **(D)** Na_2CO_3;[7,53-56] **(E)** Na_2SO_4;[11,48,57] **(F)** $KNaC_4H_4O_6$.[2]

The solvatochromic probe (1) used by Lungwitz et al.[19] was proposed for the first time by Oehlke et al.[58] This probe presents a UV/Vis band shift that is significantly affected by the IL anion

nature which allows to determine the β parameter with high accuracy. Furthermore, this probe possesses a large UV/Vis absorption coefficient in the visible region between 460 and 700 nm[58] meaning that colored ILs – which shows a UV/Vis absorption band of at most 400 nm – will not interfere in the ILs hydrogen bond acceptor ability determination, contrarily to what usually happens with the commonly used probes, such as the probes pair (2)/(3) used by Tom Welton and co-workers.[21] Probably, this feature justify why in general the β values reported by Lungwitz et al.[19] present a better correlation with the saturation solubility of the studied ABS, as can be observed in **Figure 3.12**. Although the trends here found are based on a specific IL cation, namely $[C_4C_1im]^+$, this is also valid for other ILs classes, since it has been already shown that the anion rank is maintained even if the cation is changed.[1]

Despite the good correlations that can be found between the ILs hydrogen bond acceptor ability and the IL saturation solubility in the different ABS evaluated (**Figure 3.12**), the drawbacks associated to solvatochromic parameters determination, such as the required experimental efforts, their sensitivity to ILs impurities and color, and the fact of being only possible to carry out the measurements with liquid samples, makes the number and accuracy of β values available in the literature very low.[36] Furthermore, the most part of the studies are focused on $[C_4C_1im]^+$-based ILs, and there is almost no data for other types of cations which makes unfeasible the use of β parameters in the development of a predictive model that can be used to predict the IL-based ABS formation.

Taking into account the importance of the parameter β in the polarity of ILs and, consequently, their association to the ILs ability to form ABS, as well as the simplicity in the estimation of E_{HB} from COSMO-RS which, as previously shown, presents a good correlation with β parameter,[36] E_{HB} was further used to correlate the ABS formation, according to the Equation **(3.20)**:

$$[IL]_{SS} = C \cdot E_{HB} + D \qquad \textbf{(3.20)}$$

with C and D as constants that depend on the salt employed.

The set of data available for E_{HB} can be as large as desired since this approach only requires the information on the chemical structure of the IL, without restrictions on the IL cation-anion combinations. This overcomes the drawbacks associated to the use of solvatochromic probes, not only by avoiding an extensive experimental determination of the β values for a set of ILs, but also by eliminating the obstruction to establish a coherent and complete polarity scale for any IL structure caused by the presence of impurities and water. For that purpose, in **Figure 3.13**, β

values were replaced by the COSMO-RS E_{HB} values and, not only $[C_4C_1im]^+$-based ILs were used, but a very diversified set of ILs was evaluated – **Table 3.3**.

As expected, when replacing β values by E_{HB} values, and by introducing different types of ILs cations, such as pyridinium- ammonium-, phosphonium- and cholinium-based, similar tendencies are observed for the IL-based ABS composed of the salts K_3PO_4, $K_3C_6H_5O_7$, K_2HPO_4, Na_2CO_3, Na_2SO_4 and $KNaC_4H_4O_6$, with correlation coefficients ranging between 0.738 and 0.893 (*cf.* **Table 3.3**). Using E_{HB} values, a large set of ILs can be used in the development of these correlations since E_{HB} can be easily assessed for all ILs structures considered, independently of their physical state at room temperature. Furthermore, as reported by Cláudio et al.[36], ILs with more negative values of E_{HB} present higher hydrogen bond basicities, and for these ILs the ABS formation is attained at higher $[IL]_{SS}$.

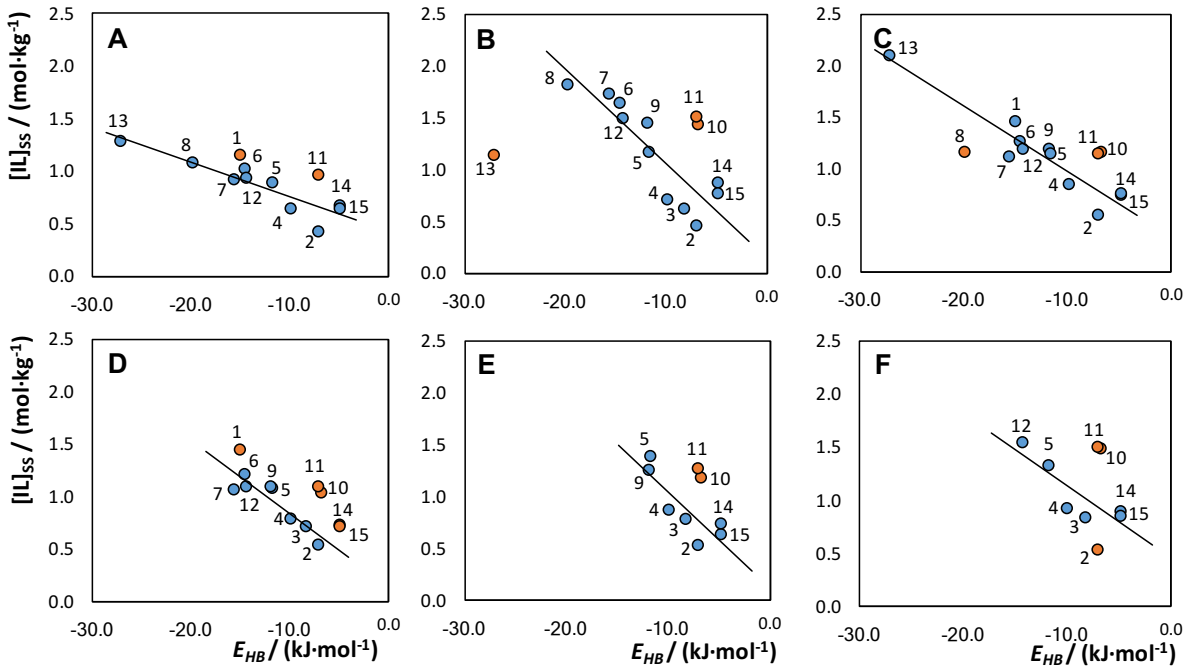

Figure 3.13. Relationship between the molality of the IL at saturation solubility necessary to undergo liquid-liquid demixing ($[IL]_{SS}$) and the hydrogen-bonding interaction energy in the equimolar cation-anion mixture (E_{HB}) of ILs, estimated by COSMO-RS, for the IL-based ABS composed of **(A)** K_3PO_4,[11,45-50] **(B)** $K_3C_6H_5O_7$,[51] **(C)** K_2HPO_4,[10,45,52] **(D)** Na_2CO_3,[7,53-56] **(E)** Na_2SO_4,[11,48,57] and **(F)** $KNaC_4H_4O_6$.[2] ILs used in each correlation (blue circles) and outsiders (orange circles) are identified in **Table 3.3**.

The ILs used in these correlations, as well as their ability to induce (✓) or not (✗) ABS formation with each salt, are summarized in **Table 3.3**. Some ABS composed with a given IL and salt were considered as outsiders (within a 95 % confidence interval) to the tendency generated with the E_{HB} values. Despite some particular cases that can be related with experimental errors, there are two ILs, the $[C_4C_1pip]Cl$ and $[C_4C_1pyr]Cl$ that, independently of the salt, were always

identified as outsiders. This suggests that the E_{HB} values for these two ILs could be wrongly estimated by COSMO-RS. It is important to have in mind that COSMO-RS is a thermodynamic model that combines quantum chemistry with statistical thermodynamic calculations, and this tool is in constant update trying to move to more accurate representations of the real properties of ILs. Nevertheless, the obtained results still demonstrate the high potential application of the predicted hydrogen-bonding interaction energies in the description of IL + salt ABS formation.

Table 3.3. ABS used to evaluate the correlation between $[IL]_{SS}$ and E_{HB} parameter: (✓) formation of ABS; (✗) no formation of ABS; (*n.a.*) no information available. ABS identified as outsiders are colored at grey. Values of the parameters C, and D of **Equation (3.20)** and respective standard deviations, σ, correlation coefficients, R^2, and number of ABS experimental data used in the correlations, N.

		SALTs					
	ILs	(A) K_3PO_4 11,45-50	(B) $K_3C_6H_5O_7$ 51	(C) K_2HPO_4 10,45,52	(D) Na_2CO_3 7,53-56	(E) Na_2SO_4 11,48,57	(F) $KNaC_4H_4O_6$ 2
(1)	$[C_2C_1im]Cl$	✓	✗	✓	✓	*n.a.*	*n.a.*
(2)	$[C_4C_1im][CF_3SO_3]$	✓	✓	✓	✓	✓	✓
(3)	$[C_4C_1im][SCN]$	*n.a.*	✓	*n.a.*	✓	✓	✓
(4)	$[C_4C_1im][N(CN)_2]$	✓	✓	✓	✓	✓	✓
(5)	$[C_4C_1im]Br$	✓	✓	✓	✓	✓	✓
(6)	$[C_4C_1im]Cl$	✓	✓	✓	✓	✗	✗
(7)	$[C_4C_1im][DMP]$	✓	✓	✓	✓	✗	*n.a.*
(8)	$[C_4C_1im][CH_3CO_2]$	✓	✓	✓	✗	✗	*n.a.*
(9)	$[C_4C_1py]Cl$	*n.a.*	✓	✓	✓	✓	✗
(10)	$[C_4C_1pip]Cl$	*n.a.*	✓	✓	✓	✓	✓
(11)	$[C_4C_1pyr]Cl$	✓	✓	✓	✓	✓	✓
(12)	$[C_6C_1im]Cl$	✓	✓	✓	✓	✗	✓
(13)	$[N_{111(2OH)}]Cl$	✓	✓	✓	*n.a.*	*n.a.*	✗
(14)	$[N_{4444}]Cl$	✓	✓	✓	✓	✓	✓
(15)	$[P_{4444}]Cl$	✓	✓	✓	✓	✓	✓
	N	10	11	11	8	7	6
	C* ± *σ	-0.033 ± 0.005	-0.09 ± 0.02	-0.064 ± 0.007	-0.07 ± 0.01	-0.09 ± 0.02	-0.07 ± 0.02
	D* ± *σ	0.42 ± 0.08	0.14 ± 0.19	0.33 ± 0.10	0.15 ± 0.16	0.12 ± 0.22	0.46 ± 0.19
	R^2	0.828	0.776	0.893	0.807	0.738	0.752

After the determination of the correlations between the molality of the IL at saturation solubility, $[IL]_{SS}$ and the E_{HB} parameter, their ability to predict the formation of ABS constituted by other ILs, which were not previously considered, was also evaluated. The obtained results are presented in **Figure 3.14**. Only ABS constituted by K_3PO_4,[11,45-50] K_2HPO_4[10,45,52] and Na_2SO_4[11,48,57] were considered, since for the remaining salts there is not enough experimental data reported in the

literature. Experimental data evaluated in these correlations are reported in **Appendix B**. The average relative deviations (ARD) were determined through **Equation (3.16)**. Remarkably, for the three salts considered, correlation coefficients (R^2) higher than 0.83 and ARD values between 12.70 and 9.53 % were obtained, indicating that the correlations previously determined for each salt can be used to predict the formation of new ABS.

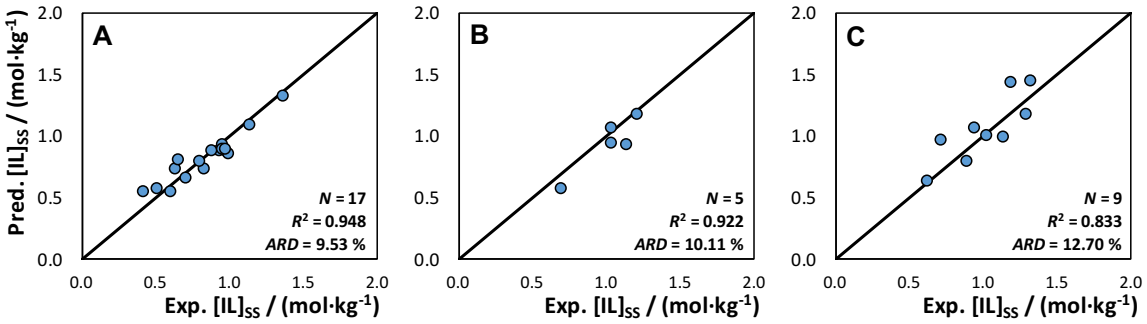

Figure 3.14. Correlation between experimental (Exp. $[IL]_{SS}$) and predicted (Pred. $[IL]_{SS}$) values by **Equation (3.20)** of IL molality at saturation solubility in ABS composed of: **(A)** K_3PO_4, **(B)** K_2HPO_4 and **(C)** Na_2SO_4. Legend: *N* – number of ABS considered; R^2 – correlation coefficient; ARD – average relative deviation.

At this point, it was demonstrated that for a common salt and using ILs E_{HB} parameters estimated by COSMO-RS, it is possible to predict the formation of new ABS without the need of additional experimental data. However, it is still need to experimentally determine a set of IL-based ABS to found the equation that correlates the ABS formation for each salt (**Table 3.3**), and, in an optimum situation, these equations should allow the prediction without the need to use experimental data.

Since each of the correlations presented in **Figure 3.13** was determined for a fixed salt, the constants C and D of **Equation (3.20)** are salt dependent. Shahriari et al.[7] reported that the molar entropy of hydration ($\Delta_{hyd}S$) of the salt ions is related with the IL-based ABS formation. The $\Delta_{hyd}S$ values for the cations and anions that compose the salts evaluated in this work, are reported in **Table 3.4**. In fact, it was possible to find a linear relation between the constants *C* and *D* determined for each salt-based ABS and the salt ions molar entropy of hydration, that are described by the **Equations (3.21)** and **(3.22)**.

Table 3.4. Molar entropy of hydration ($\Delta_{hyd}S$) for ions that compose the salts under study.[59-61]

	$\Delta_{hyd}S$ (kJ·mol^{-1})
Anions	
PO_4^{3-}	-421
$C_6H_5O_7^{3-}$	*n.a.*
HPO_4^{2-}	-272
CO_3^{2-}	-245
SO_4^{2-}	-200
$C_4H_4O_6^{2-}$	*n.a.*
Cations	
K^+	-74
Na^+	-111

$$C = (2.48\times10^{-4} \pm 4.37\times10^{-5}) \cdot \Delta_{hyd}S_{anion} - 0.119 \pm 0.012 \quad \textbf{(3.21)}$$

R^2 = 0.942; F = 32.27; N = 4

$$D = (6.13\times10^{-4} \pm 2.96\times10^{-5}) \cdot \Delta_{hyd}S_{anion} + (4.43\times10^{-3} \pm 1.33\times10^{-4}) \cdot \Delta_{hyd}S_{cation} + 0.491 \pm 0.019 \quad \textbf{(3.22)}$$

R^2 = 1.0; F = 2920; N = 4

Through **Equations (3.21)** and **(3.22)**, it is possible to conclude that the parameter C is dominated by the molar entropy of hydration of the salt anion, while parameter D depends on both anion and cation salt $\Delta_{hyd}S$. Unfortunately, there is no available data for the molar entropy of hydration of citrate and tartrate anions, and thus **Equations (3.21)** and **(3.22)** were estimated only using a N = 4. Nevertheless, these equations have, not only statistical meaning, but also are in good agreement with Shahriari et al.[7] previous findings.

To prove the **Equations (3.21)** and **(3.22)** possible application, the constants C and D for the ABS constituted by the salt K_2CO_3, that were never considered in this work until this point, were determined. By their direct application the following values were calculated for K_2CO_3-based ABS: C = -0.0743 mol^2·(kg·kJ)$^{-1}$ and D = 0.313 mol·kg^{-1}. With these two parameters, and ILs E_{HB} values, it was possible to predict the $[IL]_{SS}$ for ABS composed of K_2CO_3 salt. In **Figure 3.15** the values predicted by **Equation (3.20)** are represented as function of experimental data (these data will be presented in **chapter 3.5**). Remarkably, a correlation coefficient of 0.881 and an ARD of 12.86 %

were obtained. This result demonstrates that $[IL]_{SS}$ values of K_2CO_3-based ABS can be predicted only using the ILs E_{HB} parameters estimated by COSMO-RS and the molar entropy of hydration of both cation and anion of the salt.

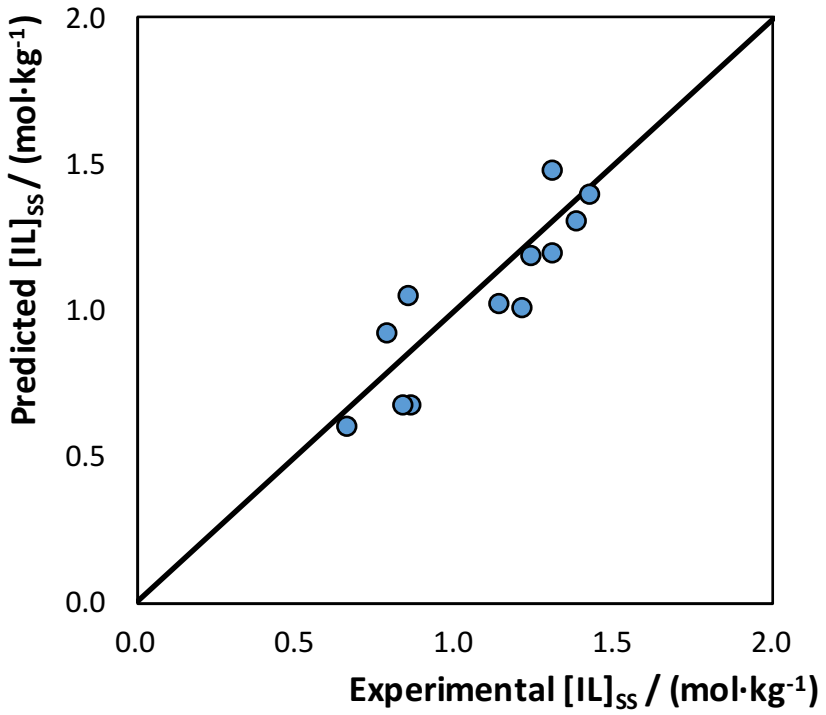

Figure 3.15. Correlation between experimental and predicted values of IL molality at saturation solubility ($[IL]_{SS}$) for K_2CO_3-based ABS. *N* = 12; R^2 = 0.881; ARD = 12.86 %.

3.2.5. Conclusions

For the first time, an effective predictive model for IL-based ABS was successfully established. It was demonstrated that the ABS ILs saturation solubility present a linear dependence with the COSMO-RS hydrogen-bonding interaction energies, allowing to predict the ability of ILs to form ABS with a specific salt. Furthermore, the determined correlation constants showed to be intrinsically related with the salt ions molar entropy of hydration. This finding allowed to expand the predictive model, and not only the change of an IL for a fixed salt, but also the modification of the salt that compose the ABS, can be now predicted with the model here developed.

3.2.6. References

(1) M.G. Freire, A.F.M. Cláudio, J.M.M. Araujo, J.A.P. Coutinho, I.M. Marrucho, J.N. Canongia Lopes, and L.P.N. Rebelo, *Chem. Soc. Rev.*, 2012, **41**, 4966−4995;
(2) T.B.V. Dinis, H. Passos, D.L.D. Lima, V.I. Esteves, J.A.P. Coutinho, and M.G. Freire, *Green Chem.*, 2015, **17**, 2570−2579;

(3) R.P. Swatloski, S.K. Spear, J.D. Holbrey, and R.D. Rogers, *J. Am. Chem. Soc.*, 2002, **124**, 4974−4975;
(4) H. Passos, M.G. Freire, and J.A.P. Coutinho, *Green Chem.*, 2014, **16**, 4786−4815;
(5) A.F.M. Cláudio, M.C. Neves, K. Shimizu, J.N. Canongia Lopes, M.G. Freire, and J.A.P. Coutinho, *Green Chem.*, 2015, **17**, 3948−3963;
(6) K.E. Gutowski, G.A. Broker, H.D. Willauer, J.G. Huddleston, R.P. Swatloski, J.D. Holbrey, and R.D. Rogers, *J. Am. Chem. Soc.*, 2003, **125**, 6632−6633;
(7) S. Shahriari, C.M.S.S. Neves, M.G. Freire, and J.A.P. Coutinho, *J. Phys. Chem. B*, 2012, **116**, 7252−7258;
(8) K.A. Kurnia, M.G. Freire, and J.A.P. Coutinho, *J. Phys. Chem. B*, 2014, **118**, 297−308;
(9) A.F.M. Cláudio, A.M. Ferreira, S. Shahriari, M.G. Freire, and J.A.P. Coutinho, *J. Phys. Chem. B*, 2011, **115**, 11145−11153;
(10) T. Mourão, A.F.M. Cláudio, I. Boal-Palheiros, M.G. Freire, and J.A.P. Coutinho, *J. Chem. Thermodyn.*, 2012, **54**, 398−405;
(11) S.P.M. Ventura, C.M.S.S. Neves, M.G. Freire, I.M. Marrucho, J. Oliveira, and J.A.P. Coutinho, *J. Phys. Chem. B*, 2009, **113**, 9304−9310;
(12) J. Palgunadi, S.Y. Hong, J.K. Lee, H. Lee, S.D. Lee, M. Cheong, and H.S. Kim, *J. Phys. Chem. B*, 2011, **115**, 1067−1074;
(13) A. Xu, J. Wang, and H. Wang, *Green Chem.*, 2010, **12**, 268−275;
(14) R.C. Remsing, R.P. Swatloski, R.D. Rogers, and G. Moyna, *Chem. Commun.*, 2006, 1271−1273;
(15) C. Reichardt, *Green Chem.*, 2005, **7**, 339−351;
(16) Y. Marcus, *Chem. Soc. Rev.*, 1993, **22**, 409−416;
(17) P.G. Jessop, D.A. Jessop, D. Fu, and P. Lam, *Green Chem.*, 2012, **14**, 1245−1259;
(18) R. Lungwitz, M. Friedrich, W. Linert, and S. Spange, *New J. Chem.*, 2008, **32**, 1493−1499;
(19) R. Lungwitz and S. Spange, *New J. Chem.*, 2008, **32**, 392−394;
(20) R. Lungwitz, V. Strehmel, and S. Spange, *New J. Chem.*, 2010, **34**, 1135−1140;
(21) M.A. Ab Rani, A. Brant, L. Crowhurst, A. Dolan, M. Lui, N.H. Hassan, J.P. Hallett, P.A. Hunt, H. Niedermeyer, J.M. Perez-Arlandis, M. Schrems, T. Welton, and R. Wilding, *Phys. Chem. Chem. Phys.*, 2011, **13**, 16831−16840;
(22) A. Brandt, J.P. Hallett, D.J. Leak, R.J. Murphy, and T. Welton, *Green Chem.*, 2010, **12**, 672−679;
(23) A. Brandt, M.J. Ray, T.Q. To, D.J. Leak, R.J. Murphy, and T. Welton, *Green Chem.*, 2011, **13**, 2489−2499;
(24) L. Crowhurst, P.R. Mawdsley, J.M. Perez-Arlandis, P.A. Salter, and T. Welton, *Phys. Chem. Chem. Phys.*, 2003, **5**, 2790−2794;
(25) T.P. Wells, J.P. Hallett, C.K. Williams, and T. Welton, *J. Org. Chem.*, 2008, **73**, 5585−5588;
(26) M.J. Kamlet, J.L. Abboud, and R.W. Taft, *J. Am. Chem. Soc.*, 1977, **99**, 6027−6038;
(27) M.J. Kamlet, J.L.M. Abboud, M.H. Abraham, and R.W. Taft, *J. Org. Chem.*, 1983, **48**, 2877−2887;
(28) M.J. Kamlet and R.W. Taft, *J. Am. Chem. Soc.*, 1976, **98**, 377−383;
(29) R.W. Taft and M.J. Kamlet, *J. Am. Chem. Soc.*, 1976, **98**, 2886−2894;
(30) S.N. Baker, G.A. Baker, and F.V. Bright, *Green Chem.*, 2002, **4**, 165−169;
(31) S. Trivedi, N.I. Malek, K. Behera, and S. Pandey, *J. Phys. Chem. B*, 2010, **114**, 8118−8125;
(32) V. Znamenskiy and M.N. Kobrak, *J. Phys. Chem. B*, 2004, **108**, 1072−1079;
(33) S.R. Mente and M. Maroncelli, *J. Phys. Chem. B*, 1999, **103**, 7704−7719;
(34) H. Niedermeyer, C. Ashworth, A. Brandt, T. Welton, and P.A. Hunt, *Phys. Chem. Chem. Phys.*, 2013, **15**, 11566−11578;
(35) R. Contreras, A. Aizman, R.A. Tapia, and A. Cerda-Monje, *J. Phys. Chem. B*, 2013, **117**, 1911−1920;
(36) A.F.M. Claudio, L. Swift, J.P. Hallett, T. Welton, J.A.P. Coutinho, and M.G. Freire, *Phys. Chem. Chem. Phys.*, 2014, **16**, 6593−6601;

(37) K.A. Kurnia, F. Lima, A.F.M. Cláudio, J.A.P. Coutinho, and M.G. Freire, *Phys. Chem. Chem. Phys.*, 2015, **17**, 18980−18990;
(38) A. Klamt, *J. Phys. Chem.*, 1995, **99**, 2224−2235;
(39) A. Klamt and F. Eckert, *Fluid Phase Equilib.*, 2000, **172**, 43−72;
(40) A. Klamt and G. Schuurmann, *J. Chem. Soc.-Perkin Trans. 2*, 1993, 799−805;
(41) J. Palomar, J.S. Torrecilla, J. Lemus, V.R. Ferro, and F. Rodriguez, *Phys. Chem. Chem. Phys.*, 2008, **10**, 5967−5975;
(42) J. Palomar, J.S. Torrecilla, J. Lemus, V.R. Ferro, and F. Rodriguez, *Phys. Chem. Chem. Phys.*, 2010, **12**, 1991−2000;
(43) University of Karlsruhe and Forschungszentrum Karlsruhe GmbH, TURBOMOLE V6.1 2009, 1989–2007, 25 GmbH, since 2007; available from http://www.turbomole.com;
(44) F. Eckert and A. Klamt, COSMOtherm Version C2.1 Release 01.08, Cosmol. GmbH Co. KG, Leverkusen, Ger. 2006;
(45) M. Zawadzki, F. A. e Silva, U. Domańska, J. A. P. Coutinho and S. P. M. Ventura, *Green Chem.*, 2016, **18**, 3527–3536;
(46) C. L. S. Louros, A. F. M. Cláudio, C. M. S. S. Neves, M. G. Freire, I. M. Marrucho, J. Pauly and J. A. P. Coutinho, *Int. J. Mol. Sci.*, 2010, **11**, 1777–1791;
(47) H. Passos, A. C. A. Sousa, M. R. Pastorinho, A. J. A. Nogueira, L. P. N. Rebelo, J. A. P. Coutinho and M. G. Freire, *Anal. Methods*, 2012, **4**, 2664–2667;
(48) A. F. M. Cláudio, A. M. Ferreira, C. S. R. Freire, A. J. D. Silvestre, M. G. Freire and J. A. P. Coutinho, *Sep. Purif. Technol.*, 2012, **97**, 142–149;
(49) M. G. Freire, C. M. S. S. Neves, J. N. C. Lopes, I. M. Marrucho, J. A. P. Coutinho and L. P. N. Rebelo, *J. Phys. Chem. B*, 2012, **116**, 7660–7668;
(50) C. M. S. S. Neves, S. P. M. Ventura, M. G. Freire, I. M. Marrucho and J. A. P. Coutinho, *J. Phys. Chem. B*, 2009, **113**, 5194–5199;
(51) H. Passos, A. R. Ferreira, A. F. M. Cláudio, J. A. P. Coutinho and M. G. Freire, *Biochem. Eng. J.*, 2012, **67**, 68–76;
(52) S. P. M. Ventura, S. G. Sousa, L. S. Serafim, Á. S. Lima, M. G. Freire and J. A. P. Coutinho, *J. Chem. Eng. Data*, 2011, **56**, 4253–4260;
(53) C. F. C. Marques, T. Mourão, C. M. S. S. Neves, Á. S. Lima, I. Boal-Palheiros, J. A. P. Coutinho and M. G. Freire, *Am. Inst. Chem. Eng. Biotechnol. Prog*, 2013, **29**, 645–654;
(54) C. Li, J. Han, Y. Wang, Y. Yan, J. Pan, X. Xu and Z. Zhang, *J. Chem. Eng. Data*, 2010, **55**, 1087–1092;
(55) A. F. M. Cláudio, C. F. C. Marques, I. Boal-Palheiros, M. G. Freire and J. A. P. Coutinho, *Green Chem.*, 2014, **16**, 259–268;
(56) F. J. Deive, M. A. Rivas and A. Rodríguez, *J. Chem. Thermodyn.*, 2011, **43**, 1153–1158;
(57) J. R. Trindade, Z. P. Visak, M. Blesic, I. M. Marrucho, J. A. P. Coutinho, J. N. Canongia Lopes and L. P. N. Rebelo, *J. Phys. Chem. B*, 2007, **111**, 4737–4741;
(58) A. Oehlke, K. Hofmann, and S. Spange, *New J. Chem.*, 2006, **30**, 533−536;
(59) Y. Marcus, *Ion Properties*. 1997, New York: Marcel Dekker, Inc;
(60) Y. Marcus, *J. Chem. Soc., Faraday Trans.*, 1991, **87**, 2995−2999;
(61) M.T. Zafarani-Moattar and A. Zaferanloo, *J. Chem. Thermodyn.*, 2009, **41**, 864−871.

3.3. Aqueous biphasic systems composed of ionic liquids and acetate-based salts: phase diagrams, densities, and viscosities

This chapter is based on the published manuscript

Maria V. Quental, Helena Passos, Kiki A. Kurnia, João A. P. Coutinho, and Mara G. Freire;[1]

"Aqueous biphasic systems composed of ionic liquids and acetate-based salts: phase diagrams, densities, and viscosities", Journal of Chemical Engineering Data 60 (2015) 1674−168.

3.3.1. Abstract

Ionic-liquid-based aqueous biphasic systems (IL-based ABS) have been largely investigated as promising extraction and purification routes. In this context, the determination of their phase diagrams and the physical properties of the coexisting phases are of high relevance when envisaging their large-scale applications. Low viscosities improve mass transfer and reduce energy consumption, while the knowledge of their densities is important for equipment design. In this work, novel phase diagrams for aqueous solutions of imidazolium-based ILs combined with acetate-based salts, namely KCH_3CO_2 or $NaCH_3CO_2$, are reported and discussed. The ability of the acetate-based salts to induce the phase separation not only depends on the ions hydration energy, but also on the concentration of "free" ions in solution. The tie-lines, tie-line lengths, and critical points are also addressed. Experimental measurements of density and viscosity of the coexisting phases, for the different systems and at several compositions and temperatures, are additionally presented. The Othmer−Tobias and Bancroft equations are also applied to ascertain the tie-lines coherence. It is here shown that low-viscous IL-based ABS, with a high difference in the densities of the coexisting phases, can be formed with organic and biodegradable salts thus offering enhanced features over conventional polymer-based systems.

3.3.2. Introduction

Aqueous biphasic systems (ABS) have been investigated for the replacement of volatile and hazardous organic compounds in liquid−liquid extraction processes.[1−4] Typical ABS consist in two aqueous-rich phases containing polymer/polymer, polymer/salt or salt/salt combinations.[5] In the past decade, ionic-liquid-(IL)-based ABS appeared as a novel alternative to polymer-rich systems

[1]**Contributions:** M.G.F. and H.P. conceived and directed this work. M.V.Q. acquired the experimental data. K.A.K. was responsible for the study of ions speciation. M.V.Q., H.P. and M.G.F interpreted the experimental data. M.V.Q., H.P. and M.G.F. wrote the final manuscript with significant contributions of the remaining authors.

because of their enhanced performance in extraction and purification approaches.[5,6] In fact, the use of ILs as phase-forming components of ABS permits the tuning of the polarities and affinities of the coexisting phases and improved extractions and selectivities can be foreseen.[5]

Reliable thermophysical data of pure ILs and their mixtures are of paramount relevance to support their industrial applications.[7–10] These data are required in the development of models for process design, energy efficiency, and control of chemical processes.[7] In addition to the knowledge of the phase diagrams and compositions of the coexisting phases, the density and viscosity are also pertinent properties for the use of IL-based ABS at a large scale. Low viscosities of the coexisting phases enhance mass transfer and reduce energy consumption, while densities are important for equipment design. Although a large number of publications reporting the phase diagrams of IL-based ABS can be found,[5] few of them report the thermophysical properties of their coexisting phases.[11–14] In literature, most works addressing IL-based ABS have considered high-charge density inorganic salts because of their strong salting-out character.[5] Nevertheless, the high concentrations of these salts required to form two-phase systems may have some adverse effects upon the (bio)molecules being purified and also lead to environmental concerns. Organic salts, known for their lower toxicity and favorable biodegradability, can also form ABS when combined with ILs in aqueous solutions. Despite these advantages, few works on IL-based ABS formed by organic salts are available.[15–22] The ability of citrate-, tartrate-, and acetate-based salts to induce ABS with ILs has been reported.[15–22] However, acetate-based salts were only tested with $[BF_4]$-based ILs,[18–20] which are nonstable in water even at room temperature,[23] and with $[CF_3SO_3]$-based compounds.[20]

In this work, a set of imidazolium-based ILs with the ability to induce ABS formation when in the presence of sodium or potassium acetate salts, namely 1-butyl-3-methylimidazolium trifluoromethanesulfonate ($[C_4C_1im][CF_3SO_3]$), 1-butyl-3-methylimidazolium thiocyanate ($[C_4C_1im][SCN]$), and 1-butyl-3-methylimidazolium dicyanamide ($[C_4C_1im][N(CN)_2]$), were selected. The ternary phase diagrams at 298 K, as well as the respective tie-lines (TLs) and tie-line lengths (TLLs), were determined. As it will be shown, the ability of the acetate-based salts to induce the phase separation not only depends on their respective hydration energy, but also on the concentration of "free" ions in solution. In addition, the TLs were also validated using the Othmer–Tobias and Bancroft equations.[24,25] Finally, the physical properties of the coexisting phases, namely density and viscosity, were characterized to gather a broader picture on the applicability of these systems.

3.3.3. Experimental procedures

Materials. Potassium acetate, KCH_3CO_2, 99 wt % of purity from Sigma-Aldrich, and sodium acetate, $NaCH_3CO_2$, 99 wt % of purity from VWR, were used as received. Several imidazolium-based ILs, namely 1-butyl-3-methylimidazolium trifluoromethanesulfonate ($[C_4C_1im][CF_3SO_3]$), 1-butyl-3-methylimidazolium thiocyanate ($[C_4C_1im][SCN]$), and 1-butyl-3-methylimidazolium dicyanamide ($[C_4C_1im][N(CN)_2]$), acquired from Iolitec and with a purity level > 98 wt %, were investigated. The cation and anion chemical structures of the studied ILs are displayed in **Figure 3.16**. It should be highlighted that other ILs were investigated to form ABS with KCH_3CO_2 and $NaCH_3CO_2$, namely 1-butyl-3-methylimidazolium bromide ($[C_4C_1im]Br$), 1-butyl-3-methylimidazolium methylsulfate ($[C_4C_1im][CH_3SO_4]$), 1-butyl-3-methylimidazolium ethylsulfate ($[C_4C_1im][C_2H_5SO_4]$), 1-butyl-3-methylimidazolium tosylate ($[C_4C_1im][TOS]$), 1-butyl-3-methylimidazolium octylsulfate ($[C_4C_1im][C_8H_{17}SO_4]$), 1-hexyl-3-methylimidazolium chloride ($[C_6C_1im]Cl$), 1-methyl-3-octylimidazolium chloride ($[C_8C_1im]Cl$), 1-butyl-1-methylpiperidinium chloride ($[C_4C_1pip]Cl$), 1-butyl-1-methylpyrrolidinium chloride ($[C_4C_1pyr]Cl$), 1-butyl-3-metylpyridinium chloride ($[C_4C_1py]Cl$), tetrabutylphosphonium chloride ($[P_{4444}]Cl$), tetrabutylammonium chloride ($[N_{4444}]Cl$), tributylmethylphosphonium tosylate ($[P_{4441}][TOS]$), tributylmethylphosphonium ethylsulfate ($[P_{4441}][C_2H_5SO_4]$), and tributylethylphosphonium diethylphosphate ($[P_{4442}][DEP]$). Nevertheless, these ILs were not able to undergo liquid–liquid demixing with the acetate-based salts investigated. Before use, IL samples were purified and dried for a minimum of 24 h at constant agitation, at a moderate temperature (≈ 353 K), and under vacuum. After this step, the purity of each IL was further confirmed using ^1H, ^{13}C, and ^{19}F (whenever applicable) NMR spectroscopy. The water employed was ultrapure water, double distilled, and treated with a Milli-Q plus 185 water purification device.

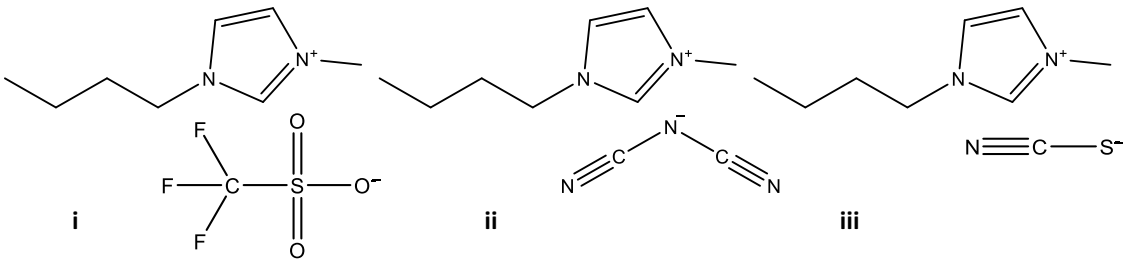

Figure 3.16. Chemical structure of the ILs studied: (i) $[C_4C_1im][CF_3SO_3]$, (ii) $[C_4C_1im][N(CN)_2]$, (iii) $[C_4C_1im][SCN]$.

Phase diagrams, tie-lines and critical points. The binodal curve of each ternary phase diagram was determined through the cloud point titration method at (298 ± 1) K and at

atmospheric pressure. The experimental procedure adopted in this work follows the method already validated by us and described in **chapter 2.1**. In brief, aqueous solutions of the acetate salts (≈ 25 wt %) and aqueous solutions of ILs with variable concentrations (from 60 wt % to 80 wt %) were prepared gravimetrically ($\pm 10^{-4}$ g) and used for the determination of the saturation curves. Drop-wise addition of the aqueous salt solution to each IL aqueous solution was carried out until the detection of a cloudy solution (biphasic region), followed by the dropwise addition of ultrapure water until the detection of a limpid solution (monophasic regime). In some situations, the addition of the IL solution to the salt-rich medium was also carried out to complete the phase diagrams. These additions were carried out under constant agitation. Each mixture composition was determined by the weight quantification of all components added within ± 10^{-4} g.

The tie-lines (TLs) of the system $[C_4C_1im][CF_3SO_3]$ + $NaCH_3CO_2$ were determined analytically (by quantifying the IL by UV spectroscopy, the water gravimetrically by evaporation down to a constant weight and the salt by weight difference), while the TLs of the systems $[C_4C_1im][SCN]$ + $NaCH_3CO_2$, $[C_4C_1im][CF_3SO_3]$ + KCH_3CO_2, $[C_4C_1im][SCN]$ + KCH_3CO_2 and $[C_4C_1im][N(CN)_2]$ + KCH_3CO_2 were determined by the lever-arm rule using **Equations (2.2)** to **(2.5)**. The tie-line length (TLL) was determined using **Equation (2.6)**.

The method described by Merchuk et al.,[27] commonly applied to describe the binodal data of ABS, is not able to correctly describe TLs highly concentrated in IL and salt.[28] Some problems were found in the application of this method to the aqueous system formed by $[C_4mim][CF_3SO_3]$ and $NaCH_3CO_2$, where no consistency of the TLs' data was found, maybe due to the highly hydrophobicity of this IL which implies an IL-rich phase with a low water content. The selected mixture, at the biphasic regime, was prepared by weighting the appropriate amounts of salt + IL + water, vigorously stirred, and further submitted to centrifugation for 30 min and at controlled temperature, (298 ± 1) K. After centrifugation, each phase was carefully separated and weighed. For the first situation, the quantification of each compound in each phase was determined as described previously. For the gravimetric method approach, each individual TL was determined by the application of the lever-arm rule to the relationship between the weight of the top and bottom phases and the overall system composition. The experimental binodal curves were fitted by least-squares regression according to **Equation (2.1)** presented in **chapter 2.1**.

The consistency of the measured TLs was further checked using the Othmer-Tobias[24]

$$\left(\frac{1-[IL]_{IL}}{[IL]_{IL}}\right) = k_1\left(\frac{1-[salt]_{salt}}{[salt]_{salt}}\right)^n \qquad \textbf{(3.23)}$$

and Bancroft[25] equations,

$$\left(\frac{[H_2O]_{salt}}{[salt]_{salt}}\right) = k_2\left(\frac{[H_2O]_{IL}}{[IL]_{IL}}\right)^r \quad \textbf{(3.24)}$$

where k_1, n, k_2, and r are fitting parameters. A linear dependency of $\log\left(\frac{1-[\mathrm{IL}]_{IL}}{[\mathrm{IL}]_{IL}}\right)$ against $\log\left(\frac{1-[\mathrm{salt}]_{salt}}{[\mathrm{salt}]_{salt}}\right)$ and $\log\left(\frac{[\mathrm{H_2O}]_{salt}}{[\mathrm{salt}]_{salt}}\right)$ against $\log\left(\frac{[\mathrm{H_2O}]_{\mathrm{IL}}}{[\mathrm{IL}]_{IL}}\right)$ indicates the consistency of the results.

The critical point of each ABS was also determined by extrapolating the TLs' slopes of individual systems followed by the fitting using **Equation (3.25)**,

$$[IL] = f[salt] + g \quad \textbf{(3.25)}$$

where *f* and *g* are the fitting parameters.

Ions speciation. The speciation of the salt ions in aqueous solution and the respective concentrations were estimated using VisualMINTEQ[29] (version 3.0), a thermodynamic speciation model, based on the MinteqA2 software with the Minteq database. Previously we confirmed the capability of VisualMINTEQ to describe the metal salt ions speciation and its impact upon the formation of IL-based ABS.[20] In these thermodynamic calculations, the concentration of salt in each ternary mixture was used as the input.

Density and viscosity. Density and viscosity measurements for both the IL-rich and organic-salt-rich phases were performed at atmospheric pressure and at the temperature range between (298.15 and 328.15) K, with an uncertainty of ± 0.02 K, using an automated SVM 3000 Anton Paar rotational Stabinger viscometer-densimeter. The dynamic viscosities have a relative uncertainty of 0.35 % while the absolute uncertainty for the density is 5×10^{-4} g·cm^{-3}. Prior to the measurements, the equipment was calibrated using standard solutions, as well as with pure ILs or their mixtures.[7,30]

3.3.4. Results and discussion

Phase diagrams, tie-lines and critical points. Ternary phase diagrams were determined for each IL + KCH_3CO_2 + H_2O (**Figure 3.17**) and IL + $NaCH_3CO_2$ + H_2O (**Figure 3.18**) system, at 298 K and at atmospheric pressure. To form ABS, that is, two aqueous rich-phases, composed of ILs and salts, only hydrophilic or water-miscible ILs should be chosen. Among all the studied ILs, only $[C_4C_1im][CF_3SO_3]$, $[C_4C_1im][SCN]$, and $[C_4C_1im][N(CN)_2]$ were able to promote the ABS formation with acetate-based salts. These ILs comprise imidazolium-based cations with a butyl chain that

turns the IL more hydrophobic that makes them more easily undergo phase separation, and anions with a low hydrogen-bond basicity or a weak ability to accept protons from water.[31] For most systems, the top phase corresponds to the IL-rich phase while the bottom phase represents the salt-rich phase. An exception was observed for the ABS containing $[C_4C_1im][CF_3SO_3]$. The phase inversion is directly related to the high density of the fluorinated anion.[32]

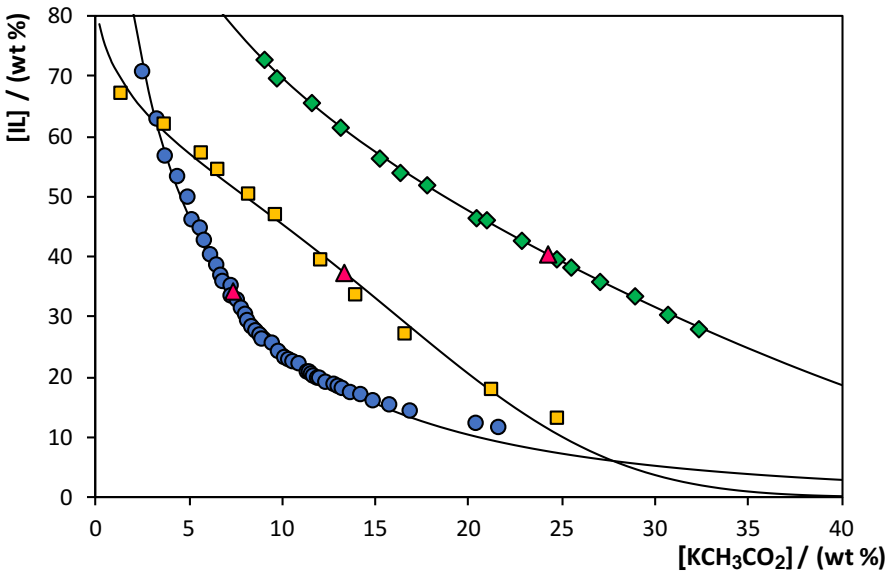

Figure 3.17. Ternary phase diagrams for ABS composed of IL + KCH_3CO_2 + H_2O: $[C_4C_1im][CF_3SO_3]$ (●); $[C_4C_1im][SCN]$ (■); $[C_4C_1im][N(CN)_2]$ (◆); critical point (▲); adjusted binodal using **Equation (2.1)** (–).

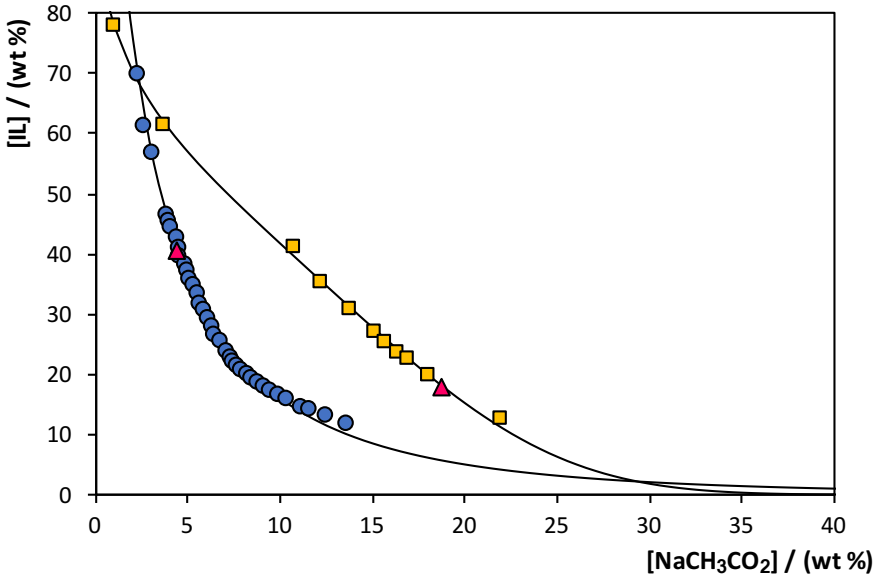

Figure 3.18. Ternary phase diagrams for ABS composed of IL + $NaCH_3CO_2$ + H_2O: $[C_4C_1im][CF_3SO_3]$ (●); $[C_4C_1im][SCN]$ (■); critical point (▲); adjusted binodal using **Equation (2.1)** (–).

In **Figure 3.17** and **Figure 3.18**, the biphasic regime is located above the solubility curve. The area of this region is proportional to the ability of each IL to undergo liquid–liquid demixing with

salt solutions. The aptitude of each IL to form two phases in the presence of ~10 wt % of KCH_3CO_2 is as follows: $[C_4C_1im][CF_3SO_3]$ > $[C_4C_1im][SCN]$ > $[C_4C_1im][N(CN)_2]$. This rank to promote phase separation is similar to previous results for ABS composed of ILs and Na_2SO_4,[33] citrate-based[22] and phosphate-based[26] salts. Previous works[34–36] have shown that water mainly interacts with ILs through its anion, in which it plays a major role as a hydrogen-bond acceptor. Furthermore, the ability of the IL anions to form ABS closely follows the decrease on their hydrogen-bond accepting strength or electron pair donation ability.[26] The same trend of ILs to promote ABS was observed for ~10 wt % of $NaCH_3CO_2$; however, it is interesting to highlight that this salt is not able to form ABS with $[C_4C_1im][N(CN)_2]$, despite its higher hydration energy ($\Delta G_{hyd}(Na^+)$ = −365 kJ·mol^{-1} and $\Delta G_{hyd}(K^+)$ = −295 kJ·mol^{-1}).[21,37]

The formation of ABS with ILs and salts is normally characterized by the occurrence of a competition between the IL and salt ions to be solvated by water. The competition is won by the salt ions due to their higher hydration energy when compared to IL ions. Consequently, there is a migration of water from the IL-solvated region toward the salt-rich phase and thus forming two liquid phases. The strength of the salt ions to be solvated by water can be characterized either by the Gibbs free energy (ΔG_{hyd}) or the molar entropy of hydration (ΔS_{hyd}). The lower ΔG_{hyd} and ΔS_{hyd} of the acetate ion when compared with other high-charge density anions, for instance PO_4^{3-},[26,38] confirms its weaker salting-out ability (according to the Hofmeister series[21,39]) and, consequently, a lower aptitude to create ABS with ILs.

As the studied salts share the same anion, the capability of the salts to promote ABS depends on their cation counterpart, Na^+ and K^+. **Figure 3.19** depicts the effect of the salt on the formation of two-phase systems. $NaCH_3CO_2$ is more able to form ABS, that is, lower amounts of salt are required for the liquid−liquid demixing. This trend is in agreement with the ΔG_{hyd} and ΔS_{hyd} of the respective salt cations: Na^+ (ΔG_{hyd} = −365 kJ·mol^{-1}, ΔS_{hyd} = −111 J·K^{-1}·mol^{-1}) and K^+ (ΔG_{hyd} = −295 kJ·mol−1, ΔS_{hyd} = −74 J·K^{-1}·mol^{-1}).[21,37] Thus, if KCH_3CO_2 can form ABS with $[C_4C_1im][N(CN)_2]$, one might also expect that $NaCH_3CO_2$, with higher ΔG_{hyd} and ΔS_{hyd}, should also form ABS. Nevertheless, the unexpected inability of $NaCH_3CO_2$ to promote phase separation with aqueous solutions of $[C_4C_1im][N(CN)_2]$ is an indication that the formation of ABS is not only governed by the Gibbs free energy of hydration (or molar entropy of hydration). In fact, the concentration of "free" ions in aqueous solution plays a major role as discussed below.

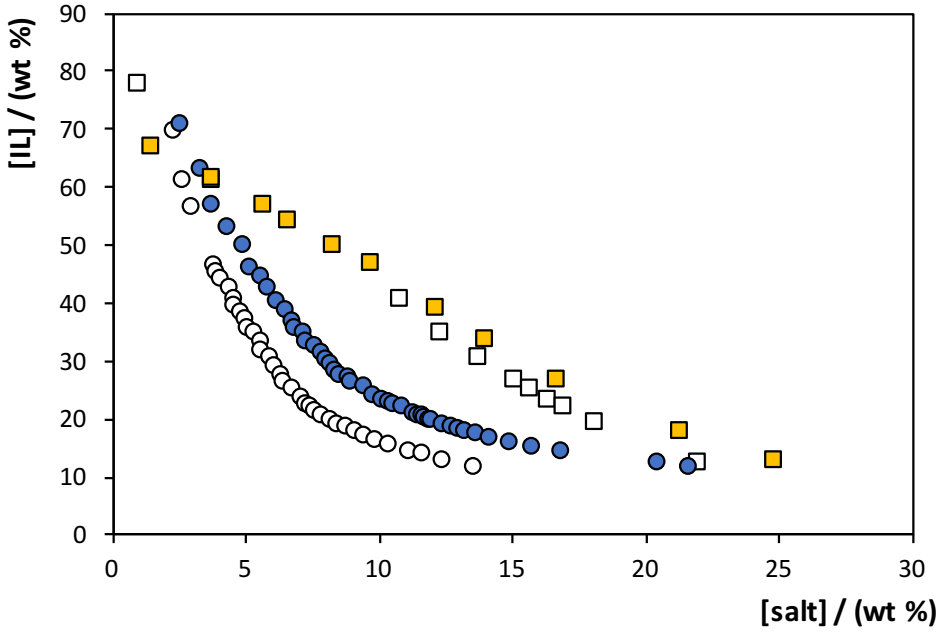

Figure 3.19. Evaluation of salt effect on the formation of $[C_4C_1im][CF_3SO_3]$- (●) and $[C_4C_1im][SCN]$-based ABS (■): KCH_3CO_2 (full symbols) and $NaCH_3CO_2$ (open symbols).

Several works[37,40–42] have addressed the presence of ion pairs of organic (or inorganic) salts in aqueous solution. For instance, using Raman spectroscopy, Fournier and co-workers[42] confirmed ion pairing of $NaCH_3CO_2$ in aqueous media. In a previous work,[20] we have shown that the ion pairing of polyvalent salt ions has a significant impact toward their ability to promote phase separation in ABS. Therefore, we turned here our attention to estimate the ions speciation that might occur in aqueous solutions of $NaCH_3CO_2$ and KCH_3CO_2 with an aim to understand the inability of the sodium-based salt to form ABS with $[C_4C_1im][N(CN)_2]$. Details on the speciation of the ions, at 298 K, along with their concentration are given in the **Appendix B**. It is shown that, for the concentration range where the salt is able to form ABS, the dissolution of $NaCH_3CO_2$ in aqueous media produces not only Na^+ and $CH_3CO_2^-$ but also $NaCH_3CO_2$. In addition, the concentration of the $NaCH_3CO_2$ ion pair increases with an increase in the concentration of salt. Although a similar trend is observed for the dissolution of KCH_3CO_2, in which it produces the KCH_3CO_2 ion pair, when comparing the ion speciation profiles of both salts, it is interesting to note that for the same concentration, the sodium-based salt presents a higher abundance of the pair $NaCH_3CO_2$. This ion pairing reduces therefore the concentration of "free" and further hydrated Na^+ and $CH_3CO_2^-$, that coupled with the weaker ability of $[C_4C_1im][N(CN)_2]$ to form ABS, support the inexistence of a two-phase system for the $NaCH_3CO_2$/$[C_4C_1im][N(CN)_2]$ combination.

The parameters obtained by the regression of the experimental binodal curves using **Equation (2.1)** are presented in **Table 3.5**. In general, good correlation coefficients were obtained for all

systems, indicating that these fittings can be used to predict data in a given region of the phase diagram where no experimental results are offered. The detailed experimental weight fraction data for each phase diagram are reported in the **Appendix B**.

Table 3.5. Correlation parameters used to describe the experimental binodal data by **Equation (2.1)** and respective standard deviations (σ) and correlation coefficients (R^2).

IL	salt	$A \pm \sigma$	$B \pm \sigma$	$10^5 (C \pm \sigma)$	R^2
$[C_4C_1im][CF_3SO_3]$	KCH_3CO_2	209.0 ± 1.8	-0.67 ± 0.03	0.01 ± 0.19	0.998
$[C_4C_1im][SCN]$		84.9 ± 3.7	-0.17 ± 0.02	18.14 ± 0.95	0.992
$[C_4C_1im][N(CN)_2]$		205.8 ± 13.9	-0.57 ± 0.02	1.00 ± 0.43	0.996
$[C_4C_1im][CF_3SO_3]$	$NaCH_3CO_2$	265.1 ± 9.7	-0.89 ± 0.02	0.01 ± 3.20	0.995
$[C_4C_1im][SCN]$		98.9 ± 1.8	-0.24 ± 0.01	9.94 ± 0.70	0.999

The experimental TLs, along with their respective length (TLL), are reported in **Table 3.6**. Their representation can be found in the **Appendix B**. In addition, the critical point of each system was also determined using **Equation (3.25)** based on a geometrical approach schematized in **Figure 3.20** for the system composed of $[C_4C_1im][N(CN)_2]$ + KCH_3CO_2 + H_2O. The critical points of all the investigated systems are depicted in **Figure 3.17** and **Figure 3.18**. For the potassium-based ABS, the content of IL at the critical point is similar among all the systems investigated, while a larger difference is noticeable in the salt amount. On the other hand, for the stronger salting-out salt, $NaCH_3CO_2$, the critical point is more dependent on the type and amount of IL and salt.

Table 3.6. Weight fraction compositions for TLs and respective TLLs of IL + KCH_3CO_2 + H_2O and IL + $NaCH_3CO_2$ + H_2O ABS, at the IL- and salt-rich phases and at the initial biphasic composition of the mixture (M) at 298 K and at atmospheric pressure (0.1 MPa). Viscosity and density properties were measured for the identified TLs (ID).[a]

IL	salt	Weight fraction composition / wt %									TLL	ID
		$[IL]_{IL}$	$[salt]_{IL}$	$[H_2O]_{IL}$	$[IL]_{M}$	$[salt]_{M}$	$[H_2O]_{M}$	$[IL]_{salt}$	$[salt]_{salt}$	$[H_2O]_{salt}$		
$[C_4C_1im][CF_3SO_3]$	KCH_3CO_2	57.41	3.74	38.85	24.22	11.83	63.95	18.31	13.23	68.46	47.76	TL1
		80.16	2.06	17.78	25.95	15.07	58.98	11.83	18.47	69.70	70.27	---
		84.15	1.85	14.00	29.88	15.11	55.01	10.67	19.80	69.53	75.63	---
$[C_4C_1im][SCN]$		64.76	2.46	32.78	40.18	13.81	46.01	2.83	31.07	66.10	68.22	TL1
		81.31	0.06	18.63	40.13	19.84	40.03	0.23	38.99	60.78	89.93	TL2
		82.76	0.02	17.22	39.94	22.23	37.83	0.04	42.93	57.03	93.18	---
$[C_4C_1im][N(CN)_2]$		63.57	12.23	24.20	39.84	26.91	33.25	18.51	40.11	41.38	52.99	---
		71.70	9.25	19.05	39.97	28.94	31.09	12.55	45.94	41.51	69.60	---
		75.10	8.18	16.72	41.18	28.88	29.94	11.78	46.81	41.41	74.18	---
		76.41	7.80	15.79	39.86	30.93	29.21	8.71	50.65	40.64	80.12	TL1
		84.27	5.77	9.96	39.88	32.96	27.16	7.06	53.06	39.88	90.53	TL2
$[C_4C_1im][CF_3SO_3]$	$NaCH_3CO_2$	73.56	2.20	24.24	29.82	11.70	58.48	6.61	17.69	75.70	68.72	---
		79.56	2.04	18.40	29.99	14.06	55.95	5.40	19.94	74.66	76.23	---
		82.22	2.24	15.54	30.08	15.54	54.38	5.32	21.20	73.48	79.22	TL1
$[C_4C_1im][SCN]$		60.68	3.97	35.35	33.60	15.12	51.23	3.86	27.11	69.03	61.34	TL1
		82.93	0.53	16.54	33.02	18.86	48.12	1.59	30.41	68.00	86.65	TL2
		88.65	0.20	11.15	33.58	20.69	45.73	0.80	32.58	66.62	93.36	---

[a] The standard uncertainty for the weight fraction is 0.01, the standard uncertainty for the temperature is 1 K, and the standard uncertainty for pressure is 10 kPa.

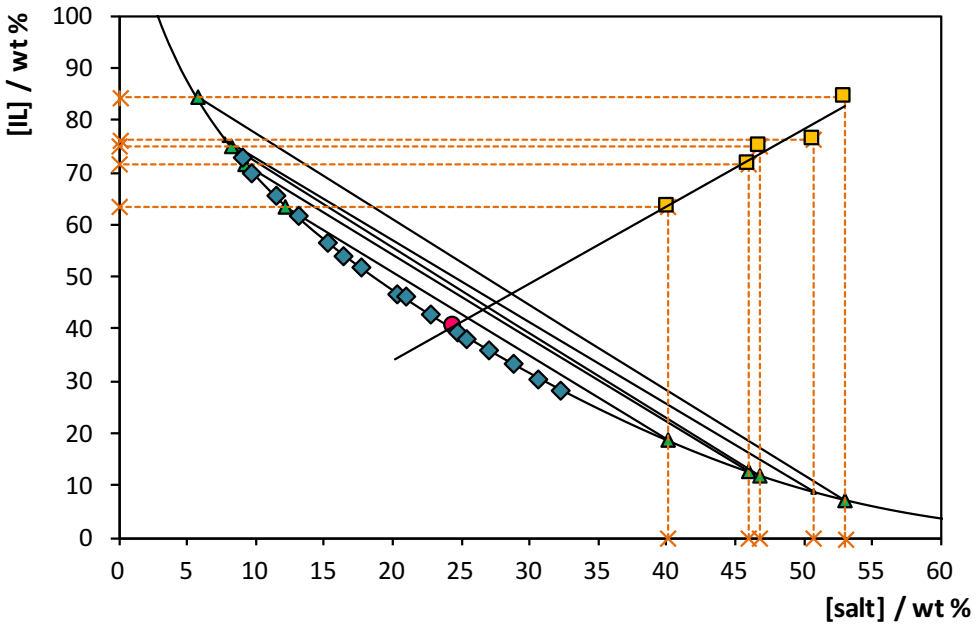

Figure 3.20. Phase diagram for the ternary system composed of $[C_4C_1im][N(CN)_2]$ + KCH_3CO_2 + H_2O: binodal curve data (◆); adjusted binodal data through **Equation (2.1)** (–); TL data (▲); TLs relation (■); critical point (●).

The consistency of the TLs was further checked using the Othmer–Tobias[24] and Bancroft[25] equations (**Equations (3.23)** and **(3.24)**), and the respective fitting parameters and correlation coefficient (R^2) are shown in **Table 3.7** (*cf.* the **Appendix B** with the graphical representation). The TL data are reliable since the obtained regression coefficients are close to 1, indicating therefore a good degree of consistency of the experimental data.

Table 3.7. Values of the fitting parameters of **Equations (3.23)** and **(3.24)** for the systems composed of IL+ salt + H_2O at 298 K, and respective standard deviations (σ) and correlation coefficients (R^2).

IL	salt	Othmer-Tobias[24] (Equation (3.23))			Bancrof[25] (Equation (3.24))		
		$n \pm \sigma$	$k_1 \pm \sigma$	R^2	$r \pm \sigma$	$k_2 \pm \sigma$	R^2
$[C_4C_1im][CF_3SO_3]$	KCH_3CO_2	2.846 ± 0.051	0.004 ± 0.036	1.000	0.275 ± 0.004	5.734 ± 0.003	1.000
$[C_4C_1im][SCN]$	KCH_3CO_2	1.970 ± 0.445	0.109 ± 0.107	0.951	0.477 ± 0.117	2.962 ± 0.066	0.943
$[C_4C_1im][N(CN)_2]$	KCH_3CO_2	1.945 ± 0.344	0.273 ± 0.030	0.914	0.271 ± 0.049	1.307 ± 0.021	0.910
$[C_4C_1im][CF_3SO_3]$	$NaCH_3CO_2$	2.264 ± 0.011	0.011 ± 0.007	1.000	0.379 ± 0.001	6.518 ± 0.001	1.000
$[C_4C_1im][SCN]$	$NaCH_3CO_2$	6.285 ± 0.645	0.001 ± 0.240	0.990	0.138 ± 0.017	2.751 ± 0.011	0.985

Density and viscosity. The characterization of the top and bottom phases in different ternary systems, at different compositions and temperatures, are important for the design and scale up of extraction processes. Hence, the density and viscosity in the temperature range between 298.15 K and 328.15 K were determined for one or two ternary compositions of each ABS studied. The

following mixture compositions were investigated: 12 wt % of KCH_3CO_2 + 24 wt % of $[C_4C_1im][CF_3SO_3]$ + 64 wt % of H_2O (TL1); 31 wt % of KCH_3CO_2 + 40 wt % of $[C_4C_1im][N(CN_2)]$ + 29 wt % of H_2O (TL1); 33 wt % of KCH_3CO_2 + 40 wt % of $[C_4C_1im][N(CN_2)]$ + 27 wt % of H_2O (TL2); 14 wt % of KCH_3CO_2 + 40 wt % $[C_4C_1im][SCN]$ + 46 wt % of H_2O (TL1); 20 wt % of KCH_3CO_2 + 40 wt % $[C_4C_1im][SCN]$ + 40 wt % of H_2O (TL2); 15 wt % of $NaCH_3CO_2$ + 30 wt % $[C_4C_1im][CF_3SO_3]$ + 64 wt % of H_2O (TL1); 15 wt % of $NaCH_3CO_2$ + 34 wt % of $[C_4C_1im][SCN]$ + 51 wt % of H_2O (TL1); 19 wt % of $NaCH_3CO_2$ + 33 wt % of $[C_4C_1im][SCN]$ + 29 wt % of H_2O (TL2) (*cf.* **Table 3.6** with the respective TLs data). **Figure 3.21** to **Figure 3.24** show the density and viscosity data, as a function of temperature, for the mixtures investigated. The complete experimental data are available in the **Appendix B**.

Viscosity is mainly dependent on intra- and intermolecular interactions. Since aqueous solutions of ILs and salts are being analyzed, H-bonding and Coulombic interactions are among the most important. An increase in temperature substantially decreases the intensity of H-bonding interactions and, therefore, the viscosity decreases with an increase in temperature, as shown in **Figure 3.21** and **Figure 3.22**.

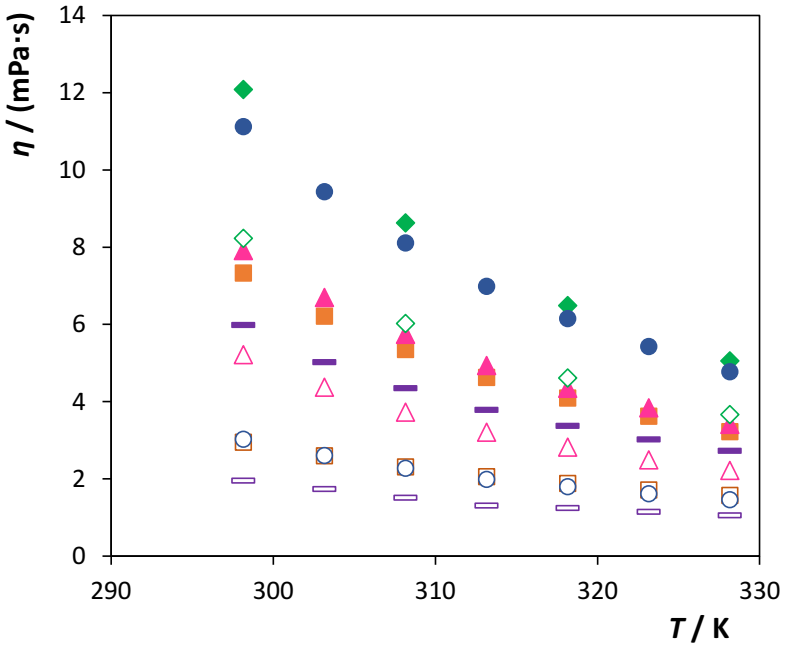

Figure 3.21. Experimental viscosity as a function of temperature for IL-rich (full symbols) and salt-rich (open symbols) phases of ternary mixtures identified in **Table 3.6** as TL1: $[C_4C_1im][CF_3SO_3]$ + KCH_3CO_2 (–); $[C_4C_1im][CF_3SO_3]$ + $NaCH_3CO_2$ (●); $[C_4C_1im][SCN]$ + KCH_3CO_2 (■); $[C_4C_1im][SCN]$ + $NaCH_3CO_2$ (▲); $[C_4C_1im][N(CN)_2]$ + KCH_3CO_2 (◆).

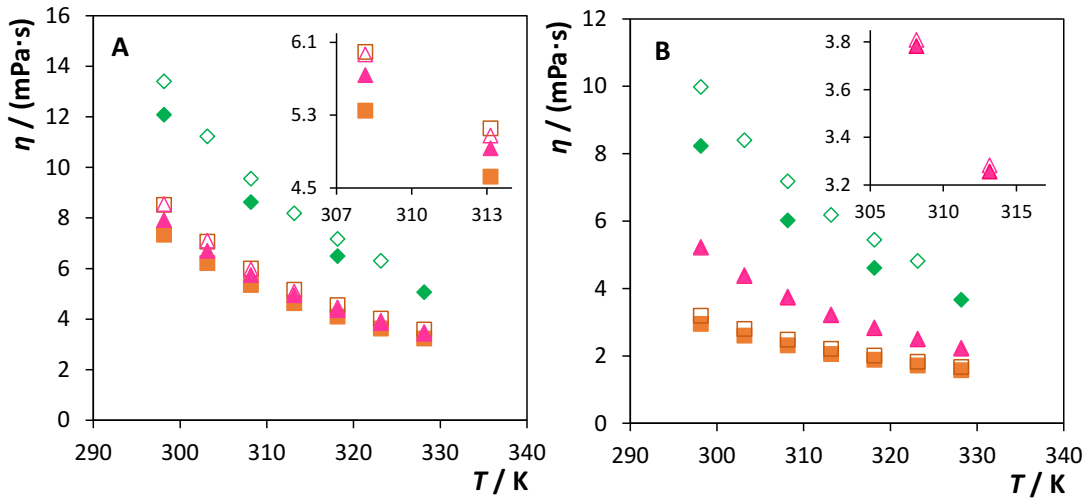

Figure 3.22. Experimental viscosity as a function of temperature for ternary mixtures identified in **Table 3.6** as TL1 (full symbols) and TL2 (open symbols): $[C_4C_1im][SCN]$ + KCH_3CO_2 (■); $[C_4C_1im][SCN]$ + $NaCH_3CO_2$ (▲); $[C_4C_1im][N(CN)_2]$ + KCH_3CO_2 (◆). **(A)** IL-rich phase; **(B)** salt-rich phase.

Figure 3.21 displays the IL anion effect on the viscosity of the IL-rich and salt-rich phases for ABS composed of KCH_3CO_2 and $NaCH_3CO_2$. At 298.15 K and at the TL1' compositions (**Table 3.6**), the viscosity of the IL-rich phase of the KCH_3CO_2-based ABS decreases in the following order: $[C_4C_1im][N(CN)_2]$ (12.08 mPa·s) > $[C_4C_1im][SCN]$ (7.33 mPa·s) > $[C_4C_1im][CF_3SO_3]$ (5.99 mPa·s). The opposite trend was observed with $NaCH_3CO_2$ where the viscosity decreases in the rank: $[C_4C_1im][CF_3SO_3]$ (11.12 mPa·s) > $[C_4C_1im][SCN]$ (7.91 mPa·s). For the salt-rich phase of ABS composed of KCH_3CO_2 the trend observed was as follows: $[C_4C_1im][N(CN)_2]$ (8.23 mPa·s) > $[C_4C_1im][SCN]$ (2.95 mPa·s) > $[C_4C_1im][CF_3SO_3]$ (1.96 mPa·s); for $NaCH_3CO_2$-based ABS the series is as follows: $[C_4C_1im][SCN]$ (5.21 mPa·s) > $[C_4C_1im][CF_3SO_3]$ (3.03 mPa·s). In general, the trend on the viscosity values of both phases seems to be closely related with their compositions. For IL-rich phases, the viscosity decreases with a decrease in the IL content and concomitant increase in the water amount (data given in **Table 3.6**). For KCH_3CO_2-based ABS at 298 K, the viscosity decreases in the order $[C_4C_1im][N(CN)_2]$ (76.41 wt % of IL, 15.79 wt % of H_2O) > $[C_4C_1im][SCN]$ (64.76 wt % of IL, 32.78 wt % of H_2O) > $[C_4C_1im][CF_3SO_3]$ (57.41 wt % of IL, 38.85 wt % of H_2O); and for $NaCH_3CO_2$-based ABS at 298 K: $[C_4C_1im][CF_3SO_3]$ (82.22 wt % of IL, 15.54 wt % of H_2O) > $[C_4C_1im][SCN]$ (60.68 wt % of IL, 35.35 wt % of H_2O). In a similar way, the viscosity of the salt-rich phase decreases with the increase on the water content and simultaneous decrease on the salt content according to the rank $[C_4C_1im][N(CN)_2]$ (50.65 wt % of salt, 40.64 wt % of water) > $[C_4C_1im][SCN]$ (31.07 wt % of salt, 66.10 wt % of water) > $[C_4C_1im][CF_3SO_3]$ (13.23 wt % of salt, 68.46 wt % of water) for

KCH_3CO_2-based ABS, and $[C_4C_1im][SCN]$ (27.11 wt % of salt, 69.03 wt % of water) > $[C_4C_1im][CF_3SO_3]$ (21.20 wt % of salt, 73.48 wt % of water) for $NaCH_3CO_2$-based ABS.

Different ABS compositions were also investigated, and from the results displayed in **Figure 3.22**, the viscosities differences among the coexisting phases generally increase with the increase of the TLL (from TL1 to TL2) due to the larger differences in the mixture compositions (*cf.* **Table 3.6**).

Comparing the viscosity values obtained for KCH_3CO_2 + $[C_4C_1im][SCN]$ and $NaCH_3CO_2$ + $[C_4C_1im][SCN]$ ABS (**Figure 3.21** and **Figure 3.22**), it seems that the type of salt used in the ABS formulation does not influence the viscosity of the IL-rich phases – probably due to their low concentration in these phases (less than 4 wt %). On the other hand, salt-rich phases are composed of *ca.* 30 wt % of each salt, and there are significant differences in the viscosity values of these phases that are further dependent on the salt used in the preparation of a given ABS.

One of the critical problems related with conventional ABS composed of polymers is the high viscosity of the polymeric-rich phase which hinders the mass transfer and adds significant energetic inputs into the process.[43] It was already demonstrated that phosphonium-K_3PO_4-based ABS display lower viscosities than polymer-based ABS.[12] In addition, a recent work comprising ABS composed of imidazolium-based ILs and K_3PO_4 reported that imidazolium-based ABS lead to coexisting phases of lower viscosity than their phosphonium counterparts.[11] In general, while the viscosities of the IL-rich phases here studied are 1.5 to 3 times higher than those of the salt-rich ones, these are of a much lower viscosity than those of typical polymer-based ABS.[44]

Density data for all the studied systems are presented in **Figure 3.23** and **Figure 3.24**. In general, the density decreases with the increase of temperature. For most systems, and for both salts, the density of the salt-rich phase is higher than the density of the IL-rich phase. An exception was observed with the $[C_4C_1im][CF_3SO_3]$-based ABS – the IL-rich phase presents a higher density than the salt-rich phase (**Figure 3.23**). This is a consequence of the low concentration of inorganic salt at the IL-rich phase and of the high density of the fluorinated IL.

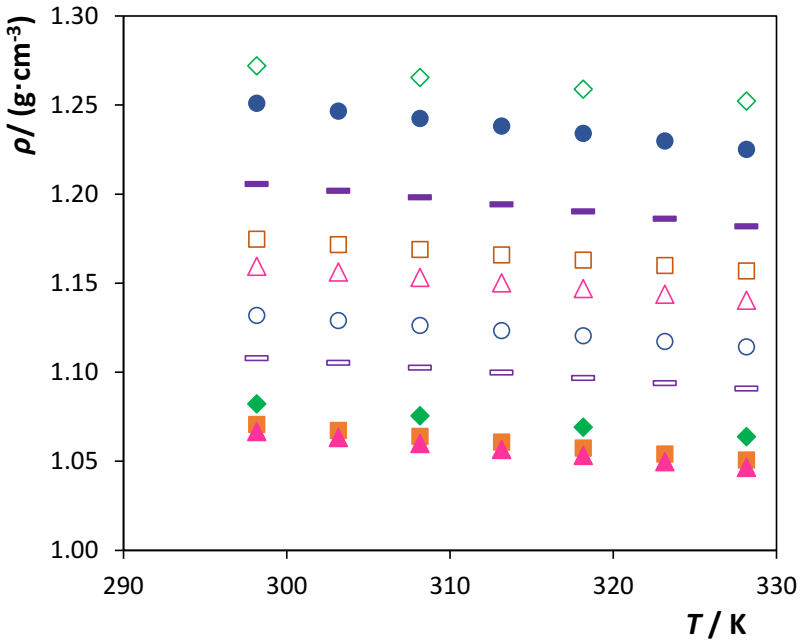

Figure 3.23. Experimental density as a function of temperature for IL-rich (full symbols) and salt-rich (open symbols) phases of ternary mixtures identified in **Table 3.6** as TL1: $[C_4C_1im][CF_3SO_3]$ + KCH_3CO_2 (–) $[C_4C_1im][CF_3SO_3]$ + $NaCH_3CO_2$ (●); $[C_4C_1im][SCN]$ + KCH_3CO_2 (■); $[C_4C_1im][SCN]$ + $NaCH_3CO_2$ (▲); $[C_4C_1im][N(CN)_2]$ + KCH_3CO_2 (◆).

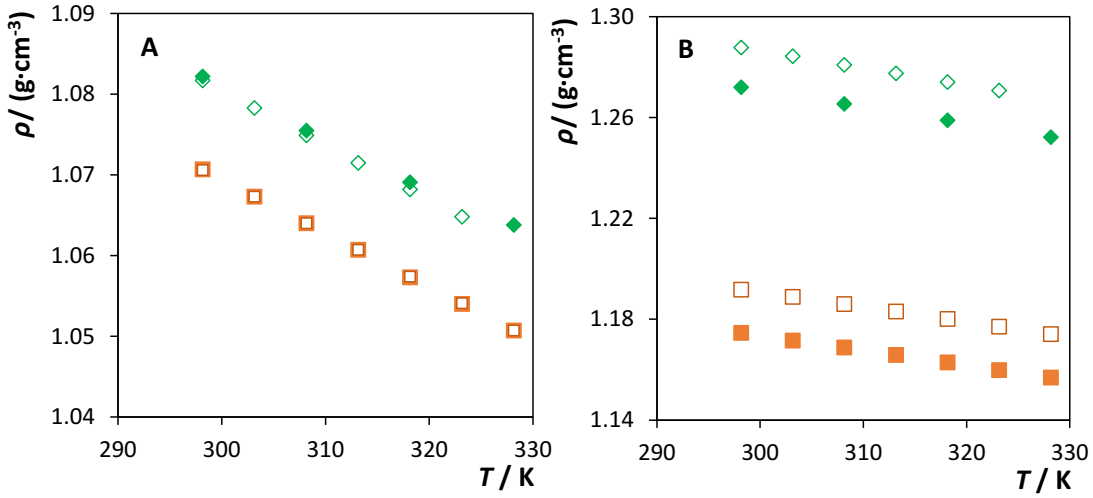

Figure 3.24. Experimental density as a function of temperature for ternary mixtures identified in **Table 3.6** as TL1 (full symbols) and TL2 (open symbols): $[C_4C_1im][SCN]$ + KCH_3CO_2 (■); $[C_4C_1im][N(CN)_2]$ + KCH_3CO_2 (◆). **(A)** IL-rich phase; **(B)** salt-rich phase.

For the ABS formed by KCH_3CO_2, the density values of the IL-rich phases at 298.15 K and at the TL1' compositions, are 1.0707 g·cm^{-3} for $[C_4C_1im][SCN]$, 1.0822 g·cm^{-3} for $[C_4C_1im][N(CN)_2]$, and 1.2058 g·cm^{-3} for $[C_4C_1im][CF_3SO_3]$. For ABS composed of $[C_4C_1im][SCN]$ + $NaCH_3CO_2$ and $[C_4C_1im][CF_3SO_3]$ + $NaCH_3CO_2$ the densities of the IL-rich phases are 1.0667 g·cm^{-3} and 1.2509

$g \cdot cm^{-3}$, respectively. These tendencies are in close agreement with other systems previously reported.[11,13] Moreover, when compared with other salts, such as K_3PO_4, the densities of the IL-rich phases are quite similar; for instance, at 298.15 K, the densities range between 1.2169 $g \cdot cm^{-3}$ ($[C_4C_1im][CF_3SO_3]$) and 1.0366 $g \cdot cm^{-3}$ ($[C_4C_1im][N(CN)_2]$).[11]

For salt-rich phases the density values at 298.15 K for both the studied salts are very similar: 1.1746 $g \cdot cm^{-3}$ for $[C_4C_1im][SCN] + KCH_3CO_2$ (TL1) and 1.1594 $g \cdot cm^{-3}$ for $[C_4C_1im][SCN] + NaCH_3CO_2$ (TL1). These results indicate that the change of the cation of the salt does not induce considerable variations in the densities of the coexisting phases. Nevertheless, the differences between the IL-rich and salt-rich phases cannot be neglected (**Figure 3.23**). As observed for viscosity, the density differences between the phases increase with the TLL (from TL1 to TL2 – **Figure 3.24** and **Table 3.6**). For the IL-rich phase the density values are very close for the two TLLs tested (they are overlapped). On the other hand, for the salt-rich phase, an increase in the TLL leads to an increase in the density values as presented in **Figure 3.24**. In fact, for TL2, the amount of salt at the salt-rich phase is higher (shown in **Table 3.6**).

Compared with that of typical polymer–salt ABS,[45] the differences in the densities of the coexisting phases are higher for IL-based ABS. This is a very relevant result since higher density differences allow an easier and faster separation of the coexisting phases in ABS.

3.3.5. Conclusions

ILs are currently seen as potential phase-forming promoters of ABS to be used in liquid-liquid separation processes. With a goal to develop more benign systems, we report here novel ternary phase diagrams, TLs, TLLs, and critical points for ABS composed of imidazolium-based ILs and two biodegradable organic salts (potassium and sodium acetate). It was found that the phase-separation ability of the investigated ILs follows the order $[C_4C_1im][CF_3SO_3]$ > $[C_4C_1im][SCN]$ > $[C_4C_1im][N(CN)_2]$. Sodium acetate revealed to be a stronger salting-out agent or having a higher capacity to form ABS. Furthermore, the coherence of the TL data was ascertained using the Othmer–Tobias and Bancroft equations. The densities and viscosities of the coexisting phases at given mixtures of all IL-based ABS were also determined. The system formed by KCH_3CO_2 and $[C_4C_1im][CF_3SO_3]$ presents the lower viscosity values, while the system constituted by KCH_3CO_2 + $[C_4C_1im][N(CN)_2]$ is the most viscous. Nevertheless, the viscosities of the coexisting phase of the investigated IL-based ABS were found to be substantially lower than those observed in typical polymer-based systems, representing thus a major contribution for the development of industrial processes based on ILs. At last, it was observed that the differences in the densities of the

coexisting phases are higher for IL-based ABS than for polymer-based systems, allowing therefore an easier and faster separation of the coexisting phases.

3.3.6. References

(1) P.A. Albertsson, *Partitioning of Cell Particles and Macromolecules*; Wiley-Interscience: New York, 1986;
(2) J.C. Merchuk, B.A. Andrews, and J.A. Asenjo, *J. Chromatogr. B Biomed. Sci. Appl.*, 1998, **711**, 285−293;
(3) R. Hatti-Kaul, *Mol. Biotechnol.*, 2001, **19**, 269−277;
(4) H.-O. Johansson, G. Karlström, F. Tjerneld, and C.A. Haynes, *J. Chromatogr. B Biomed. Sci. Appl.*, 1998, **711**, 3−17;
(5) M.G. Freire, A.F.M. Cláudio, J.M.M. Araújo, J.A.P. Coutinho, I.M. Marrucho, J.N. Canongia Lopes, and L.P.N. Rebelo, *Chem. Soc. Rev.*, 2012, **41**, 4966−4995;
(6) K.E. Gutowski, G.A. Broker, H.D. Willauer, J.G. Huddleston, R.P. Swatloski, J.D. Holbrey, and R.D. Rogers, *J. Am. Chem. Soc.*, 2003, **125**, 6632−6633;
(7) A. Bhattacharjee, C. Varanda, M.G. Freire, S. Matted, L.M.N.B.F. Santos, I.M. Marrucho, and J.A.P. Coutinho, *J. Chem. Eng. Data*, 2012, **57**, 3473−3482;
(8) J.-Y. Wang, F.-Y. Zhao, Y.-M. Liu, X.-L. Wang, and Y.-Q. Hu, *Fluid Phase Equilib.*, 2011, **305**, 114−120;
(9) L. G. Sanchez, J.R. Espel, F. Onink, G.W. Meindersma, G. W., and A.B. de Haan, *J. Chem. Eng. Data*, 2009, **54**, 2803−2812;
(10) M. Tariq, P.A.S. Forte, M.F.C. Gomes, J.N.C. Lopes, and L.P.N. Rebelo, *J. Chem. Thermodyn.*, 2009, **41**, 790−798;
(11) A.F.M. Cláudio, M.G. Freire, C.S.R. Freire, A.J.D. Silvestre, and J.A.P. Coutinho, *Sep. Purif. Technol.*, 2010, **75**, 39−47;
(12) C.L.S. Louros, A.F.M. Cláudio, C.M.S.S. Neves, M.G. Freire, I.M. Marrucho, J. Pauly, and J.A.P. Coutinho, *Int. J. Mol. Sci.*, 2010, **11**, 1777−1791;
(13) C.M.S.S. Neves, M.G. Freire, and J.A.P. Coutinho, *RSC Adv.*, 2012, **2**, 10882−10890;
(14) M.G. Freire, C.L.S. Louros, L.P.N. Rebelo, and J.A.P. Coutinho, *Green Chem.*, 2011, **13**, 1536− 1545;
(15) M.T. Zafarani-Moattar and S. Hamzehzadeh, *J. Chem. Eng. Data*, 2009, **54**, 833− 841;
(16) M.T. Zafarani-Moattar and S. Hamzehzadeh, *Fluid Phase Equilib.*, 2011, **304**, 110−120;
(17) J. Han, Y. Wang, Y. Li, C. Yu, and Y. Yan, *J. Chem. Eng. Data*, 2011, **56**, 3679−3687;
(18) J. Han, C. Yu, Y. Wang, X. Xie, Y. Yan, G. Yin, and W. Guan, *Fluid Phase Equilib.*, 2010, **295**, 98−103;
(19) J. Han, Y. Wang, C. Yu, Y. Yan, and X. Xie, *Anal. Bioanal. Chem.*, 2011, **399**, 1295−1304;
(20) K.A. Kurnia, M.G. Freire, and J.A. Coutinho, *J. Phys. Chem. B*, 2013, **118**, 297−308;
(21) S. Shahriari, C.M.S.S. Neves, M.G. Freire, and J.A.P. Coutinho, *J. Phys. Chem. B*, 2012, **116**, 7252−7258;
(22) H. Passos, A.R. Ferreira, A.F.M. Cláudio, J.A.P. Coutinho, and M.G. Freire, *Biochem. Eng. J.*, 2012, **67**, 68−76;
(23) M.G. Freire, C.M.S.S. Neves, I.M. Marrucho, J.A.P. Coutinho, and A.M. Fernandes, *J. Phys. Chem. A*, 2009, **114**, 3744−3749;
(24) D.F. Othmer and P.E. Tobias, *Ind. Eng. Chem.*, 1942, **34**, 693−696;
(25) P. Gonzalez-Tello, F. Camacho, G. Blázquez, and F.J. Alarcón, *J. Chem. Eng. Data*, 1996, **41**, 1333−1336;
(26) T. Mourão, A.F.M. Cláudio, I. Boal-Palheiros, M.G. Freire, and J.A.P. Coutinho, *J. Chem. Thermodyn.*, 2012, **54**, 398−405;
(27) J.C. Merchuk, B.A. Andrews, and J.A. Asenjo, *J. Chromatogr. B*, 1998, **711**, 285−293;

(28) E. Alvarez-Guerra, S.P.M. Ventura, J.A.P. Coutinho, and A. Irabien, *Fluid. Phase Equilibr.*, 2014, **371**, 67−74;
(29) J. Gustafsson, *Visual MINTEQ A Free Equilibrium Speciation Model*; KTH: Sweden, 2006; http://www.lwr.kth.se/English/ OurSoftware/vminteq/;
(30) C.M.S.S. Neves, K.A. Kurnia, J.A.P. Coutinho, I.M. Marrucho, J.N.C. Lopes, M.G. Freire, and L.N.P. Rebelo, *J. Phys. Chem. B*, 2013, **117**, 10271− 10283;
(31) A.F.M. Cláudio, L. Swift, J.P. Hallett, T. Welton, J.A.P. Coutinho, and M.G. Freire, *Phys. Chem. Chem. Phys.*, 2014, **16**, 6593−6601;
(32) H. Tokuda, K. Hayamizu, K. Ishii, M.A.B.H. Susan, and M. Watanabe, *J. Phys. Chem. B*, 2004, **108**, 16593−16600;
(33) A.F.M. Cláudio, A.M. Ferreira, S. Shahriari, M.G. Freire, and J.A.P. Coutinho, *J. Phys. Chem. B*, 2011, **115**, 11145−11153;
(34) M.G. Freire, P.J. Carvalho, A.M.S. Silva, L.M.N.B.F. Santos, L.P.N. Rebelo, and I.M. Marrucho, *J. Phys. Chem. B*, 2009, **113**, 202−211;
(35) L.E. Ficke and J.F. Brennecke, *J. Phys. Chem. B*, 2010, **114**, 10496−10501;
(36) S. Cha, M. Ao, W. Sung, B. Moon, B. Ahlstrom, P. Johansson, Y. Ouchi, and D. Kim, *Phys. Chem. Chem. Phys.*, 2014, **16**, 9591−9601;
(37) D.W. Archer and C.B. Monk, *J. Chem. Soc.*, 1964, 3117−3122;
(38) S.P.M. Ventura, C.M.S.S. Neves, M.G. Freire, I.M. Marrucho, J. Oliveira, and J.A.P. Coutinho, *J. Phys. Chem. B*, 2009, **113**, 9304−9310;
(39) F. Hofmeister, *Archiv. Exp. Pathol. Pharm.*, 1888, **24**, 247−260;
(40) P.G. Daniele, A. De Robertis, C. De Stefano, S. Sammartano, and C. Rigano, *J. Chem. Soc., Dalton Trans.*, 1985, 2353−2361;
(41) J.L. Oscarson, S.E. Gillespie, J.J. Christensen, R.M. Izatt, and P.R. Brown, *J. Solution Chem.*, 1988, **17**, 865−885;
(42) P. Fournier, E.H. Oelkers, R. Gout, and G. Pokrovski, *Chem. Geol.* 1998, **151**, 69−84;
(43) F. van Rantwijk and R.A. Sheldon, *Chem. Rev.*, 2007, **107**, 2757−2785;
(44) L.-M. Mei, D.-Q. Lin, Z.-Q. Zhu, and Z.-X. Han, *J. Chem. Eng. Data*, 1995, **40**, 1168−1171;
(45) I. Regupathi, R. Govindarajan, S. Pandian Amaresh, and T. Murugesan, *J. Chem. Eng. Data*, 2009, **54**, 3291−3295.

3.4. Alternative probe for the determination of the hydrogen-bond acidity of ionic liquids and their aqueous solutions

This chapter is based on the published manuscript

Pedro P. Madeira, Helena Passos, Joana Gomes, João A.P. Coutinho and Mara G. Freire[1]; "Alternative probe for the determination of the hydrogen-bond acidity of ionic liquids and their aqueous solutions", Physical Chemistry Chemical Physics 19 (2017) 11011−11016.

3.4.1. Abstract

Although highly relevant to *a priori* select adequate solvents for a given application, the determination of the hydrogen-bond acidity or proton donor ability of aqueous solutions of ionic liquids (ILs) is a difficult task due to the poor solubility of the commonly used probes in aqueous media. In this work, we demonstrate the applicability of the pyridine-*N*-oxide (PyO) probe to determine the hydrogen-bond acidity of both neat ILs and their aqueous solutions, based on ^{13}C NMR chemical shifts, and the suitability of these values to appraise the ability of ILs to form aqueous biphasic systems (ABS).

3.4.2. Introduction

Due to their unique properties and enhanced performance, ionic liquids (ILs) have received increasing attention as suitable candidates for various applications, such as in organic synthesis, catalysis, polymerization, as solvent media for chemical reactions, and in separation/extraction processes.[1-4] They are salts composed of bulk organic cations combined with either organic or inorganic anions, whose asymmetry and dispersed charge leads to low melting temperatures, by general definition below 373 K. Important features associated to most ILs include their negligible vapor pressure, good thermal and chemical stabilities, and the ability to dissolve a wide variety of solutes. Furthermore, ILs are extremely versatile and often referred to as "tuneable", "tailor", "taskspecific" or "designer" solvents. The versatility of these compounds has its roots on the possibility of adjusting their physical and chemical properties by changing their constituting ions.

In addition to the large number of available ILs, the finetuning of their physicochemical properties can be further extended by mixing ILs with molecular liquids. Their aqueous solutions are particularly important, with applications in many fields.[4,5] One particular sub-set of this

[1]**Contributions:** M.G.F. and J.A.P.C. conceived and directed this work. H.P. and J.G. acquired the experimental data. P.P.M., H.P., M.G.F and J.A.P.C. interpreted the experimental data and wrote the final manuscript.

strategy comprises IL-water mixtures for liquid-liquid phase separation and extraction processes.[6,7] In this field, a large interest has been given to IL-based aqueous biphasic systems (ABS) as alternative concentration and purification platforms of a wide variety of value-added compounds.[4] However, to better predict their applicability at an industrial level, the physicochemical characterization of their coexisting phases is a crucial requirement.

An important criterion for choosing the most appropriate solvent for a particular application is the knowledge of its polarity, which encompasses all non-specific and specific interactions. It has been previously demonstrated that the IL polarity influences its solvation ability, enzymes activities, reaction rates and mechanisms, among others.[4,8-10] To appraise the polarity of solvents, several polarity scales are known and well-described in the literature, most of which are based on the interactions of solvatochromic dyes with the target solvent.[11] Solute-solvent interactions include multiple types, such as electrostatic, dipole-dipole, dipole-induced dipole, hydrogen bonding, and electron pair donor–acceptor interactions. A quantitative estimation of the solvent polarity aiming at explaining and/or predicting other solvent dependent phenomena can be adequately obtained through a multi-parameter approach. The most widely accepted multiparametric polarity scale is the one proposed by Kamlet and Taft (KT),[12-15] which has been used to correlate solvent effects (XYZ) on reaction rates, phase equilibria, and spectroscopic properties, through linear solvation energy relationships (LSER) equations of the form

$$XYZ = (XYZ)_0 + s\pi^* + a\alpha + b\beta \qquad \textbf{(3.26)}$$

where $(XYZ)_0$ is the value for the reference system, π^* represents the solvent's dipolarity/polarizability, α is the hydrogen bond donating ability (hydrogen-bond acidity), and β is the hydrogen-bond accepting ability (hydrogen-bond basicity). The parameters a, b and s represent the solute coefficients, which characterizing the respective influence of the π^*, α, and β terms on the XYZ property under study.

The determination of the β and π^* parameters by the identification of the solvatochromic peak maxima of selected probes is relatively straightforward. For example, the UV-Vis spectrum of the non-protonic indicators *N*,*N*-diethyl-4-nitroaniline or 4-nitroanisole in non-hydrogen bond acceptors solvents is shifted bathochromically by increasing the solvent dipolarity, and solvent effects on the peak shift depend only on π^*. For β, the magnitudes of the enhanced bathochromic displacements attributable to hydrogen bonding by 4-nitroaniline relative to *N*,*N*-diethyl-4-nitroaniline, and by 4-nitrophenol relative to 4-nitroanisole, are compared to the same solvent acceptors. The chemical structures of the referred solvatochromic dyes are shown in **Figure 3.25**.

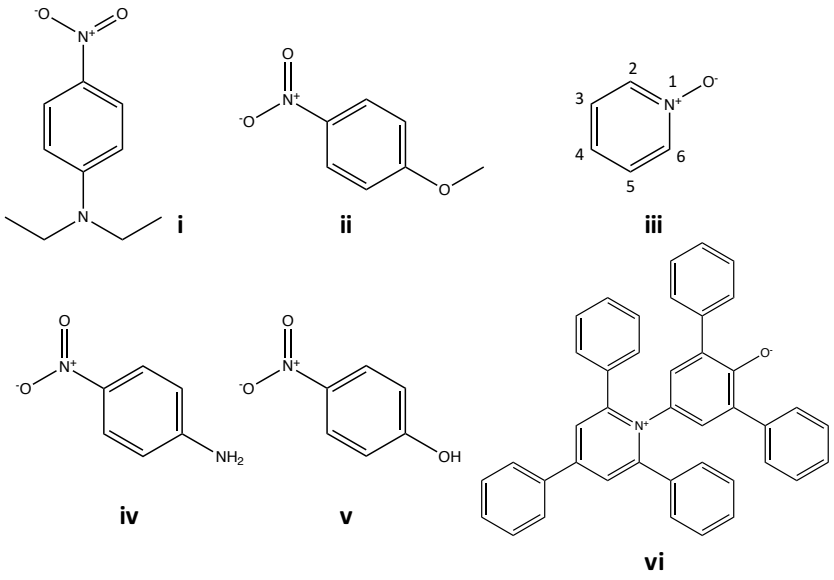

Figure 3.25. Examples of solvatochromic dyes: (i) *N*,*N*-diethyl-4-nitroaniline, (ii) 4-nitroanisole, (iii) pyridine-*N*-oxide, (iv) 4-nitroaniline, (v) 4-nitrophenol, (vi) Reichardt's dye.

Similarly to β, α values are obtained using the solvatochromic comparison method. However, no structurally similar pairs of probes are used, and amongst all the KT parameters, α also has been the most controversial parameter, particularly regarding their values for ILs.[16] Generally, the KT solvatochromic probe used to obtain α values is based on the displacement of the solvatochromic band observed in the spectrum of pyridinium *N*-phenolate betaine dye (Reichardt's dye, **Figure 3.25**). Although this dye has been used for long and known to be strongly dependent on the hydrogen bond donor ability of the solvent,[17-19] it also shows a strong dependency on some other solvent properties. For molecular solvents, it has been reported[20] that this probe is only 1.11 times more sensitive to α than to π^*, and that it presents a slight dependence on β.[20] This scenario is even worsened for ILs, since electrostatic interactions are also mapped by the dye.[21-26] Other probe solutes have been used to evaluate the hydrogen bond donor properties by means of UV-visible spectroscopy or by ^{13}C or ^{31}P nuclear magnetic resonance (NMR),[27] but all have shown dependences on others solvent properties.[13] More importantly, the absorption spectrum of the Reichardt's dye in concentrated salt solutions is extremely diffuse,[28, 29] while this dye is almost insoluble in water and aqueous salt solutions, precluding its use in the characterization of aqueous solutions of ILs or in the characterization of the coexisting phases of IL-based ABS.

To overcome some of the aforementioned problems, pyridine-*N*-oxide (PyO, **Figure 3.25**) was proposed as an alternative probe based on the replacement of the methoxyl group of 4-nitroanisole by a hydrogen-bond acceptor group.[30] However, the solvatochromic effect observed

(283-254 nm) falls within the absorption region of many solvents, including some ILs, thus detracting a widespread spectroscopic utility of this probe. A more adequate solution was further proposed using the same dye as a probe to characterize the hydrogen-bond acidity of 26 molecular solvents, yet through ^{13}C NMR chemical shifts measurements.[31] Schneider et al.[31] determined the α values of 26 molecular solvents by the ^{13}C chemical shifts of PyO according to the following equations:

$$\alpha_{24} = 2.32 - 0.15 \times d_{24} \quad \textbf{(3.27)}$$

$$\alpha_{34} = 0.40 - 0.16 \times d_{34} \quad \textbf{(3.28)}$$

where α is the KT hydrogen bond donating ability of the solvent, d_{24} and d_{34} are the differences (in ppm) of the ^{13}C NMR chemical shifts, δ, of carbons 2 and 3, respectively, with respect to that of carbon 4 of PyO (*cf.* **Figure 3.25** with the carbons number identification). According to Marcus,[27] the standard deviation of the α values obtained by Schneider *et al.*[31] are estimated to be 0.07, while their dependence on other solvent properties, such as π^* or β, are negligible. Based on this possibility, in the present work, we explored the applicability of this probe/method for the determination of the α parameter of ILs and of their aqueous solutions, being the aqueous solutions particularly relevant since they could not be widely characterized by the common Reichardt's dye probe, as previously highlighted.

3.4.3. Experimental procedures

Materials. The following ILs were investigated in what concerns the determination of the hydrogen-bond acidity of pure compounds: 1-alkyl-3-methylimidazolium bis(trifluoromethylsulfonyl)imide ([$C_nC_1$im][NTf_2], with *n* = 1, 3, 4 6 and 8, all 99 wt % pure), 1-butyl-3-methylimidazolium trifluoromethanesulfonate ([C_4C_1im][CF_3SO_3], 99 wt % pure), 1-butyl-3-methylimidazolium tetrafluoroborate ([C_4C_1im][BF_4], 99 wt % pure), 1-butyl-3-methylimidazolium dicyanamide ([C_4C_1im][$N(CN)_2$], 98 wt % pure), 1-butyl-3-methylimidazolium hexafluorophosphate ([C_4C_1im][PF_6], 99 wt % pure), 1-butyl-3-methyl-imidazolium thiocyanate ([C_4C_1im][SCN], 98 wt % pure), 1-butyl-3-methylimidazolium acetate ([C_4C_1im][CH_3CO_2], 98 wt % pure), 1-butyl-1-methylpiperidinium bis(trifluoromethylsulfonyl)imide ([C_4C_1pip][NTf_2], 99 wt % pure), 1-butyl-1-methyl-pyrrolidinium bis(trifluoromethylsulfonyl)imide ([C_4C_1pyr][NTf_2], 99 wt %), 1-propyl-3-methylpyridinium bis(trifluoromethylsulfonyl)imide ([C_3C_1py][NTf_2], 98 wt % pure), and trihexyltetradecylphosphonium bis(trifluoromethylsulfonyl)imide ([$P_{666,14}$][NTf_2], 98 wt % pure).

The hydrogen-bond acidity was determined for aqueous solutions of the following ILs at different concentrations: 1-alkyl-3-methylimidazolium chloride ([$C_nC_1$im]Cl, with *n* = 4 and 6, 99 wt % and 98 wt % pure, respectively), tetrabutylammonium chloride ([N_{4444}]Cl, 97 wt % pure); cholinium chloride ([$N_{111(2OH)}$]Cl, 98 wt % pure), 1-butyl-1-methylpyrrolidinium chloride ([C_4C_1pyr]Cl, 99 wt % pure), 1-butyl-3-methylpyridinium chloride ([C_4C_1py]Cl, 98 wt % pure), [C_4C_1im][CF_3SO_3], [C_4C_1im][$N(CN)_2$], [C_4C_1im][SCN], and [C_4C_1im][CH_3CO_2]. All imidazolium-, pyridinium-, and pyrrolidinium-based ILs were purchased from Iolitec. [$P_{666,14}$][NTf_2] was kindly offered by Cytec, and [N_{4444}]Cl and [$N_{111(2OH)}$]Cl were purchased from Sigma-Aldrich. The chemical structures of cations and anions that composed the studied ILs are presented in **Appendix B.** In order to remove traces of water and volatile compounds, individual samples of each IL were dried at a moderate temperature (*ca*. 323 K) and at high vacuum (ca. 10^{-1} Pa), under constant stirring, and for a minimum period of 48 h, prior to the determination of the hydrogen-bond acidity of each neat IL and prior to the preparation of each aqueous solution. The water content was found to be below 0.1 wt%. IL aqueous mixtures were prepared by weight with an uncertainty of $\pm 10^{-4}$ g. PyO was commercially obtained from Sigma-Aldrich with a purity of 95 %.

NMR measurements. In this work, NMR chemical shifts (δ) were obtained in ppm using a Bruker Avance 300 spectrometer (operating at 300.13 MHz for ^{1}H and 75.47 MHz for ^{13}C NMR). Solutions containing 0.25 mol.dm^{-3} of PyO in each sample aimed to be characterized, and a solution of tetramethylsilane (TMS) in pure deuterated water (99.9% D) as internal standard, were used in NMR tubes adapted with coaxial inserts. The TMS/D_2O solution was always used as the inner part of the concentric tubes, while each sample was used in the outer part of the NMR tube. Using this approach, it is possible to guarantee that the TMS standard and D_2O are not in direct contact with the sample, avoiding thus possible interferences or deviations in the 13C NMR chemical shifts. The standard deviation of α values obtained is estimated to be 0.07. Further details on the NMR experimental procedure and spectra analysis are given in the **Appendix B**.

3.4.4. Results and discussion

Table 3.8 presents the KT parameters for the pure ILs studied in this work. KT parameters for common molecular solvents can be found in **Appendix B**.

Table 3.8. Solvatochromic parameters for the ILs studied in the present work.

IL	α_{24}	α_{34}	α_{RD}[a]	β[a]	π^*[a]
$[C_1C_1im][NTf_2]$	0.58	0.51	0.82	0.20	0.97
$[C_3C_1im][NTf_2]$	0.51	0.44	0.78	0.23	0.96
$[C_4C_1im][NTf_2]$	0.48	0.39	0.69	0.27	0.94
$[C_6C_1im][NTf_2]$	0.50	0.40	0.64	0.27	0.95
$[C_8C_1im][NTf_2]$	0.44	0.37	0.64	0.28	0.94
$[C_4C_1im][CF_3SO_3]$	0.39	0.32	0.62[b]	0.49[b]	1.00[b]
$[C_4C_1im][BF_4]$	0.42	0.33	0.62[b]	0.49[b]	1.00[b]
$[C_4C_1im][N(CN)_2]$	0.39	0.32	0.54[b]	0.60[b]	1.05[b]
$[C_4C_1im][PF_6]$	0.44	0.36	0.68[b]	0.21[b]	1.02[b]
$[C_4C_1im][SCN]$	0.40	0.31	0.43[c,d]	0.71[c,d]	1.06[c,d]
$[C_4C_1im][CH_3CO_2]$	0.25	0.19	0.43[b]	1.20[b]	0.96[b]
$[C_4C_1pip][NTf_2]$	0.36	0.26	0.44	0.26	0.94
$[C_4C_1pyr][NTf_2]$	0.44	0.35	0.47	0.28	0.94
$[C_3C_1py][NTf_2]$	0.79	0.80	0.51	0.26	0.98
$[P_{666,14}][NTf_2]$	0.34	0.27	0.24	0.46	0.86

[a]values taken from ref. 32 unless otherwise indicated; [b]data from ref. 16; [c]data from ref. 33; [d]a different set of dyes was used (see ref. 33)

The analysis of the data illustrated in **Figure 3.26**, which also considers the α values of molecular solvents, shows that α_{24} and α_{34} are strongly correlated according to:

$$\alpha_{24} = 0.061_{\pm 0.009} + 1.01_{\pm 0.02}\alpha_{34} \quad \textbf{(3.29)}$$

(NP = 37; R^2 = 0.992; SD = 0.033; F = 4156)

where NP is the number of experimental points, R is the correlation coefficient, SD the standard deviation, and F is the ratio of variance. It should be noted that acetic acid, benzyl alcohol, and cyclohexane were considered as outliers.[31] As shown, all ILs fit within the given equation which also comprises values for molecular solvents, meaning that the physicochemical information of all solvents (including ILs), *i.e.*, the solvents ranking in terms of hydrogen-bond acidity provided by both scales, is in close agreement. This general correlation that includes both organic solvents and ILs show that electrostatic interactions are not mapped by the current probe.

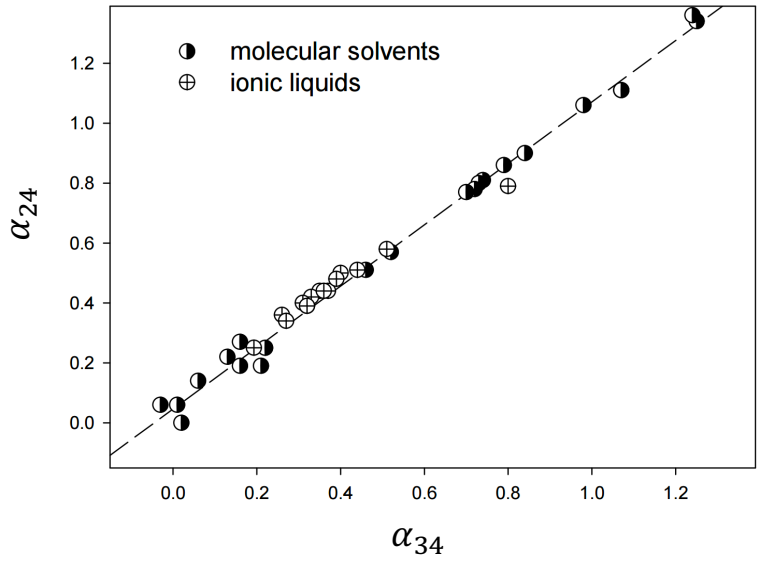

Figure 3.26. Values of α_{24} plotted against the α_{34} values obtained from ^{13}C NMR of PyO: molecular solvents (◑) and ILs (⊕).

The α_{24} values of pure ILs (**Table 3.8**) and molecular solvents (**Appendix B**), determined from the ^{13}C NMR data of PyO, are compared with the data obtained with the Reichardt's dye (α_{RD}) in **Figure 3.27**. The straight correlation presented in **Figure 3.27** is given by the following equation,

$$\alpha_{24} = 0.88_{\pm 0.03}\alpha_{RD} \quad \textbf{(3.30)}$$

(NP = 37; SD = 0.1; F = 650; p < 0.0001)

where NP is the number of experimental points, SD the standard deviation, F the ratio of variance and p is the common statistic p-value based on the null hypothesis. The obtained straight correlation supports the suitability of PyO as an alternative probe to characterize the hydrogen-bond donor properties of molecular solvents, as well as of ILs, and that it can be used as an individual probe/method capable of ranking the hydrogen bond acidity of a given set of solvents.

Equation (3.30) allows a backwards calculation and the determination of the widely used $ET_{(30)}$ (or E_T^N) single parameter polarity scales, according to the following equations:

$$ET_{(30)} = (\alpha_{RD} + 2.03 + 0.72\pi^*)/0.0649 \quad \textbf{(3.31)}$$

$$E_T^N = \left(ET_{(30)} - 30.7\right)/32.4 \quad \textbf{(3.32)}$$

The experimental $ET_{(30)}$ values obtained with the Reichardt's dye probe and those calculated with **Equations (3.30)**, **(3.31)**, and **(3.32)** using the PyO probe to obtain the α values are given in **Appendix B** (both for molecular organic solvents and ILs).

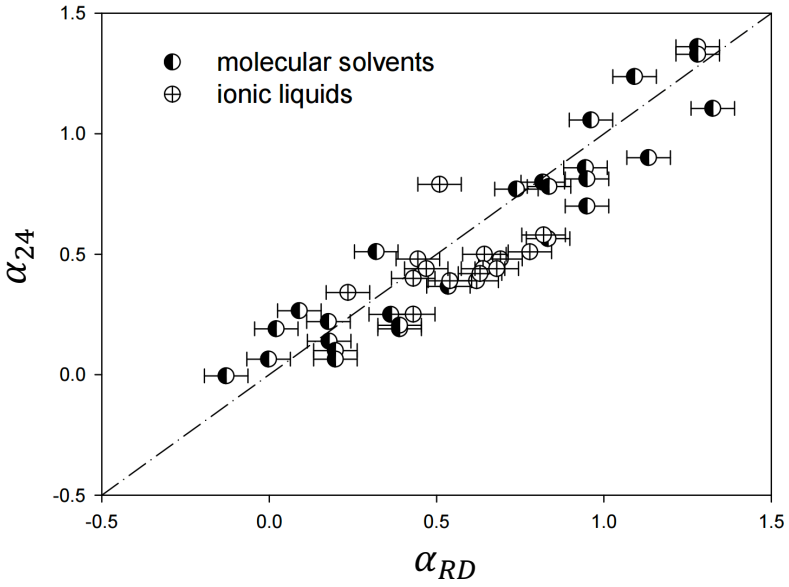

Figure 3.27. Values of α_{24} obtained from ^{13}C NMR chemical shifts deviations of PyO plotted against the α values obtained with the Reichardt's probe (α_{RD}): molecular solvents (◑) and ILs (⊕).

Amongst the three KT solvatochromic parameters, given in **Table 3.8**, the α and β parameters are recognized to cover a wider range of values, being π^* usually less divergent.[16,32,35] The β parameter of the ILs studied in the present work ranges from 0.20 (for $[C_1C_1im][NTf_2]$) up to 1.18 (for $[C_4C_1im][CH_3CO_2]$), π^* varies between 0.89 (for $[C_4C_1im][CH_3CO_2]$) and 1.06 (for $[C_4C_1im][SCN]$), and α_{24} ranges between 0.25 (for $[C_4C_1im][CH_3CO_2]$) and 0.79 (for $[C_3C_1py][NTf_2]$). The hydrogen bond donor strength of an IL is recognized to be dominated by the cation, depending only slightly upon the anion.[16,32,35] This effect was also verified in the current work when evaluating the α values obtained for the $[C_4C_1im]$-based ILs (α_{24} = 0.42 ± 0.03, $[C_4C_1im]^+$ combined with a wide variety of anions, such as $[NTf_2]^-$, $[CF_3SO_3]^-$, $[BF_4]^-$, $[N(CN)_2]^-$, $[PF_6]^-$ and $[SCN]^-$). The only exception was observed with $[C_4C_1im][CH_3CO_2]$ that displays an extremely low α_{24} value, and where similar trends were obtained with the Reichardt's probe.[16,23] The reason behind the low hydrogen-bond acidity of the acetate-based IL is not yet clear, but could have its origin on the strong hydrogen bond interactions occurring between the imidazolium cation and the acetate anion, as a result of this anion high hydrogen bond basicity, reducing consequently the α value. On the other hand, the hydrogen-bond acidity of imidazolium-based ILs, as measured with the PyO probe, decreases with the increase in the number of carbon atoms at the alkyl side

chains, in agreement with the literature data obtained with different probes/methods.[32,33,36,37] For the ILs studied sharing the $[NTf_2]^-$ anion, their acidity increases in the order: $[P_{666,14}][NTf_2]$ < $[C_4C_1pip][NTf_2]$ < $[C_4C_1pyr][NTf_2]$ < $[C_4C_1im][NTf_2]$ <$[C_3C_1py][NTf_2]$, as measured by the PyO probe. A slight different acidity ordering is obtained when using the Reichardt's dye, and according to: $[P_{666,14}][NTf_2]$ <$[C_4C_1pip][NTf_2]$ < $[C_4C_1pyr][NTf_2]$ < $[C_3C_1py][NTf_2]$ <$[C_4C_1im][NTf_2]$. It is well-known that the characteristics of hydrogen-bonding (H-bonding) in ILs cover an extremely wide and diverse range. These comprise conventional H-bonding and blue-shifted H-bonding, dihydrogen H-bonding, inverse H-bonding, resonance assisted H-bonding, charge-assisted H-bonding, ionic H-bonding, among others.[38] The sensitivity of chemically distinct solvatochromic- or NMR-based probes are probe-specific, which could thus lead to slightly divergent polarity scales. In particular, PyO has been described to participate in very strong positive/negative charge-assisted H-bonding,[39, 40] which could be the reason behind the differences observed for the ranking on the α values for $[C_3C_1py][NTf_2]$ *vs* $[C_4C_1im][NTf_2]$.

As previously mentioned, the physicochemical properties of ILs can be further tuned by mixing these ionic species with molecular solvents, such as water or ethanol. Nevertheless, the a priori knowledge of the polarity of ILs and their mixtures with other solvents is a crucial requirement for carrying out reactions, as well as separation processes. Despite its relevance, there are however few data in the literature regarding the polarity of IL-water mixtures[41-44] – a major consequence of the Reichardt's dye almost null solubility in aqueous solutions. After addressing the potential of the PyO probe to determine the hydrogen-bond acidity of neat ILs, we further explored its applicability to determine the α parameter of IL-water mixtures. Both IL-water mixtures of partial miscibility (mainly derived from the solid of the ILs appraised state at room temperature, **Figure 3.28**) and complete miscibility (**Figure 3.29**) were studied. All detailed data, including some examples of the obtained NMR spectra, are presented in the **Appendix B**.

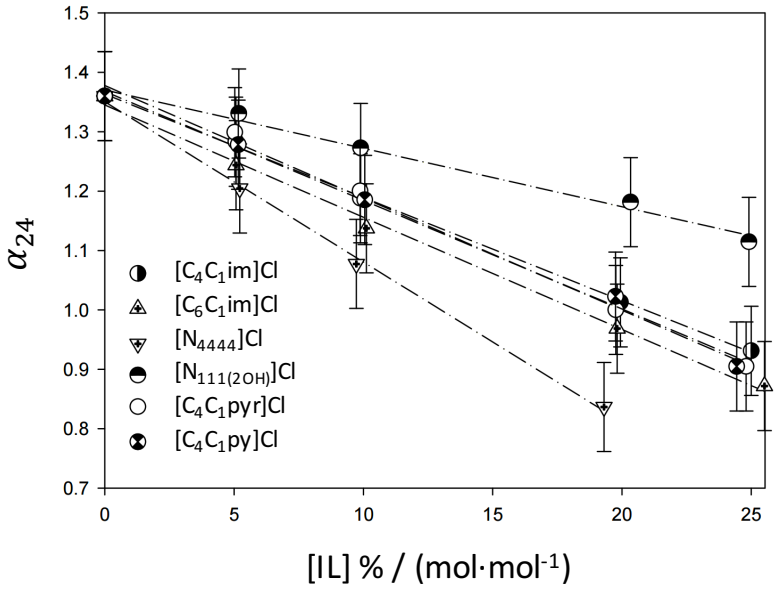

Figure 3.28. α_{24} values for partially miscible IL-water mixtures as a function of the IL concentration.

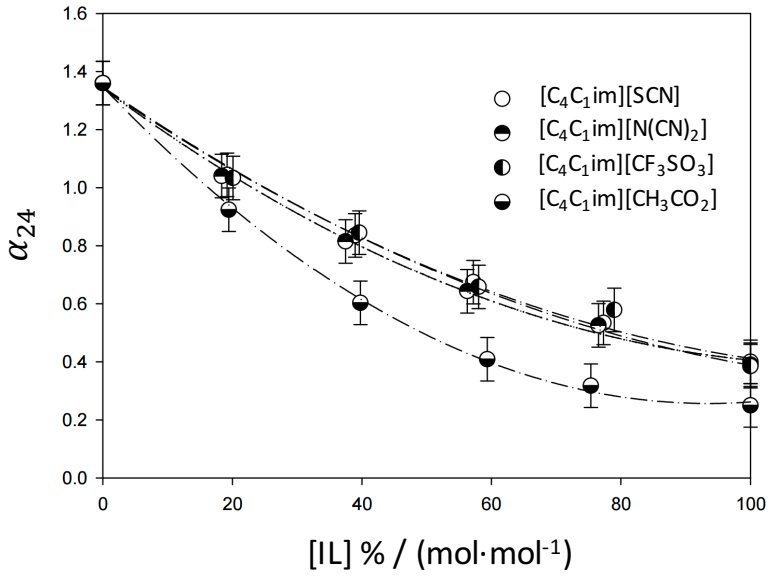

Figure 3.29. α_{24} values for the completely miscible IL-water mixtures as a function of the IL concentration.

For all studied IL-water mixtures, the hydrogen-bond acidity decreases as a function of the IL concentration, meaning that water has a higher ability to donate protons than aqueous solutions of ILs. In both sets appraised, the hydrogen bond acidity of IL aqueous solutions follows the ILs ranking discussed above. For instance, at a fixed concentration of IL, aqueous solutions of $[N_{4444}]Cl$ display a lower ability to donate protons than aqueous solutions of $[N_{111(2OH)}]Cl$ – an expected trend given the more hydrophobic character of $[N_{4444}]Cl$, afforded by the four butyl chains attached to the nitrogen central atom, when compared to the more hydrophilic $[N_{111(2OH)}]Cl$,

composed of shorter aliphatic moieties and an extra –OH group. For the first set of IL-water mixtures (**Figure 3.28**), where concentrations up to 25 % of IL (in mole fraction) were investigated, there is a linear correlation between the hydrogen bond donor acidity and the IL concentration. On the other hand, for the second set of IL water mixtures (**Figure 3.29**) investigated, an almost ideal behavior is observed for the $[C_4C_1im][SCN]$-, $[C_4C_1im][N(CN)_2]$- and $[C_4C_1im][CF_3SO_3]$-water mixtures, whereas for the $[C_4C_1im][CH_3CO_2]$-water mixture a non-ideal behavior is perceived. Khupse and Kumar[41] also observed a non-linear behavior of the α parameter (measured with the Reichardt's dye) in binary water-IL mixtures composed of $[BF_4]$-based ILs and interpreted the results based on preferential solvation models, in which the deviations from the ideal behavior result from a different tendency of the probe to be solvated by the several solvents. However, it should be highlighted that no such extreme non-ideal behavior, as reported by these authors,[41] was here observed. This suggests that the probe used in this work could be better solvated by IL-water mixtures, further confirming the applicability of PyO to determine the hydrogen-bond donor properties of ILs and of IL aqueous solutions.

Ultimately, the practical outcome of a polarity scale is to explain or predict solvent effects on diverse types of physicochemical phenomena. In this regard, we used the hydrogen-bond acidity data obtained in the current work for aqueous solutions of ILs along with data of phase equilibria of ternary IL-water-salt mixtures reported in the literature[7,45-47] to obtain new insights on the molecular-level phenomena ruling the phase splitting of IL-salt ABS. A strong correlation between the α values of the IL-water mixtures and the ability of each IL to create ABS was observed, as depicted in **Figure 3.30**. All the ILs presented in **Figure 3.30** share the same chloride anion. The effect of the IL anion was not considered in this type of correlations since the studied $[C_4C_1im]$-based ILs, all have, with the exception of $[C_4C_1im][CH_3CO_2]$, and within the experimental uncertainty, the same α_{24} value. This is a main result of the hydrogen-bond acidity being governed by the IL cation as discussed before. The capability of each IL to create ABS was addressed by the IL/salt concentrations required to form two aqueous phases, *i.e.* by taking the values at each binodal curve in which the concentration of IL ([IL], in $mol \cdot kg^{-1}$) is equal to the concentration of the salt ([salt], in $mol \cdot kg^{-1}$). Two salts (K_3PO_4 and $K_3C_6H_5O_7$) that are able to form ABS with a large variety of ILs[7, 45-47] were used here as main examples. The α values presented in **Figure 3.30** correspond to an IL concentration of 20 % (in mole fraction). It should be mentioned however that similar correlations are obtained for different IL-water compositions, as would be expected from the almost linear behavior of the α values of IL-water mixtures illustrated in **Figure 3.28** and **Figure 3.29**.

The results illustrated in **Figure 3.30** reveal that the closer is the α_{24} value of the IL-water mixture to that of water (1.36) or the higher the ability of a given IL-water mixture to donate protons, which further translates into a higher affinity of a given IL for water, the larger is the value of the respective binodal curve or the larger is the amount of IL and salt required to create an ABS. In an ABS, IL and salt ions compete for water molecules, being well-accepted that this type of systems is formed due to the salting-out ability of the salt over the IL in aqueous media.[7,45-47] For the ILs evaluated, the immiscibility region in ABS decreases according to the series: $[N_{4444}]Cl$ > $[C_6C_1im]Cl$ > $[C_4C_1pyr]Cl$ > $[C_4C_1im]Cl$, regardless of the salt,[7,45-47] and thus the systems formed by $[N_{4444}]Cl$ require a lower amount of salt to undergo liquid-liquid demixing, whereas the opposite is observed with $[C_4C_1im]Cl$. In summary, the correlations shown in **Figure 3.30** reveal that the higher the hydrogen-bond acidity of a given IL-water mixture (which ranks the IL in terms of affinity for water) the more difficult it is to create an ABS, confirming thus the usefulness of hydrogen-bond acidity data to predict the ability of ILs to create aqueous two-phase systems.

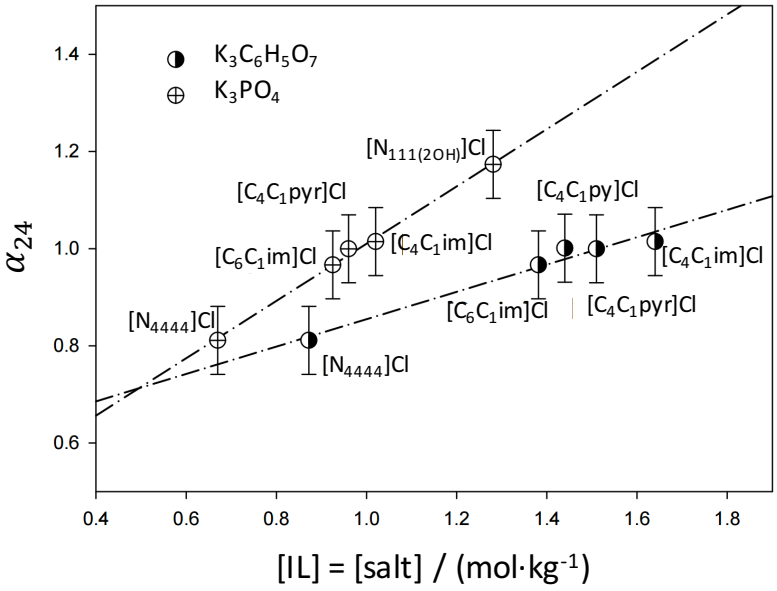

Figure 3.30. α_{24} values for IL-water mixtures (chloride-based ILs) versus the capability of each IL to create ABS (addressed by the values at each binodal curve in which the concentration of IL is equal to the concentration of salt in molality).

3.4.5. Conclusions

In this work we demonstrated that the differences of the ^{13}C NMR chemical shifts of carbon 2 (or 3), with respect to that of carbon 4, of PyO can be used to determine the hydrogen bond acidity or hydrogen bond donation ability of neat ILs and of their aqueous solutions. Furthermore,

this approach to obtain the α values does not require the determination of other solvent properties, such as π^* or β. Compared to the current available scales, a wider scale for the hydrogen-bond acidity of ILs and of their aqueous solutions can be established with the PyO probe and ^{13}C NMR analysis. Taking into account the utility of polarity scales to predict other physicochemical phenomena, it was here demonstrated that the hydrogen bond acidity of aqueous solutions of ILs closely correlates with the ILs ability to create ABS or to be salted-out by conventional salts in aqueous ternary mixtures.

3.4.6. References

(1) J. P. Hallett and T. Welton, *Chem. Rev.*, 2011, **111**, 3508−3576;
(2) Y. Chauvin, L. Mussmann, and H. Olivier, *Angew. Chem. Int. Ed.*, 1995, **34**, 2698−2700;
(3) A. J. Carmichael, D. M. Haddleton, S. A. F. Bon, and K. R. Seddon, *Chem. Commun.*, 2000, 1237−1238;
(4) M. G. Freire, A. F. M. Cláudio, J. M. M. Araújo, J. A. P. Coutinho, I. M. Marrucho, J. N. C. Lopes, and L. P. N. Rebelo, *Chem. Soc. Rev.*, 2012, **41**, 4966−4995;
(5) Y. Kohno and H. Ohno, *Chem. Commun.*, 2012, **48**, 7119−7130;
(6) F. J. Deive, A. Rodríguez, A. B. Pereiro, J. M. M. Araújo, M. A. Longo, M. A. Z. Coelho, J. N. C. Lopes, J. M. S. S. Esperança, L. P. N. Rebelo, and I. M. Marrucho, *Green Chem.*, 2011, **13**, 390−396;
(7) H. Passos, A. R. Ferreira, A. F. M. Cláudio, J. A. P. Coutinho, and M. G. Freire, *Biochem. Eng. J.*, 2012, **67**, 68−76;
(8) T. Welton, *Chem. Rev.*, 1999, **99**, 2071−2083;
(9) J. G. Huddleston, H. D. Willauer, R. P. Swatloski, A. E. Visser, and R. D. Rogers, *Chem. Commun.*, 1998, 1765−1766;
(10) A. E. Visser, R. P. Swatloski, and R. D. Rogers, *Green Chem.*, 2000, **2**, 1−4;
(11) C. Reichardt and T. Welton, *Solvents and Solvent Effects in Organic Chemistry: Fourth Edition*, 2010;
(12) M. J. Kamlet and R. W. Taft, *J. Am. Chem. Soc.*, 1976, **98**, 377−383;
(13) R. W. Taft and M. J. Kamlet, *J. Am. Chem. Soc.*, 1976, **98**, 2886−2894;
(14) M. J. Kamlet, J. L. Abboud, and R. W. Taft, *J. Am. Chem. Soc.*, 1977, **99**, 6027−6038;
(15) M. J. Kamlet, J. L. M. Abboud, M. H. Abraham, and R. W. Taft, *J. Org. Chem.*, 1983, **48**, 2877−2887;
(16) M. A. Ab Rani, A. Brant, L. Crowhurst, A. Dolan, M. Lui, N. H. Hassan, J. P. Hallett, P. A. Hunt, H. Niedermeyer, J. M. Perez-Arlandis, M. Schrems, T. Welton, and R. Wilding, *Phys. Chem. Chem. Phys.*, 2011, **13**, 16831−16840;
(17) K. Dimroth, C. Reichardt, T. Siepmann and F. Bohlmann, *Justus Liebigs Annalen der Chemie*, 1963, **661**, 1−37;
(18) C. Reichardt, *Angew. Chem. Int. Ed.*, 1965, **4**, 29−40;
(19) F. W. Fowler, A. R. Katritzky, and R. J. D. Rutherford, *J. Chem. Soc. B: Phys. Org.*, 1971, 460−469;
(20) Y. Marcus, *J. Solution Chem.*, 1991, **20**, 929−944;
(21) H. Weingärtner, *Angew. Chem. Int. Ed.*, 2008, **47**, 654−670;
(22) V. Znamenskiy and M. N. Kobrak, *J. Phys. Chem. B*, 2004, **108**, 1072−1079;
(23) A. F. M. Cláudio, L. Swift, J. P. Hallett, T. Welton, J. A. P. Coutinho, and M. G. Freire, *Phys. Chem. Chem. Phys.*, 2014, **16**, 6593−6601;
(24) L. Crowhurst, P. R. Mawdsley, J. M. Perez-Arlandis, P. A. Salter, and T. Welton, *Phys. Chem. Chem. Phys.*, 2003, **5**, 2790−2794;

(25) S. Zhang, Z. Chen, X. Qi, and Y. Deng, *New J. Chem.*, 2012, **36**, 1043−1050;
(26) C. Chiappe and C. S. Pomelli, *Theor. Chem. Acc.*, 2012, **131**, 1−7;
(27) Y. Marcus, *Chem. Soc. Rev.*, 1993, **22**, 409−416;
(28) L. A. Ferreira, P. Parpot, J. A. Teixeira, L. M. Mikheeva and B. Y. Zaslavsky, *J. Chromatogr. A*, 2012, **1220**, 14−20;
(29) T. V. Doherty, M. Mora-Pale, S. E. Foley, R. J. Linhardt, and J. S. Dordick, *Green Chem.*, 2010, **12**, 1967−1975;
(30) E. I. Vorkunova and Y. A. Levin, *Zh. Obshch. Khim*, 1984, **54**, 1349−1352;
(31) H. Schneider, Y. Badrieh, Y. Migron and Y. Marcus, *Z. Phys. Chem.*, 1992, **177**, 143−156;
(32) K. A. Kurnia, F. Lima, A. F. M. Cláudio, J. A. P. Coutinho and M. G. Freire, *Phys. Chem. Chem. Phys.*, 2015, **17**, 18980−18990;
(33) S. Spange, R. Lungwitz and A. Schade, *J. Mol. Liq.*, 2014, **192**, 137−143;
(34) V. Balevicius, Z. Gdaniec and K. Aidas, *Phys. Chem. Chem. Phys.*, 2009, **11**, 8592–8600;
(35) P. G. Jessop, D. A. Jessop, D. Fu and L. Phan, *Green Chem.*, 2012, **14**, 1245−1259;
(36) V. Strehmel, R. Lungwitz, H. Rexhausen and S. Spange, *New J. Chem.*, 2010, **34**, 2125−2131;
(37) H. Tokuda, S. Tsuzuki, M. A. B. H. Susan, K. Hayamizu and M. Watanabe, *J. Phys. Chem. B*, 2006, **110**, 19593−19600;
(38) P. A. Hunt, C. R. Ashworth and R. P. Matthews, *Chem. Soc. Rev.*, 2015, **44**, 1257−1288;
(39) L. Goliç, D. Hadţi and F. Lazarini, *J. Chem. Soc. D*, 1971, 860a-860a;
(40) P. Gilli, V. Bertolasi, L. Pretto, V. Ferretti, and G. Gilli, *J. Am. Chem. Soc.*, 2004, **126**, 3845−3855;
(41) N. D. Khupse and A. Kumar, *Journal of Physical Chemistry B*, 2011, **115**, 711−718;
(42) A. Sarkar and S. Pandey, *J. Chem. Eng. Data*, 2006, **51**, 2051−2055;
(43) M. Ali, A. Sarkar, M. Tariq, A. Ali and S. Pandey, *Green Chem.*, 2007, **9**, 1252−1258;
(44) A. Sarkar, M. Ali, G. A. Baker, S. Y. Tetin, Q. Ruan and S. Pandey, *J. Phys. Chem. B*, 2009, **113**, 3088−3098;
(45) S. P. M. Ventura, C. M. S. S. Neves, M. G. Freire, I. M. Marrucho, J. Oliveira and J. A. P. Coutinho, *J. Phys Chem. B*, 2009, **113**, 9304−9310;
(46) H. Passos, A. C. A. Sousa, M. R. Pastorinho, A. J. A. Nogueira, L. P. N. Rebelo, J. A. P. Coutinho and M. G. Freire, *Anal. Methods*, 2012, **4**, 2664−2667;
(47) S. Shahriari, C. M. S. S. Neves, M. G. Freire and J. A. P. Coutinho, *J. Phys. Chem. B*, 2012, **116**, 7252−7258.

3.5. Which factors drive the solutes partition in ionic-liquid-based aqueous biphasic systems?

This chapter is based on the manuscript under preparation

Helena Passos, Teresa B. V. Dinis, Emanuel V. Capela, Pedro P. Madeira, Mara G. Freire and João A. P. Coutinho;[1] "Which factors drive the solutes partition in ionic-liquid-based aqueous biphasic systems?", 2017.

3.5.1. Abstract

Aqueous biphasic systems (ABS) composed of ionic liquids (ILs) have been successfully used in the extraction and purification of a large range of biocompounds. However, the widespread use of ABS at an industrial level has been limited by a poor understanding of the mechanisms which rule the partition of the biomolecules between the phases, which thus limits the ability to design ABS for a specific application and converts the development of a novel ABS-based separation on a trial and error process. In this work, a physicochemical characterization of several IL-based ABS was performed. The differences between the properties of the phases of ABS composed of various imidazolium-based ILs, two different salts – Na_2SO_4 and K_2CO_3 – and water were investigated. The Gibbs free energy of transfer of a methylene group between the phases in equilibrium, $\Delta G(CH_2)$, were estimated from the partition of an homologous series of dinitrophenylated amino acids in the studied ABS. The solvatochromic parameters of the coexisting phases, namely the dipolarity/polarizability (π^*), hydrogen-bonding donor acidity (α) and hydrogen-bonding acceptor basicity (β), were also measured using adequate probes.

3.5.2. Introduction

Aqueous biphasic systems (ABS) are used in liquid-liquid extraction processes suitable for biomolecules since they consist of two immiscible aqueous phases that can be formed by the mixture of two polymers, a polymer with a salt or two salts dissolved in aqueous media.[1–3] Besides these common ABS, in 2003 Rogers and co-workers[4] demonstrated that ABS could also be created by mixing ionic liquids (ILs) and inorganic salts. IL-based ABS present additional advantages when compared with polymer-based ABS, namely a lower viscosity, quick phase separation and higher extraction efficiencies for a wide range of biomolecules. After a decade of studies, IL-based ABS

[1]**Contributions:** M.G.F. and J.A.P.C. conceived and directed this work. H.P., T.B.V.D. and E.V.C. acquired the experimental data. H.P., P.M. and J.A.P.C. interpreted the experimental data and wrote this manuscript.

are nowadays considered one of the most promising media for application in the extraction and separation of a broad range of biocompounds.[5]

As a technology ABS present several advantages, namely an easy scale-up, high capacity and low cost. Their application to the large-scale recovery and purification of biological compounds was already demonstrated.[1–3,6,7] However, the use of ABS at an industrial level has been plagued by a poor understanding of the mechanisms which rule the partition of the biomolecules between the phases, limiting the ability to design ABS for a specific application, and converting the development of a novel ABS-based separation on a trial and error process. With the purpose of improving the understanding of the partition of biomolecules in ABS, several works reporting insights on the physicochemical characterization of the partition of biomolecules in ABS composed of polymer/polymer and polymer/salt have been carried out.[8–15] It seems clear that the distribution of compounds in these ABS is ruled by the differences in the solute-solvent interactions occurring in the coexisting phases.[8]

Amongst the approaches available for the ABS physicochemical characterization in terms of solvation ability, the Gibbs free energy of transfer of a methylene group between the phases and the Kamlet-Taft Linear Solvation Energy Relationship (LSER) have been successfully used for the description of solute partition in ABS composed of polymers and salts.[3,4,8–18] The relative hydrophobicity of the coexisting phases in ABS has been shown[3,4,16–18] to be an important factor controlling the molecules partition. This property can be assessed through the analysis of the partition of an homologous series of compounds with aliphatic alkyl side-chains of increasing length. The logarithm of the partition coefficient is linearly dependent on the equivalent number of methylene groups in the alkyl side-chain, $n(CH_2)$, as described in **Equation (3.33)**.

$$\ln(K) = C + E \cdot n(CH_2) \qquad \textbf{(3.33)}$$

The parameters C and E are characteristic constants for a given ABS. The C is the partition of the non-alkyl moiety of the molecule, and has been suggested to represent the difference in the polar/electrostatic properties of the phases, if dinitrophenyl-amino acids (DNP-amino-acids) are used. E is related with the Gibbs free energy of transfer of a methylene group between the phases in equilibrium, $\Delta G(CH_2)$, and has been suggested to be a measure of the relative hydrophobicity of the phases, given by the following equation:[3]

$$\Delta G(CH_2) = -RTE \qquad \textbf{(3.34)}$$

where R is the universal gas constant and T the absolute temperature. $\Delta G(CH_2)$ has also been suggested to be a measure of the free energy for cavity formation.[13]

Although the $\Delta G(CH_2)$ was found to be useful for the characterization of polymer/polymer-[11–13] and polymer/salt-based ABS[15], the assessment of this parameter depends on the ability to measure the partition coefficient of a homologous series of compounds, which may be very difficult when these molecules present a high affinity for one of the phases and the partition coefficients are extreme.[18]

Polarity is the most widely used approach for solvents characterization and is defined as the sum of all possible specific and non-specific interactions between a solvent and a solute, without considering the interactions associated to solute chemical transformations.[19,20] Since it is impossible to describe the multiple possible solute-solvent interactions using a single parameter, Kamlet and Taft proposed a multiparametric approach which is based on the use of a set of solvatochromic probes, allowing the assessment of different interactions for the same solvent,[21–23] such as dipolarity/polarizability (π^*), hydrogen bond donor (α), and hydrogen bond acceptor (β) ability. These properties allow the development of correlations for the description of a variety of properties using the LSER model[21–23] given by the following equation:

$$(XYZ) = (XYZ)_0 + s\pi^* + a\alpha + b\beta \qquad \textbf{(3.35)}$$

where (XYZ) is the value for a particular solvent-dependent property, $(XYZ)_0$ is the value for the reference system, and s, a, and b are the solute-dependent coefficients characterizing the respective influence of π^*, α and β terms on the (XYZ) property under study.[21–23] There are several examples of the successful application of this approach to correlate the properties of solvents and solvent mixtures, such as the phases of an ABS.[8–14]

Despite previous efforts concerning the physicochemical characterization of polymer/polymer and polymer/salt ABS by the determination of solvatochromic parameters and relative hydrophobicity of the coexisting phases,[8–10,14,15] their application to IL-based ABS has been very limited and hampered by experimental difficulties as discussed below.[18,24–26] Although nowadays a large database is available for π^*, α, and β for pure ILs,[20,27–29] no solvatochromic parameters for the IL-based ABS phases are available and only relative hydrophobicities for a small number of systems have been reported.[18,24–26] However, due the increased interest in the use of IL-based ABS in the extraction, separation and purification of biomolecules[5] this information is of high relevance to understand the mechanisms which rule the ABS formation and the solute partition in these systems. With this purpose, the properties of ABS composed of imidazolium-based IL, two

different salts – K_2CO_3 and Na_2SO_4 – and water, at 298 K were characterized in this work. Different probes were used to assess the solvatochromic parameters dipolarity/polarizability, hydrogen-bond donor acidity, and hydrogen-bond acceptor basicity of the coexisting phases of ABS. Partition coefficients of a series of DNP-amino-acids were determined to infer on the relative hydrophobicity and electrostatic properties of the coexisting phases and to allow a comparison between the results obtained by the two approaches. The ILs investigated were selected to allow the study of the IL anion impact on the properties of the IL-based ABS.

3.5.3. Experimental procedures

Materials. ABS composed of ILs and the salts K_2CO_3 (99 wt % pure from Sigma-Aldrich) or Na_2SO_4 (99.82 wt % pure from José Manuel Gomes dos Santos, LDA) were studied. The following ILs were used: 1-butyl-3-methylimidazolium trifluoromethanesulfonate, $[C_4C_1im][CF_3SO_3]$ (99 wt %), 1-butyl-3-methylimidazolium thiocyanate, $[C_4C_1im][SCN]$ (>98 wt %), 1-butyl-3-methylimidazolium tosylate, $[C_4C_1im][TOS]$ (99 wt %), 1-butyl-3-methylimidazolium dicyanamide, $[C_4C_1im][N(CN)_2]$ (>98 wt %) 1-butyl-3-methylimidazolium ethylsulfate, $[C_4C_1im][C_2H_5SO_4]$ (98 wt %), 1-butyl-3-methylimidazolium methylsulfate, $[C_4C_1im][CH_3SO_4]$ (99 wt %), 1-butyl-3-methylimidazolium bromide, $[C_4C_1im]Br$ (99 wt %), 1-butyl-3-methylimidazolium dimethylphosphate, $[C_4C_1im][DMP]$ (>98 wt %), 1-butyl-3-methylimidazolium methylacetate, $[C_4C_1im][CH_3CO_2]$ (>98 wt %), 1-butyl-3-methylimidazolium methanesulfonate, $[C_4C_1im][CH_3SO_3]$ (98 wt %), and 1-butyl-3-methylimidazolium chloride, $[C_4C_1im]Cl$ (99 wt %) from Iolitec and 1-butyl-3-methylimidazolium octylsulfate, $[C_4C_1im][C_8H_{17}SO_4]$ (>95 wt %) from Aldrich. To reduce the water and volatile compounds content to negligible values, ILs individual samples were dried under constant stirring at vacuum and moderate temperature (≈ 323 K) for a minimum of 48 h. After this step, the purity of each IL was checked by ^1H and ^{13}C NMR spectra and found to be in accordance with the purity given by the suppliers. Phosphate buffered saline (PBS) tablets from Sigma were used to buffer the aqueous solutions used in Na_2SO_4-based ABS preparation at a pH of 7.4. Four different dinitrophenylated (DNP) amino acids were used in the Gibbs free energy determination: *N*-(2,4-dinitrophenyl)glycine (≥98 wt % pure) and *N*-(2,4-dinitrophenyl)-L-valine (>98 wt % pure) were obtained from Sigma-Aldrich, while *N*-(2,4-dinitrophenyl)-L-alanine (>98 wt % pure) and *N*-(2,4-dinitrophenyl)-L-leucine (>99 wt % pure) were supplied from Tokyo Chemical Industry (TLC). The solvatochromic probes *N*,*N*-diethyl-4-nitroaniline, 99 % of purity from Fluorochem, 4-nitroaniline, 99 % of purity from Aldrich, and pyridine-*N*-oxide 95 % of purity from

Aldrich were also used. The water used was ultra-pure water, double distilled, passed by a reverse osmosis system and further treated with a Mili-Q plus 185 water purification apparatus.

Phase diagrams and tie-lines. The limit between the monophasic and biphasic regions for the studied systems was determined through the cloud point titration method at (298 ± 1) K and atmospheric pressure. Aqueous solutions of K_2CO_3 at 50 wt % or Na_2SO_4 at 20 wt % and aqueous solutions of the different [C_4C_1im]-based ILs at variable concentrations were prepared gravimetrically (≈10^{-4} g) and used for the determination of the respective binodal curves. In the preparation of solutions used in the determination Na_2SO_4-based ABS binodal curves a PBS solution was used instead of pure water, to control the pH of the systems and fix it at values close to 7. No pH control was carried out for K_2CO_3-based ABS. Repetitive drop-wise addition of the salt solution to each IL aqueous solution was carried out until the detection of a cloudy mixture. Then, repetitive drop-wise of double distilled water was added until the detection of a clear and limpid mixture. Drop-wise additions were performed under constant stirring. The ternary system compositions corresponding to the description of the phase diagrams were determined by weight quantification of all components added to the mixture within ± 10^{-4} g.

The tie-lines (TLs) were determined by a gravimetric method originally described by Merchuk et al.[30], as described in **chapter 2.1**. A mixture composition at the biphasic region was gravimetrically prepared, vigorously stirred, and allowed to reach the equilibrium by the separation of the phases for at least 12 h at (298 ± 1) K. After the separation step, both top and bottom phases were weighted.

The experimental binodal curves were fitted according to **Equation (2.1)** presented in **chapter 2.1**. The obtained results are provided in the **Appendix B**. For the determination of TLs, it was applied the lever-arm using **Equations (2.2)** to **(2.5).** However, for a better approximation of the real composition of TLs, it was defined that the result of lever-arm rule must meet a set of premises (**Equations (3.36)** to **(3.38)**), namely:

$$w(IL)_M = \frac{w_{IL} \times [IL]_{IL}}{100} + \frac{w_{salt} \times [IL]_{salt}}{100} \quad \textbf{(3.36)}$$

$$w(salt)_M = \frac{w_{IL} \times [salt]_{IL}}{100} + \frac{w_{salt} \times [salt]_{salt}}{100} \quad \textbf{(3.37)}$$

$$\frac{[salt]_{salt} - [salt]_M}{[salt]_M - [salt]_{IL}} = \frac{w_{IL}}{w_{salt}} \quad \textbf{(3.38)}$$

where the indexes M, IL and $salt$ correspond to the mixture, IL- and salt-rich phases, respectively. $w(IL)_M$ and $w(salt)_M$ are the amounts of IL and salt in the mixture point preparation, while w_{IL} and w_{salt} represent the weight of IL- and salt-rich phases, respectively. The solution of the referred system gives the concentration of IL and salt in the top and bottom phases. The tie-line length (TLL) was calculated using **Equation (2.6)**.

DNP-amino-acids partition coefficients. DNP-amino-acids were prepared in a concentration of 0.2 wt % in a PBS aqueous solution. For each mixture point a total of six replicates were prepared in Eppendorf tubes containing different amounts of DNP-amino-acids stock solutions (0, 20, 40, 60, 80 and 100 µL). The Eppendorf tubes were agitated using an Eppendorf Thermomixer Comfort equipment at 1200 rpm and 298 K during 30 min. To guarantee the complete separation of ABS coexisting phases and DNP-amino-acids partition, the systems were centrifuged at 298 K in a VWR Micro Star 17 microcentrifuge during 30 minutes at 3500 rpm. Finally, samples of IL and salt-rich phases were collected and diluted to further analysis by UV-spectroscopy at 362 nm using a BioTeck Synergy HT microplate reader. The DNP-amino-acids partition coefficients (K_{DNP-AA}) were determined through the slope of the straight line obtained when the absorbances in the top phase are plotted against the absorbances in the bottom phase and considering the dilution factors used.

Solvatochromic parameters determination. The solvatochromic probes *N*,*N*-diethyl-4-nitroaniline (1), 4-nitroaniline (2) and pyridine-*N*-oxide (3) were used to determine the dipolarity/polarizability, π^*, hydrogen-bond acceptor basicity, β, and hydrogen-bond donor acidity, α, in both phases of the ABS studied. For each mixture point a total of three replicates were prepared in Eppendorf tubes. After centrifugation and collection of a sample of each phase of the system, *N*,*N*-diethyl-4-nitroaniline (≈ 0.30 mg), 4-nitroaniline (≈ 0.30 mg) and pyridine-*N*-oxide (0.25 mol·dm^{-3}) were added to the samples. After agitation in a vortex mixer the samples containing the probes *N*,*N*-diethyl-4-nitroaniline and 4-nitroaniline were scanned in a UV-Vis spectrophotometer (BioTeck Synergy HT microplate reader) at 298 K to determine the longest wavelength absorption band of each probe in both phases. The β and π^* solvatochromic parameters were determined by the following equations:

$$\beta = \frac{\left(\Delta\nu^{IL} - \Delta\nu^{cyclohexane}\right)\times 0.76}{\Delta\nu^{DMSO} - \Delta\nu^{cyclohexane}} \quad \textbf{(3.39)}$$

$$\Delta\nu^i = \nu_1^i - \nu_2^i \quad \textbf{(3.40)}$$

$$\pi^* = \frac{\nu_1^{IL} - \nu_1^{cyclohexane}}{\nu_1^{DMSO} - \nu_1^{cyclohexane}} \quad \textbf{(3.41)}$$

where ν_n^i is the experimental wave number in 10^3 cm^{-1} of probe n in the solvent i. The analyses were carried out in triplicate and average standard deviation for each wavelength measured was always bellow 0.5 nm for both probes.

Samples containing the probe pyridine-*N*-oxide were analyzed by ^{13}C nuclear magnetic resonance (NMR) in neat solvent, using a Bruker Avance 300 at 300.13 MHz, with deuterium oxide (D_2O) as solvent and trimethylsilyl propanoic acid (TSP) as the internal reference. The ^{13}C NMR chemicals shifts $\delta(C_i)$ in ppm of the carbons atoms in positions i = 2 and 4 of pyridine-*N*-oxide (formula II) were determined and α was calculated by Equation **(3.42)**.

$$\alpha = 0.15 \times d_{24} + 2.32 \quad \textbf{(3.42)}$$

with $d_{24} = \delta_4 - \delta_2$, $d_{34} = \delta_4 - \delta_3$ and δ_i the chemical shift of pyridine-*N*-oxide carbon i. The analyses were carried out in duplicate and average standard deviations for each chemical shift measured were always bellow 0.02 ppm. The solvatochromic solvent parameters of pure water and pure ILs were also determined using the same probes and procedures for comparison purposes.

COSMO-RS. The IL cation-anion hydrogen-bonding energies (E_{HB}) were calculated using the thermodynamic model COnductor-like Screening MOdel for Real Solvents (COSMO-RS). The standard process of COSMO-RS calculations employed in this chapter, as well as the values of E_{HB}, were previously reported in **chapter 3.2**.

3.5.4. Results and discussion

Phase diagrams. The binodal curves of [C_4C_1im]-based ILs + K_2CO_3 + H_2O ABS without pH control, and [C_4C_1im]-based ILs + Na_2SO_4 + H_2O ABS at pH of 7.4 were determined at (298 ± 1) K and atmospheric pressure. The respective ternary phase diagrams are presented in **Figure 3.31** while the experimental data are reported in the **Appendix B**.

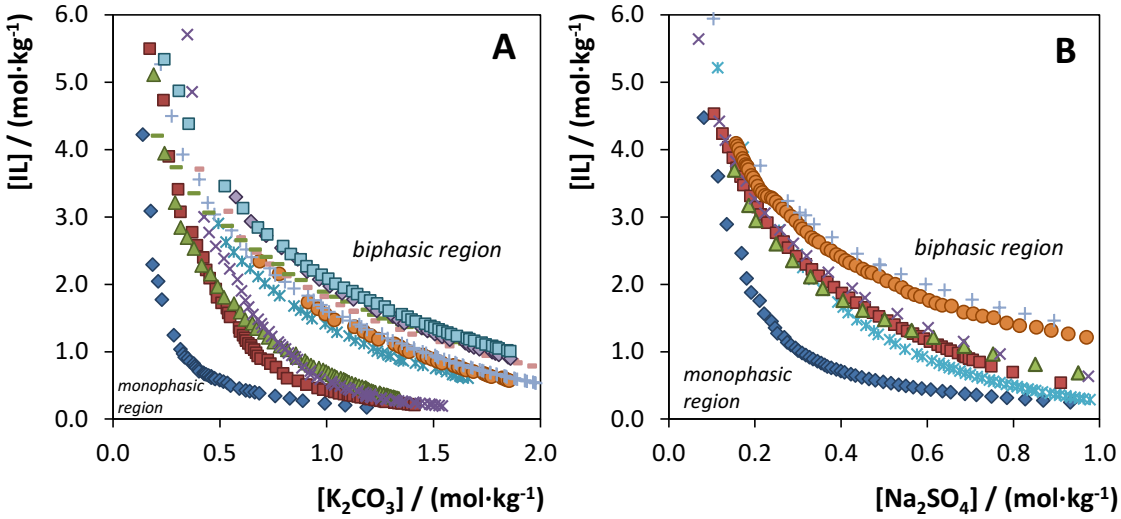

Figure 3.31. Ternary phase diagrams composed of (**A**) $[C_4C_1im]$-based IL + K_2CO_3 + H_2O and (**B**) $[C_4C_1im]$-based IL + Na_2SO_4 + H_2O: $[C_4C_1im][CF_3SO_3]$ (◆); $[C_4C_1im][SCN]$ (■); $[C_4C_1im][TOS]$ (▲); $[C_4C_1im][N(CN)_2]$ (×); $[C_4C_1im][C_2H_5SO_4]$ (✳); $[C_4C_1im][C_8H_{17}SO_4]$ (✱) $[C_4C_1im][CH_3SO_4]$ (●); $[C_4C_1im]Br$ (+); $[C_4C_1im][DMP]$ (-); $[C_4C_1im][CH_3CO_2]$ (–); $[C_4C_1im][CH_3SO_3]$ (◆); and $[C_4C_1im]Cl$ (■).

In **Figure 3.31** the solubility curves are represented in molality units for a better understanding on the impact of the ILs structure in the behavior of the phase diagrams. Since the ILs studied share a common cation, **Figure 3.31** depicts the effect of the IL anion nature on the ABS formation when K_2CO_3 (**Figure 3.31 A**) and Na_2SO_4 (**Figure 3.31 B**) are used. For all ABS reported the biphasic region is located above the binodal curve, and the closer is the binodal to the axis the higher is the capability of the IL to form ABS. Through the analysis of **Figure 3.31 A** and considering the binodal curves points where the IL concentration is equal to that of the salt, also designated as the molality of the IL at saturation solubility, $[IL]_{SS}$, the IL anion ability to form an ABS with K_2CO_3 is as follows: $[CF_3SO_3]^-$ (0.53 mol·kg^{-1}) > $[SCN]^-$ (0.79 mol·kg^{-1}) > $[N(CN)_2]^-$ (0.86 mol·kg^{-1}) ≈ $[TOS]^-$ (0.88 mol·kg^{-1}) >> $[C_2H_5SO_4]^-$ (1.14 mol·kg^{-1}) > $[CH_3SO_4]^-$ (1.21 mol·kg^{-1}) > Br^- (1.24 mol·kg^{-1}) > $[DMP]^-$ (1.31 mol·kg^{-1}) > $[CH_3CO_2]^-$ (1.38 mol·kg^{-1}) > $[CH_3SO_3]^-$ (1.39 mol·kg^{-1}) ≈ Cl^- (1.43 mol·kg^{-1}). Similarly, for Na_2SO_4 the following trend is observed (**Figure 3.31 B**): $[CF_3SO_3]^-$ (0.51 mol·kg^{-1}) > $[C_8H_{17}SO_4]^-$ (0.69 mol·kg^{-1}) > $[SCN]^-$ (0.76 mol·kg^{-1}) > (0.83 mol·kg^{-1}) $[TOS]^-$ ≈ $[N(CN)_2]^-$ (0.83 mol·kg^{-1}) >> $[CH_3SO_4]^-$ (1.06 mol·kg^{-1}) > Br^- (1.13 mol·kg^{-1}). Independently of the salt and pH conditions, the observed trends are in close agreement with previous studies using other inorganic or organic salts.[31–34] In fact, the effect of the ILs anion in ABS formation is well studied in the literature and is related with the ability of the IL anion to hydrogen-bond with water, *i.e.*, IL anions with lower hydrogen bond donor basicity values, β, present a higher ability to form ABS.[35] This relation was previously studied in **chapter 3.2**. It was suggested that a linear dependence

could be observed if $[IL]_{SS}$ is represented as a function of the pure ILs β values. Furthermore, and as previously reported by Cláudio et al.,[35] COSMO-RS[36–39] hydrogen bond energy, E_{HB}, correlate well with the β solvatochromic parameter and, as shown in **chapter 2.2**, it could be used instead of the β values in the development of correlations with this property, allowing to overcome the drawbacks associated to the experimental determination of this parameter. **Figure 3.32** shows the correlation between the IL anions ability to form ABS, here described by $[IL]_{SS}$ binodal points, and the COSMO-RS hydrogen-bonding energies (E_{HB}) of ILs.

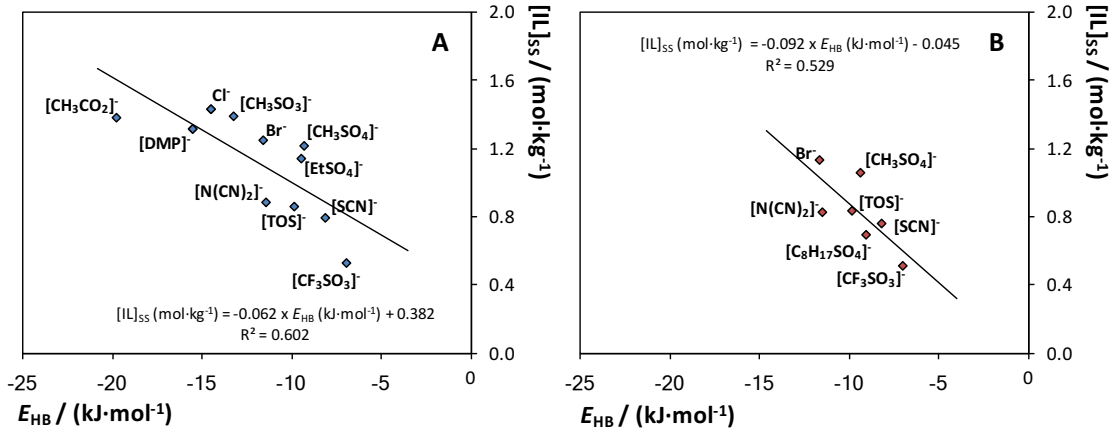

Figure 3.32. Molality of the IL at saturation solubility ($[IL]_{SS}$) as a function of COSMO-RS hydrogen-bonding energies (E_{HB}): **(A)** K_2CO_3-based ABS; **(B)** Na_2SO_4-based ABS.

Several experimental TLs and respective length (TLL) were determined for each ABS. In **Table 3.9** are presented only the TLs that will be used in the following discussion, while the remaining are reported in **Appendix B**.

Table 3.9. Experimental data for TLs and TLLs of [C_4C_1im]-based ILs + salt + H_2O ABS.

IL	Weight fraction composition / wt %						TLL
	$[IL]_{IL}$	$[salt]_{IL}$	$[IL]_{M}$	$[salt]_{M}$	$[IL]_{Salt}$	$[salt]_{salt}$	
IL + K_2CO_3 + H_2O ABS (no pH control)							
[C_4C_1im][CF_3SO_3]	58.32	1.04	37.05	4.40	8.85	9.13	50.13
[C_4C_1im][SCN]	54.83	1.86	27.78	8.77	3.96	14.97	52.91
	45.96	4.19	26.85	10.27	6.29	16.81	41.62
	46.91	3.99	28.34	10.16	4.28	18.16	44.92
[C_4C_1im][TOS]	50.46	3.31	26.85	12.01	1.37	21.40	52.32
	53.31	2.82	28.01	12.21	0.96	22.25	55.85
	55.81	2.43	29.55	12.25	0.67	23.05	58.86
[C_4C_1im][$N(CN)_2$]	60.81	3.04	29.08	10.80	3.01	17.18	59.51
[C_4C_1im]Br	49.87	3.11	26.80	15.50	3.33	28.23	52.89
[C_4C_1im][DMP]	45.32	5.78	23.50	21.59	2.09	37.10	53.38
[C_4C_1im]Cl	43.10	4.46	21.94	19.92	3.11	33.67	49.53
IL + Na_2SO_4 + H_2O ABS (at pH = 7.4)							
[C_4C_1im][CF_3SO_3]	52.55	1.30	35.13	3.93	11.19	7.54	41.82
[C_4C_1im][SCN]	46.37	1.56	34.06	5.00	5.91	12.85	42.01
[C_4C_1im][TOS]	44.35	3.33	32.76	8.00	4.35	19.50	43.14
[C_4C_1im][$N(CN)_2$]	41.68	2.42	31.69	6.40	1.95	18.40	42.82
[C_4C_1im]Br	40.32	4.14	29.73	11.50	6.79	28.01	41.15

Gibbs free energy of methylene transfer between the ABS phases. Using a series of homologues DNP-amino-acids, the Gibbs free energy of transfer of a methylene group, $\Delta G(CH_2)$, from the aqueous salt-rich to the aqueous IL-rich phase was determined for the ABS listed in **Table 3.9**. The DNP-amino-acids partition coefficients are reported in **Appendix B**. **Figure 3.33** displays the relationships experimentally obtained for the logarithm of the partition coefficient of four DNP-amino-acids (K_{DNP-AA}), obtained in K_2CO_3- and Na_2SO_4-based ABS, and the number of equivalent methylene groups in their alkyl-side chain ($n(CH_2)$), which is correlated by **Equation (3.33)**. From this correlation, it was possible to assess the difference of electrostatic properties and relative hydrophobicity of the coexisting phases (parameters C and E, respectively), while the $\Delta G(CH_2)$ was obtained from **Equation (3.34)**. The final results are reported in **Table 3.10**.

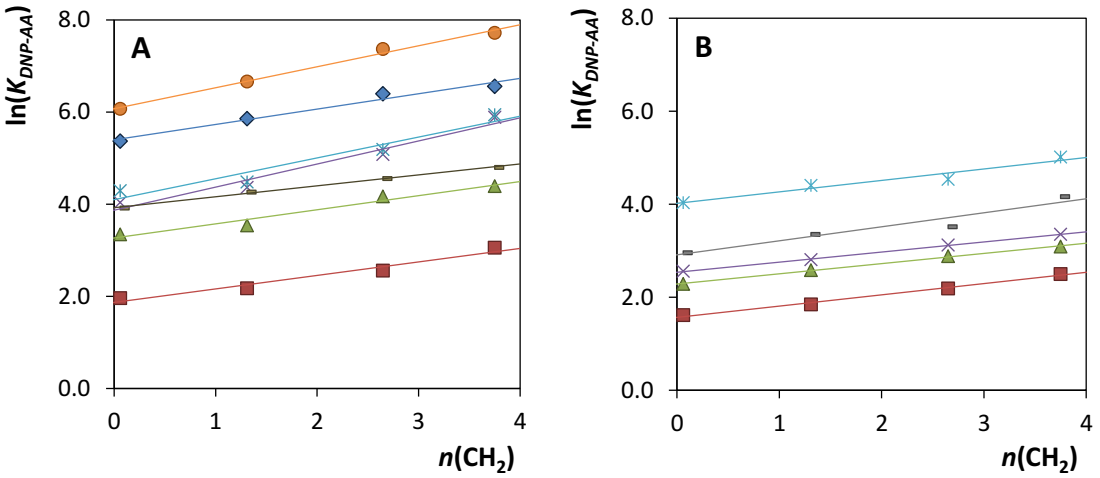

Figure 3.33. Logarithm of partition coefficients for homologous series of DNP-amino-acids in ABS composed of [C_4C_1im]-based ILs and **(A)** K_2CO_3 or **(B)** Na_2SO_4 as a function of the number of equivalent methylene groups, $n(CH)_2$: [C_4C_1im][CF_3SO_3] (■); [C_4C_1im][SCN] (▲); [C_4C_1im][$N(CN)_2$] (×); [C_4C_1im][TOS] (▬); [C_4C_1im]Br (✳); [C_4C_1im]Cl (◆); [C_4C_1im][DMP] (●).

Table 3.10. Parameters C and E (**Equation (3.33)**) and Gibbs free energy of transfer of a methylene group between the coexisting phases, $\Delta G(CH_2)$ (**Equation (3.34)**), in IL-based ABS.

IL	TLL	C	E	$\Delta G(CH_2)$ / kJ·mol^{-1}
IL + K_2CO_3 + H_2O ABS (no pH control)				
[C_4C_1im][CF_3SO_3]	50.13	1.868 ± 0.106	0.293 ± 0.042	-0.726 ± 0.103
[C_4C_1im][SCN]	52.91	3.268 ± 0.111	0.306 ± 0.044	-0.759 ± 0.108
[C_4C_1im][TOS]	52.32	3.924 ± 0.023	0.237 ± 0.009	-0.588 ± 0.023
[C_4C_1im][$N(CN)_2$]	59.51	3.868 ± 0.180	0.501 ± 0.070	-1.242 ± 0.175
[C_4C_1im]Br	52.89	4.099 ± 0.210	0.453 ± 0.082	-1.123 ± 0.082
[C_4C_1im][DMP]	53.38	6.071 ± 0.029	0.456 ± 0.029	-1.130 ± 0.072
[C_4C_1im]Cl	49.53	5.398 ± 0.100	0.334 ± 0.039	-0.828 ± 0.098
IL + Na_2SO_4 + H_2O ABS (at pH = 7.4)				
[C_4C_1im][CF_3SO_3]	41.82	1.568 ± 0.039	0.242 ± 0.015	-0.600 ± 0.038
[C_4C_1im][SCN]	42.01	2.286 ± 0.017	0.218 ± 0.007	-0.542 ± 0.016
[C_4C_1im][TOS]	43.14	2.911 ± 0.154	0.302 ± 0.060	-0.749 ± 0.150
[C_4C_1im][$N(CN)_2$]	42.82	2.536 ± 0.012	0.218 ± 0.005	-0.540 ± 0.011
[C_4C_1im]Br	41.15	4.019 ± 0.107	0.246 ± 0.042	-0.610 ± 0.104

The partition coefficients of DNP-amino-acids to the IL-rich phase are very high, with values ranging between ~5 and ~2250 (*cf.* the **Appendix B**). This extreme partition of DNP-amino-acids made the quantification in the salt-rich phase very difficult due to the low concentration of these molecules in these phases. This difficulty justifies the large deviations reported in **Table 3.10** for some systems and represents one of the limitations of this methodology when involving IL-based

ABS. When the extracted molecules present high affinities for one of the phases of the biphasic system, it may be impossible to accurately determine the $\Delta G(CH_2)$.

From the data reported in **Table 3.10** it is possible to observe that for the studied systems, independently of the salt used and the pH, $\Delta G(CH_2)$ is always negative, meaning that the transfer of a nonpolar CH_2 group from the salt- to the IL-rich phase is favorable, and that IL-rich phases are more hydrophobic than salt-rich phases in IL-based ABS. The $\Delta G(CH_2)$ of IL + K_2CO_3 ABS ranges from -0.588 to -1.242 kJ·mol^{-1}, while a much smaller variation is observed for ABS composed of Na_2SO_4 (-0.540 to -0.749 kJ·mol^{-1}).

The Gibbs free energies of transfer of a methylene group between the coexisting phases in IL-based ABS were previously reported by Wu et al.[25,26] The authors evaluated the effect of the anion[25] and the cation[26] of amino-acid-based ILs in $\Delta G(CH_2)$ values, and observed a strong relation between the ILs hydrophobicity (thus the ILs ability to form an ABS) and this parameter. Although the $\Delta G(CH_2)$ values reported in **Table 3.10** are close to those reported by Wu et al.[25,26], it is impossible to observe a similar behavior in the systems studied in this work. It should be noted that Wu et al.[25,26] determined the $\Delta G(CH_2)$ values at a fixed mixture point while in this work a constant TLL value was used. It is well known that the size of the TL presents a high impact on the extraction ability of an ABS. With the increase of the TLL, the ABS moves from the critical point, where the two coexisting phases present the same composition, to two phases with increasingly distinct compositions and properties, resulting in the increase of the driving force for the molecules partition. Thus, when a fixed mixture point is used in a set of systems which only differ in the IL nature, different TLL will be obtained for each system, as can be gauged from **Figure 3.31**, and consequently, not only the IL nature will influence the molecules extraction or properties determination, but also the TLL. In the case of $\Delta G(CH_2)$, as the TLL increases (larger differences between the phases compositions), the Gibbs free energy value will also increase,[4,14] and similar results to those reported by Wu et al.[25,26] could be obtained, but these would lead to a wrong interpretation of the phases relative hydrophobicities as the results are dominated by the TLL effect rather than the nature of the phases.

The effect of the methylene group in the $ln(K)$ is independent of the nature of the partitioned solutes, which means that E is a characteristic of the system under study. On the other hand, the contribution of the polar group of the aliphatic solutes, represented by constant C, depends on both the composition of the ABS and the solute being partitioned. Since a homologous series of solutes was used, the effect of the solute nature will be constant and the differences observed in the parameter C result only from the composition of the studied systems.

For the studied IL-based ABS, the parameter C is considerably higher than 1, ranging between 1.868 and 6.071 for K_2CO_3-based ABS and between 1.568 and 4.019 for Na_2SO_4-based ABS (*cf.* **Table 3.10**). These results suggest that the polar group of DNP-amino-acids has a significant effect on the solutes partition in IL-based ABS. Furthermore, it is possible to observe a good linear relation between the parameter *C* and the COSMO-RS hydrogen-bonding energies (E_{HB}) of ILs that compose the studied systems – **Figure 3.34**. This relation indicates that, for these systems, C is a good measure of the polar/hydrogen bonding interactions differences of the coexisting phases of IL-based ABS.

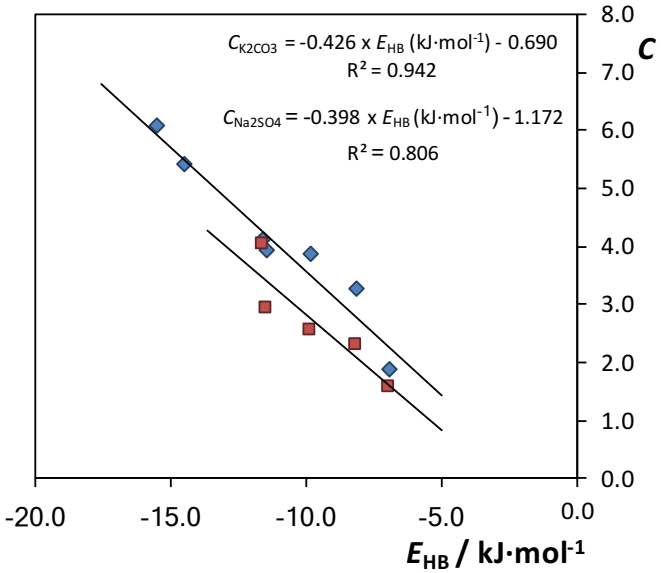

Figure 3.34. Constant C as a function of COSMO-RS hydrogen-bonding energies (E_{HB}) for K_2CO_3-based ABS (■) and Na_2SO_4-based ABS (◆).

The influence of the methylene group influence seems to be also very important, since the partition coefficients of DNP-amino-acids increase considerably with the number of methylene groups – *cf.* **Appendix B**. However, a direct comparison of C and E absolute values does not allow to understand which type of interactions influences more the partition of DNP-amino-acids. For example, considering the partition of DNP-leucine in the ABS composed of $[C_4C_1im][CF_3SO_3]$ + K_2CO_3 + H_2O, the contribution of DNP-amino-acid polar group is represented by the value of C, *i.e.* 1.868, while the contribution of the methylene groups is equal to 1.70 (product of the parameter E by the number of equivalent methylene groups that in this case is 3.75). This means that the influence of both groups is positive and very similar for this case. However, considering the partition of the same DNP-amino-acid in $[C_4C_1im]Cl$ + K_2CO_3 + H_2O system, the contributions of both polar and non-polar groups are 5.398 and 1.252, respectively, which means that the influence of polar group is 4.31 times higher than the non-polar group of the solute, suggesting

that, despite the increase in the partition coefficient with the number of methylene groups, polar/hydrogen bonding interactions are the main driving force for this partition. Furthermore, this effect is even more evident the lower is the number of CH_2 equivalent groups presents in the DNP-amino-acid. In **Figure 3.35** and **Figure 3.36** are represented the ratios between the contribution of polar groups (*i.e.* electrostatic interactions) over the contribution of non-polar groups (*i.e.* dispersive-type interactions) – $R_{polar/non-polar}$ – for all DNP-amino-acids partition in K_2CO_3 and Na_2SO_4-based ABS, respectively. The number of equivalent methylene groups for DNP-glycine, DNP-valine, DNP-alanine and DNP-leucine are 0.06, 1.31, 2.65 and 3.75, respectively. Since DNP-glycine has a $n(CH_2)$ close to 0, the contribution of the hydrophobic interactions in its partition is almost null and $R_{polar/non-polar}$ becames significantly high. Nevertheless, even when DNP-amino-acids with higher $n(CH_2)$ are considered, the contribution of the polar group of the aliphatic solutes is always higher than the methylene groups influence (the ratio is always higher than unity) – *cf.* **Figure 3.35** and **Figure 3.36**. Furthermore, similarly to what was previously observed for the parameter C (**Figure 3.34**), this ratio tends to increase with the E_{HB} of the IL that composes the system. In fact, ILs with higher COSMO-RS hydrogen-bonding energies will be able to easily hydrogen bond with the solutes and consequently the effect of the polar group in the partition of the DNP-amino-acids will increase. However, if the system is constituted by an IL with lower E_{HB} value and higher hydrophobic character, such as the $[C_4C_1im][CF_3SO_3]$, the influence of the methylene groups in the partition will be higher and the contributions will be more similar (ratio closer to 1) – *cf.* **Figure 3.35** and **Figure 3.36**.

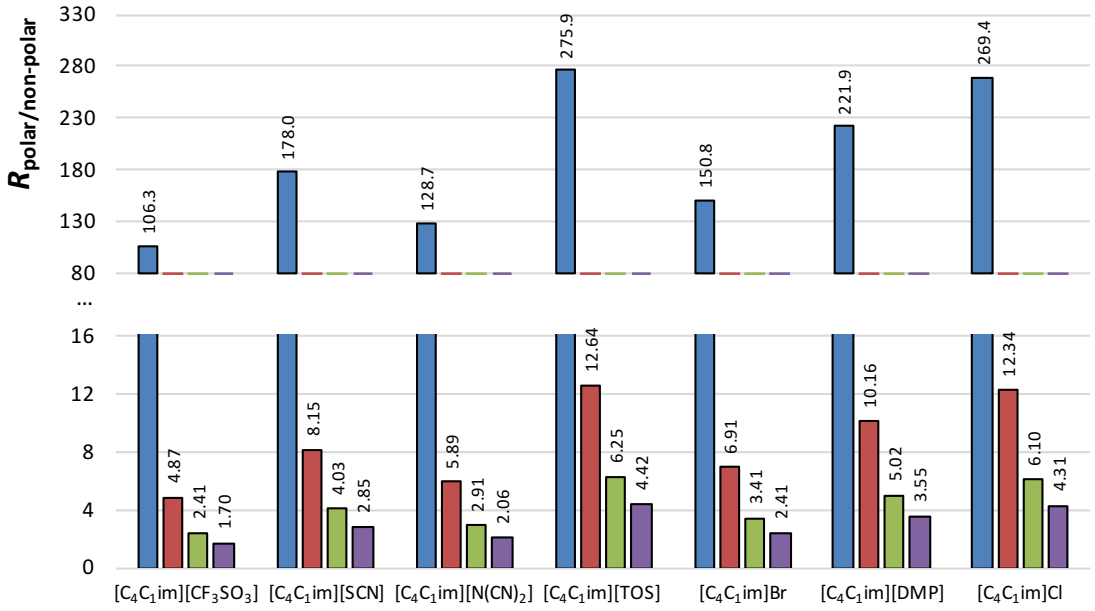

Figure 3.35. Ratio between the contribution of polar groups (*i.e.* electrostatic interactions) over the contribution of non-polar groups (*i.e.* dispersive-type interactions), $R_{polar/non-polar}$, of DNP-amino-acids (DNP-glycine – blue bars; DNP-valine – red bars; DNP-alanine – green bars and DNP-leucine – purple bars) partition in K_2CO_3-based ABS.

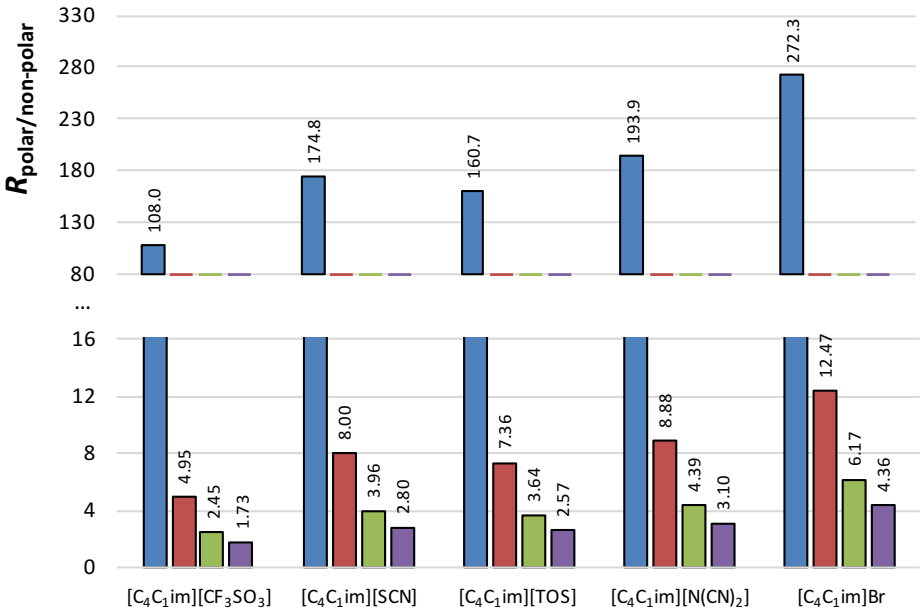

Figure 3.36. Ratio between the contribution of polar groups (*i.e.* electrostatic interactions) over the contribution of non-polar groups (*i.e.* dispersive type interactions), $R_{polar/non-polar}$, of DNP-amino-acids (DNP-glycine – blue bars; DNP-valine – red bars; DNP-alanine – green bars and DNP-leucine – purple bars) partition in Na_2SO_4-based ABS.

Figure 3.37 depicts the comparison of $\Delta G(CH_2)$ values for different types of liquid-liquid systems previously reported in the literature. Since several factors could affect the $\Delta G(CH_2)$

value of a system, whenever possible, $\Delta G(CH_2)$ determined at similar TLLs were chosen from the data reported in the literature. Comparing the relative hydrophobicity of different types of ABS, IL-based ABS[25,26] present very similar values to polymer/salt[15,40] and considerably higher than polymer/polymer[3,13] aqueous systems. Nevertheless, due the very distinct chemical composition of their phases, binary systems composed of organic solvent/water[16] and micellar[41] systems are those which present the largest differences in the solvation ability between the phases. Furthermore, whenever possible the contribution of the polar groups over the non-polar groups ($R_{polar/non-polar}$) was also calculated and represented in **Figure 3.37**. As expected, the ratio between the polar and non-polar groups contributions is lower in the systems that present higher$\Delta G(CH_2)$. Through this parameter is possible to see that for IL-based ABS the polar group contribution is always slightly higher than the non-polar group, while for polymer-salt ABS this ratio tends to be closer to 1. For organic solvents-water systems, the polar group presents a non-favorable impact on the solutes partition for the organic phase. These results clearly show the different nature of IL-based ABS when compared with other types of biphasic systems.

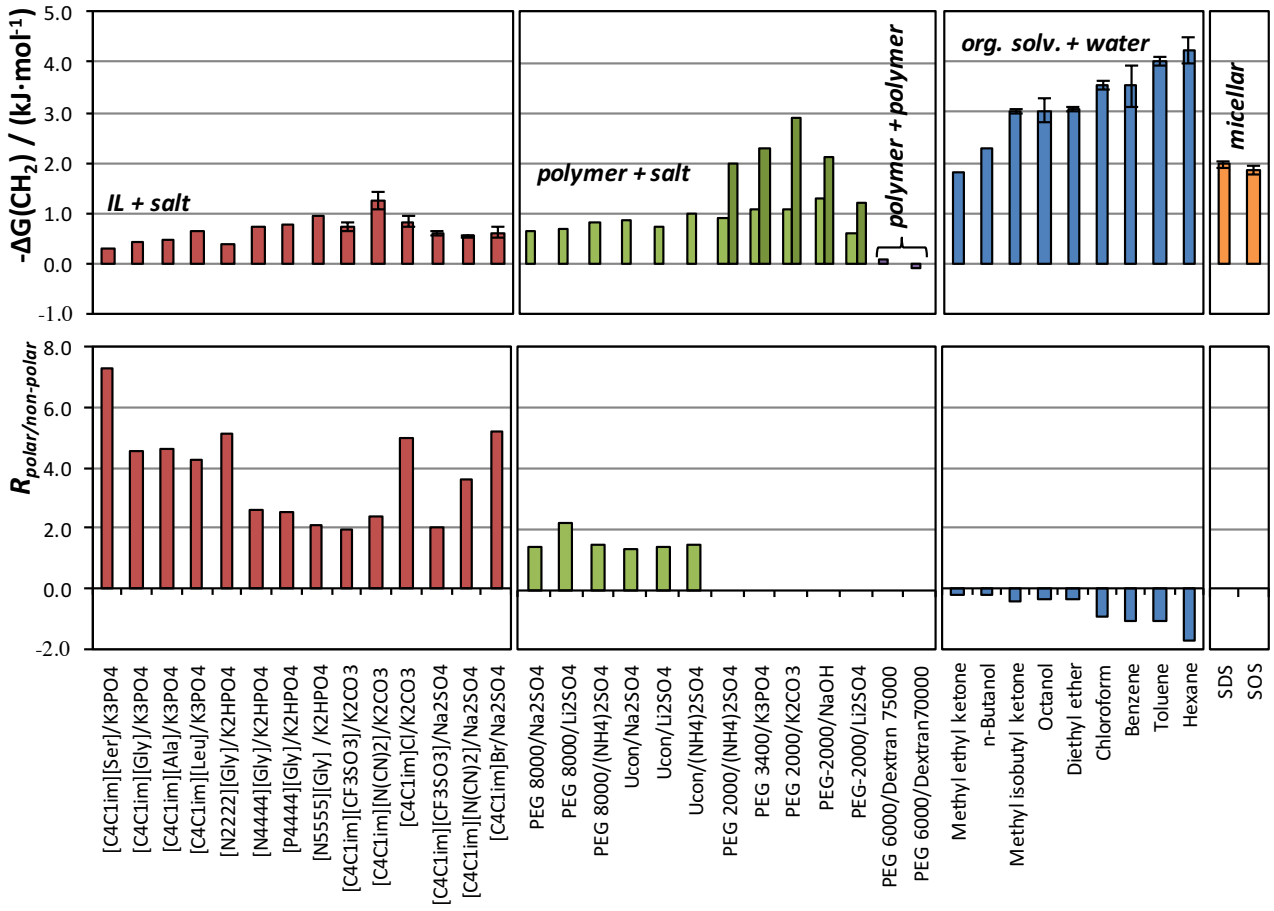

Figure 3.37. Gibbs free energy of transfer of a methylene group between the coexisting phases of different types of liquid-liquid system and ratio of solutes polar and non-polar groups contributions in the partition: ABS composed of IL/salt,[25,26] polymer/salt (light green – smallest TL; darker green – largest TL),[15,40] polymer/polymer,[3,13] and binary systems composed of organic solvents/water[16] and micellar-systems.[41]

Solvatochromic parameters. The Kamlet-Taft parameters – solvent dipolarity/polarizability, π^*, solvent hydrogen-bond donor acidity, α, and solvent hydrogen bond acceptor basicity, β – of IL-rich and salt-rich phases of IL-K_2CO_3 and IL-Na_2SO_4 ABS, and their differences, were determined at a constant TLL value, and the obtained results are presented in **Table 3.11**.

Table 3.11. Solvatochromic parameters and their differences in the coexisting phases of IL-based ABS.

IL	TLL	π^*_{IL}	π^*_{salt}	$\Delta\pi^*$	α_{IL}	α_{salt}	$\Delta\alpha$	β_{IL}	β_{salt}	$\Delta\beta$
IL + K_2CO_3 + H_2O ABS (no pH control)										
[C_4C_1im][CF_3SO_3]	50.13	1.09	1.24	-0.15	1.13	1.34	-0.21	0.44	0.34	0.10
[C_4C_1im][SCN]	52.91	1.21	1.29	-0.08	1.17	1.34	-0.17	0.41	0.34	0.07
[C_4C_1im][TOS]	52.32	1.12	1.24	-0.12	1.21	1.33	-0.12	0.56	0.44	0.12
[C_4C_1im][$N(CN)_2$]	59.51	1.18	1.28	-0.10	1.15	1.33	-0.18	0.41	0.35	0.06
[C_4C_1im]Br	52.89	1.27	1.29	-0.02	1.21	1.31	-0.10	0.49	0.44	0.05
[C_4C_1im][DMP]	53.38	1.20	n.s.[a]	---	1.18	1.30	-0.12	0.59	n.s.[a]	---
[C_4C_1im]Cl	49.53	1.26	n.s.[a]	---	1.21	1.31	-0.10	0.53	n.s.[a]	---
IL + Na_2SO_4 + H_2O ABS (at pH = 7.4)										
[C_4C_1im][CF_3SO_3]	41.82	1.12	1.21	-0.09	1.17	1.35	-0.18	0.41	0.37	0.04
[C_4C_1im][SCN]	42.01	1.23	1.28	-0.05	1.23	1.35	-0.12	0.40	0.36	0.04
[C_4C_1im][TOS]	43.14	1.17	1.24	-0.07	1.26	1.35	-0.09	0.53	0.46	0.07
[C_4C_1im][$N(CN)_2$]	42.82	1.20	1.27	-0.07	1.21	1.34	-0.13	0.39	0.34	0.05
[C_4C_1im]Br	41.15	1.31	1.32	-0.01	1.26	1.36	-0.10	0.46	0.41	0.05

[a] not soluble (n.s.)

Each of the solvatochromic parameters presented in **Table 3.11** were obtained from a set of single solvatochromic probes as previously described in the Experimental Section. The use of single probes versus multiple probes, as first suggested by Kamlet et al.,[42] for solvatochromic parameters determination is still a controversial issue in the literature. Since the use of a series of selected probes requires a considerable experimental effort to determine the respective values of any new solvents, several authors demonstrated that good results could be achieved with single solvatochromic probes.[8,10,20] Furthermore, it should be noted that solvatochromic parameters are not fundamental physical properties of a solvent with an exact value, but only a scale of the effect of the solvent upon solute species that are sensitive to interactions with the solvent.[20]

Despite the considerably low solubility of *N*,*N*-diethyl-4-nitroaniline and 4-nitroaniline in water (< 1g·L^{-1}),[43] the ILs hydrotropic effect[44] contributed to enhance the solubility of these two poorly soluble dyes making them good probes in Kamlet-Taft parameters determination for IL-based ABS. However, it was not possible to dissolve *N*,*N*-diethyl-4-nitroaniline in the salt-rich phases of [C_4C_1im][DMP]-K_2CO_3 and [C_4C_1im]Cl-K_2CO_3-based ABS, making impossible the

determination of π^* and β of the bottom phases, and consequently the $\Delta\pi^*$ and $\Delta\beta$ of these systems. Since the amount of *N*,*N*-diethyl-4-nitroaniline dissolved in these phases was lower than the probe water solubility, it seems that the presence of a high concentration of salt in these two samples induced the probe precipitation. In **chapter 3.4**. it was demonstrated that the probe pyridine-*N*-oxide, proposed by Marcus et al.,[45] could be used to determine the hydrogen-bond donor ability of highly concentrated salt aqueous solutions, for which the conventional used Reichardt dye presents low solubility and aggregation problems.

From the data reported in **Table 3.11**, it is possible to observe that, independently of the salt used, the salt-rich phases always present higher dipolarity/polarizability values than IL-rich phases in the ABS studied. However, the π^* values range is larger for the IL-rich phases than the salt-rich phases, that present dipolarity/polarizability values close to that of pure water ($\pi^*_{H_2O} = 1.26$). In **Table 3.12** are presented the Kamlet-Taft parameters for water and some pure ILs.[35,46] Since pure ILs dipolarity/polarizability is considerably lower than water, it is expected that binary solutions of water and ILs will present lower dipolarity/polarizability, as observed for the studied IL-rich phases. However, these results are very distinct from those observed for ABS composed of polymers and/or salts where in general both phases presented a higher dipolarity/polarizability than water.[10,14] Nevertheless, from the solutes partition point of view, the most important parameter is the difference in the solvatochromic parameters between the coexisting phases. The differences between the π^* values of the coexisting phases in IL-based ABS are slightly larger than those observed in polymer systems.[10,14] Considering the $\Delta\pi$ values for K_2CO_3- and Na_2SO_4-based ABS it is possible to observe a decreasing tendency of the absolute value of this parameter with the decrease of the IL hydrophobicity.

Table 3.12. Kamlet-Taft parameters of pure water and ILs.

Solvent	π^*	α	β
water	1.26[(a)]	1.36[(a)]	0.15[(a)]
$[C_4C_1im][CF_3SO_3]$	0.98[(b)]	0.39[(a)]	0.48[(b)]
$[C_4C_1im][SCN]$	[(d)]	0.39[(a)]	[(d)]
$[C_4C_1im][N(CN)_2]$	0.60[(c)]	0.40[(a)]	1.05[(c)]
$[C_4C1im][DMP]$	0.96[(b)]	[(d)]	1.12[(b)]

[a] parameters determine in this work; [b] parameters from ref. 35; [c] parameters from ref. 46;
[d] it was not possible determine the parameters due the IL strong color or high viscosity.

The solvatochromic parameter that seems to be less influenced by the composition of the IL-based ABS is the hydrogen bond donor acidity. In fact, this parameter is almost constant in salt-rich phases with values close to that of pure water ($\alpha_{H_2O} = 1.36$), while slight oscillations are observed in IL-rich phases. Although the IL anion plays a secondary role, the hydrogen bond donor

acidity is mainly determined by the IL cation. Since a common IL cation was used in this study this justifies the small variations observed for this parameter. However, the differences between the coexisting phases ($\Delta\alpha$) are considerably higher than those observed for the dipolarity/polarizability and the hydrogen bond acceptor basicity. This behavior is similar to that observed in ABS constituted by polymers and salts.[10,14]

Similarly to polymer-polymer- and polymer-salt-based ABS,[9,10,14] the hydrogen bond acceptor basicity values of IL-based ABS coexisting phases are considerably superior to those of pure water (**Table 3.12**), with IL-rich phases presenting higher values than salt-rich phases. It is possible to observe in **Table 3.12** that ILs present considerably a higher hydrogen-bond acceptor ability than water, which means that their addition to an aqueous solution will increase the β value of the mixture. The hydrogen-bond acceptor ability is mainly controlled by the IL anion which justifies the large variations observed in β for the various systems studied. As observed in dipolarity/polarizability, also $\Delta\beta$ for K_2CO_3-based ABS seems to decrease with the IL hydrophobicity. However, it is not clear the existence of a tendency in Na_2SO_4-based ABS.

To better understand how solvatochromic parameters behave along the phase diagram of an IL-based ABS, a fine analysis was carried out with the water-$[C_4C_1im][TOS]$-K_2CO_3 ternary system. The Kamlet-Taft parameters were determined in binary solutions of $[C_4C_1im][TOS]$ + water and K_2CO_3 + water, and in monophasic and biphasic ternary mixtures of $[C_4C_1im][TOS]$-K_2CO_3 ABS. The compositions of each mixture are reported in **Appendix B**. In **Figure 3.38**, the π^*, α and β parameters are represented as a contour plot on the ternary phase diagram of $[C_4C_1im][TOS]$-K_2CO_3 ABS. As discussed above, it was not possible to dissolve the probe *N*,*N*-diethyl-4-nitroaniline in binary solutions of K_2CO_3 and water, and consequently only the hydrogen-bond donor ability was determined for these samples.

From **Figure 3.38 A**, it is possible to observe that the dipolarity/polarizability is mostly affected by water and K_2CO_3 concentrations. The addition of salt species to highly diluted aqueous solutions slightly increases the value of π^*, but when water concentration is below 80 wt % the dipolarity/polarizability decreases significantly. The hydrogen-bond donor ability of the ternary mixture seems to be ruled by the water content of the solution, since the color scale changes in the same direction of the water weight percentage (**Figure 3.38 B**). Although not as clear, a similar tendency is seen for the hydrogen-bond acceptor ability (**Figure 3.38 C**). Furthermore, while the α value increases with the water content, the β decreases with the addition of hydrogen-bond acceptor species into the solution, such as the IL.

Concerning the TLL effect on the Kamlet-Taft parameters, the coexisting phases present symmetrical behaviors. For example, with the TLL increase, the π^* of salt-rich phases increases while it decreases in IL-rich phases (**Figure 3.38 A**). A similar behavior was observed with hydrogen-bond acceptor ability (**Figure 3.38 C**). As the IL concentration in the salt-rich phase decreases with the increase of the TLL, π^* and β values for this phase became closer to the pure water solvatochromic parameters, while the increase of IL concentration in the IL-rich phase induces the opposite behavior. Thus, $\Delta\pi^*$ and $\Delta\beta$ increase significantly with the TLL, contrarily to what is observed for ABS composed of polymers and salts, where these two parameters are essentially independent of the TLL.[10,14] On the other hand, the α of the coexisting phases, and $\Delta\alpha$, present a similar behavior to that observed for polymer-salt ABS.[10,14] The salt-rich phase has a hydrogen bond donor acidity close to pure water and independent of the TLL, while the IL-rich phase value decreases considerably with the TLL. Since the water amount in salt-rich phases is almost constant, while it changes considerably in IL-rich phases with the increase of the TLL, these trends are probably related with the water concentration in the phases as discussed above.

As previously mentioned, the solvatochromic parameters differences between the coexisting phases in ABS are the most important factors to understand the partition of a solute. The ABS constituted by ILs and salts here studied present a considerably large variation on these differences with a high dependency on the type of the IL and salt that compose the system and their concentrations in the mixture, suggesting that these systems can be tuned for the improved extraction of a specific solute.

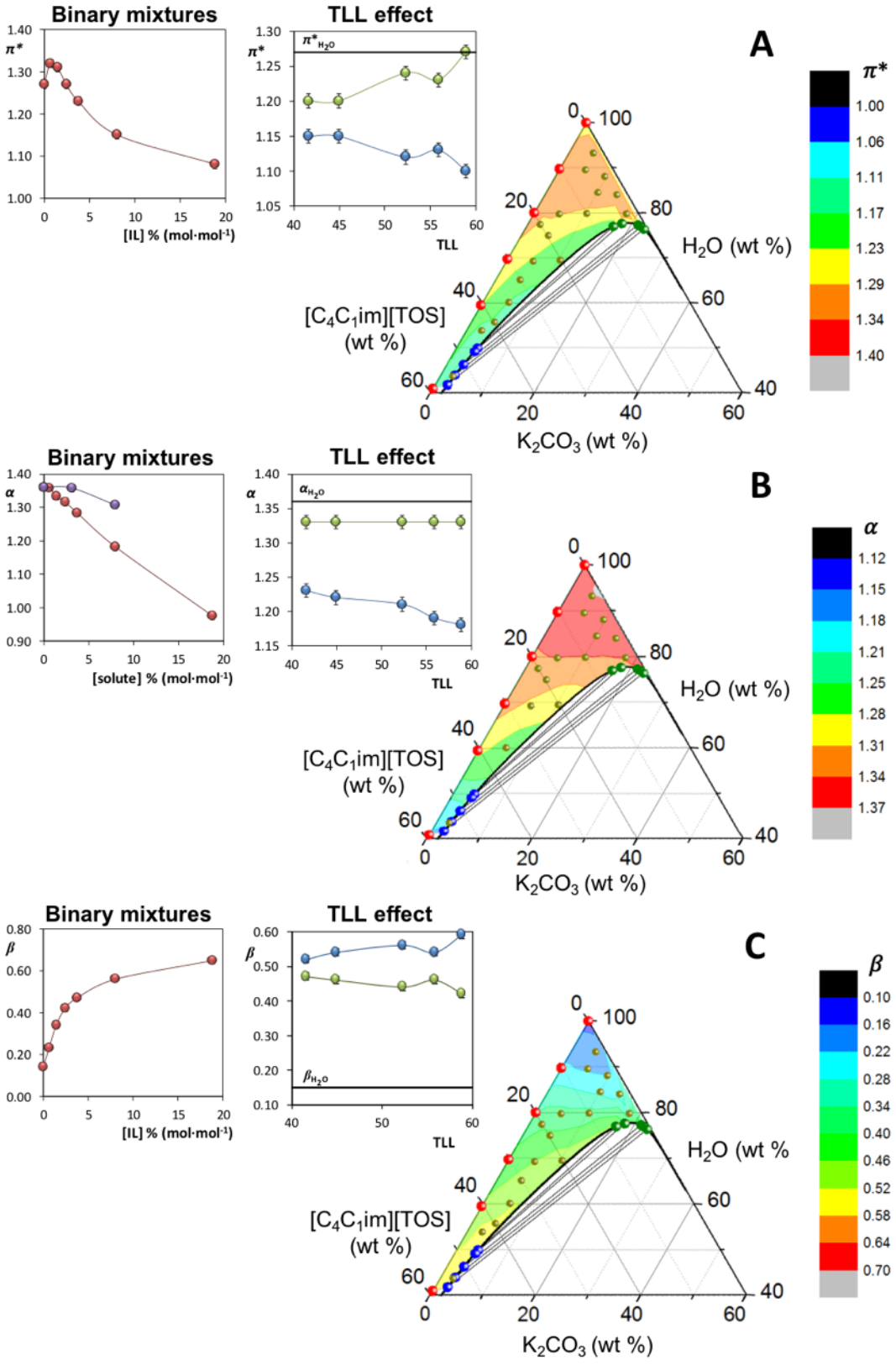

Figure 3.38. The effect of ABS composition in Kamlet-Taft parameters: **(A)** π^*, **(B)** α, and **(C)** β. $[C_4C_1im][TOS]$-K_2CO_3-based ABS: binary mixtures of $[C_4C_1im][TOS]$ and water (red circles), binary mixtures of K_2CO_3 and water (purple circles); IL-rich phases (blue circles); salt-rich phases (green circles).

3.5.5. Conclusions

Aiming at better understanding the mechanisms which rule the partition of molecules in ABS composed of ILs and salts, the Gibbs free energy of a methylene group transfer and the solvatochromic parameters of the phases in equilibrium were here determined. The relative hydrophobicity of a wide range of ABS composed of [C_4C_1im]-based ILs and K_2CO_3 or Na_2SO_4, at 298 K, were determined by the partition of a series of DNP-amino-acids. It was observed that the partition of DNP-amino-acids in IL-salt ABS is mainly ruled by hydrogen-bond interactions with the ILs, *i.e.* by electrostatic interactions. The relative hydrophobicity of the phases presents a significant effect that increases with the increase of the IL hydrophobic character. Contrarily to what was previously reported in the literature, no relation was found between the ΔG_{CH_2} and the IL ability to induce the ABS formation, which could be related with the use of a fixed TLL instead of a fixed mixture point as usually reported. When a fixed TLL is used to compare the relative hydrophobicity (or other property) of ABS which only differ in the IL anion nature, it is possible to make constant the molecules partition driving force generated by the TLL, and thus only the IL anion nature will be responsible for the variations observed in the system properties. It was also evaluated how the solvatochromic parameters – dipolarity/polarizability (π^*), hydrogen-bonding donor acidity (α) and hydrogen-bonding acceptor basicity (β) – of the coexisting phases of IL-based ABS change with the composition. The ABS constituted by ILs and salts here studied, present a considerably large variation on the solvatochromic parameters differences between the coexisting phases with a high dependency on the type of IL and salt that compose the system and their concentrations in the mixture.

3.5.6. References

(1) P. Å. Albertsson, *Partition of cell particles and macromolecules*, 2nd ed.; John Wiley & Sons Inc.: New York, 1971;
(2) H. Walter, D.E. Brooks, D. Fisher, *Partitioning in aqueous two-phase systems: theory, methods, use, and applications to biotechnology*; Academic Press: Orlando, Florida, 1985;
(3) B.Y. Zaslavsky, *Aqueous two-phase partitioning: Physical chemistry and bioanalytical applications*; Marcel Dekker Inc.: New York, 1994;
(4) K.E. Gutowski, G.A. Broker, H.D. Willauer, J.G. Huddleston, R.P. Swatloski, J.D. Holbrey, R.D. Rogers, *J. Am. Chem. Soc.*, 2003, **125**, 6632–6633;
(5) M.G. Freire, A.F.M. Cláudio, J.M.M. Araújo, J.A.P. Coutinho, I.M. Marrucho, J.N.C. Lopes, L.P.N. Rebelo, *Chem. Soc. Rev.*, 2012, **41**, 4966–4995;
(6) A. Frerix, P. Geilenkirchen, M. Müller, M.-R. Kula, and J. Hubbuch, *Biotechnol. Bioeng.*, 2007, 96, 57–66;
(7) P.A.J. Rosa, A.M. Azevedo, S. Sommerfeld, W. Bäcker, M.R. Aires-Barros, *Biotechnol. Adv.*, 2011, **29**, 559–567;

(8) B.Y. Zaslavsky, V.N. Uversky, A. Chait, *Biochim. Biophys. Acta*, 2016, **1864**, 622–644;
(9) P.P. Madeira, C.A. Reis, A.E. Rodrigues, L.M. Mikheeva, A. Chait, B.Y. Zaslavsky, *J. Chromatogr. A*, 2011, **1218**, 1379–1384;
(10) J.G. Huddleston, H.D. Willauer, R.D. Rogers, *Phys. Chem. Chem. Phys.*, 2002, **4**, 4065–4070;
(11) P.P. Madeira, A. Bessa, L. Álvares-Ribeiro, M.R. Aires-Barros, A.E. Rodrigues, B.Y. Zaslavsky, *J. Chromatogr. A*, 2013, **1274**, 82–86;
(12) P.P. Madeira, A. Bessa, D.P.C. de Barros, M.A. Teixeira, L. Álvares-Ribeiro, M.R. Aires-Barros, A.E. Rodrigues, A. Chait, B.Y. Zaslavsky, *J. Chromatogr. A*, 2013, **1271**, 10–16;
(13) M.L. Moody, H.D. Willauer, S.T. Griffin, J.G. Huddleston, R.D. Rogers, *Ind. Eng. Chem. Res.*, 2005, **44**, 3749–3760;
(14) O. Rodríguez, S.C. Silvério, P.P. Madeira, J.A. Teixeira, E.A. Macedo, *Ind. Eng. Chem. Res.*, 2007, **46**, 8199–8204;
(15) S.C. Silvério, P.P. Madeira, O. Rodríguez, J.A. Teixeira, E.A. Macedo, *J. Chem. Eng. Data*, 2008, **53**, 1622–1625;
(16) B.Y. Zaslavsky, L.M. Miheeva, S.V. Rogozhin, *J. Chromatogr. A*, 1981, **216**, 103–113;
(17) B.Y. Zaslavsky, L.M. Miheeva, S.V. Rogozhin, *J. Chromatogr. A*, 1981, **212**, 13–22;
(18) N.J. Bridges, K.E. Gutowski, R.D. Rogers, *Green Chem.*, 2007, **9**, 177–183;
(19) C. Reichardt, T. Welton, *Solvents and solvent effects in organic chemistry*, 4th ed.; Wiley-VCH: Weinheim, 2010;
(20) M.A. Ab Rani, A. Brant, L. Crowhurst, A. Dolan, M. Lui, N.H. Hassan, J.P. Hallett, P.A. Hunt, H. Niedermeyer, and J.M. Perez-Arlandis, *Phys. Chem. Chem. Phys.*, 2011, **13**, 16831–16840;
(21) M.J. Kamlet, R.W. Taft, *J. Am. Chem. Soc.*, 1976, **98**, 377–383;
(22) R.W. Taft, M.J. Kamlet, *J. Am. Chem. Soc.*, 1976, **98**, 2886–2894;
(23) M.J. Kamlet, J.L. Abboud, R.W. Taft, *J. Am. Chem. Soc.*, 1977, **99**, 6027–6038;
(24) Y. Pei, J. Wang, K. Wu, X. Xuan, X. Lu, *Sep. Purif. Technol.*, 2009, **64**, 288–295;
(25) C. Wu, J. Wang, H. Wang, Y. Pei, Z. Li, *J. Chromatogr. A*, 2011, **1218**, 8587–8593;
(26) C. Wu, J. Wang, Z. Li, J. Jing, H. Wang, *J. Chromatogr. A*, 2013, **1305**, 1–6;
(27) L. Crowhurst, P.R. Mawdsley, J.M. Perez-Arlandis, P.A. Salter, T. Welton, *Phys. Chem. Chem. Phys.*, 2003, **5**, 2790–2794;
(28) C. Chiappe, C.S. Pomelli, S. Rajamani, *J. Phys. Chem. B*, 2011, **115**, 9653–9661;
(29) C. Chiappe, D. Pieraccini, *J. Phys. Org. Chem.*, 2005, **18**, 275–297;
(30) J.C. Merchuk, B.A. Andrews, J.A. Asenjo, *B. Biomed. Sci. Appl.*, 1998, **711**, 285–293;
(31) A.F.M. Cláudio, A.M. Ferreira, S. Shahriari, M.G. Freire, J.A.P. Coutinho, *J. Phys. Chem. B*, 2011, **115**, 11145–11153;
(32) H. Passos, A.R. Ferreira, A.F.M. Cláudio, J.A.P. Coutinho, and M.G. Freire, *Biochem. Eng. J.*, 2012, **67**, 68–76;
(33) S.P.M. Ventura, C.M.S.S. Neves, M.G. Freire, I.M. Marrucho, J. Oliveira, J.A.P. Coutinho, *J. Phys. Chem. B*, 2009, **113**, 9304–9310;
(34) S.P.M. Ventura, S.G. Sousa, L.S. Serafim, Á.S. Lima, M.G. Freire, and J.A.P. Coutinho, *J. Chem. Eng. Data*, 2012, **57**, 507–512;
(35) A.F.M. Cláudio, L. Swift, J.P. Hallett, T. Welton, J.A.P. Coutinho, and M.G. Freire, *Phys. Chem. Chem. Phys.*, 2014, **16**, 6593–6601;
(36) A. Klamt, G. Schüürmann, *J. Chem. Soc. Perkin Trans. 2*, 1993, **No. 5**, 799;
(37) A. Klamt, *COSMO-RS from quantum chemistry to fluid phase thermodynamics and drug design.* Elsevier: Amsterdam, Boston 2005;
(38) A. Klamt, *J. Phys. Chem.*, 1995, **99**, 2224–2235;
(39) A. Klamt, and F. Eckert, *Fluid Phase Equilib.*, 2000, **172**, 43–72;

(40) H.D. Willauer; J.G. Huddleston, R.D. Rogers, *Ind. Eng. Chem. Res.*, 2002, **41**, 2591–2601;
(41) M.F. Vitha, P.W. Carr, *Sep. Sci. Technol.*, 1998, **33**, 2075–2100;
(42) M.J. Kamlet, J.L. Abboud, M.H. Abraham, and R.W. Taft, *J. Org. Chem.*, 1983, **48**, 2877–2887;
(43) S.H. Yalkowsky and Y. He, *Handbook of aqueous solubility data*; CRC Press LLC: Boca Raton, 2003;
(44) A.F.M. Cláudio, M.C. Neves, K. Shimizu, J.N. Canongia Lopes, M.G. Freire, and J.A.P. Coutinho, *Green Chem.*, 2015, **17**, 3948–3963;
(45) H. Schneider, Y. Badrieh, Y. Migron, and Y. Marcus, *Zeitschrift für Phys. Chemie*, 1992, **177** (Part_2), 143–156;
(46) A. Brandt, J.P. Hallett, D.J. Leak, R.J. Murphy, and T. Welton, *Green Chem.*, 2010, **12**, 672–679;

4. An application example of IL-based ABS

4.1. One-step extraction and concentration of estrogens for an adequate monitoring of wastewater using ionic-liquid-based aqueous biphasic systems

This chapter is based on the published manuscript

Teresa B. V. Dinis, Helena Passos, Diana L. D. Lima, Valdemar I. Esteves, João A. P. Coutinho and Mara G. Freire[1], "One-step extraction and concentration of estrogens for an adequate monitoring of wastewater using ionic-liquid-based aqueous biphasic systems",

Green Chemistry 17 (2015) 2570–2579.

4.1.1. Abstract

Ethinylestradiol (EE2) is a synthetic hormone that has been recognized as one of the most prominent endocrine disruptors found in the aqueous environment. Nevertheless, the low content of EE2 in wastewater makes its identification/quantification unfeasible – a major drawback for the evaluation of its persistence and environmental impact. In this context, a novel extraction/concentration method for EE2 from wastewater is proposed here based on aqueous biphasic systems (ABS) composed of ionic liquids (ILs). ABS formed by several hydrophilic ILs and $KNaC_4H_4O_6$ were initially screened and optimized, with extraction efficiencies of EE2 for the IL-rich phase ranging between 92 and 100 %. Remarkable results were obtained with systems that allow the complete extraction of EE2 in a single-step, and without loss of EE2 or the saturation of the extractive phase. Further, the concentration factors of EE2 attainable with these systems were investigated by a suitable manipulation of the composition of the phase-forming components and the corresponding volumes of the coexisting phases. An outstanding concentration of EE2 up to 1000-fold (from $ng \cdot L^{-1}$ to $\mu g \cdot L^{-1}$) in a single extraction and concentration step was achieved for the first time with IL-based ABS. These systems are straightforwardly envisaged for the monitoring of wastewater as one-step extraction and concentration routes for a wide array of endocrine disrupting chemicals while allowing an adequate evaluation of their environmental impact.

4.1.2. Introduction

In the past few years, endocrine disrupting compounds (EDCs) have gained significant relevance due to their association with adverse human health effects and environmental concerns. The United States Environmental Protection Agency (USEPA), defines EDCs as

[1]**Contributions:** M.G.F. and J.A.P.C. conceived and directed this work. T.B.V.D. and H.P. acquired the experimental data. D.L.D.L. and V.I.E. were involved in HPLC quantifications. H.P. and M.G.F interpreted the experimental data. H.P., M.G.F. and J.A.P.C. wrote the final manuscript with significant contributions of the remaining authors.

"exogenous agents that interfere with the production, release, transportation, binding, action, or elimination of the natural hormones in the body, responsible for the maintenance of homeostasis and the regulation of the development process".[1]

17α-Ethinylestradiol, EE2 (**Figure 4.1**), is a synthetic steroid hormone classified as an endocrine disruptor. This compound derives from 17β-estradiol (E2) and displays the most potent estrogenic activity amongst the estrogens found in sewage effluents.[2] EE2 is widely used for medical purposes, for instance, in hormone replacement therapy,[3] in the treatment of prostate and breast cancers and in oral contraception,[4] since it mimics the natural estrogens produced by humans (causing endocrine disruption) and is rapidly absorbed by the organism. The EE2 extensive consumption by humans and further excretion are responsible for its actual presence and persistence in effluents of different sewage treatment plants (up to 64 ng·L^{-1})[5,6] as well as in surface waters (up to 27 ng·L^{-1}).[5,7]

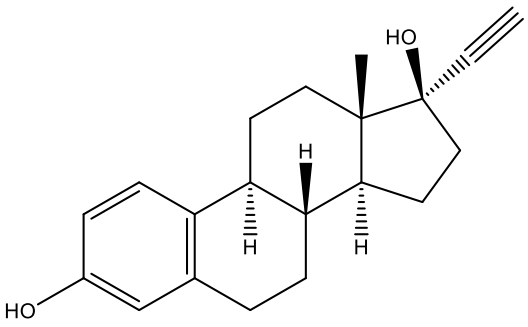

Figure 4.1. Chemical structure of EE2.

In 2012, the Legislative Commission of Water Framework Directive[8] classified EE2 as a priority substance with a significant risk to or via the aquatic environment. Its high stability, low volatility and high octanol-water partition coefficient (K_{OW}) are responsible for its high resistance to degradation and broad bioaccumulation in aquatic organisms.[9] Moreover, the concentration of EE2 has been increasing in sewage effluents, all around the world, due to its widespread use and resistance to degradation.[9–11] Risk assessment bioassays showed the high toxicity of EE2, even at a ng *per* L level, on a wide number of aquatic species.[12,13] All these claims pointed out the need for finding an effective treatment process for EE2. For instance, physical (sorption, membrane filtration, etc.), biological (activated sludge, etc.) and advanced oxidation (photolysis, strong oxidizers, etc.) processes have been investigated for such a purpose.[9,14] However, an accurate monitoring of the EE2 content in aqueous samples is crucial to evaluate the efficiency of these processes. Furthermore, a complemented identification and risk assessment of EE2 in the aquatic environment is of vital importance.[12,15] Several techniques to identify and quantify EE2, such as high performance liquid chromatography (HPLC),[4,16–18] liquid chromatography (LC)[19–21] and gas chromatography (GC),[22–24] combined with mass spectrometry (MS), have been used. Nevertheless, the presence of unknown EDCs in complex matrices of wastewater and the high detection limits of the equipment traditionally used are the major shortcomings in the EE2

identification and quantification.[20,23] Additional and complex pre-treatment processes, using volatile and hazardous organic solvents, are usually employed to purify and to concentrate EE2 from real samples. This pre-treatment stage is also time-consuming and expensive.[25] In this context, the development of alternative methodologies to concentrate EE2 from aqueous media while allowing their appropriate quantification is a challenging task.

Aqueous biphasic systems (ABS) fall within the liquid–liquid extraction (LLE) techniques and involve the partition of molecules from one aqueous phase to another. Typically, these systems are formed by different pairs of solutes (polymer-polymer, polymer-salt or salt-salt) dissolved in water, and above specific concentrations the system undergoes a two phase separation.[26] In addition to their large water content, the non-volatile nature of polymers and salts allows the phase forming components to be recovered and recycled, and hence, ABS are a more benign alternative to traditional liquid–liquid extraction routes which use volatile and hazardous organic compounds. Classical ABS have already been investigated as extraction/concentration techniques.[27,28]

In addition to the more conventional polymer-based systems, in 2003, Gutowski et al.[29] demonstrated that hydrophilic ionic liquids (ILs) can also form ABS by the addition of inorganic salts. After this proof of principle, in the following years it was shown that IL-based ABS can be formed with organic salts, amino acids, carbohydrates or polymers.[30] ILs belong to the molten salts category, and due to the large differences in size and shape of the constituting ions they cannot easily form an ordered crystalline structure, and thus, present melting points below a general temperature of 373 K. Due to their ionic nature, most ILs present unique characteristics, such as a negligible vapor pressure, non-flammability, high thermal and chemical stabilities and a high solvation capacity.[30–33] Still, one of the most important features that has attracted both academia and industry is their aptitude as "designer solvents", *e.g.* the capacity to be synthesized for a given task as a result of their plentiful cation and anion combinations.[34–39]

IL-based ABS were extensively explored for the extraction and purification of a wide variety of biomolecules.[30,40–42] The main advantage of using ILs in the formation of ABS rests on the possibility of tailoring their phases' polarities and affinities by an appropriate combination of their ions[43] and, therefore, exceptional results were already accomplished.[30] It was recently reported that they can be used for the extraction and concentration of alkaloids and bisphenol A from human fluids.[44,45] Yet, only concentration factors up to 100-fold were reported.[44] Furthermore, most of the previously reported systems are composed of ILs and high-charge density inorganic salts[30] which led to some environmental concerns. Taking this into consideration, and although no

enrichment factors were investigated, in recent studies, biodegradable and more biocompatible organic salts were introduced in the composition of IL-based ABS.[46,47]

In this work, we propose the use of novel ABS composed of ILs and a biodegradable organic salt as a concentration strategy for EE2 from wastewater. For this purpose, we initially determined the phase diagrams of IL-based ABS to infer on their formation aptitude. After their evaluation, the ability of IL-based ABS as a new alternative to the current concentration steps used in the EE2 identification and quantification was investigated.

4.1.3. Experimental procedures

Materials. EE2, (17α)-17-ethinylestra-1,3,5(10)-triene-3,17-diol, was supplied by Sigma, with a purity level of ≥ 98 wt% (**Figure 4.1**). The ILs studied were: 1-butyl-3-methylimidazolium bromide, [C_4C_1im]Br (99 wt%); 1-butyl-3-methylimidazolium trifluoroacetate, [C_4C_1im][CF_3CO_2] (>97 wt%); 1-butyl-3-methylimidazolium trifluoromethanesulfonate, [C_4C_1im][CF_3SO_3] (99 wt%); 1-butyl-3-methylimidazolium thiocyanate, [C_4C_1im][SCN] (>98 wt%); 1-butyl-3-methylimidazolium tosylate, [C_4C_1im][TOS] (98 wt%); 1-ethyl-3-methylimidazolium dicyanamide, [C_2C_1im][$N(CN)_2$] (>98 wt%); 1-butyl-3-methylimidazolium dicyanamide, [C_4C_1im][$N(CN)_2$] (>98 wt%); 1-hexyl-3-methylimidazolium dicyanamide, [C_6C_1im][$N(CN)_2$] (>98 wt%); tetrabutylammonium chloride, [N_{4444}]Cl (≥97 wt%); and tetrabutylphosphonium chloride, [P_{4444}]Cl (98 wt%). All imidazolium-based ILs were purchased from Iolitec. [P_{4444}]Cl was kindly offered by Cytec Industries Inc., and [N_{4444}]Cl was purchased from Sigma-Aldrich. The molecular structures of the investigated ILs are illustrated in **Figure 4.2**. Ten more ILs were tested. However, it was not possible to form ABS with these ILs – their names and acronyms are reported in the **Appendix C.** For the reduction of the water and volatile compounds content to negligible values, IL individual samples were dried under constant stirring under vacuum and at moderate temperature (~353 K) for a minimum of 24 h. After this procedure, the purity of each IL was checked by ^{1}H, ^{13}C and ^{19}F (whenever possible) NMR spectra and deemed in accordance with the purity given by the suppliers. The organic salt potassium sodium tartrate tetra-hydrated, $KNaC_4H_4O_6{\cdot}4H_2O$ (> 99 wt%) was acquired from Fluka. The water used was double distilled, passed through a reverse osmosis system and further treated with Milli-Q plus 185 water purification apparatus. HPLC grade methanol and acetonitrile, 99.9%, were from Fischer Chemical and HiPerSolv Chromanorm, respectively.

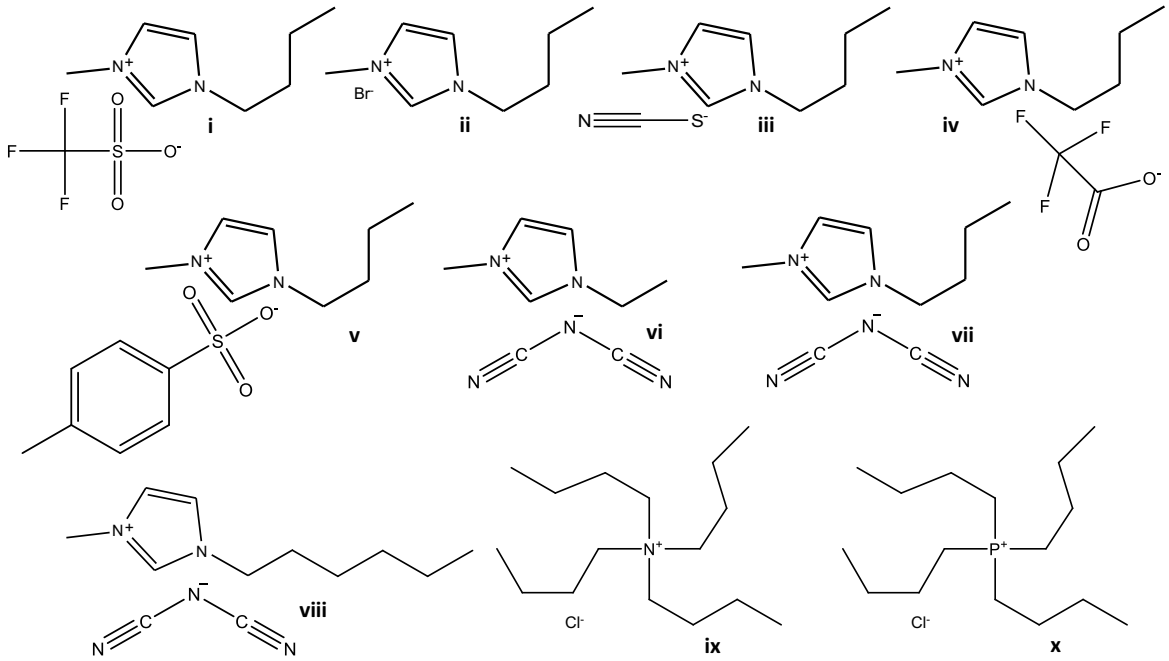

Figure 4.2. Chemical structures of the ILs used to form ABS: (i) $[C_4C_1im][CF_3SO_3]$; (ii) $[C_4C_1im]Br$; (iii) $[C_4C_1im][SCN]$; (iv) $[C_4C_1im][CF_3CO_2]$; (v) $[C_4C_1im][TOS]$; (vi) $[C_2C_1im][N(CN)_2]$; (vii) $[C_4C_1im][N(CN)_2]$; (viii) $[C_6C_1im][N(CN)_2]$; (ix) $[N_{4444}]Cl$; (x) $[P_{4444}]Cl$.

Phase diagrams and tie-lines. The saturation (binodal) curve of each ABS, which represents the limit between the monophasic and biphasic regions, was determined through the cloud point titration method at (298 ± 1) K and atmospheric pressure. The experimental procedure adopted in this work follows the method already validated by us and described in **chapter 2.1**. Aqueous solutions of $KNaC_4H_4O_6$ at 35 wt% and aqueous solutions of the different hydrophilic ILs at variable concentrations (between 35 and 85 wt%) were prepared gravimetrically ($\pm 10^{-4}$ g) and used for the determination of the respective binodal curves. Repetitive drop-wise addition of the organic salt solution to each IL aqueous solution was carried out until the detection of a cloudy mixture. Then, repetitive drop-wise addition of double distilled water was carried out until the detection of a clear and limpid mixture. Whenever necessary, IL aqueous solutions were added to the salt solutions to complete the phase diagrams. Drop-wise additions were performed under constant stirring. The ternary system compositions corresponding to the description of the phase diagrams were determined by weight quantification of all components added to the mixture within $\pm 10^{-4}$ g. The experimental binodal curves were fitted by least-squares regression according to **Equation (2.1)** presented in **chapter 2.1**.

For the determination of each tie-line (TL), a mixture composition at the biphasic region was gravimetrically prepared, vigorously stirred, and allowed to reach the equilibrium by the separation of both phases for at least 12 h at (298 ± 1) K. After the separation step, both top and

bottom phases were weighed. Finally, each individual TL was determined by the application of the lever-arm rule using **Equations (2.2)** to **(2.5)**. The tie-line length (TLL) was determined using **Equation (2.6)**.

Extraction of ethinylestradiol. For the screening of improved IL-based ABS for the one-step extraction and concentration of EE2, several ternary (biphasic) systems (IL + $KNaC_4H_4O_6$ + water) were prepared. The weight fraction percentage of each component was established taking into account a constant weight ratio between the coexisting phases of approximately 1. EE2, *ca.* 2.0 × 10^{-3} g, was added to each ternary mixture or individual experiments. The ternary mixture was vigorously stirred and left for achieving the equilibrium for at least 12 h, at (298 ± 1) K, aiming at allowing the complete partition of EE2 between the two phases. After the separation of the top and bottom phases, the detection and quantification of EE2 was carried out through UV-spectroscopy, using a Shimadzu UV-1700, Pharma-Spec Spectrometer, at a wavelength of 284 nm. Blank controls of the ternary mixture were always prepared to eliminate possible interferences of the IL and $KNaC_4H_4O_6$. Three samples of each aqueous phase were analyzed, in at least three individual systems, in order to determine the extraction efficiencies of EE2 and the respective standard deviations.

The percentage extraction efficiencies of EE2, $EE_{EE2}\%$, were estimated by **Equation (4.1)**:

$$EE_{\mathrm{EE2}}\% = \frac{Abs_{\mathrm{EE2}}^{\mathrm{IL}} \times w_{\mathrm{IL}}}{Abs_{\mathrm{EE2}}^{\mathrm{IL}} \times w_{\mathrm{IL}} + Abs_{\mathrm{EE2}}^{\mathrm{salt}} \times w_{\mathrm{salt}}} \qquad \textbf{(4.1)}$$

where Abs_{EE2}^{IL} and Abs_{EE2}^{salt} are the absorbance values of EE2 in the IL-rich and $KNaC_4H_4O_6$-rich aqueous phases (taking into account the respective dilution factors – in weight) and w_{IL} and w_{salt} are the weights obtained for the IL-rich and $KNaC_4H_4O_6$-rich phases, respectively.

Concentration of ethinylestradiol in the [C_4C_1im][$N(CN)_2$]-based ABS. The larger TL of the liquid-liquid ABS composed of [C_4C_1im][$N(CN)_2$] + $KNaC_4H_4O_6$ + H_2O was determined by means of the preparation of several ternary systems and further addition of $KNaC_4H_4O_6$ until the detection of a solid phase. Once the equation commonly applied to describe the binodal data is not able to correctly describe the regions of the solubility curve for high IL and salt concentrations,[49] the concentration of each compound in both phases of this TL was analytically determined. [C_4C_1im][$N(CN)_2$] was quantified through UV-spectroscopy, using a Shimadzu UV-1700, PharmaSpec Spectrometer, at a wavelength of 212 nm. Blank controls were prepared to eliminate interferences caused by the salt in the $KNaC_4H_4O_6$-rich phase. The water content in each phase was determined by evaporation, by means of an air oven at ~333 K, until a constant weight of the

non-volatile mixture $[C_4C_1im][N(CN)_2]$ + $KNaC_4H_4O_6$ was achieved. The $KNaC_4H_4O_6$ amount was determined by the weight difference. This process was carried out in duplicate to ascertain on the associated standard deviations. In general, shorter TLs obtained by the quantification of all phase-forming components agree well with those obtained by the mass-balance method proposed by Merchuk et al.[48]

The concentration factor of EE2 along the characterized TL was evaluated by the preparation of ternary systems at different compositions and at different weight ratios (weight of water added to the system per weight of the IL-rich phase): 100 and 1000. It should be noted that along the same TL the composition of each phase is maintained while varying only the volume or weight ratio of the phases. In these two situations, and where lower detection limits are required, EE2 was quantified using a Shimadzu HPLC Prominence system equipped with a fluorescence detector. This device consists of a degasser DGU-20A5, a bomb LC-20AD, and a column oven CTO-10ASVP. An ACE® C18 column-PFP (5 µm, 150 mm × 4.6 mm) connected to an ACE® 5 C18 4.6 mm i.d. guard column was used for the separation. The mobile phase consisted of a water-acetonitrile mixture (55:45, v/v), at a flow rate of 0.8 $mL \cdot min^{-1}$, with an injection volume of 20 µL. The detection/quantification of EE2 was performed using a Shimadzu Prominence RF-20A XS fluorescence detector at an excitation wavelength of 280 nm and an emission wavelength of 310 nm.[25] Both the column and cell temperature were maintained at 298 K. Three individual samples of the IL-rich phase were analyzed in order to determine the recovery of EE2 and the respective standard deviations. Individual standard stock solutions of EE2 were prepared in methanol at a concentration of 100 $mg \cdot L^{-1}$ and were further diluted at appropriate concentrations (between 2.5 and 100 $\mu g \cdot L^{-1}$) using ultrapure water to obtain the calibration curve. Water and acetonitrile used in the mobile phase were pretreated by filtration using 0.2 µm polyamide membrane filters from Whatman.

pH determination. The pH values (±0.02) of both the IL-rich and salt-rich phases were measured at (298 ± 1) K using a Mettler Toledo SevenMulti pH meter.

4.1.4. Results and discussion

Phase diagrams and tie-lines. New ternary phase diagrams were determined for several ILs + $KNaC_4H_4O_6$ + H_2O ABS, at (298 ± 1) K and at atmospheric pressure. The obtained liquid-liquid phase diagrams are depicted in **Figure 4.3** (the detailed weight fraction data are provided in the **Appendix C**). For all the phase diagrams, the biphasic region is localized above the solubility curve while the monophasic region is presented below. In general, the larger the biphasic region, the

higher is the capacity of the IL to undergo liquid-liquid demixing and to form an ABS, *i.e.*, the easier the IL is salted-out by the salt.

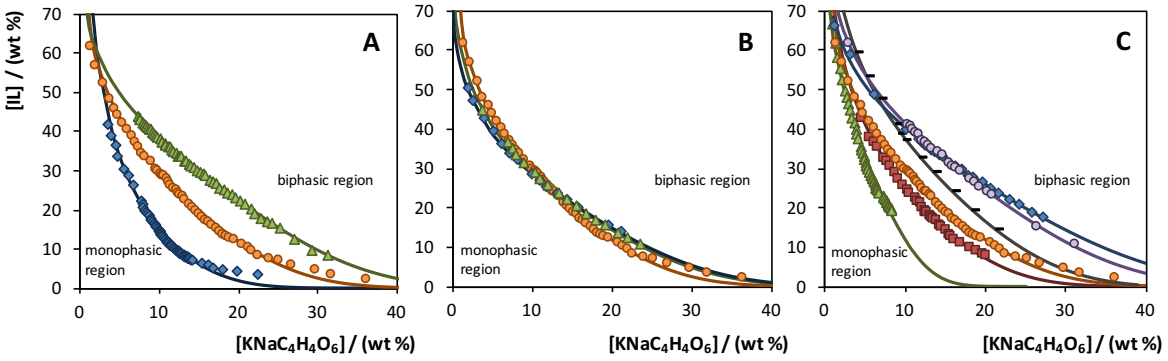

Figure 4.3. Evaluation of the **(A)** cation alkyl side chain length, **(B)** cation core and **(C)** anion nature in the ternary phase diagrams composed of IL + water + $KNaC_4H_4O_6$ at (298 ± 1) K: **(A)** $[C_2C_1im][N(CN)_2]$ (▲), $[C_4C_1im][N(CN)_2]$ (●), $[C_6C_1im][N(CN)_2]$ (◆); **(B)** $[P_{4444}]Cl$ (▲), $[N_{4444}]Cl$ (◆), $[C_4C_1im][N(CN)_2]$ (●); **(C)** $[C_4C_1im][CF_3SO_3]$ (▲)[57], $[C_4C_1im][SCN]$ (■), $[C_4C_1im][N(CN)_2]$ (●), $[C_4C_1im][TOS]$ (-), $[C_4C_1im][CF_3CO_2]$ (●), $[C_4C_1im]Br$ (◆). Adjusted binodal data by **Equation (2.1)** (–).

The ILs investigated allow addressing the effect of their chemical structures (cation alkyl side chain length and cation and anion nature) on the phase diagrams behavior or ABS formation aptitude. **Figure 4.3 A** depicts the effect of the imidazolium cation alkyl side chain length on the formation of ABS, and follows the order: $[C_2C_1im][N(CN)_2] \ll [C_4C_1im][N(CN)_2] \ll [C_6C_1im][N(CN)_2]$. Longer aliphatic chains at the cation enhance the IL hydrophobicity and lead to a wider biphasic region.[50,51] **Figure 4.3 B** presents the influence of the cation core, with the $[N_{4444}]Cl$ and $[P_{4444}]Cl$ ILs, on the liquid-liquid demixing. The phase diagram for $[C_4C_1im][N(CN)_2]$ is also depicted as one imidazolium-based fluid reference. Both $[N_{4444}]$- and $[P_{4444}]$-based ILs have an identical ability for the formation of ABS due to their similar chemical structures (four butyl chains at the cation which are responsible for their high hydrophobicity). The effect of the IL anion nature on the ABS formation is shown in **Figure 4.3 C**, where the following order was observed: $Br^- \approx [CF_3CO_2]^- < [TOS]^- < [N(CN)_2]^- < [SCN]^- \ll [CF_3SO_3]^-$. This rank is in close agreement with previous studies using other inorganic or organic salts[46,52–55] and it is related to the ability of the IL anion to hydrogen-bond with water: IL anions with lower hydrogen bond basicity values (β) present a higher ability to form ABS.[56]

Besides its biodegradable and biocompatible features, $KNaC_4H_4O_6$ presents a significant salting-out effect. This is an important characteristic while foreseeing the use of ABS for the one-step extraction and concentration of a target analyte since it will permit to obtain considerably long TLs, and thus, high concentration factors.

The experimental TLs, *i.e.*, the composition of the phases for a given mixture point, along with their respective lengths (TLL), are reported in **Table 4.1**. The pH values of both phases in each ABS are also shown in **Table 4.1**. The pH values of the coexisting phases range from neutral to slightly alkaline (6.23–9.24) and are useful to explore the possibility of using these ABS as extractive platforms for specific compounds and/or compounds that may suffer speciation.

Table 4.1. Experimental data for TLs and TLLs of IL + $KNaC_4H_4O_6$ ABS and respective pH values of the coexisting phases.

IL	Weight fraction composition / wt %								
	$[IL]_{IL}$	$[salt]_{IL}$	pH_{IL}	$[IL]_{M}$	$[salt]_{M}$	$[IL]_{salt}$	$[salt]_{salt}$	pH_{salt}	TLL
$[C_4C_1im]Br$	35.41	12.98	6.93	34.13	13.92	26.80	19.27	7.11	10.67
$[C_4C_1im][CF_3SO_3]$	62.09	1.16	6.23	40.82	4.57	19.28	8.03	6.29	43.36
$[C_4C_1im][CF_3CO_2]$	41.56	9.95	9.10	27.12	19.87	8.75	32.50	8.99	39.82
	37.86	11.87	9.24	25.72	19.98	13.16	28.37	8.88	29.71
$[C_4C_1im][SCN]$	59.72	1.98	6.63	27.25	15.19	2.55	25.22	6.68	61.71
	55.66	2.45	6.64	23.05	14.99	5.11	21.88	6.70	54.15
	49.31	3.37	6.40	31.23	10.28	8.29	19.05	6.44	43.92
$[C_4C_1im][TOS]$	57.71	4.24	7.21	38.20	14.93	1.72	34.90	7.34	63.84
	49.84	6.06	7.10	32.91	14.98	4.49	29.94	6.96	51.25
	45.17	7.40	7.10	30.38	15.05	6.96	27.16	7.11	43.02
	41.37	8.64	7.01	29.64	14.59	9.83	24.66	6.93	35.37
$[C_2C_1im][N(CN)_2]$	45.89	6.39	8.69	33.90	15.04	4.22	36.46	8.71	51.39
	43.05	7.64	8.78	32.00	14.98	9.97	29.61	8.68	39.71
$[C_4C_1im][N(CN)_2]$	61.75	1.32	8.64	19.91	30.01	2.39	36.17	8.69	68.84
	54.78	2.55	8.76	29.86	15.09	3.37	28.41	8.63	57.55
	50.69	3.28	8.52	29.92	13.50	5.66	25.41	8.55	50.18
	46.37	4.22	8.61	29.88	12.29	8.23	22.87	8.74	42.44
$[C_6C_1im][N(CN)_2]$	49.51	2.87	7.99	22.86	2.87	7.00	14.25	8.30	44.01
	44.99	3.33	8.04	20.04	10.06	8.66	13.12	7.99	37.62
$[P_{4444}]Cl$	41.58	4.75	6.60	28.09	14.93	2.44	34.29	6.72	49.03
	37.16	6.30	6.65	24.84	15.58	3.93	31.34	6.73	41.61
	35.20	7.10	6.65	24.80	15.20	4.40	30.56	6.82	38.72
$[N_{4444}]Cl$	46.95	2.58	8.06	30.01	15.04	2.41	35.34	7.94	55.29
	36.61	5.87	8.11	25.17	15.03	4.12	31.88	8.24	41.62

Extraction of ethinylestradiol. For a successful extraction, an appropriate manipulation of the phases' properties, which control the selectivity and the partition of the solute of interest, is always required. This approach was taken into consideration by scanning systems with different ILs and by manipulating their phases' compositions and volumes (*cf.* the **Appendix C**), as presented and discussed below.

The extraction efficiencies of EE2, and respective standard deviations, in ABS formed with different ILs, $KNaC_4H_4O_6$ and H_2O are depicted in **Figure 4.4** (*cf.* the **Appendix C** with the detailed values). To avoid dissimilarities in the extraction efficiencies that could result from the differences in the composition of the coexisting phases, all the partition experiments were carried out at a fixed TLL (≈ 43) – **Table 4.1**.

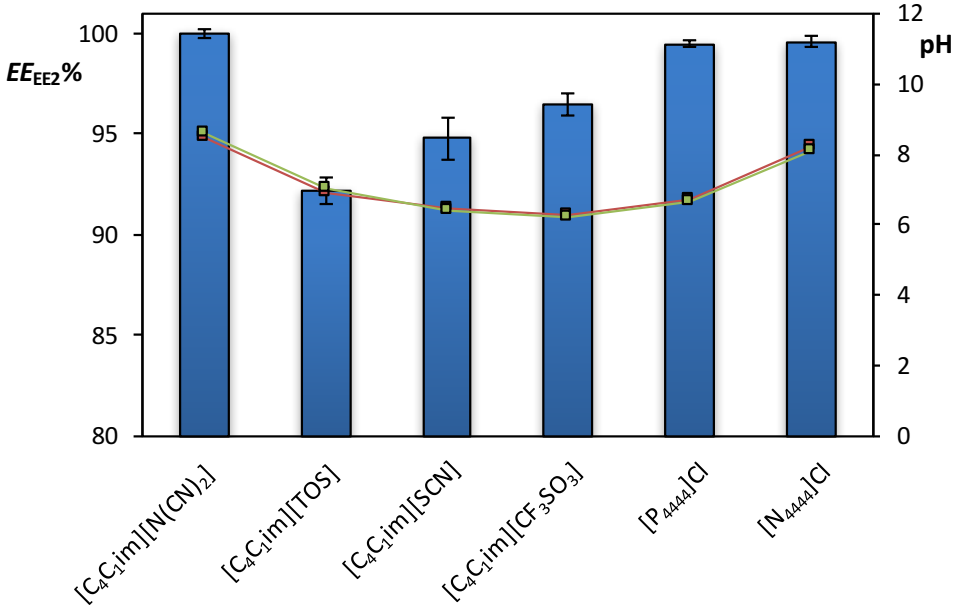

Figure 4.4. Extraction efficiencies of EE2, EE_{EE2}%, in several ABS at (298 ± 1) K: IL-rich phase pH (■); salt-rich phase pH (■).

EE2 preferentially migrates towards the IL-rich phase in all investigated ABS, with extraction efficiencies higher than 92%. The higher affinity of EE2 for the IL-rich phase correlates well with its octanol–water partition coefficient (K_{ow}) value. The $log(K_{ow})$ of EE2 is 4.15,[9] meaning that the synthetic hormone has a preferential affinity for more hydrophobic phases, which, in these systems, corresponds to the IL-rich phase. Since the pH values of each phase range between 6.2 and 8.6, and EE2 is mostly present in its neutral form, possible electrostatic interactions between the salt or IL ions and the charged EE2 species are neither significant nor responsible for the solute preferential migration.

As depicted in **Figure 4.4**, the EE2 extraction efficiency is strongly related to the hydrophobicity of the IL that forms a given ABS. The extraction efficiencies of EE2 decrease in the order: $[C_4C_1im][N(CN)_2]$ > $[P_{4444}]Cl$ ≈ $[N_{4444}]Cl$ > $[C_4C_1im][CF_3SO_3]$ > $[C_4C_1im][SCN]$ > $[C_4C_1im][TOS]$. Outstandingly, with the ABS composed of $[C_4C_1im][N(CN)_2]$ and $KNaC_4H_4O_6$ it was possible to achieve a complete extraction of EE2 for the IL-rich phase in a single-step.

Figure 4.5 depicts the impact of TLL on the EE2 extraction with $[C_4C_1im][N(CN)_2]$-based ABS (detailed data in the **Appendix C**). $[C_4C_1im][N(CN)_2]$ was chosen since this IL leads to the best extraction efficiency (100% of extraction achieved in a single-step) and allows working with long TLs that further provides the highest concentration factors.

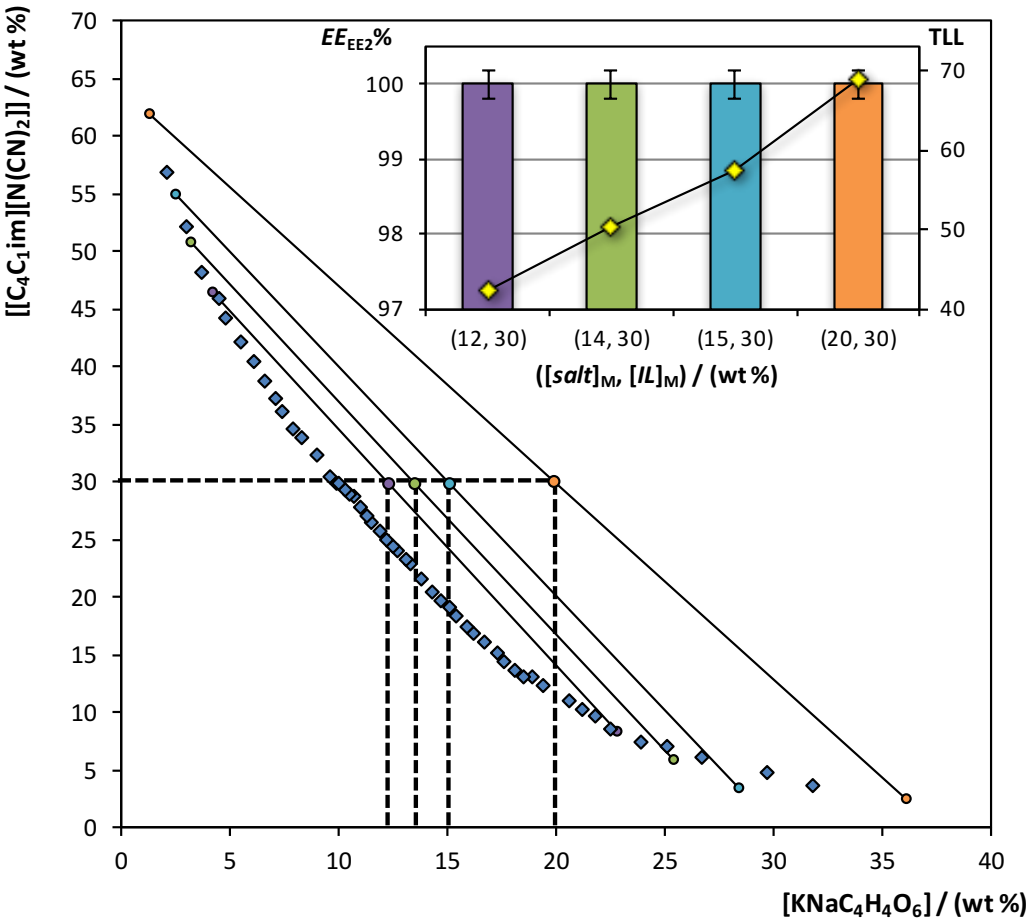

Figure 4.5. Evaluation of the TLL in the extraction efficiencies of EE2, EE_{EE2}%, in the $[C_4C_1im][N(CN)_2]$ + $KNaC_4H_4O_6$ + H_2O ABS, at (298 ± 1) K: binodal curve data (◆); TL data (●); TLL values (◆).

From **Figure 4.5**, it is possible to conclude that the TLL (at least in the range studied) does not affect the extraction capacity for EE2 and a complete extraction is always attained. The TLL values range from 46.7 to 68.8, which means that it is possible to optimize the process to be more economical and environmentally benign by decreasing the concentration of IL without losing the complete extraction efficiency.

Concentration of ethinylestradiol in $[C_4C_1im][N(CN)_2]$-based ABS. The main characteristic of ABS to be used as concentration platforms comprises the presence of very long TLs. Indeed, the longer the TL, the higher the concentration factor that can be achieved. For a one-stage extraction-concentration step, the complete extraction of the target analyte for the IL-rich phase

is required. At this stage, we should also guarantee that the IL-rich phase does not saturate with the extracted biomolecule; otherwise, the accurate quantification of EE2 in the IL-rich phase will be not accomplished leading to underestimated results. The ABS composed of $[C_4C_1im][N(CN)_2]$ + $KNaC_4H_4O_6$ + H_2O was selected here since it led to a single-step complete extraction of EE2, without saturation of the IL-rich phase, and allowed working with long TLs.

Figure 4.6 depicts the solubility curve of the $[C_4C_1im][N(CN)_2]$ + $KNaC_4H_4O_6$ + H_2O system, as well as the TL and mixture points investigated. The extraction efficiency values and respective standard deviations for different initial compositions along the same and largest TL are also shown in **Figure 4.6**.

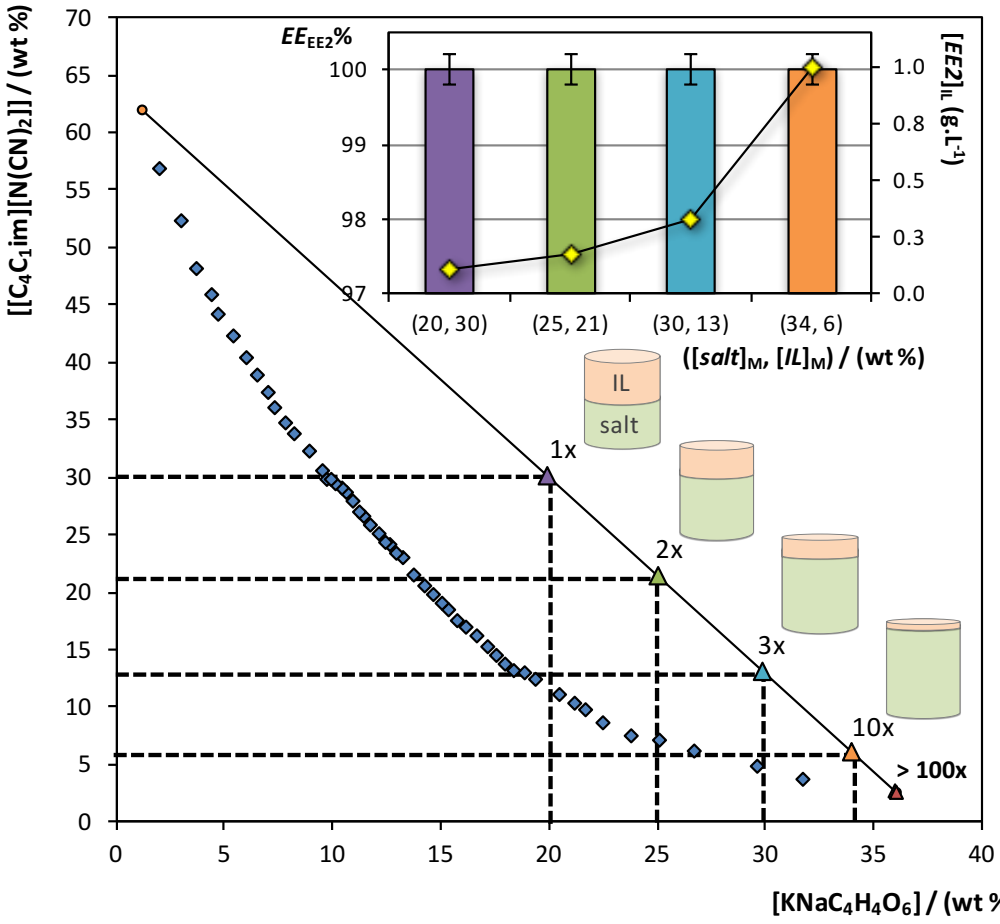

Figure 4.6. Extraction efficiencies of EE2, EE_{EE2}%, for different initial compositions along the same TL in the $[C_4C_1im][N(CN)_2]$ + $KNaC_4H_4O_6$ + H_2O ABS, at (298 ± 1) K: binodal curve data (◆); TL data (●); initial compositions (▲); EE2 final concentration in the IL-rich phase, $[EE2]_{IL}$ (◆).

Different initial compositions (*cf.* the **Appendix C**) along the same TL, and with a TLL value circa 69, lead to different weight ratios of the coexisting phases (IL-rich and salt-rich phases). Nevertheless, since the aim of this work is the concentration of an aqueous sample containing EE2 in wastewater, it should be taken into account that the amount of the real sample added to the

system is the same as the amount of water required to create the initial mixture point. Thus, in this situation, the concentration factor is equal to the total amount of water added to the mixture point divided by the IL-rich phase amount (phase for which EE2 is completely extracted). Yet, even if the IL-rich phase and water present similar densities ($[C_4C_1im][N(CN)_2]$-rich phase density at 298 K ≈ 1.04 $g \cdot cm^{-3}$ as experimentally determined by us), for higher concentration factors this difference becomes significant and should be considered. Therefore, in the following results regarding the concentration factors, volumes are considered instead of the weights of water and of the coexisting phases.

The complete extraction of EE2 was always attained for all the mixture compositions evaluated – **Figure 4.6**. The weight ratio between the water (containing EE2) added in the mixture and the IL-rich phase ranges from 1.12 to 10.03, which means that it is possible to concentrate the synthetic hormone by reducing the volume of the IL-rich phase without losing complete extraction performance. Indeed, this possibility of concentrating EE2 may overcome the main problem on its detection derived from its low concentrations in sewage treatment plants and wastewater. For the mixture point with a concentration factor of 10.03, it was experimentally possible to concentrate EE2 up to 200-fold regarding its saturation solubility in water (4.8 $mg \cdot L^{-1}$).[9]

In a wastewater real sample, EE2 is present in concentrations in the order of $ng \cdot L^{-1}$. Therefore, when dealing with real samples, a concentration factor of 10 is still not sufficient. Thus, the $[C_4C_1im][N(CN)_2]$-based ABS was further tested for higher concentration factors using an HPLC with a fluorescence detector for that purpose. Concentration factors of 100 and 1000 can be obtained in the largest TL of the ternary system (**Figure 4.6**). The mixture points required to create these conditions are: 2.69 wt% of $[C_4C_1im][N(CN)_2]$ + 36.00 wt% of $KNaC_4H_4O_6$ and 2.43 wt% of $[C_4C_1im][N(CN)_2]$ + 36.15 wt% of $KNaC_4H_4O_6$, respectively.

Standard samples with initial concentrations of ~450 and 90 $ng \cdot L^{-1}$ were used to evaluate the EE2 extraction efficiency and the concentration factors of 100 and 1000 afforded by the $[C_4C_1im][N(CN)_2]$-based ABS. The major goal is to reach a final concentration of EE2 at the IL-rich phase higher than the HPLC lower limit detection (3.1 $\mu g \cdot L^{-1}$). The EE2 recovery results obtained were 98 ± 8% and 102 ± 10% for a concentration factor of 100 and 1000, respectively. Therefore, the concentration of EE2 in wastewater can be increased at least up to 1000-fold, in a single-step, without losing EE2 and without saturating the IL-rich phase, simply by the tuning of the mixture point composition for a minimum IL-rich phase volume. Furthermore, the phase-forming components of the phase containing EE2, mainly IL and water, do not interfere with the HPLC quantification. In summary, the proposed methodology allows to increase the EE2 concentration

by, at least, three orders of magnitude (from $ng \cdot L^{-1}$ to $\mu g \cdot L^{-1}$), and enables its appropriate identification and quantification.

The economical and sustainable viability of the proposed method to detect EE2 in sewage treatment plants is also ensured. The amount of IL used for ABS formation is inversely proportional to the concentration factor required. For instance, for a real water sample of ≈ 61 mL, (ABS with a total volume of 100 mL) only 2.69 g or 2.43 g of $[C_4C_1im][N(CN)_2]$ is required to reach a concentration factor of 100 and 1000, respectively.

The analysis of effluent samples requires analytical techniques with high sensitivity because of their complex matrices and low concentration of marker pollutants. LC-MS and LC-MS/MS, due to high sensitivity and selectivity, have been selected as the techniques of choice for environmental analysis of steroid hormones.[58] However, they display several drawbacks, namely, the use of expensive devices, high maintenance costs and require skilled analysts. Therefore, these techniques are unaffordable for many analytical laboratories. Compared with LC-MS and LC-MS/MS, HPLC coupled either to UV or a fluorescence detector is a simpler, cheaper, easy-to-use and extensively available technique. Yet, due to its higher detection limits, a pre-concentration step is always required. To this end, HPLC conjugated with solid-phase extractions (SPE) or liquid-liquid extractions are regularly used.[59–61] Both these pre-concentration techniques require large quantities of toxic and volatile organic solvents and are time-consuming. Low-cost dispersive liquid-liquid micro extraction (DLLME) has also been proposed[44,45] and successfully applied for the concentration of steroid hormones, with an enrichment factor of 178 and an extraction efficiency of 89% for EE2.[25] Compared to these methods, IL-based ABS do not require the use of volatile organic solvents and allow obtaining a complete extraction of EE2 (with no loss of solute) and significantly higher concentration factors. Furthermore, it is possible to tune the ABS properties through the change of the IL nature creating, therefore, a new plethora of concentration systems for other target analytes present in wastewater. The concentration factors here obtained are also far superior to those previously reported with IL-based ABS with maximum enrichment factors of 10 in the extraction of opium alkaloids or steroid hormones from biological fluids,[62,63] and up to 100 in the extraction of bisphenol A from human fluids.[44]

4.1.5. Conclusions

Aiming at overcoming one of the major limitations in the analysis and monitoring of wastewater, a novel methodology is proposed here to concentrate EE2 by the application of IL-based ABS. As a first approach, their ternary phase diagrams were determined and the single-step

extraction capacity of several IL-based ABS was addressed. Extraction efficiencies ranging between 92% and 100% were obtained for the IL-rich phase revealing the high affinity of EE2 to the most hydrophobic phase. In particular, outstanding extraction efficiencies, *i.e.*, the complete extraction of EE2 in a single-step, were attained with $[C_4C_1im][N(CN)_2]$-based ABS. Therefore, these types of systems were further tested to optimize the concentration factors of EE2. It was found that by tuning the mixture point composition for a minimum IL-rich phase volume, the EE2 concentration in wastewater can be increased at least up to 1000-fold in a single-step. The proposed methodology allows the increase of the EE2 concentration by three orders of magnitude (from $ng \cdot L^{-1}$ to $\mu g \cdot L^{-1}$), thus overcoming the detection limits of conventional analytical equipment commonly used in the analysis and monitoring of wastewater. These systems are straightforwardly envisaged for the monitoring of wastewater as potential one-step extraction and concentration routes for a wide array of endocrine disrupting chemicals or other trace pollutants.

4.1.6. References

(1) USEPA, *Endocrine Disruptors Research*, http://www.epa. gov/research/endocrinedisruption/index.htm, Accessed 09.14;
(2) A. C. Johnson and J. P. Sumpter, *Environ. Sci. Technol.*, 2001, **35**, 4697–4703;
(3) D. Nasuhoglu, D. Berk and V. Yargeau, *Chem. Eng. J.*, 2012, **185**, 52–60;
(4) D. Matejicek and V. Kuban, *Anal. Chim. Acta*, 2007, **588**, 304–315;
(5) G.-G. Ying, R. S. Kookana and Y.-J. Ru, *Environ. Int.*, 2002, **28**, 545–551;
(6) Z. Yu, B. Xiao, W. Huang and P. A. Peng, *Environ. Toxicol. Chem.*, 2004, **23**, 531–539;
(7) A. K. Sarmah, G. L. Northcott and F. F. Scherr, *Environ. Int.*, 2008, **34**, 749–755;
(8) EWA, http://www.ewaonline.de, Accessed 01.13;
(9) C. P. Silva, M. Otero and V. Esteves, *Environ. Pollut.*, 2012, **165**, 38–58;
(10) R. J. Williams, A. C. Johnson, J. J. L. Smith and R. Kanda, *Environ. Sci. Technol.*, 2003, **37**, 1744–1750;
(11) O. Braga, G. A. Smythe, A. I. Schäfer and A. J. Feitz, *Environ. Sci. Technol.*, 2005, **39**, 3351–3358;
(12) T. Frische, J. Bachmann, D. Frein, T. Juffernholz, A. Kehrer, A. Klein, G. Maack, F. Stock, H.-C. Stolzenberg, C. Thierbach and S. Walter-Rohde, *Toxicol. Lett.*, 2013, **223**, 306–309;
(13) A. Lange, G. C. Paull, T. S. Coe, Y. Katsu, H. Urushitani, T. Iguchi and C. R. Tyler, *Environ. Sci. Technol.*, 2009, **43**, 1219–1225 ;
(14) H. M. Maes, S. X. Maletz, H. T. Ratte, J. Hollender and A. Schaeffer, *Environ. Sci. Technol.*, 2014, **48**, 12354–12361 ;
(15) T. A. Ternes, M. Stumpf, J. Mueller, K. Haberer, R. D. Wilken and M. Servos, *Sci. Total Environ.*, 1999, **225**, 81–90;
(16) T. Benijts, W. Lambert and A. De Leenheer, *Anal. Chem.*, 2004, **76**, 704–711;
(17) T. Vega-Morales, Z. Sosa-Ferrera and J. J. Santana-Rodriguez, *J. Hazard. Mater.*, 2010, **183**, 701–711;
(18) N. Yoshioka, Y. Akiyama and K. Teranishi, *J. Chromatogr. A*, 2004, **1022**, 145–150;
(19) H. C. Chen, H. W. Kuo and W. H. Ding, *Chemosphere*, 2009, **74**, 508–514;
(20) M. Henriques, V. Cardoso, A. Rodrigues, E. Ferreira, M. Benoliel and C. Almeida, *J. Water Resource Prot.*, 2010, **2**, 818–829;

(21) B. J. Vanderford, R. A. Pearson, D. J. Rexing and S. A. Snyder, *Anal. Chem.*, 2003, **75**, 6265–6274;
(22) H. G. J. Mol, S. Sunarto and O. M. Steijger, *J. Chromatogr. A*, 2000, **879**, 97–112;
(23) G. Saravanabhavan, R. Helleur and J. Hellou, *Chemosphere*, 2009, **76**, 1156–1162;
(24) S. D. Richardson, *Anal. Chem.*, 2002, **74**, 2719–2741;
(25) D. L. D. Lima, C. P. Silva, M. Otero and V. I. Esteves, *Talanta*, 2013, **115**, 980–985;
(26) P. A. Albertsson, *Partitioning of Cell Particles and Macromolecules*, Wiley-Interscience, New York, 1986;
(27) M. Milosevic, K. J. J. Staal, B. Schuur and A. B. de Haan, *Desalination*, 2013, **324**, 99–110;
(28) X. Xie, Y. Wang, J. Han and Y. Yan, *Anal. Chim. Acta*, 2011, **687**, 61–66;
(29) K. E. Gutowski, G. A. Broker, H. D. Willauer, J. G. Huddleston, R. P. Swatloski, J. D. Holbrey and R. D. Rogers, *J. Am. Chem. Soc.*, 2003, **125**, 6632– 6633;
(30) M. G. Freire, A. F. M. Cláudio, J. M. M. Araujo, J. A. P. Coutinho, I. M. Marrucho, J. N. Canongia Lopes and L. P. N. Rebelo, *Chem. Soc. Rev.*, 2012, **41**, 4966–4995;
(31) J. F. Brennecke and E. J. Maginn, *AIChE J.*, 2001, **47**, 2384– 2389;
(32) S. Aparicio, M. Atilhan and F. Karadas, *Ind. Eng. Chem. Res.*, 2010, **49**, 9580–9595;
(33) T. Kakiuchi, *Anal. Chem.*, 2007, **79**, 6442–6449;
(34) T. D. Ho, C. Zhang, L. W. Hantao and J. L. Anderson, *Anal. Chem.*, 2013, **86**, 262–285;
(35) H. Passos, M. G. Freire and J. A. P. Coutinho, *Green Chem.*, 2014, **16**, 4786–4815;
(36) D. K. Bwambok, S. K. Challa, M. Lowry and I. M. Warner, *Anal. Chem.*, 2010, **82**, 5028–5037;
(37) J. F. B. Pereira, A. S. Lima, M. G. Freire and J. A. P. Coutinho, *Green Chem.*, 2010, **12**, 1661–1669;
(38) C. D. Tran, D. Oliveira and S. Yu, *Anal. Chem.*, 2006, **78**, 1349–1356;
(39) K. R. Seddon, *J. Chem. Technol. Biotechnol.*, 1997, **68**, 351– 356;
(40) A. F. M. Cláudio, C. F. C. Marques, I. Boal-Palheiros, M. G. Freire and J. A. P. Coutinho, *Green Chem.*, 2014, **16**, 259–268;
(41) M. Taha, F. A. e Silva, M. V. Quental, S. P. M. Ventura, M. G. Freire and J. A. P. Coutinho, *Green Chem.*, 2014, **16**, 3149–3159;
(42) F. J. Deive, A. Rodriguez, A. B. Pereiro, J. M. M. Araujo, M. A. Longo, M. A. Z. Coelho, J. N. C. Lopes, J. M. S. S. Esperança, L. P. N. Rebelo and I. M. Marrucho, *Green Chem.*, 2011, **13**, 390–396;
(43) J. F. B. Pereira, L. P. N. Rebelo, R. D. Rogers, J. A. P. Coutinho and M. G. Freire, *Phys. Chem. Chem. Phys.*, 2013, **15**, 19580–19583;
(44) H. Passos, A. C. A. Sousa, M. R. Pastorinho, A. J. A. Nogueira, L. P. N. Rebelo, J. A. P. Coutinho and M. G. Freire, *Anal. Methods*, 2012, **4**, 2664–2667;
(45) M. G. Freire, C. M. S. S. Neves, I. M. Marrucho, J. N. Canongia Lopes, L. P. N. Rebelo and J. A. P. Coutinho, *Green Chem.*, 2010, **12**, 1715–1718;
(46) H. Passos, A. R. Ferreira, A. F. M. Cláudio, J. A. P. Coutinho and M. G. Freire, *Biochem. Eng. J.*, 2012, **67**, 68–76;
(47) J. Han, C. Yu, Y. Wang, X. Xie, Y. Yan, G. Yin and W. Guan, *Fluid Phase Equilib.*, 2010, **295**, 98–103;
(48) J. C. Merchuk, B. A. Andrews and J. A. Asenjo, *J. Chromatogr., B: Biomed. Appl.*, 1998, **711**, 285–293;
(49) E. Alvarez-Guerra, S. P. M. Ventura, J. A. P. Coutinho and A. Irabien, *Fluid Phase Equilib.*, 2014, **371**, 67–74;
(50) S. P. M. Ventura, S. G. Sousa, L. S. Serafim, Á. S. Lima, M. G. Freire and J. A. P. Coutinho, *J. Chem. Eng. Data*, 2011, **56**, 4253–4260;
(51) C. M. S. S. Neves, S. P. M. Ventura, M. G. Freire, I. M. Marrucho and J. A. P. Coutinho, *J. Phys. Chem. B*, 2009, **113**, 5194–5199;
(52) S. P. M. Ventura, C. M. S. S. Neves, M. G. Freire, I. M. Marrucho, J. Oliveira and J. A. P. Coutinho, *J. Phys. Chem. B*, 2009, **113**, 9304–9310;
(53) A. F. M. Cláudio, A. M. Ferreira, S. Shahriari, M. G. Freire and J. A. P. Coutinho, *J. Phys. Chem. B*, 2011, **115**, 11145–11153;

(54) C. Li, J. Han, Y. Wang, Y. Yan, J. Pan, X. Xu and Z. Zhang, *J. Chem. Eng. Data*, 2009, **55**, 1087–1092;
(55) S. P. M. Ventura, S. G. Sousa, L. S. Serafim, Á. S. Lima, M. G. Freire and J. A. P. Coutinho, *J. Chem. Eng. Data*, 2012, **57**, 507–512;
(56) A. F. M. Cláudio, L. Swift, J. P. Hallett, T. Welton, J. A. P. Coutinho and M. G. Freire, *Phys. Chem. Chem. Phys.*, 2014, **16**, 6593–6601;
(57) S. Shahriari, C. M. S. S. Neves, M. G. Freire and J. A. P. Coutinho, *J. Phys. Chem. B*, 2012, **116**, 7252–7258;
(58) M. Petrović, M. D. Hernando, M. S. Díaz-Cruz and D. Barceló, *J. Chromatogr. A*, 2005, **1067**, 1–14;
(59) S. Rodriguez-Mozaz, M. J. Lopez de Alda and D. Barceló, *Anal. Chem.*, 2004, **76**, 6998–7006;
(60) X. Du, X. Wang, Y. Li, F. Ye, Q. Dong and C. Huang, *Chromatographia*, 2010, **71**, 405–410;
(61) M. Rezaee, Y. Yamini and M. Faraji, *J. Chromatogr. A*, 2010, **1217**, 2342–2357;
(62) C. He, S. Li, H. Liu, K. Li and F. Liu, *J. Chromatogr. A*, 2005, **1082**, 143–149;
(63) S. Li, C. He, H. Liu, K. Li and F. Liu, *J. Chromatogr. B: Biomed. Appl.*, 2005, **826**, 58–62.

5. FINAL REMARKS
AND FUTURE WORK

Aqueous biphasic systems (ABS) composed of ionic liquids (ILs) combine all the advantages of these alternative solvents with the advantages of ABS, making this type of systems valuable in processes of extraction and separation of a wide range of compounds. The high versatility of IL-based ABS was here demonstrated by the determination and characterization of new phase diagrams of ternary and quaternary systems composed of protic ILs, Good's buffers, or IL-IL mixtures mixed with salts and/or polymers, and by inferring on the IL-based ABS properties. It was shown that the use of protic ILs allows the development of highly temperature dependent ABS, which could be used to induce reversible phase separation. Similarly, it was shown that self-buffering systems could be prepared if Good's buffers are used in IL-based ABS formulation. Furthermore, and for the first time, it was here demonstrated that ABS composed of a mixture of two ILs with very distinct polarities – $[C_4C_1im]Cl$ and $[C_4C_1im][CF_3SO_3]$ – and a salt, should be considered as a quaternary system instead of a pseudo-ternary system, since each IL presents its own impact on the system. Considering the mechanisms which rules the formation of ABS, it was possible to prepare systems with three coexisting phases – aqueous multiphasic systems (MuPS) – by the correct selection of four phase forming components: K_3PO_4 + PEG 600 + $[N_{111(2OH)}]^+$-based IL + water. It was also evaluated the real nature of ABS composed of deep eutectic solvents (DES), demonstrating that the DES integrity is destroyed in ABS by the disruption of the DES hydrogen-bond complex and preferential solvation of the isolated components by water. All the new systems developed here presented improved extractions and selectivities in the partition of several molecules, such as proteins, amino acids and textile and food dyes.

The number of possibilities to form an IL-based ABS is huge and is still growing. Thus, there is an increasing need to create methodologies to predict their formation and ability to extract target compounds. In this work, preliminary results on the PC-SAFT potential application as a tool to predict the LLE behavior of ternary mixtures composed of ILs, salts and water, based only in IL-water binary mixtures experimental data, was demonstrated. Still in this ambit, it was shown the existence of a relation between the COSMO-RS hydrogen-bonding interaction energies of ILs and their ability to induce ABS formation and, based on this, a new methodology able to predict with good accuracy the formation of IL-based systems was developed. The physicochemical properties of ABS composed of ILs and acetate-based salts were also studied to infer on their potential application in industrial processes. Furthermore, a new probe for the determination of the hydrogen bond donor acidity of highly concentrated ILs aqueous solutions was here disclosed. To infer on the mechanisms which rules the partition of molecules between the coexisting phases, two different methodologies were tested: the Gibbs free energy of transfer of a methylene group

between the coexisting phases and the Kamlet-Taft solvatochromic parameters. Both types of characterization allowed a deep understanding on the type of interactions that are present in the phases of ABS composed of different ILs and salts.

To close this work, the application of IL-based ABS to allow a more accurate monitoring of wastewaters is here shown as a main example. In particular, ABS were used to extract and concentrate the endocrine disruptor, ethinylestradiol (EE2). The complete extraction of EE2 in a single-step was attained with $[C_4C_1im][N(CN)_2]$-based ABS. Furthermore, by the tuning of the mixture point composition for a minimum IL-rich phase volume, the EE2 concentration in wastewater was increased at least up to 1000-fold, demonstrating the IL-based ABS potential in one-step extraction and concentration routes for the further the quantification of a wide array of endocrine disrupting chemicals or other trace pollutants.

Despite all the promising results here disclosed, additional future work in the IL-based ABS arena is still required, such as:

- Determination of the ILs partition between the coexisting phases of the ABS composed of IL-IL mixtures, and evaluation of the degree of ions exchange in these systems;
- Determination of the polarity of the ABS phases for systems composed of mixtures of ILs using the Gibbs free energy of transfer of a methylene group and/or the Kamlet-Taft solvatochromic parameters;
- Evaluation of other types of salts and polymers in the formation of aqueous multiphasic systems to increase the range of possible systems to allow the tuning of the phases properties, such as the pH, viscosity and polarity, while envisaging an increase in the number of potential applications of these systems;
- Development of the PC-SAFT to describe IL-based ABS using other types of experimental data of binary and ternary mixtures;
- Evaluation of the capacity of the predictive model based on the COSMO-RS hydrogen-bonding interaction energies to predict new types of ABS composed of distinct ILs and salts;
- Determination of the Gibbs free energy of a methylene group transfer and the Kamlet-Taft solvatochromic parameters of ABS composed of ILs with distinct cations, to infer on the IL cation effect;
- Optimization of the experimental procedure of the one-step extraction and concentration methodology to make feasible its application at an industrial scale;

- Development of simultaneously temperature- and pH-dependent IL-based ABS to design switchable systems with more degrees of freedom.

6. List of publications

Co-author in:

1. Helena Passos, Ana R. Ferreira, Ana Filipa M. Cláudio, João A. P. Coutinho, Mara G. Freire; "Characterization of Aqueous Biphasic Systems Composed of Ionic Liquids and a Citrate-Based Biodegradable Salt", Biochemical Engineering Journal, 2012, 67, 68-76;
2. Helena Passos, Ana C. A. Sousa, M. Ramiro Pastorinho, António J. A. Nogueira, Luís Paulo N. Rebelo, João A. P. Coutinho and Mara G. Freire; "Ionic-Liquid-Based Aqueous Biphasic Systems for Improved Detection of Bisphenol A in Human Fluids", Analytical Methods, 2012, 4, 2664-2667;
3. Hugo F. D. Almeida, Helena Passos, José A. Lopes-da-Silva, Ana M. Fernandes, Mara G. Freire and João A. P. Coutinho; "Thermophysical Properties of Acetate-Based Ionic Liquids", Journal of Chemical & Engineering Data, 2012, 57, 3005-3013;
4. Helena Passos, Margarida P. Trindade, Tatiana S. M. Vaz, Luiz P. da Costa, Mara G. Freire and João A. P. Coutinho; "The impact of self-aggregation on the extraction of biomolecules in ionic-liquid-based aqueous two-phase systems", Separation and Purification Technology, 2013, 108, 174-180;
5. Helena Passos, Imran Khan, Fabrice Mutelet, Mariana B. Oliveira, Pedro J. Carvalho, Luís M. N. B. F. Santos, Christoph Held, Gabriele Sadowski, Mara G. Freire and João A. P. Coutinho; "Vapor-liquid equilibria of water + alkylimidazolium-based ionic liquids: measurements and Perturbed-Chain Statistical Associating Fluid Theory modelling", Industrial & Engineering Chemistry Research, 2014, 53, 3737-3748.
6. Mafalda R. Almeida, Helena Passos, Matheus Pereira, Álvaro Lima, João A.P. Coutinho, Mara G. Freire; "Ionic liquids as additives to enhance the extraction of antioxidants in aqueous two-phase systems", Separation and Purification Technology, 2014, 128, 1-10.
7. Helena Passos, Mara G. Freire and João A. P. Coutinho; "Ionic liquids solutions as extractive solvents of value-added compounds from biomass", Green Chemistry, 2014, 16, 4786-4815.
8. Teresa B.V. Dinis, Helena Passos, Diana L. D. Lima, Valdemar I. Esteves, João A. P. Coutinho and Mara G. Freire; "One-step extraction and concentration of estrogens for an adequate monitoring of wastewaters using ionic-liquid-based aqueous biphasic systems", Green Chemistry, 2015, 17, 2570-2579.
9. Andreia Luís, Teresa B.V. Dinis, Helena Passos, João A. P. Coutinho, Mohamed Taha and Mara G. Freire; "Good's buffers as novel phase-forming components of ionic-liquid-based aqueous biphasic systems", Biochemical Engineering Journal, 2015, 101, 142–149.

10. Maria V. Quental, Helena Passos, Kiki A. Kurnia, João A. P. Coutinho and Mara G. Freire; "Aqueous biphasic systems composed of ionic liquids and acetate-based salts: phase diagrams, densities and viscosities", Journal of Chemical & Engineering Data, 2015, 60, 1674-1682.

11. Helena Passos, Andreia Luís, João A. P. Coutinho and Mara G. Freire; "Thermoreversible (Ionic-Liquid-Based) Aqueous Biphasic Systems", Scientific Reports, 2016, 6, 20276.

12. Helena Passos, Daniel J. P. Tavares, Ana M. Ferreira, Mara G. Freire and João A.P. Coutinho; "Are aqueous biphasic systems composed of deep eutectic solvents ternary or quaternary systems?", Sustainable Chemistry and Engineering, 2016, 4, 2881-2886.

13. Marta L. S. Batista, Helena Passos, Bruno J. M. Henriques, Edward J. Maginn, Simão P. Pinho, Mara G. Freire, José R. B. Gomes and João A. P. Coutinho; "Why are some cyano-based ionic liquids better glucose solvents than water?", Physical Chemistry Chemical Physics, 2016, 18, 18958-18970.

14. Belinda Soares, Helena Passos, Carmen S. R. Freire, João A. P. Coutinho, Armando J. D. Silvestre and Mara G. Freire; "Ionic liquids in chromatographic and electrophoretic techniques: toward additional improvements on the separation of natural compounds", Green Chemistry, 2016, 18, 4582-4604.

15. Pedro P. Madeira, Helena Passos, Joana Gomes, João A. P. Coutinho and Mara G. Freire; "Alternative probe for the determination of the hydrogen-bond acidity of ionic liquids and their aqueous solutions", Physical Chemistry Chemical Physics, 2017, 19, 11011-11016.

16. Teresa B. V. Dinis, Helena Passos, Diana L. D. Lima, João A. P. Coutinho, Valdemar I. Esteves, and Mara G. Freire; "Simultaneous extraction and concentration of water pollution tracers using ionic-liquid-based systems"; Journal of Chromatography A, 2017, submitted.

17. Ana M. Ferreira, Helena Passos, Akiyoshi Okafuji, Mara G. Freire, João A. P. Coutinho and Hiroyuki Ohno; "Designing the thermal behaviour of aqueous biphasic systems composed of ammonium-based zwitterions", Green Chemistry, 2017, submitted.

18. Helena Passos, Sara Costa, Ana M. Fernandes, Mara G. Freire, Robin D. Rogers and João A.P. Coutinho; "Double salting-out effect: a required phenomenon in the formation of ionic-liquid-based aqueous multiphase systems", Chemical Communications, 2017, submitted.

Estes anexos só estão disponíveis para consulta através do CD-ROM.
Queira por favor dirigir-se ao balcão de atendimento da Biblioteca.

Serviços de Biblioteca, Informação Documental e Museologia
Universidade de Aveiro